SELF-SATURATING MAGNETIC AMPLIFIERS

WESTINGHOUSE—McGRAW-HILL
ENGINEERING BOOKS FOR INDUSTRY

Bean, Chackan, Moore, and Wentz—TRANSFORMERS FOR THE ELECTRIC POWER INDUSTRY

Beck—LIGHTNING PROTECTION FOR ELECTRIC SYSTEMS

Gibbs—TRANSFORMER PRINCIPLES AND PRACTICE (2d ed.)

Lynn, Pula, Ringelman, and Timmel—SELF-SATURATING MAGNETIC AMPLIFIERS

Marbury—POWER CAPACITORS

PREVIOUSLY PUBLISHED McGRAW-HILL BOOKS
BY WESTINGHOUSE AUTHORS

James and Markle—CONTROLLERS FOR ELECTRIC MOTORS

Veinott—FRACTIONAL HORSEPOWER ELECTRIC MOTORS (2d ed.)

Wagner and Evans—SYMMETRICAL COMPONENTS

Self-saturating Magnetic Amplifiers

GORDON E. LYNN, M.S.E.E.

THADDEUS J. PULA, Dr. Eng.

JOHN F. RINGELMAN, B.S. Eng. Phys.

FREDERICK G. TIMMEL, M.S.E.E.

All members of the Air Arm Division,
Westinghouse Electric Corp., Baltimore, Md.

McGRAW-HILL BOOK COMPANY, INC.

New York Toronto London 1960

SELF-SATURATING MAGNETIC AMPLIFIERS

 Library of Congress Catalog Card Number 60-6979

39250

THE MAPLE PRESS COMPANY, YORK, PA.

Preface

The desirability of a text devoted principally to magnetic amplifiers employing self-saturation has been recognized for years by practitioners in the field. The rapid multiplication of the fields of application of magnetic amplifiers after the introduction of the self-saturating technique by Logan indicates the importance of this contribution to the art. Unfortunately, introduction of the technique of self-saturation, together with the evolution of essentially square-loop core materials, did not result in immediate recognition of the simplifications in the concepts of the mechanics of operation made possible by these developments. The rapid expansion of the technology following the new developments necessitated training engineers to apply the new device. Numerous papers appeared in the technical journals explaining the operation of the devices, describing new circuits, and advancing new concepts of operation. To aid the beginner in obtaining a background in the field, linear phenomena and terms were used almost exclusively, since the student was not prepared to assimilate nonlinear concepts as they were understood at that time.

In the years immediately following World War II, the explanations of how magnetic amplifiers work were concerned largely with dynamic flux-current loops and the determination of average ampere-turns during a half-cycle. The concepts were based in large measure on observations of simple saturable reactor circuits. The observations and conclusions drawn from them were manipulated to satisfy best the conditions existing in self-saturating circuits such as the doubler, bridge, and center-tapped circuits. The resultant explanations were incomplete, cumbersome, and difficult for an engineer new to the field to grasp. More recently, new concepts have been advanced and more use has been made of simplifications made possible by the self-saturating technique, by essentially square-loop materials, and by diodes with nearly ideal reverse characteristics. In addition, the application of magnetic amplifiers in complex feedback-control mechanisms has stimulated the development of engineers conversant with both magnetic-amplifier and feedback-control technologies. As a result, techniques of the latter field have been applied to the former with excellent results. It is the purpose of this text to present a thorough treatment of self-saturating magnetic amplifiers, stressing simplicity of approach for the undergraduate, yet emphasizing rigor in analysis for the graduate student or practicing engineer. We have scrupulously attempted to avoid impractical idealizations of nonlinear functions wherever such idealizations would disguise the true operation of a physically realizable amplifier. In the chapters to follow, modern concepts of magnetic-amplifier operation will be explained. In the process, the reader will be taken step by step from the basic, underlying assumptions involving circuital laws through a moderate amount of magnetic theory to an understanding of the mechanics of self-saturating magnetic amplifiers. Sections have been included to refresh the reader's memory of transformer theory, feedback-control theory, and magnetic theory. The practitioner familiar with these fields is at liberty to skip over these sections without loss of clarity.

With a reasonable groundwork laid concerning the operation of magnetic amplifiers, the later chapters are intended to provide a background for magnetic-amplifier design. Chapter 6 presents a brief discussion of test methods applicable to core materials for magnetic amplifiers and test data of use as design aids. A logical method for pursuing a design from application to finished amplifier is presented in Chap. 7. Following this, a few commonly encountered design problems are discussed in Chap. 8, and suggestions are made for minimizing harmful effects. The book concludes with a discussion of the advantages and disadvantages of magnetic amplifiers and a few typical applications of the various circuits considered in preceding chapters.

Our material has been drawn from many sources in our somewhat heterogeneous backgrounds. The order of presentation of the subject matter follows closely a course in saturating-core devices presented to Westinghouse engineers of the Air Arm Division for several years. The suggestions and criticisms of these students have helped us considerably in selecting the format for presentation. The portion of the first chapter devoted to a review of transformer theory, for example, was included at their request.

Insofar as possible the symbols and nomenclature used are those recommended by the Definitions and Theory Subcommittees of the AIEE Magnetic Amplifiers Committee. The system of units chosen is the rationalized MKS system. Unfortunately for the field, until the recent past magnetic data have been presented in emu units by materials manufacturers. The engineer was constrained, therefore, to think in terms of gauss and oersteds, and it is difficult now for practitioners in the art (including the authors) to change to teslas and ampere-turns/meter.

Acknowledgment is gratefully made for the support and encouragement provided by the management of the Westinghouse Air Arm Division during the past two years. Particular thanks are extended to Messrs. N. V. Petrou, J. F. Harris, and H. M. Watson. We are also indebted to many people for assistance in the preparation of this text. Particular thanks are due Mr. W. C. Bullock both for ideas contributed and for his discerning criticisms of the rough draft of several chapters. Mr. B. C. Knudson and Dr. M. Lauriente were most helpful in discussions of the problems of semiconductor and magnetic materials. Various members of the Magnetic Devices Section of the Air Arm Division, Westinghouse Electric Corporation, were responsible for the derivation of equations and for supplying and reducing data. Of particular assistance was the work of Mr. J. J. Biess on derivations for Chap. 7. The patience of our typist, Mrs. M. G. Klein, who bore with our infinite changes with good humor, is gratefully acknowledged. The understanding of our wives, who rendered considerable assistance during the chores of proofreading, was very gratifying and we take this opportunity to thank them for their encouragement and aid throughout the preparation of the book.

G. E. Lynn
T. J. Pula
J. F. Ringelman
F. G. Timmel

List of Symbols

A Cross-sectional area of core
A_W Available window area
B Bias subscript
B Flux density (magnetic induction)
B_m Maximum flux density
B_r Remanent flux density
B_{sat} Saturation flux density
C Capacitance
C Centigrade
$C(s)$ Generalized output as a function of frequency
D Impedance/turns² core constant
E_{ac} Effective value of e_{ac}
E_B Average or d-c value of bias voltage
E_d Average voltage across N_d (half-cycle average)
E_i Total average interstage voltage loss
E_L Average value of load voltage
E_m Peak magnitude of source voltage
E_{NG} Average voltage across N_G (half-cycle average)
E_{NS} Average voltage across N_S (half-cycle average)
E_Q Quiescent voltage across R_D
E_S Average or d-c value of signal voltage
$E_{S\max}$ Maximum d-c voltage of E_S
E_T Forward threshold voltage of rectifier
E_1 Inverse voltage on REC_1
E_{1m} Peak magnitude of primary voltage
E_2 Inverse voltage on REC_2
E_{2m} Peak magnitude of voltage across winding 2
$F(s)$ Frequency function
G Gate subscript
G Material gain
$G(s)$ Transfer function
$G_{v/NI}$ Volts per ampere-turn gain
$(G_{v/NI})_0$ Volts per ampere-turn gain at $N^2/R = 0$
$G_{v/v}$ Volts per volt gain
G_1 Block diagram transfer function
H Magnetic field intensity
H Transfer function of feedback loop
H_i Field intensity at inner rim
H_o Field intensity at outer rim
H_0 Reset field intensity to achieve $\Delta B = B_m$
H_1 Reset field intensity to achieve ΔB_1
H_2 Reset field intensity to achieve Δ_{B2}
I Intensity of magnetization
I Current
$I_{\text{d-c}}$ Reset current in constant-current flux reset test
I_f Forward current of diode
I_0 Amplitude constant of the diode equation
I_r Reverse current of diode
I_S Average signal-circuit current

K Kelvin
K Amplification constant
K_c Closed-loop amplification constant
K_f Feedback amplification constant
K_v Voltage gain constant
L Reactor
L Inductance
L_e Source inductance
M_0 Spontaneous magnetization intensity at 0°K
M_s Spontaneous magnetization intensity
N Number of turns
N_B Bias winding turns
N_d Pickup winding turns
N_F Feedback winding turns
N_G Gate winding turns
N_S Signal winding turns
N_1 Turns on winding 1
N_2 Turns on winding 2
P_L D-c load power
P_S D-c signal power
R Resistance
R_B Bias-circuit resistance
R_{BL} Self-bias resistance
R_D Mixing resistance for push-pull operation
R_e Source resistance
R_e Driving resistance in sine-current test
R_f Forward resistance of rectifier
R_i Inside radius
R_i Resistance of interstage circuit
R_G Gate-circuit resistance
R_L Load resistance
R_o Outside radius
R_{NG} Resistance of gate winding
R_p Resistance of primary winding
R_r Reverse resistance of rectifier
R_{REC} Forward resistance of rectifier
R_S Signal-circuit resistance
$R(s)$ Generalized input
REC Rectifier
S Signal subscript
Sw Switch
T Temperature, °K
T Time interval
T Bucking transformer
T_T Dead-time interval
V Developed junction potential
V Reference voltage for sine-current test
V' Reference voltage for sine-current test
VSA Volt-second area
VSTR Volt-second transfer ratio
Z_s Secondary impedance
a Turns ratio, N_1/N_2
a Volts/turn constant
b Resetting ampere-turn constant
c Integration constant
$\overline{d\phi}/dt$ Average rate of change of flux
e Charge of an electron
e Instantaneous voltage magnitude
e_{a-b} Voltage across points a-b
e_{ac} Supply voltage
e_d Instantaneous voltage across pickup winding
e_{fr} Voltage across N_G in absence of backfiring
e_L Instantaneous load voltage
e_{NG} Instantaneous voltage across gate winding
e_r Instantaneous voltage of reset source
e_{REC} Instantaneous rectifier voltage
e_{RS} Instantaneous voltage across R_S
e_s Instantaneous source voltage
e_S Instantaneous signal voltage
e_1 Voltage across winding N_1

e_2	Voltage across winding N_2
exp	Exponent of ϵ
f	Frequency in cps
$f(t)$	Time function
i_e	Excitation current
i_L	Instantaneous load current
i_m	Magnetizing current component of primary current
i_{mG}	Magnetizing current of gate winding
i_S	Instantaneous signal current
$\bar{\imath}_S$	Average signal current during flux reset
i_1	Current in one-half of load circuit
i_1	P/N_1 for hypothetical loop
i_1	Load-current component of primary current
i_1	Primary current
i_L	Current in one-half of load circuit
i_2	Secondary current
i_2	P/N_2 for hypothetical loop
j	Complex operator
k	Slope of B-H loop
k	Coefficient of coupling
k	Boltzmann constant
k	Amplification constant
l	Length
mmf	Magnetomotive force
mmf_0	Magnetomotive force for a given core derived from H_0
p	Magnetomotive force of hypothetical rectangular loop
s	Complex frequency variable
(s)	Denotes frequency function
t	Time
(t)	Denotes time function
$\Phi(s)$	Frequency-dependent portion of $G(s)$
α	Threshold mmf
α	Firing angle
α	Angle at which flux change starts
α	Defined constant
β	Magnetomotive force for saturation
β	Angle at which flux change ends
β	Firing angle
β'	Firing angle
γ	Angle at which flux change starts
γ	Quiescent firing angle
δ	Angle at which flux change ends
ΔB_1	Standard flux change for H_1
ΔB_2	Standard flux change for H_2
ΔE_L	Change in average load voltage
$\Delta E_{L(n)}$	Total load voltage change through the nth half-cycle
ΔH	$H_2 - H_1$
Δmmf	Incremental mmf for a given core derived from ΔH
$\Delta\theta$	Phase difference
$\Delta\phi$	Change in flux
ϵ	Base of Napierian logarithms
θ	Curie temperature
μ	Permeability
ϕ	Flux
ϕ_i	Initial flux state or level
ϕ_m	Saturation flux
ϕ_{sat}	Saturation flux
Ψ	Phase angle
ω	Angular frequency
ω_G	Gating frequency

Contents

1

Fundamental Concepts

Magnetic amplifiers differ from most other electrical components in one principal respect. In achieving optimum operation of a magnetic amplifier, many nonlinearities must be emphasized and utilized rather than minimized.[1] This emphasis on nonlinear operation is very real and must be recognized before an intimate understanding of magnetic-amplifier operation can be achieved. If the essential nonlinearities are admitted, magnetic amplifiers reveal themselves to be reasonable devices obeying the same basic laws as any other electromagnetic-circuit component. This chapter, therefore, will first illustrate the pitfalls associated with a carry-over of linear concepts to a nonlinear field and will then lay a groundwork of basic assumptions on which the following chapters will build. To the reader who has become thoroughly accustomed to using the results of derivations based on the assumption of component linearity, the return to basic relationships and the casting aside of already mastered linear techniques may be somewhat upsetting. However, the rewarding results should be a renewed appreciation of the basic relationships which apply to both linear and nonlinear circuit theory as well as a firmer foundation for an understanding of self-saturating magnetic amplifiers.

1-1. NONLINEAR PHENOMENA

Many brief, "simplified" descriptions of the operation of magnetic amplifiers exist in the literature, or are invented to convey a limited understanding of magnetic amplifiers in a two-minute talk. These thumbnail descriptions often take a form similar to "the control of an a-c impedance in series with a load." While this is probably as adequate a one-sentence description as can be formulated, its implications frequently confuse a beginner in the field when he tries to learn more about the mechanics of magnetic-amplifier operation. To most electrical engineers, well-versed in linear transformer theory, the operation of an iron-cored reactor can be adequately represented by a vector diagram in which current and voltage are nearly in quadrature.[2] Any such attempt to represent a magnetic amplifier by a vector diagram results in a false impression of its true behavior. If one represents a magnetic amplifier as a controlled impedance, it would seem logical to visualize it as a controlled inductance. Therefore, when the "inductive reactance" is large compared to the load resistance, the current should be largely out of phase with applied voltage, and when the "inductive reactance" is small, current should be largely in phase with applied voltage. *This concept is totally inapplicable.* It is discussed here because it is encountered time

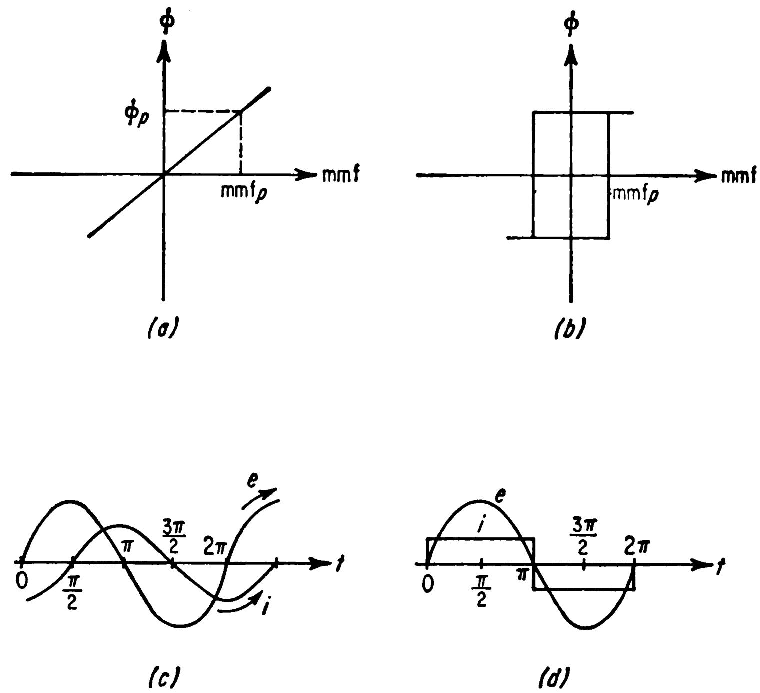

FIG. 1-1. Comparison of magnetic and circuital characteristics of idealized linear and nonlinear core materials.

and time again when electrical engineers with diverse specialties meet to discuss magnetic amplifiers. It arises from an extension of the behavior of nearly linear reactors to extremely nonlinear reactors.

To illustrate some of the difference between linear and nonlinear reactors, a comparison is made in Fig. 1-1 between the idealized flux-magnetomotive force characteristics of two types of core materials and between the voltage-current relationships when these materials are used in reactors. Figure 1-1*a* presents the idealized flux-magnetomotive force characteristic of a linear material while Fig. 1-1*b* presents a material displaying saturation, hysteresis, and zero energy storage. The voltage-current relationships existing at the terminals of a resistanceless winding on a core of each of these materials when a sinusoidal voltage source is connected across the terminals are shown in Fig. 1-1*c* and *d* for the linear and nonlinear material, respectively. It is assumed in this instance that the magnitude and frequency of the applied voltage will not result in saturation of the nonlinear material. Obviously, any statement concerning the magnitude and phase of the current in the case represented by Fig. 1-1*d* must be approached with caution. Since the phenomena involved in the operation of such a circuit include a change of flux with respect to time, it would seem that the term inductance should be applicable. However, any concepts associated with a linear inductance such as linear resonance with a capacitor must be abandoned. The nonlinear phenomenon known as ferroresonance may be observed.[3] The present discussion is introduced only to emphasize the basic point that when some nonlinearity of a device is the fundamental characteristic governing operation, no useful analysis can be made by assuming this characteristic to be linear in order to make the mathematics tractable. This is not to imply that nonlinearities may *never* be linearized—only that essential nonlinearities may not.

The principal nonlinearity introduced by the core material is seen to exist in the hysteresis observed in the relationship between flux ϕ and magnetomotive force. To review the origin of hysteretic characteristics, a flux-mmf characteristic as shown in Fig. 1-1*b* will be discussed very briefly. If it is assumed that a core of such a ferromagnetic material is initially unmagnetized, the flux is at zero with zero applied field. If a sufficiently small positive magnetomotive force is applied, no flux change will occur because, as will be discussed in greater detail in Chap. 2, the domain walls which determine the flux state of the material will not move if the applied mmf is sufficiently small. As the mmf is increased very slowly, a value of mmf will be reached at which, for this highly idealized material, flux begins to change. With no further increase in mmf, flux will continue changing in this idealized material until positive saturation is reached. This flux change required a change of time, but did not require an increase in mmf. When a sufficiently long period of time has elapsed, the material reaches saturation, and a further increase in mmf has no effect on the flux state. All of the energy supplied to change flux from zero to positive saturation was dissipated in this idealized material by the irreversible movement of the domain walls. None of the energy was stored in a reversible process. Therefore, upon decrease of the mmf to zero, no flux change will occur, since no energy is available to move the domain walls. The flux remains at its remanent state (positive saturation in this idealized material). If the mmf is reversed, a minimum negative magnetomotive force must be applied to start a flux change in the negative direction. Again, once flux starts to change, it continues changing with no change in mmf until negative saturation is reached. Application of a positive mmf of sufficient magnitude starts flux toward positive saturation again and the material is now in a cyclic state. It is seen that the material has two values of flux, positive and negative saturation, for any value of mmf less than the critical value which initiates flux change. The "lagging behind" of flux as mmf is returned to zero from its critical value gives rise to the term "hysteresis loop" to describe the phenomenon.

1-2. APPLICABLE ELECTROMAGNETIC EQUATIONS

In discussing the operation of magnetic-amplifier circuits, it is often convenient, because of the extreme nonlinearities involved, to break down the operation of a circuit into successive time intervals. The dependent variables are assumed linear with respect to the significant independent parameters throughout any one interval of time. The slopes of the variables may, however, have different values, including zero or infinity, in different intervals. This method is commonly described as piecewise linear analysis.[4] Wherever this method is used in the following chapters, the transition from one time interval to the next will be marked by the effective application or removal of some energy source to or from some circuital component.

Kirchhoff's Laws. During any particular time interval under discussion, the general form of Kirchhoff's laws will apply. That is, around any closed circuit, the summation of instantaneous voltages is zero and the summation of instantaneous currents into any junction is zero. Once again, these are the basic laws—any linear concepts previously derived from application of these laws to linear components in elementary circuit courses must be reexamined before they are applied to magnetic amplifiers.

Faraday's Law. Throughout the following chapters Faraday's law of electromagnetic induction will be regarded as a fundamental postulate. In addition to using the familiar form of the mathematical expression of this law,

$$e = N \frac{d\phi}{dt} \tag{1-1}$$

it often will be convenient to refer to it in its equivalent integral form

$$\Delta\phi = \frac{1}{N} \int_{t_1}^{t_2} e \, dt \tag{1-2}$$

In this latter form a flux change is shown to be equivalent to a voltage-time product or a volt-second area. Thus, when N (the number of turns of a winding on a core) is known, an expression is available which relates the flux change in a core to the corresponding time integral of the voltage appearing at the terminals of an open-circuited winding.

Ampère's Law. Another important concept in considering magnetic amplifiers is some form of Ampère's law. This has been stated variously as

$$\oint H\,dl = I \tag{1-3}$$

and

$$\oint B\,dl = \mu I \tag{1-4}$$

To make Eq. (1-4) equivalent to the fundamental relationship of Eq. (1-3) requires that

$$B = \mu H \tag{1-5}$$

In considering ferromagnetic materials, it is seen that μ is extremely nonlinear with respect to H, assuming values from as high as 4×10^5 to as low as 4.

The significance of Eq. (1-3) is that it demonstrates that a magnetic field cannot exist without current flow. In the most general case, this current need be only that due to electron spin. However, to cause an appreciable flux change in a ferromagnetic material requires, in practice, the flow of circuital current.[5]

1-3. TRANSFORMER REVIEW

Many points in the operation of self-saturating magnetic amplifiers can best be explained using transformer theory. Therefore, a brief review of the more important concepts in this field is included at this point for emphasis.

The Idealized Transformer. An ideal transformer can be imagined by postulating that one has a toroidal core of lossless core material of infinite permeability, that the windings have zero resistance, that the displacement currents due to the capacitances of the windings are zero, and either that the cross-sectional area of the core is infinite or that the maximum flux density of the core material is infinite. This last restriction, of course, need not be met as long as the material is operated in the region in which the condition of infinite permeability is fulfilled. Consider, for instance, the conditions implied by Fig. 1-2. Figure 1-2*a* is the circuit to be considered and Fig. 1-2*b* represents the flux-mmf characteristic of an idealized material which exhibits saturation at some level of flux. It will be assumed that the voltage of the source e_s is sinusoidal with a frequency and a finite magnitude that never result in a core flux as great as ϕ_m. If, for the moment, the load resistance R_L is assumed to be infinite, the following relationships can be established. First, since

R_L is infinite, the secondary current i_2 must be zero. Second, since i_2 is zero, i_1 must be zero. If i_1 were other than zero with i_2 zero, a net mmf would exist which would violate the flux-mmf relationship enforced by the characteristic of Fig. 1-2*b*. Third, the voltage across terminals 3 and 4 will be equal to e_sN_2/N_1. Since no provision has been made for losses

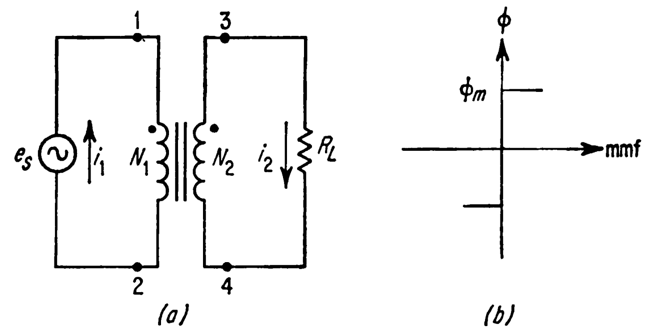

FIG. 1-2. Idealized transformer circuit. (*a*) Circuit diagram; (*b*) flux-mmf characteristic.

to occur in the primary circuit, all of the voltage e_s appears across terminals 1 and 2 and the flux change in the core during one half-cycle of e_s will be

$$\Delta\phi = \frac{1}{\omega N_1} \int_{\omega t=0}^{\omega t=\pi} e_s \, d\omega t \tag{1-6}$$

If it is assumed that $e_s = E_{1m} \sin \omega t$

$$\Delta\phi = \frac{E_{1m}}{\omega N_1} \int_{\omega t=0}^{\omega t=\pi} \sin \omega t \, d\omega t \tag{1-7}$$

With a core material of infinite permeability, all of the flux is constrained to be within the core and there can be no leakage flux which links one winding without linking the other. As a result, the flux change due to e_s causes the appearance of voltage at terminals 3 and 4 and

$$\Delta\phi = \frac{E_{2m}}{\omega N_2} \int_{\omega t=0}^{\omega t=\pi} \sin \omega t \, d\omega t \tag{1-8}$$

Equating the right-hand sides of Eqs. (1-7) and (1-8) and simplifying, we obtain

$$E_{2m} = \frac{E_{1m}N_2}{N_1} \tag{1-9}$$

If R_L is now assumed to be less than infinity, some current i_2 will flow,

$$i_2 = \frac{e^2}{R_L} \tag{1-10}$$

As long as some voltage e_2 is present across terminals 3 and 4, flux must be changing in the core. If flux is changing, there can be no mmf (because of the assumed flux-mmf relationship) and, therefore,

$$i_1N_1 = i_2N_2 \tag{1-11}$$

Since a lossless case has been assumed, the voltage relationships are the same as they were for the case with R_L infinite.

The Nonideal Transformer. In going from the ideal to the nonideal transformer, practicalities will be introduced consecutively. The effect of losses in the core material will be considered first. These losses can be divided into two classes—so-called d-c losses which do not change materially with impressed frequency (as, for instance, hysteresis loss in joules/cycle) and frequency-sensitive losses (as, for instance, eddy-current loss). Regardless of how these losses are distributed, an operating flux-mmf characteristic can be obtained at the frequency, applied voltage waveshape, and external circuit impedances of interest. The applied voltage referred to is the voltage appearing across the terminals of the transformer, not the voltage at the source terminals. Since this book is concerned for the most part with magnetic amplifiers, only core materials suitable for magnetic amplifiers will be considered.

It must be recognized that an idealized material such as was represented by the characteristic of Fig. 1-2*b* can never be achieved since, in a practical material, an infinite permeability cannot be attained, and since all practical materials display the phenomenon of hysteresis discussed in the previous section.

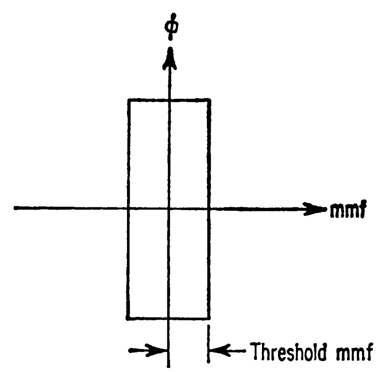

FIG. 1-3. Flux-mmf characteristic exhibiting hysteresis.

To illustrate the effect of core-material losses, the characteristic of Fig. 1-3 will be postulated, indicating the presence of hysteresis and showing that some mmf must be present before a flux change can occur. Once this "threshold" mmf has been established, however, the incremental permeability is assumed to be infinite. Although the assumption of infinite incremental permeability is somewhat unrealistic, it may be closely approached in practical materials and the concept is very useful in the present phase of the discussion. Applying this material to the circuit of Fig. 1-2*a*, under no-load conditions (R_L is infinite), the voltage relationships remain unchanged from those derived using the previous material characteristics of Fig. 1-2*b*. However, a primary current is present in the form of a square wave of supply frequency, as shown in Fig. 1-4*a*. This current must flow because of the mmf requirements of the core material. Since there are no resistances in the primary circuit, flux must be changing in the core at all times. If flux is to change, the mmf shown in Fig. 1-3 must be present at all times. As the voltage reverses polarity, the mmf also changes polarity, but the absolute magnitude of the mmf is always constant. The resulting primary current

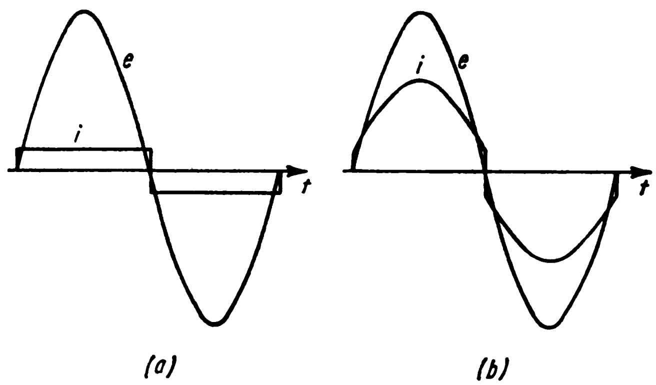

FIG. 1-4. Waveshapes resulting from use of hysteretic core material of Fig. 1-3. (*a*) Applied voltage and magnetizing current; (*b*) applied voltage and primary current under load.

with an infinite load resistance is commonly referred to as "magnetizing current."

When R_L is finite, i_2 will not be zero and will be sinusoidal as before. The primary current under these conditions will be a square wave with a sinusoidal component superimposed, as in Fig. 1-4*b*. If the operating flux-mmf characteristic is as assumed in Fig. 1-3, then the net mmf $(N_1i_1 - N_2i_2)$ must always be equal instantaneously to the value determined by Fig. 1-3. Therefore, the primary current must always consist of the basic magnetizing current plus a component due to secondary current. This component may be determined from Eq. (1-11).

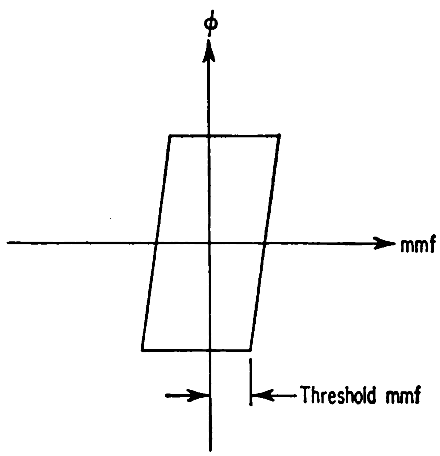

FIG. 1-5. Flux-mmf characteristic with nonvertical sides.

The significance of a loop with nonvertical sides will be considered next. The assumed operating loop will be as shown in Fig. 1-5. Again considering the circuit of Fig. 1-2*a*, the magnetizing current can be approximated now by a square wave with a cosinusoid superimposed, as in Fig. 1-6*a*. With a finite R_L, i_2 is again nonzero and sinusoidal. The total primary current is the instantaneous sum of i_2N_2/N_1 and the magnetizing current, as in Fig. 1-6*b*. The voltage relationships are no longer as straightforward as they were when a material of infinite permeability was postulated. There will be some flux which links only the turns of one winding, and not those of the other. This necessitates the introduction of the concept of coupling between the windings. With nontoroidal core configurations or inferior core material, the coupling between windings is represented by a coefficient of coupling, usually denoted as k. When toroidal cores, properly constructed of material usually employed in magnetic amplifiers, are considered, k is so near unity that the difference is neglected and leakage flux is assumed to be zero. The voltage relationships existing when core material having a characteristic similar to that shown in Fig. 1-5 is used in the core of the transformer of Fig. 1-2*a*, then, may be assumed to be the same as those

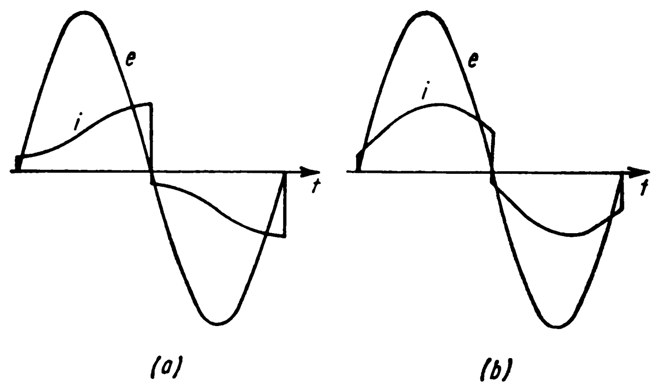

FIG. 1-6. Waveshapes resulting from use of core material of Fig. 1-5. (*a*) Applied voltage and magnetizing current; (*b*) applied voltage and primary current under load.

derived for the more idealized characteristics. It is important to note at this point that leakage flux may be neglected only when saturation does not occur (which has been assumed throughout this section).

The deviations from ideal conditions which have been considered have been only the limitations imposed by a practical core material. Before discussing circuit limitations, it may be of benefit to consider the energy relationships imposed by the core-material characteristics described up to this point. The highly idealized characteristic of Fig. 1-2*b* implies that no mmf is required to change flux. Since no current flows, no energy is exchanged between the source and the core material. The transformer neither dissipates nor stores energy, but acts simply as a means of coupling the load R_L to the source e_s.

A transformer utilizing a core material with a characteristic similar to that of Fig. 1-3 will dissipate an amount of energy which is proportional to the area enclosed by the flux-mmf characteristic. It is interesting to note that, since the magnetizing current through the primary winding always has the same instantaneous polarity as the terminal voltage, as indicated by Fig. 1-4*a*, this material stores no energy. The circuit, therefore, is totally dissipative. In contrast, a transformer using a material with the characteristic illustrated in Fig. 1-1*a* has a current-terminal voltage relationship like the one in Fig. 1-1*c* and all the energy delivered to the primary winding during the period $\pi/2$ to π is returned to the primary circuit during the period π to $3\pi/2$. With the latter material, no energy is dissipated and the circuit is purely reactive.

From the point of view of energy exchange, there is no difference in the operation of transformers using the material either of Fig. 1-3 or of Fig. 1-5. For neither material is there any energy storage, and the dissipated energy is proportional to the area enclosed by the flux-mmf characteristic.

With these points clearly in mind, the limitations of circuit components will be considered. The most serious limitation on the circuit components involved is that the resistance and reactance of any component can approach, but can never equal, zero. The circuit of Fig. 1-2*a*, therefore, must be modified to account for the inevitable losses and voltage drops.

Before introducing other circuit concepts, it may be well to consider the problem of how to designate the voltage-current relationship of iron-cored reactors of the type which has been discussed. It has been demonstrated that, since a wound toroid of a square-loop material does not store energy, the word inductance is misleading. Some authors have dubbed the voltage-current relationship "resistance" since flux change in such a device is an essentially dissipative phenomenon. The term "reactor," however, is almost universally used to describe the component consisting of a core with windings. Since "reactance" again implies energy storage, "impedance" is frequently used to label the voltage-current relationship, since an impedance can be 100 per cent dissipative. However, the essential nonlinear nature of the device must always be recognized even though the term impedance has strong linear connotations.

A reasonably complete transformer circuit is shown in Fig. 1-7*a*. Figure 1-7*b* represents its equivalent circuit with the transformer and secondary parameters replaced by equivalent impedances. In Fig. 1-7*b*, R_s represents the source resistance, and L_s the source inductance. The nonlinear magnetizing impedance is represented simply by a block. The transformation ratio N_1/N_2 is represented by a. It will be noted that, in going from Fig. 1-7*a* to Fig. 1-7*b*, the secondary impedances are multiplied by the factor a^2. The proof of the validity of this transformation is included here for the sake of the practicing engineer who may no longer be familiar with the derivation. From Fig. 1-7*a*, lumping all secondary impedance quantities into an equivalent impedance Z_s and recognizing

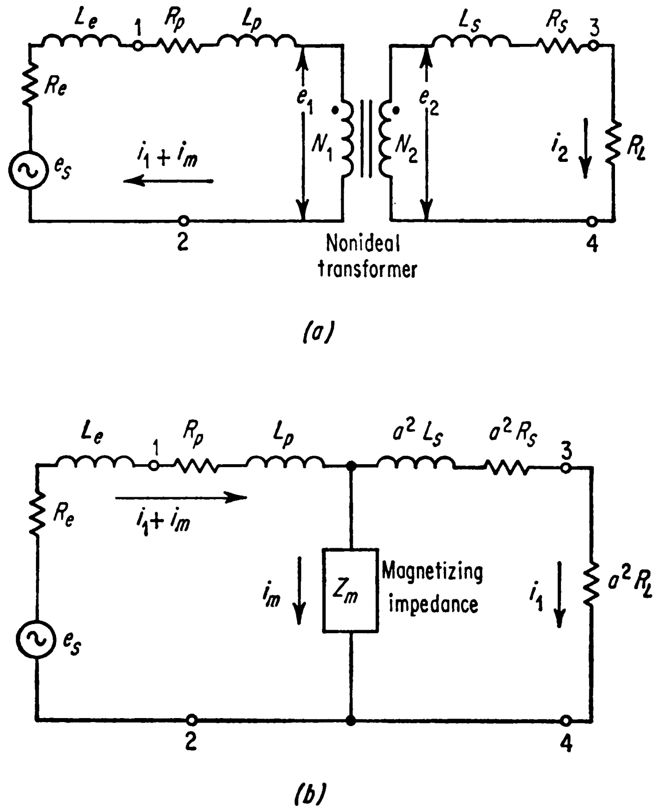

FIG. 1-7. Nonideal transformer. (a) Circuit diagram; (b) equivalent circuit.

that Z_s may be nonlinear, it is seen that

$$e_2 = i_2 Z_s \tag{1-12}$$

However, since all resistances and leakage inductances have been represented outside the transformer,

$$e_1/N_1 = d\phi/dt = e_2/N_2$$

whence

$$e_2 = e_1 N_2/N_1 \tag{1-13}$$

Also, with the primary current consisting of a magnetizing current i_m and a load component i_1, from the restriction of the flux-mmf characteristic,

$$i_2 = i_1 N_1/N_2 \tag{1-14}$$

Substituting Eqs. (1-13) and (1-14) into Eq. (1-12)

$$e_1 \frac{N_2}{N_1} = i_1 N_1 \frac{Z_s}{N_2}$$

or

$$e_1 = i_1 (N_1/N_2)^2 Z_s$$

and

$$e_1/i_1 = a^2 Z_s \tag{1-15}$$

It is important to note once again that this relationship recognizes that Z_s may be nonlinear. Also, referring to Fig. 1-7*b*, it is seen that the equivalent circuit adequately expresses the relationships derived from the original diagram.

Admittedly, the circuit of Fig. 1-7*b* is still not rigorous, since interwinding and intrawinding capacitances have been omitted as has a possible source capacitance. These additional elements are usually negligible and, where they are not, are usually difficult to define adequately. If they can be defined analytically, they may be added to the above diagram. A treatment including them is considered beyond the scope of this text. They are mentioned here simply because, in extreme designs, their effect may be noticed in practice. When these effects are encountered in magnetic-amplifier design, the physical components are redesigned to minimize capacitances. For the purposes of this text, therefore, it will

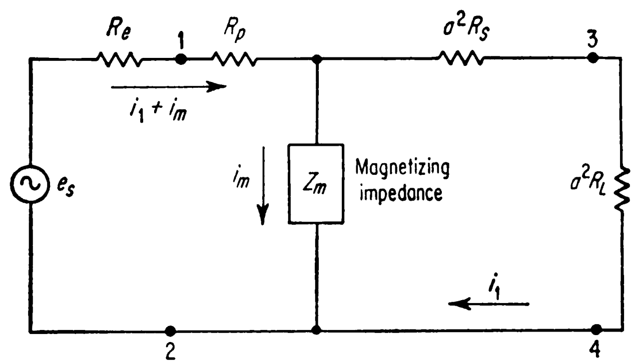

FIG. 1-8. Simplified equivalent circuit.

be assumed that the capacitances of the circuits considered are so small that the displacement currents are negligible.

Since the assumption of leakage flux prior to saturation adds a complication of considerable magnitude and since for nearly all practical cases leakage flux is negligible prior to saturation, it will be assumed that the effective permeability is sufficiently high that the leakage inductances may be neglected. With this condition imposed, the equivalent circuit of Fig. 1-7*b* reduces to that of Fig. 1-8.

If R_L is assumed infinite, i_1 is zero and the primary current is only the magnetizing current i_m. In Chap. 2 the significance of a sine-flux loop as contrasted with a sine-current loop will be discussed and the differences analyzed. For the moment it will simply be assumed that an operating characteristic similar to that of Fig. 1-5 is applicable. With this assumption made, and assuming that the resistance $(R_p + R_e)$ has a value large enough that when the magnetizing current is at its maximum value, the voltage drop across the resistance is appreciable with respect to the peak value of e_s, the instantaneous voltages around the primary circuit will be as shown in Fig. 1-9. The source voltage e_s has been assumed sinusoidal and the resistances linear.

The waveshapes of Fig. 1-9 are applicable only when steady-state conditions exist. The problem of transients in nonlinear circuits is too complex to be considered in this section and will be discussed in the appropriate sections only as necessity demands. To illustrate the piecewise linear approach which is used in this text to solve nonlinear problems, a digression will be made to explain how the waveshapes of Fig. 1-9 are obtained.

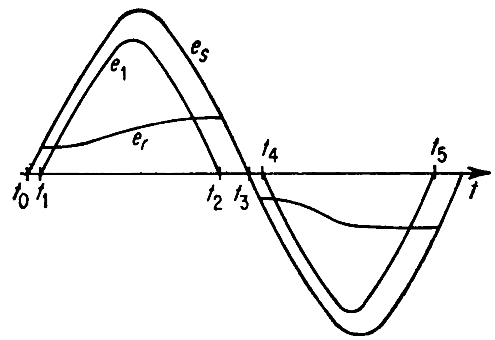

FIG. 1-9. Waveshapes existing in primary circuit with R_L infinite.

If steady-state conditions exist at the end of a negative half-cycle of supply voltage, the flux in the core must be at the maximum negative value it can attain when operating at the assumed e_s in the given circuit. Since no energy storage occurs anywhere in the circuit of Fig. 1-8, the current must go through zero when the applied voltage goes through zero. If the mmf is zero and flux is at negative maximum, the initial condition has been established with reference to the flux-mmf characteristic of Fig. 1-5.

As e_s starts a positive half-cycle, current is limited by the total resistance of the circuit and rises instant by instant with the applied voltage. From t_0 to t_1, then

$$e_s = i_m(R_e + R_p) \tag{1-16}$$

When the current amplitude has risen to the value required for the threshold mmf of the core material, a discontinuity occurs. From the start of the positive half-cycle of supply voltage (designated as t_0 in Fig. 1-9) until the threshold mmf value of current is reached at t_1, there can be no flux change in the core and, therefore, e_1, the voltage across the primary magnetizing impedance, has been zero. At t_1, flux starts to change in the core, and from t_1 to t_2

$$e_s = i_m(R_e + R_p) + N_1 \frac{d\phi}{dt}$$

But since, from Fig. 1-5, $\phi = ki_m$ from t_1 to t_2

$$e_s = i_m(R_e + R_p) + kN_1 \frac{di_m}{dt} \tag{1-17}$$

At time t_2, the voltage drop due to the magnetizing current through $(R_e + R_p)$ is equal to e_s once again. Then from t_2 to t_4, Eq. (1-16) is again applicable. At time t_4 in the negative half-cycle, Eq. (1-17) is again valid until time t_5, etc. Thus, the waveforms of Fig. 1-9 are obtained.

If R_L is finite, the secondary current reflected into the primary circuit causes an additional voltage drop across the primary-circuit resistance, lowering and further distorting the voltage across the magnetizing impedance. The existence of the secondary resistance results in a loss in the secondary circuit and the voltage appearing across the load is compared in Fig. 1-10 with the sinusoidal voltage which would be obtained in the idealized case.

Many of the points which have been discussed will be expanded in later sections. If the student has a grasp of the operation of transformers at the level discussed above, little difficulty should be encountered in understanding those portions of the mechanics of operation of magnetic amplifiers which follow from a consideration of the voltage-current relationships for individual reactors. It should now be obvious that when transformers containing square-loop core materials are considered, a conventional vector diagram approach cannot be used. In the development of the vector diagram, it is first assumed that a sinusoidal voltage is applied to the transformer terminals, resulting in a sinusoidal variation of flux with time. The sinusoidal flux is shown by the flux-mmf relationship of Fig. 1-1a to lead the sinusoidal self-induced voltage by 90°, and is assumed in phase with the magnetizing current. It has been seen that with square-loop core materials the magnetizing current goes through zero at the same time as the applied voltage. The discrepancy arises because the conventional approach assumes that the magnetizing impedance can be adequately represented by a linear resistance and a linear inductance, thus preserving sinusoidal waveshapes throughout. While this is probably an adequate assumption for low-grade transformer steels employed in configurations introducing appreciable air gaps, it is no longer tenable when applied to toroidal cores of a square-loop material.

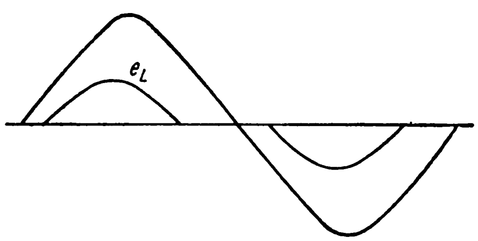

FIG. 1-10. Load voltage compared with sinusoid.

1-4. INTRODUCTION TO AMPLIFIERS

In the previous section it was seen that by choosing proper values for the transformation ratio N_1/N_2, it is possible to obtain a higher voltage at the load than exists at the source. Alternatively, it is possible to have a larger current flowing through the load than flows through the source. In a general sense, then, it might be said that a transformer exhibits current or voltage gain. It is not, however, an amplifier, since the power supplied by the source is equal to or greater than the power delivered to the load.

The American Standard Definitions of Electrical Terms defines an amplifier as "a device for increasing the power associated with a phenomenon without appreciably altering its quality, through control by the amplifier input of a larger amount of power supplied by a local source to the amplifier output."[6] This is, perhaps, a restrictive definition, but it will be used throughout this text. At times it seems more convenient in the literature to speak loosely of demodulators, impedance matching devices, and similar assemblies of hardware as amplifiers, provided they have a local source of energy. These latter categories may or may not supply larger amounts of power to the load than are available at the input terminals. By definition, then, these devices are not amplifiers unless the output power exceeds the input power.

The power amplification which is a necessary condition for an amplifier may be achieved through either voltage or current amplification or both. For instance, an amplifier with an input of 1 volt across 100,000 ohms may have an output of 0.1 volt across 10 ohms. This represents a power amplification of 100, a current amplification of 1,000, and a voltage amplification of 0.1. Had the output been 10 volts across 100,000 ohms, the power amplification would have been the same but the current and voltage amplifications would each have been 10.

In this treatment, the amplification factor has been discussed as though it were a constant of the amplifier. This is far from being true, since the amplification may vary with many parameters, particularly input frequency. In fact, one of the criteria for an amplifier is its band width, or the frequency range over which the amplification is relatively constant.

It will be recognized that many types of devices display control by the amplifier input of a larger amount of power supplied by a local source to the amplifier output. Among the components that would satisfy such a definition are grid-controlled vacuum and gas-filled tubes, magnetic and dielectric amplifiers, transistors, rotating amplifiers such as the Rototrol, and even separately excited generators.

The grid-controlled high-vacuum tube probably comes closest to satisfying the restriction that an amplifier should increase "the power associated with a phenomenon without appreciably altering its quality . . . ." Even with high-vacuum tubes, however, it is recognized that restrictions must be placed on certain parameters to achieve optimum amplification. Depending on the application, for instance, vacuum-tube amplifiers are classified as operating class A, AB, B, or C. These designations are based upon the amount of distortion of the input signal which occurs in the output.

In addition to the distortion, which is caused by nonlinearities and by noise, a certain phase difference exists between the output and the input. This phase difference is often spoken of as the phase shift across the amplifier. In communication equipment, this phase shift can often be ignored, since the desired objective is to reproduce, at a higher power level, the intelligence contained in the signal without concern for the time correspondence between input and output. It is sufficient in these cases to avoid unwanted coupling between input and output circuits to preserve stability. In automatic feedback control systems, however, the phase shift across an amplifier can be a parameter of major importance. The magnitude of this phenomenon is a function of signal frequency as well as of the constants of the amplifier.

It is seen, then, that the output of an amplifier is compared to the input with respect to magnitude and phase shift. The comparison between output and input most often made is the ratio of the two, expressed as the ratio of output to input. This is defined as the transfer function of the amplifier. The most common method of expressing the transfer function is to transform the quantities involved into the frequency domain by means of the Laplace transform.[7] Standard nomenclature for the transfer function so expressed is $G(s)$. When used in this manner, $G(s)$ may be further reduced to an amplification constant and a frequency-dependent term, $K\Phi(s)$. In some treatments, $G(s)$ is defined as including only the frequency-dependent portion. This practice, however, seems to be losing favor to the inclusion of the amplification constant in the expression. The latter method will be used in this book.

REFERENCES

1. Finzi, L. A.: Introducing Young Engineers to the Appreciation of Magnetic Amplifier Problems, *Trans. AIEE*, vol. 77, part I, pp. 119–126, 1958.
2. Lee, Reuben: "Electronic Transformers and Circuits," 2d ed., John Wiley & Sons, Inc., New York, 1955.
3. Odessey, P. H., and E. Weber: Critical Conditions in Ferroresonance, *Trans. AIEE*, vol. 57, p. 444, 1938.
4. Hochrainer, A.: The Calculation of Non-linear Networks with the Aid of Line-segment Characteristics, *Elektrotech. u. Maschinenbau*, vol. 70, pp. 376–386, Sept. 1, 1953 (in German).
5. Skilling, H. H.: "Fundamentals of Electric Waves," 2d ed., John Wiley & Sons, Inc., New York, 1948.
6. American Standards Association: "American Standard Definitions of Electrical Terms," p. 45, AIEE, New York, 1941.
7. Goldman, Stanford: "Transformation Calculus and Electrical Transients," Prentice-Hall, Inc., Englewood Cliffs, N.J., 1949.

2

Basic Material Properties

Every technological field suffers from restrictions imposed by the limitations of the materials which can be processed for use in the field. Self-saturating magnetic amplifiers are peculiarly restricted by the characteristics of the materials for two major components, the cores of the reactors and the rectifiers used to provide self-saturation. In this chapter the properties of materials commonly used for these components will be discussed. The treatment of the theories concerning the cause of the properties of interest will necessarily be brief, since a complete coverage is beyond the scope of this text. For a more detailed description, the attention of the reader is directed to the applicable items in the references at the end of the chapter.

2-1. FERROMAGNETIC MATERIALS

A reasonably complete understanding of ferromagnetism is not necessary for a rough acquaintance with magnetic amplifiers, but the subtler points of magnetic-amplifier operation require the student to have at least some knowledge of the broader aspects of domain theory. The sections immediately following will present the rudiments of modern ferromagnetic theory and will show how, at least qualitatively, the flux-mmf characteristics are related to domain phenomena.

2-2. DOMAIN STRUCTURE

A moving charge creates a magnetic field. Therefore, an electron orbiting about an atomic nucleus causes a magnetic field. For an atom of reasonably high atomic number, the several electrons, all moving in the orbits prescribed by quantum theory, will give rise to individual orbital magnetic moments which, in the aggregate, tend to cancel each other. In addition to the orbital magnetic moment, a moment exists due to the spin of each electron. Since, by quantum theory, the magnetic moment due to spin can be only in one or the other of two directions, these moments also tend to cancel each other in the aggregate.[1]

In many elements, the interaction between atoms in the solid state is the result of so-called "exchange forces" which provide the covalent binding energy required to hold the solid together. In most elements, these exchange forces align the atoms of the molecule in a manner which causes cancellation of the net spin magnetic moments of the individual atoms. This is apparently not invariably true, however. There are currently three hypotheses advanced to explain the cases where a large net spin magnetic moment does exist. While these explanations are of only peripheral interest in the design of magnetic amplifiers, a brief discussion of the three schools will be given for the student who likes a "feel" for the origin of the phenomena to be discussed later.

The atomic orbital approach adopted by one school holds that for a small group of elements, including principally iron, cobalt, nickel, and a few rare earths and alloys of these elements, the interaction between the atomic separation distances in a crystal and the total energy ranges of the $3d$ or $4f$ electron energy bands is such that the exchange forces cause a parallel alignment of magnetic spin moments for adjacent atoms. This is considered, by this school, to be the basis of ferromagnetism.[2]

A molecular orbital, or collective electron approach, also exists, wherein the interpretation of ferromagnetism is based on the overriding of the negative exchange energy by the positive contribution due to the statistical ordering effect of adjacent parallel spins. This again holds true only for certain atomic separation distances, energy band ranges, etc.[3,4]

Another school has recently proposed a third explanation based on spin-orbit interactions between the $3d$ or $4f$ and the valence electrons.[5]

An understanding of the subtleties of the above controversial theories concerning the origin of ferromagnetism is not necessary to obtain a grasp of the fundamentals of domain theory and its influence on the dynamics of flux-mmf characteristics. It is probably sufficient to recognize that the alignment of the spin magnetic moments results in small domains or regions within a given crystal which are spontaneously magnetized to saturation in a given direction. This leads, then, to a discussion of the interplay of various energy forms as they contribute to the size, shape, and dynamic properties of these spontaneously magnetized regions or domains.[6]

The size and shape of these spontaneously magnetized small domains are functions of the various energy forms which will assume values to make the total energy of the system a minimum. It is well known, for instance, that a ferromagnetic material may be lengthened or shortened by placing it in a suitable magnetic field. This magnetostrictive effect is particularly noticeable in the case of nickel. The change in length has associated with it a certain magnetostrictive energy. In addition to the magnetostrictive energy, another energy form exists which influences the size and shape of domains. This magnetostatic energy causes formation of domains of closure which tend to minimize the total energy required in a given crystal.

Consider, for instance, a unit volume within a single crystal, as illustrated in Fig. 2-1. If the uncompensated magnetic moments of the electrons are all aligned to make a positive contribution to the field as shown

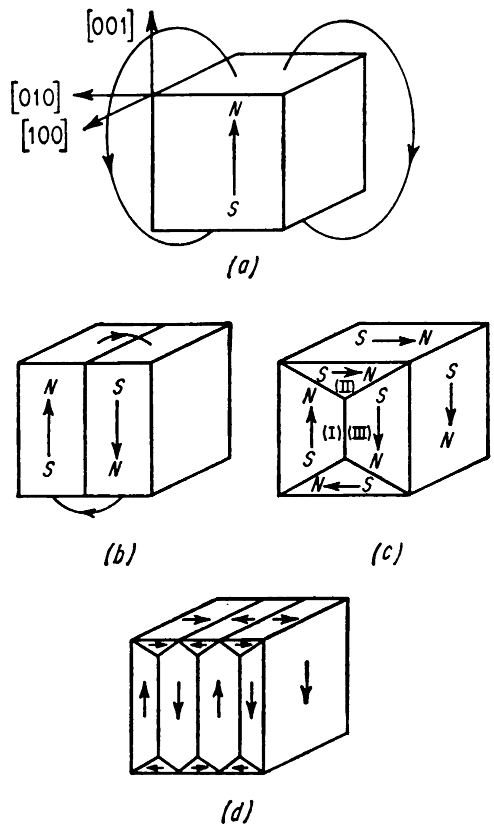

Fig. 2-1. Possible domain configurations within a volume of a single crystal. (*a*) Single domain; (*b*) introduction of a domain wall; (*c*) domains of closure; (*d*) minimum free-energy configuration.

by the north-south arrow of Fig. 2-1*a*, the entire volume is spontaneously magnetized in the direction shown and, if the volume is isolated, a large amount of magnetostatic energy is required to maintain the field in the resulting air gap. A configuration requiring less magnetostatic energy is shown in Fig. 2-1*b*. For this configuration the length of the air gap has been considerably reduced and, consequently, the energy required to maintain the air-gap field has been similarly reduced.

Still another type of energy has been introduced in Fig. 2-1*b* by the formation of a line of demarcation between the two domains shown.

Because the exchange forces between atoms tend to force parallel alignment of the spin magnetic moments, a large amount of energy would be required to maintain two contiguous atoms in antiparallel alignment. Much less energy is required if the antiparallel arrangement takes place gradually over a region many atoms wide, so that the moment of each atom is displaced a small amount from the moment of the atom nearest it. This minimizing of the total energy required to maintain a given configuration gives rise to walls between domains known variously as domain walls or Bloch walls (after Felix Bloch, who first investigated this phenomenon).[7] Thus the magnetostatic energy has been reduced by changing from the configuration of Fig. 2-1*a* to that of Fig. 2-1*b* and a new type of energy introduced, domain-wall energy. The total energy required to maintain the configuration now has three components—magnetostrictive, magnetostatic, and domain-wall energies.

The magnetostatic energy can be further reduced by introducing domains of closure with boundaries which make equal angles with the fields of the two domains, as shown in Fig. 2-1*c*. This configuration, however, would result in large stresses within the closure domains due to magnetostrictive effects, raising the amount of magnetostrictive energy required to maintain the configuration. A more typical configuration resulting in minimum total energy would be as shown in Fig. 2-1*d*. Here, by the formation of more domains, the total volume of the Bloch walls has been increased, and, therefore, the wall energy has been increased, but the magnetostrictive energy has been reduced.

It will be noted that the domain configuration of the unit volume illustrated in Fig. 2-1*d* produces zero external field. The spontaneous magnetization of each domain is not apparent unless the specimen is treated in a manner introduced by Bitter and extended by Williams and other workers in whose treatment colloidal particles of ferromagnetic material collect at the domain boundaries, revealing the pattern.[8]

A form of energy associated with domain formation which has not yet been discussed is a function of crystalline structure and is known as anisotropy energy. There are many different forms of crystalline structure, of which only three are of primary interest in a discussion of ferromagnetics. These three are the body-centered-cubic (iron), the face-centered-cubic (nickel), and the hexagonal-close-packed (cobalt) structures. In discussing anisotropy energy it will be necessary to consider briefly the fundamentals of crystalline structure. An understanding of at least the basic terminology of crystals is quite essential to an understanding of ferromagnetic materials, since references to the subject occur frequently in literature on magnetic materials cloaked in esoteric phrases such as "grain-oriented," "domain-oriented," "easy direction of magnetization," and so forth.

2-3. CRYSTALLINE STRUCTURE

A crystal is simply an orderly arranged spatial pattern or lattice of atoms. Within a single crystal, the pattern repeats itself regularly in three dimensions. A diagram of a portion of the lattice of crystalline iron is shown in Fig. 2-2. Appropriate planes have been passed through the crystal, resulting in "faces." One face has been shaded to aid in visualizing the structure. It will be observed that six unit crystals have been shown, each consisting of eight atoms at corner locations (shown black) and one atom at the center (shown white). No attempt has been made to relate the size of the dots and the distances between them to the actual size of the atom and atomic spacing. The positions shown represent the relative positions of the atomic centers; the outermost orbital electrons of each atom are shared by neighboring atoms.

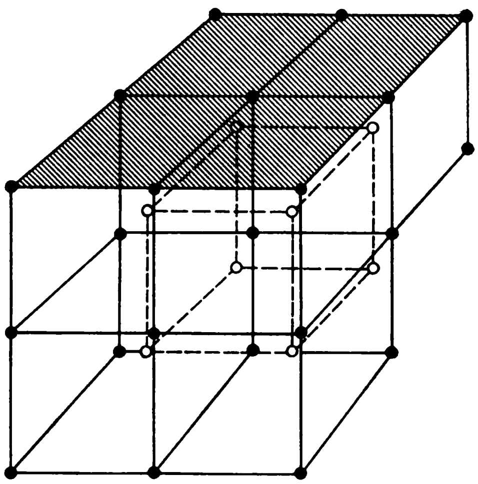

FIG. 2-2. Diagrammatic representation of a portion of an iron crystal.

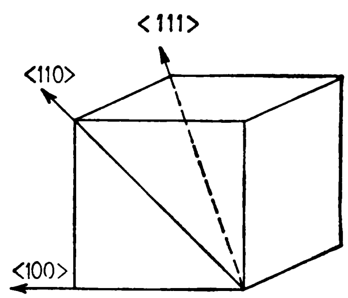

FIG. 2-3. The three principal crystallographic directions for a cubic crystal.

In Fig. 2-3, the three principal crystallographic directions are shown for a cubic crystal. These directions are identified by their Miller indices. The [100] direction is along a cube edge in the x direction and, due to the symmetry of the structure, any cube edge may be referred to as a $<100>$ direction, although it might more properly be called a [001], [010], etc. The [110] direction is a face diagonal in the xy plane, while the [111] direction is a long, or body, diagonal.[9] The crystalline anisotropy energy is a measure of the difference between external fields which must be applied in these various directions to magnetize the material to saturation.

The materials with which one usually works are of the polycrystalline type. Each crystal of such an aggregate, probably measuring tens or hundreds of millions of atoms in each direction, may normally be composed (assuming the specimen has never been subjected to an external magnetic field) of numerous domains in the general fashion shown in

Fig. 2-1*d*. Each such domain includes tens or hundreds of thousands of atoms in any direction. It is possible in the laboratory to grow a sizable single-crystal specimen. By suitable techniques it is possible to determine the crystallographic directions of the single-crystal specimen. This specimen may then be considered as a block which, due to its homogeneous structure, has the same crystallographic properties as a unit cell.

A technique for determining the energy of anisotropy is to cut, from a single crystal, picture-frame specimens as shown in Fig. 2-4. A separate specimen is cut to contain each principal crystallographic direction. Such a specimen constitutes a closed magnetic path about the particular crystallographic direction to which it is cut. By suitable techniques, the relationship between the intrinsic induction and field strength can be determined experimentally for such a picture-frame sample. Typical results for the three principal directions are shown in Fig. 2-5 for a specimen of silicon-iron. The difference in energy between that required to

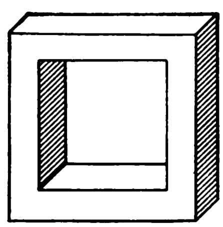

Fig. 2-4. Typical picture-frame configuration.

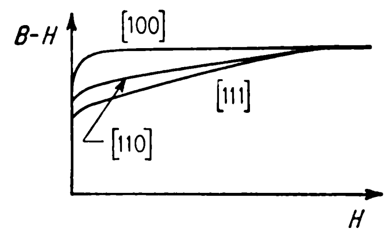

Fig. 2-5. Magnetizing characteristics in three crystallographic directions for silicon-iron.

magnetize the specimen in the <110> or <111> direction and that required in the <100> direction is the anisotropy energy. For the example of silicon-iron material, the <100> direction is the direction of easy magnetization.

To minimize losses, it is desirable in practice to magnetize many ferromagnetic materials used in components of an electrical circuit in the easy direction of magnetization. Since, as was stated before, the materials with which one usually works are polycrystalline, it is desirable that the individual crystals, or grains, be aligned or oriented so that an easy direction of magnetization of the majority of grains will be parallel to the applied field. In general, attaining this preferred orientation is a complex function of chemical composition, rolling technique, and annealing treatment. Metallurgists have evolved the techniques which result in grain orientation in a predictable direction with respect to the rolled sheet. Treatment of a polycrystalline specimen to reveal the domain structure reveals that domain walls extend across grain boundaries in patterns that differ only slightly from the patterns obtained from single-crystal specimens.

2-4. APPLICATION OF AN EXTERNAL FIELD

The next step is to consider the behavior of domains in the presence of an external field. A typical single-crystal specimen in an unmagnetized state will have the magnetization vectors of its numerous domains randomly distributed in either direction along each of the three easy directions of magnetization, as shown in a highly symbolic manner in Fig. 2-6. If an external field is applied, the magnetization vectors of some of the domains will be found to be aligned more nearly parallel to the applied field direction than those of others at the time of field application. These preferred domains will grow in volume at the expense of those less favorably oriented until the entire specimen is essentially a single domain. Upon further increase of the field, the magnetization vector of this domain is rotated into concurrence with the field direction and the specimen is now saturated. This process is frequently illustrated in a manner similar to that shown in Fig. 2-7. Bozorth implies that,

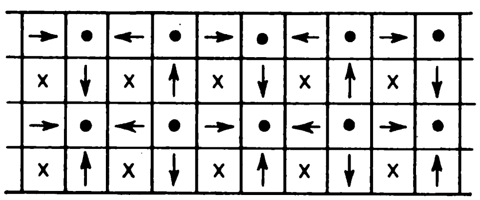

FIG. 2-6. Symbolic representation of the domain configuration of an unmagnetized specimen.

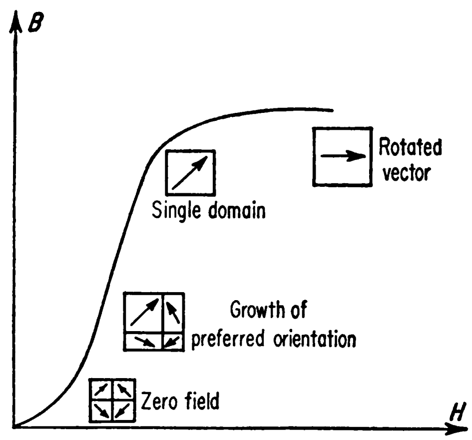

FIG. 2-7. Magnetization processes in an initially unmagnetized specimen.

using an initially demagnetized specimen, the application of a very low field strength results in a reversible wall movement associated with the movement of 90° walls (walls which separate domains with magnetization vectors separated by 90° rather than 180°).[10] In Fig. 2-1*c* the wall between domains (I) and (II) is called a 90° wall while the wall between domains (I) and (III) is a 180° wall. Higher field strengths result in irreversible wall movements. Rotation of the direction of magnetization is a reversible phenomenon. When the large external field is removed, therefore, the flux change due to irreversible domain wall motion is not reversed, and the sample will be at its remanent induction at zero field.

2-5. MECHANISM OF MAGNETIZATION

Magnetizing an initially unmagnetized specimen to saturation involves phenomena which are seldom of primary interest in a study of magnetic amplifiers. As will be seen in later chapters, the major problems associated with magnetic amplifiers involve changing flux in a core which is at its remanent state. If a sufficiently large alternating field is applied to a ferromagnetic material, the magnetization vectors will be aligned parallel to the field first in one direction and then in a direction 180° from the initial direction. When the applied field is sufficiently large and the alternations occur at a sufficiently slow rate, the domain walls will be swept out as the field increases from zero and the vectors will be aligned parallel to the field, as previously described. As the field decreases to zero, the reversible effects take place and the specimen is at its remanent state. As the field reverses, new domain walls are formed and swept out, and the magnetization vectors are aligned parallel to the applied field in the direction opposite from that of the previous saturated condition. The induction is said to change from positive saturation to negative saturation (where the assignment of polarity is arbitrary) and, if induction is plotted against applied field strength, the resultant is called a "major dynamic hysteresis loop."

It has been demonstrated that the behavior of a ferromagnetic material in an external magnetic field is a function not only of the atomic structure of the material, but of the direction of the applied field with respect to the crystalline structure as well. It has also been demonstrated that, upon removal of the external field, the domains tend to remain to a greater or lesser extent in the same state as that which existed in the presence of the field (remanence). If no change of intrinsic induction (B minus H) occurred upon removal of the field, the material would exhibit truly "square-loop" properties. This means that if the external field were reduced to zero, the remanent intrinsic induction would equal the saturation intrinsic induction.

Even in a single-crystal specimen, produced under carefully controlled laboratory conditions, there will be some change in domain state upon the removal of an external field. Zero change in state implies that the easy direction of magnetization of the single-crystal specimen is concurrent with the applied field and that there are no stresses in the specimen caused by microscopic crystal imperfections. Obviously, since we are discussing macroscopic effects requiring a specimen which can at least be seen by the naked eye, it is, at the present time, impossible to produce a specimen containing no impurities or crystal defects.

Since the concurrence of the easy direction of magnetization and the direction of the applied field requires a "lining-up" procedure, perfection can never be achieved. Figure 2-8*a* illustrates a condition in which the magnetization vectors of the domains are all aligned in the easy direction of magnetization and Fig. 2-8*b* shows how these vectors would be rotated by application of a sufficiently strong external field almost, but not quite, concurrent with the direction of easy magnetization. Upon removal of the external field, these vectors would rotate back to their original direction. The solid interior lines of Fig. 2-8 are simply to indicate where domain walls existed in the demagnetized state. No wall exists between contiguous regions in which the magnetization vectors are in the same direction. Such a condition results in a single domain.

The effects of the presence of imperfections or flaws in the crystal lattice are to rotate slightly the magnetization vectors of the associated domains and to impede the passage of the moving domain walls. Therefore, even if the external field were perfectly aligned with an easy direction of magnetization of the majority of the domains, the magnetization vectors of those domains affected by crystal imperfections would still undergo a rotational effect upon removal of the field.

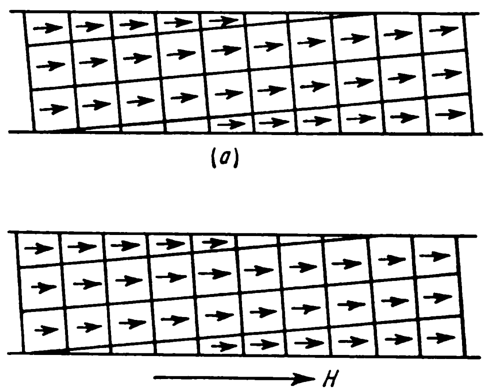

Fig. 2-8. Symbolic representation of the domain configuration of a magnetized specimen. (a) In the absence of an external field; (b) in the presence of an external field.

The rotation of the magnetization vector from alignment with an easy direction of magnetization to alignment with an externally applied field is a reversible process. This is true whether the vector associated with the domain considered is misaligned because the external field is skewed with respect to the easy direction of magnetization or a lattice imperfection has caused the vector to be misaligned from the direction occupied by the majority of the domain vectors. This reversibility of the phenomenon of domain rotation is in contrast to the almost total irreversibility of domain-wall movement (of 180° walls).

Assuming that a specimen is at its remanent state, the change of induction with the application of a step-change of applied field is a function of the magnitude of the applied field and also of time. Failure of magnetic phenomena to occur independently of time is often a source of confusion to a newcomer to the field of magnetics. It is also the source of many problems for the practitioner in the field.

Let it be assumed that a nickel-iron specimen has been subjected to a large, slowly alternating external field and that this field is removed when the specimen is at negative saturation, leaving the specimen at its negative remanent state. The polarity of the field at the time of its removal, then, was negative by definition. If a very small positive field is applied, no flux change will occur. This is, perhaps, an oversimplification since, due to imperfections, a very small, reversible flux change will occur. It is best at this time, however, to assume that no flux change will occur if the magnitude of the applied field is sufficiently small. The absence of flux change can be attributed to the fact that no domain walls exist because of the previous history of the specimen and that, since domain walls represent a certain energy, not sufficient energy has been supplied by the external field to form new walls.

It has been postulated that certain flaws, impurities, or imperfections will exist at the surface of the specimen and that these will serve as centers of nucleation for the formation of domain walls when sufficient energy is supplied by the external field.[11] Once the walls are formed, they propagate through the material at a velocity which is a function of the magnitude of the applied field (assuming no interior imperfections are present to stop wall motion). When two walls meet, they merge and the propagation continues over the combined front, as shown in Fig. 2-9.[12] In this figure, four nucleation centers of reverse magnetization are shown on the two surfaces. The walls originating at points A and B are propagating out along a hemispherical front, while those originating at points C and D have merged over a portion of their area, the unmerged portions continuing to propagate in the normal fashion.

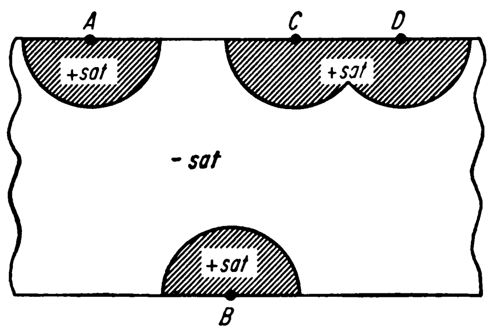

FIG. 2-9. Propagation of domain walls from nucleating centers.

The amount of energy required to cause nucleation of a domain wall at a nucleation center is not constant. It is thought that if the applied field is increased from zero in small increments, a field strength will be found at which only a very few nucleation centers are activated. Since the number of domain walls formed are few and since the velocity of propagation is low (because the velocity is a direct function of applied field strength), a comparatively long time will elapse before the walls are swept out. Had a larger field been applied in a step from zero, more walls would have been formed and these would have moved faster, resulting in a much shorter time before the flux stopped changing as a result of the applied field.

There are several factors which govern the velocity of domain-wall propagation. The three principal factors are eddy currents (both regional and local), spin relaxation phenomena, and lattice imperfections. If a strong field is applied and many nucleation centers contribute to domain-wall formation, the wall resulting from the merger of many walls originating from points close together resembles a plane front propagating toward the center of the specimen. This front gives rise to regional or macroscopic eddy currents which retard the advance of the wall and which represent a heat loss. If the applied field is comparatively weak, the eddy currents resulting from the movement of a few walls in isolated areas are more localized or "microscopic" in character. They still retard wall movement and are responsible for an energy loss, but the energy loss is less than from the macroscopic losses of the previous case.

The spin relaxation phenomena are associated with impurities, particularly interstitial carbon, in the crystal and with some anomalous causes. The lag associated with the latter is often referred to as Jordan lag and has not as yet been satisfactorily explained. Crystal imperfections cause a portion of the domain wall to "hang up" in a local region while the rest of the wall progresses. The major portions unite past the obstruction while the obstructed portion stretches out to keep contact. Eventually the stretched portion snaps and recedes to form a pattern about the imperfection, while the now undistorted main wall proceeds unimpeded. It is believed that the Barkhausen effect is a result of these sudden changes in wall configuration, particularly in materials exhibiting less rectangular hysteresis loops.

2-6. FACTORS AFFECTING PROPERTIES OF TAPE CORES

Many magnetic amplifiers with modest gain, response time, and stability requirements can be built from stacked laminations for operation at low power supply frequencies. For higher supply frequencies or high-performance amplifiers it is desirable that toroidal tape-wound cores be used. The many processes involved in producing these tape cores all affect the properties of the end product. A brief description of the metallurgical and packaging processes is included here to provide some background in these fields.

The exact procedures used vary widely, depending upon the material and the individual producer. A silicon-iron, for instance, is not particularly strain-sensitive and cores fabricated from it are frequently used without an elaborate packaging arrangement. It is usually sufficient to provide only layer insulation between the core and the windings placed on it. Nickel-irons, in the range of 45 to 90 per cent nickel, on the other hand, are highly strain-sensitive and must be protected from mechanical strains by a rigid box. For environments where vibration may be encountered, a damping fluid may be injected into the box to protect the core further.

A 50 per cent nickel-iron will be used to illustrate typical processing methods.[13] Very high-purity materials are used in the initial melt, typically nickel and iron produced by an electrolysis method to avoid contamination. In addition to the major constituents, most manufacturers add minor ingredients to achieve what they hope will be a satisfactory end product. An example of a melt which yielded good tape properties is:

nickel–50 per cent	manganese–1.0 per cent
iron oxide–0.05 per cent	iron–48.95 per cent

The nickel and iron were vacuum-melted in a magnesia crucible; then the iron oxide and manganese were added while the melt was under a helium atmosphere. The melt was then cast in a stainless steel mold. To help eliminate impurities which might have contaminated the material during the melting and casting operations, the top 15 per cent of the ingot was cut off after cooling. The ingot was then hot-rolled at a temperature of 950°C to a thickness of about 0.150 in. After the resulting strip was sanded to remove scale, it was cold-rolled in two operations, first to a thickness of 0.025 in. and then to 0.002 in.

The material at this point in processing is in sheets which resemble common aluminum foil. The treatment between cold-rolling and boxing is reasonably standard. The sheets are slit to the desired width (usually between ⅛ in. and 2 in.) and wrapped on reels in the fashion of motion-picture film. During the cold-rolling and slitting operations, the material usually accumulates a coating of grease which must be removed before further treatment if contamination is to be avoided. The slitting operation may leave a burr on the edge of the strip; this also must be removed.

The material is now ready to be wound into cores. To form the cores, the tape is wound on a mandrel to give the desired inside diameter. In this winding process, a thin insulating film is coated onto one side of the tape. This film insulates one layer from the next, preventing the circulation of eddy currents between adjacent layers. The film must be thin since it contributes no magnetic properties and it is desirable to have as high a space factor as possible. Typically for a 0.002-in. material, the magnetic material occupies 80 to 90 per cent of the total volume of the unboxed core. The film must also be stable at high temperatures. This is because the core will be annealed after the film is applied, and the film must not react with the core material, even at high temperatures, or the magnetic properties of the core will be seriously degraded. Magnesium hydroxide has been in use for many years to provide this film, but new developments in methylates are now providing better space factors.[14]

A desired maximum total flux change is achieved by the tape being wound on the mandrel either a given number of wraps or to a desired outside diameter. The result is a tightly wound spiral of coated tape with a given height and the desired inside and outside diameters. The cross-sectional area of the core will determine the total flux change, since the flux density is fixed by the gross chemical composition which, in turn, is controlled during melting. The severe cold reduction causes the desired orientation of crystalline structure to be achieved during subsequent annealing, putting a <100> direction parallel to the direction of rolling.

All of these processes tend to introduce strains and impurities. To improve this raw product and to complete the desired orientation, the core is placed in an annealing oven after removal from the winding mandrel. The annealing process consists, typically, of a 1-hr anneal at about 1000°C in a reducing atmosphere, usually hydrogen or dissociated ammonia. The high temperature relieves the strains in the material and allows proper grain growth. The reducing atmosphere removes those impurities which migrate to the surface.

After cooling, the cores are placed in a rigid box, usually of phenolic or aluminum and phenolic construction. Depending upon the manufacturer, the damping compounds which attenuate differential motion between the core and the box are added either before placing the core in the box or afterward. Silicone compounds are usually used, in the form of high-viscosity liquids or pastes or putties. The boxes are sealed and the cores are ready for the wire-winding operation. Any handling of the cores after annealing and before sealing the boxes must be done with care to avoid strains which will remain to affect operation. Tolerances on the box dimensions must be maintained within close limits to avoid squeezing the core, and the viscosity of the damping compound must be neither too high nor too low throughout the temperature range to which the core will be subjected.

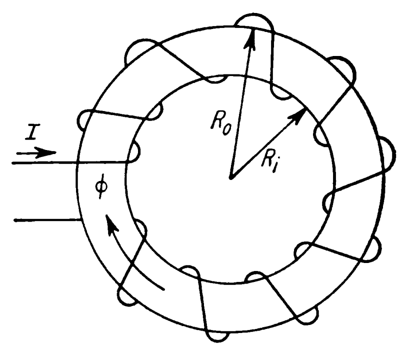

FIG. 2-10. Diagram of a toroidal reactor.

The toroidal configuration yields a minimum air gap and permits maximum use of the inherent characteristics of superior materials. Certain geometrical properties of the magnetic path become apparent under these conditions, however. With a negligible air gap, the difference in path length between the inner wraps and outer wraps of tape is apparent. This difference may usually be neglected in the presence of an air gap in the magnetic path because the field strength required to maintain a given flux density across the air gap masks the difference between the mmfs required to achieve that flux density in the different path lengths in the material. Consider the condition illustrated in Fig. 2-10.

In this illustration, the mmf is NI, where N is the number of turns of the winding. The field strength is NI/l. For a wrap of material on the inner rim of the core, therefore,

$$H_i = \frac{NI}{2\pi R_i}$$

and, for a wrap on the outer rim of the core,

$$H_0 = \frac{NI}{2\pi R_0}$$

Since R_0 is greater than R_i, H_i must always be greater than H_0. It is seen, then, that the field strength varies across the radial width of the core. It will be seen later that the ratio of the inner to the outer diameter of a core affects the flux-mmf characteristic of the core and, eventually, the gain of the magnetic amplifier in which the core is used.[15]

2-7. HYSTERESIS LOOPS

The most common way to display the magnetic properties of a material is by the use of a hysteresis loop, or plot of flux density B, as a function of field strength H. This loop is also called a B-H loop or a flux-current loop. The terms are not always used interchangeably nor do they always mean the same thing to different people. There are three major differentiations made among loops: d-c loop, sine-flux loop, and sine-current loop. The latter two are sometimes lumped under a heading of dynamic-hysteresis loops. Another differentiation is between major and minor hysteresis loops.

Static Loops. A d-c hysteresis loop is usually a loop obtained by plotting data from a "ballistic" test (or, more recently, from special quasi-static loop tests). The name "ballistic" derives from the ballistic galvanometer used as an integrating device to measure flux change. Excellent detailed descriptions of this test are available in most electrical-measurements texts.[16] For the purposes of this text it is sufficient to explain that the method consists of driving a core to negative saturation by means of a biasing mmf. A signal mmf, variable in small increments, is alternately applied and removed in a step function in opposition to the bias mmf, the signal mmf being increased by a small amount before each application. The flux change (or, more precisely, the integral of the voltage generated in a pickup winding which is proportional to the flux change) resulting from each application is read on a ballistic galvanometer. The mean length of magnetic path is calculated and the average magnetic field strength determined by dividing the net mmf (the algebraic difference between signal and bias mmfs) by the mean path length. The saturation flux level is taken as one-half the total flux change obtained by making the signal mmf twice the biasing mmf. A typical loop for a 50 per cent nickel-iron core is shown in Fig. 2-11. These data were obtained on a commercial-grade polycrystalline specimen.

Stewart has shown that this method, when applied to a single-crystal specimen, may result in a region of infinite slope which accounts for the major portion of the total flux change.[17] This results from the fact that a larger mmf is required to nucleate a domain wall than to keep a nucleated

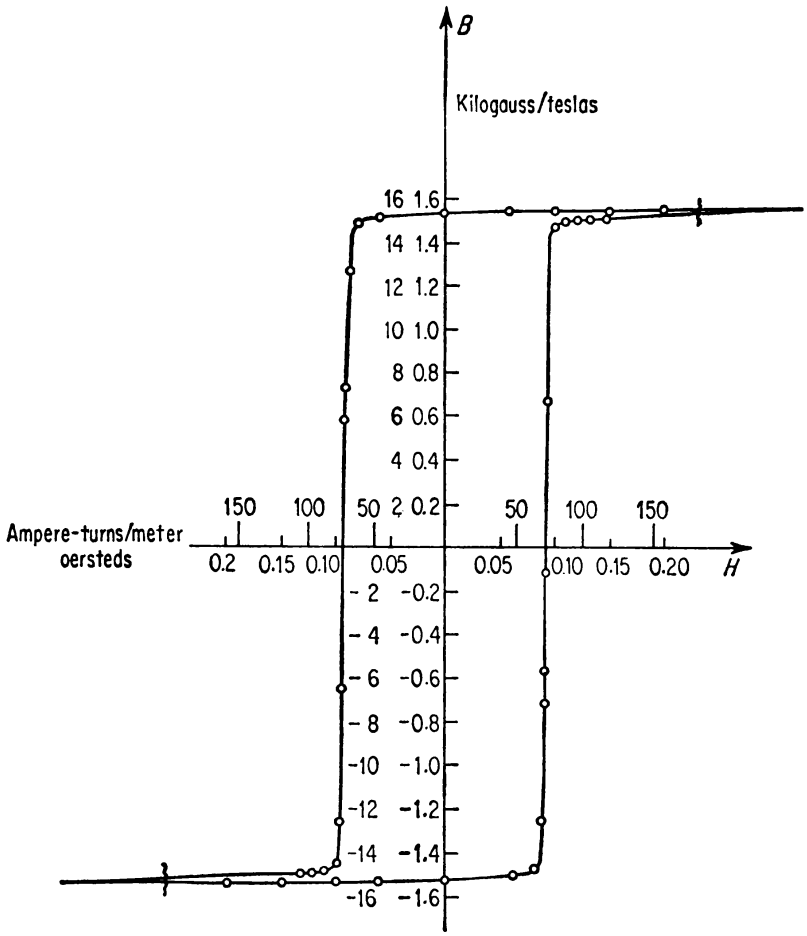

FIG. 2-11. Static *B-H* loop for a 50 per cent nickel-iron material.

wall moving. The presence of imperfections (particularly inclusions) slows down wall movement and may even halt it. If wall movement is stopped, flux change ceases. Upon application of a somewhat larger field in a ballistic type of measurement, the wall moves faster and may sweep past an imperfection which had previously stopped it. Stewart shows a plot of I against H where H was automatically varied to maintain the rate of change of I with respect to time constant. This is reproduced in Fig. 2-12. It can be seen that a ballistic method would have resulted in a loop with infinite slope between points A and B. It is seen, also, that the ballistic method would result in a larger energy loss than the method which maintains domain-wall velocity constant. Stewart speculates that, given a single-crystal specimen with only one domain wall, it would be possible, with an automatic feedback control with sufficient speed of response, to trace out a loop with zero energy loss if the impediments to wall motion could be adequately represented by the assumptions he made. He points out, however, that if the obstacle is, for instance, a nonmagnetic inclusion about which supplementary domains form, zero energy loss is not possible under any conditions.

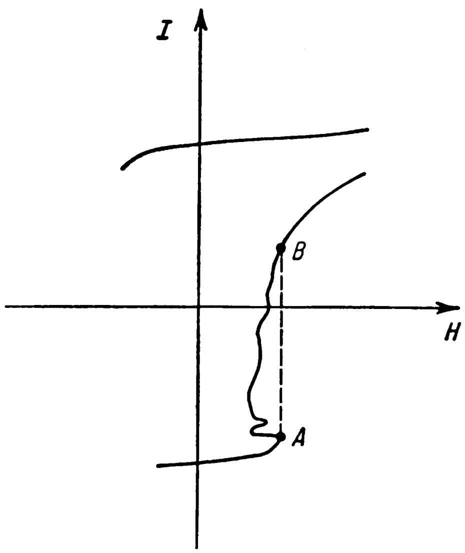

FIG. 2-12. *I-H* curve of a single-crystal specimen. (*From K. H. Stewart, Ferromagnetic Domains, Cambridge University Press, New York,* 1954.)

The name d-c hysteresis loop, then, is seen to be something of a misnomer. What is usually meant is the ballistic hysteresis loop. To obtain a close approximation to the ballistic loop, loop tracers have been employed recently in which the mmf is varied very slowly with respect to time.[18] In some models several minutes may elapse in tracing a loop. The principal disadvantage in this method is that it requires a very low drift d-c amplifier. Loops obtained with these devices may have double-valued portions of the loop, or fail to close, at saturation because of amplifier drift.

Dynamic Loops. Since the number of applications for core material in which magnetization takes place in a manner simulated by ballistic or low-frequency loop-tracer methods is limited, methods have been evolved for determining induction as a function of power-frequency alternations of magnetic potential (another term for mmf). The two methods most commonly used are the sine-flux and sine-current tests.

In the sine-current test, the magnetic potential is varied sinusoidally, or nearly so. Figure 2-13 shows the *B-H* relationship (where H is the mean field intensity) and the H-time relationship from which it resulted. Essentially all of the flux change during a positive half-cycle occurs between points a and b of the hysteresis loop. This requires that this flux change take place between points a' and b' of the sine wave of magnetic potential or in the corresponding time interval t_a to t_b. The voltage appearing across the terminals of the winding providing the mmf will be comparatively high in this interval of time, therefore, and will be virtually zero throughout the rest of the half-cycle when the rate of change of flux is very small. To supply a sinusoidal current into such a nonlinear impedance requires that the supply be a good approximation to a current source.

The sine-flux loop is obtained by varying the flux density sinusoidally with respect to time. If a voltage source (as contrasted with a current

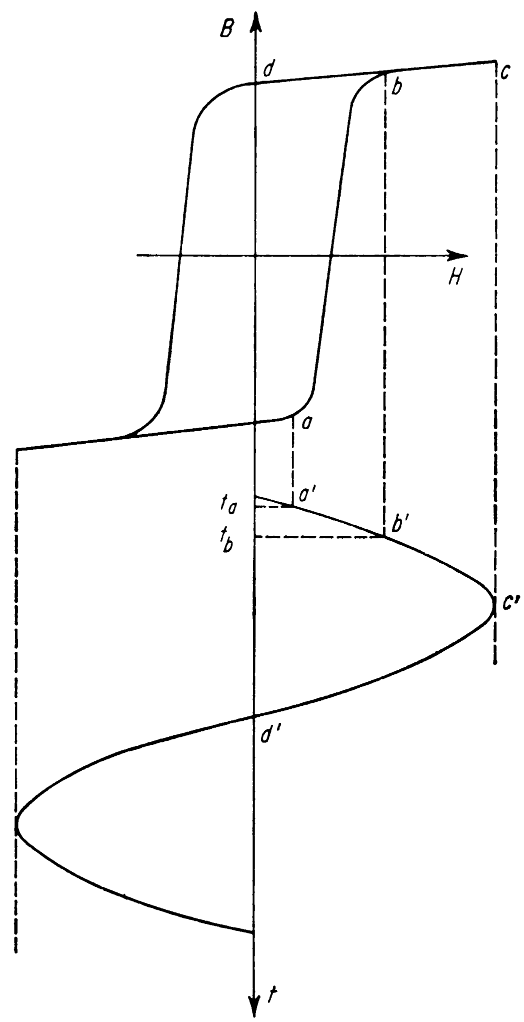

FIG. 2-13. Current sine-wave and resulting B-H loop.

source) is connected across the terminals of a winding on a core, the source voltage will be related to the time rate of flux change by Faraday's law if the winding has negligible resistance. If the source voltage is sinusoidal, Eq. (2-1) is obtained

$$E_m \sin \omega t = N \frac{d\phi}{dt} \tag{2-1}$$

By integrating Eq. (2-1), Eq. (2-2) is obtained

$$\phi = \frac{E_m}{\omega N} \cos \omega t + c \tag{2-2}$$

If the initial conditions are properly chosen, the constant of integration c in Eq. (2-2) is made zero and flux varies sinusoidally with respect to time.

In Fig. 2-14a, a typical sine-flux hysteresis loop is shown and the corresponding time relationships of voltage, field intensity, and flux are shown in Fig. 2-14b, c, and d, respectively.

A comparison of sine-flux loop with a sine-current loop for the same core is made in Fig. 2-15.[19] The larger amount of energy required to maintain a sinusoidal field strength can be ascribed to the much shorter length of time allowed for an equivalent flux change. To obtain a sinusoidal flux variation, a period equivalent to nearly a half-cycle of supply frequency is available to change flux from $-B_r$ to the upper knee. The same flux change under the influence of a sinusoidal field must occur in about one-sixth of a half-cycle. As was seen earlier, a more rapid change of flux requires a larger field and, hence, more energy loss. The four-

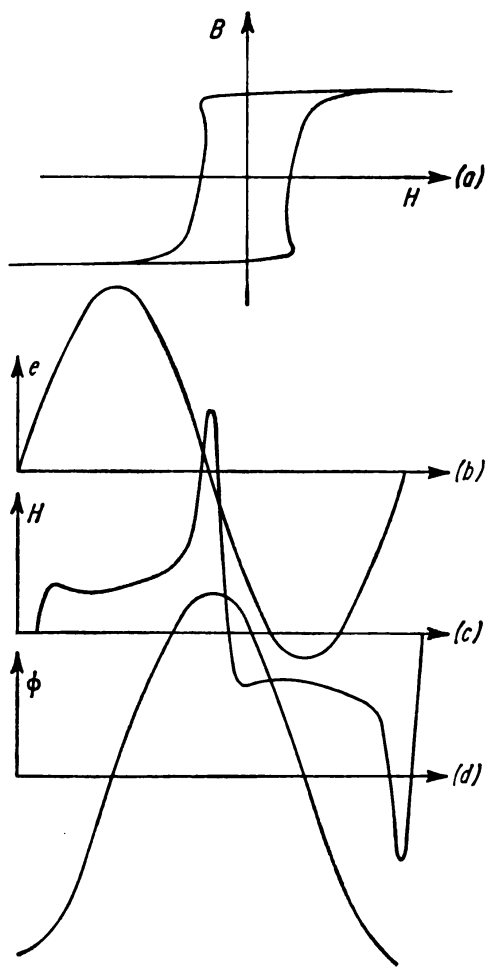

FIG. 2-14. Sine-flux loop and associated waveshapes. (a) Sine-flux B-H loop; (b) voltage-time relationship; (c) field intensity-time relationship; (d) flux-time relationship.

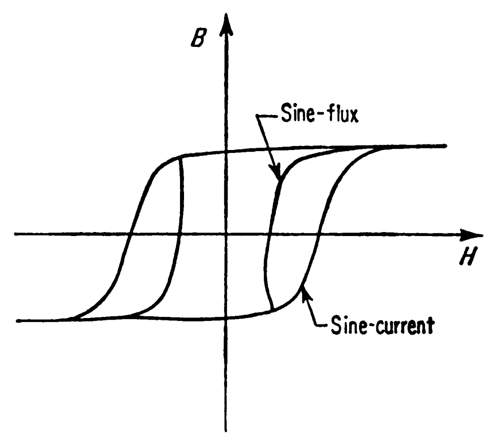

FIG. 2-15. Comparison of sine-flux and sine-current B-H loops.

valued nature of the sine-flux loop can be attributed to the fact that, with no requirement that the mmf be held constant, the source supplies enough current to nucleate domain walls and, once domain walls are moving, the impedance represented by the winding increases, causing a decrease in current.

2-8. TEMPERATURE EFFECTS

The spontaneous magnetization phenomenon is associated with interatomic forces within a crystal which, in turn, are dependent upon interatomic spacing. Consequently, the thermal energy acquired by the atoms at increased temperatures, which increases the average interatomic spacing, affects spontaneous magnetization and, therefore, the saturation value of flux density. It can be shown that the saturation value of induction B_{sat} has a maximum at absolute zero and, in general, obeys a hyperbolic tangent law, becoming zero at a temperature called the Curie temperature.[20] Above the Curie point the material behaves as a paramagnetic substance. The ratio of spontaneous magnetization intensity M_s to the magnetization intensity at absolute zero M_0 is expressed as

$$\frac{M_s}{M_0} = \tanh \frac{M_s/M_0}{T/\theta}$$

where T is the absolute temperature and θ the Curie temperature. A typical curve for iron is shown in Fig. 2-16.

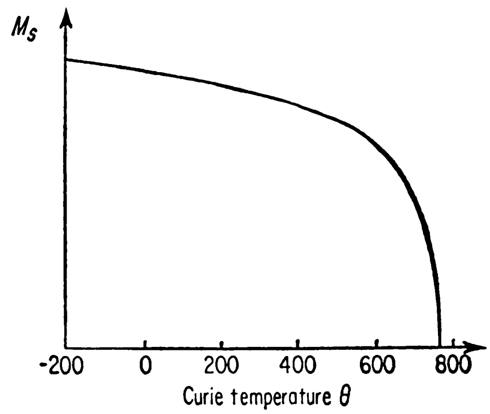

FIG. 2-16. Variation of saturation magnetization with temperature for iron.

The Curie point varies over quite wide limits for different elements, alloys, and crystal structures. The Curie temperature of cobalt, for instance, is about 1120°C, and that for nickel about 360°C. A newly improved iron-cobalt-vanadium alloy[21] has a virtual Curie point of about 960°C, but undergoes a phase transformation at 850°C. This alloy has a high-saturation flux density and is more easily worked than most iron-cobalt alloys. Further development should produce a very useful magnetic material. The presently used nickel-irons have a Curie point between 500 and 600°C. Silicon-iron, with only small additions of silicon, has a Curie point very close to that of iron (about 750°C).

The effects of temperature on permeability and coercive force have not been investigated as fully as other phenomena. In general, increasing temperature decreases the coercive force, at least for a range of temperatures about room temperature. Permeability increases with increasing temperature. The properties of coercive force and permeability cannot be correlated directly with magnetic-amplifier performance. The effects of temperature on amplifier performance will be discussed more fully in Chap. 8.

2-9. FERRITES

The oldest known highly magnetic material is probably the lodestone, known to mineralogists as magnetite and to chemists as Fe_3O_4. From its chemical symbolism, it will be recognized that this compound is not a metal nor a compound of two metals. It is one of a large family of compounds frequently called ferrites, having a composition $MOFe_2O_3$, where the M denotes a divalent ion.

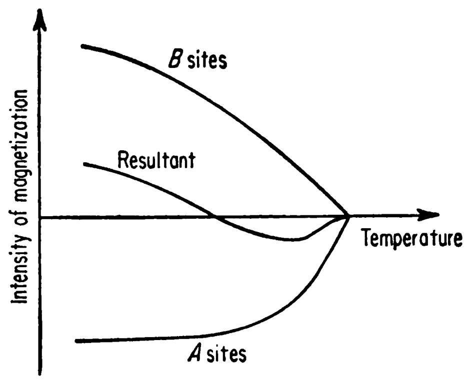

FIG. 2-17. Variation of saturation magnetization with temperature for a typical ferrite.

The ferrites display a phenomenon which has been named ferrimagnetism to distinguish it from ferromagnetism.[22] In ferrites, certain crystalline positions are occupied by atoms having a spontaneous magnetic moment antiparallel to atoms occupying certain other positions. These positions have been designated as *A* and *B* sites. As a result of this antiparallel arrangement, which is in disagreement with classic domain theory, the net magnetization is much less than would be measured if all sites were occupied by atoms with parallel moments.

The magnetization of the two types of sites does not always vary as the same function of temperature, giving rise to a possibility of reversal of net magnetization as temperature is varied. This is illustrated in Fig. 2-17, where the magnetization at saturation of the two sites is plotted as a function of temperature and the resultant magnetization is shown as the algebraic sum of the individual magnetizations.

Because of the antiparallelism, ferrimagnetic substances tend to have substantially lower net saturation magnetizations than most of the widely used ferromagnetic materials. However, they have other characteristics which make them useful in some applications. In particular, certain ferrites display a peculiar resonance phenomenon of highly directional qualities at microwave frequencies which make them extremely valuable for obtaining desirable attenuation characteristics.

Application of these materials in magnetic amplifiers has been minimal because of their low saturation characteristic, but even in this field they may prove useful at high frequencies because of their extremely high resistivity. This property results in dynamic loops which are little wider than the static loop. The loops can be quite rectangular, particularly if the material is properly prestressed.[23] Preparation of the cores is quite simple, in comparison with metallic tape cores, and the finished product is more rugged than its metallic counterpart, eliminating the need for elaborate packaging techniques.

2-10. EFFECTS OF NUCLEAR RADIATION ON MAGNETIC MATERIALS

The nature of ferromagnetic materials results in far less damage from nuclear radiation than is done to semiconductor materials. The types of nuclear radiation are discussed to some extent in Sec. 2-14, where the damage to semiconductors is assessed. Most damage from exposure to radiation occurs from the rupture of the easily disturbed covalent bonds typical of semiconductors and most organic compounds. Metals in the conductor classification already have "free" electrons and the production of more by exposure to moderate doses of radiation does not materially affect their properties.

It is possible to affect the magnetic properties of ferromagnetic materials by exposure to high radiation fluxes. Assessment of the nature and magnitude of the damage is in a pioneer state at the present time. Most studies of radiation damage have been concerned with the materials which are most susceptible to radiation. At this moment, several studies of damage to ferromagnetic materials are projected or in actual progress. The results of these studies, however, will probably not be available for several months.

One study[24] devoted to the problem indicates that the major damage to core material suitable for self-saturating magnetic amplifiers consists of loss of loop rectangularity and increased dynamic coercive force. This study was made at a total integrated neutron flux of 2.7×10^{18} neutrons/cm^2. It was, unfortunately, a "one-sample" study and a statistical evaluation of damage was not possible.

Where cobalt alloys are used, the phenomenon of secondary radiation may arise. It is well known that a radioactive isotope of cobalt, cobalt-60, has a long half-life. A cobalt alloy may, therefore, continue emitting dangerous amounts of radiation even after the irradiating field is removed. This poses a maintenance and servicing problem.

2-11. RECTIFIERS

As was indicated earlier, the properties of rectifying devices are nearly as important to satisfactory operation of self-saturating magnetic amplifiers as the properties of magnetic materials. Rectifying devices assume many forms, among which are synchronous switches, high-vacuum electron tubes, gas-filled electron tubes, electrolytic rectifiers, metal-plate rectifiers, and crystal diodes. In all probability all of the above have been tried in magnetic amplifiers. For one reason or another most are unsuitable and only metal-plate rectifiers and crystal diodes are in widespread use. Germanium and silicon junction diodes are assuming a more and more dominant role and will probably continue to replace plate rectifiers as allowable ratings are increased and costs are decreased.

***P-N* Junction Diodes.** Among the elements in the periodic table, those in Group IV are characterized by crystalline growth through formation of covalent (homopolar) bonds. A diamond is an excellent example of this type of structure. Among the Group IV elements are germanium and silicon. Since, in the discussions which follow, the broad aspects of rectification across a *P-N* junction will be equally applicable to both elements, only silicon will be treated. While germanium devices were available commercially prior to silicon and have since achieved widespread application, certain superior qualities of silicon make it more logical to treat its properties in detail, leaving it to the interested reader to consult the literature for a fuller treatment of germanium.

The semiconducting elements earned their name by virtue of their electrical conductivity, which lies between that of the insulators and that of the conductors. At absolute zero the conductivity of semiconductors should be zero. As temperature rises conductivity rises, which is the reverse of the conductivity-versus-temperature characteristic of the metallic conductors. This behavior is attributable to the nature of the homopolar bonds between atoms in the crystalline structure. These bonds may be broken by thermal energy; at room temperature sufficient bonds have been broken for a measurable current to be obtained by application of reasonable potential across the crystal. Typical resistivities at room temperature for materials in the "conductor" category are 1.72×10^{-6} ohm-cm for copper, 10×10^{-6} ohm-cm for iron, 100×10^{-6} ohm-cm for Nichrome resistance wire, and 3500×10^{-6} ohm-cm for carbon. For insulating materials, typical values are 9×10^{13} ohm-cm for ordinary glass, 9×10^{15} for mica, and 10^{18} for hard rubber. For pure germanium, a value of 50 ohm-cm is reasonable. For germanium containing controlled impurities the value may vary between 0.1 to 50 ohm-cm. For pure silicon, the resistivity is about 60×10^{3} ohm-cm. Silicon, then, has a resistivity about 10^{10} times that of ordinary conductors and about 10^{-10} times that of an insulator such as glass.

The rectifying properties are obtained by addition of small amounts of impurities to the intrinsic material while the latter is in its liquid phase. By suitable techniques, large single crystals of ultrapure silicon can be obtained which are thus "doped" with Group V elements in one region and Group III elements in a second region. As the doped material crystallizes, these impurities enter into solid solution with the base or intrinsic material and occupy normal lattice sites (as against interstitial positions) in the crystal. The homopolar bonds thus formed with the intrinsic material leave the impurity atom with an unbonded electron in the case of Group V elements (donor atoms) or a place for an electron in the case of Group III elements (acceptor atoms).[25] As long as the unbonded electron from a Group V element remains in the immediate neighborhood of the parent atom, there is no net electrical charge. Similarly, as long as no electron occupies the bonding position left free by a Group III atom there is no net electrical charge. This is illustrated diagrammatically in Fig. 2-18. The donor material is commonly referred to as *n* (negative) type and the acceptor material as *p* (positive) type. The lattice positions where an unbonded electron exists are shown as minus signs in the *n*-type material and the "holes" where no electron completes a bond are shown as plus signs in the *p*-type material.

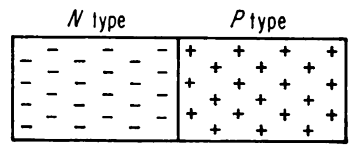

FIG. 2-18. Symbolic representation of an *N*-*P* junction.

At near absolute zero temperature, the electrons occupying unbonded positions in the *n*-type material are uninhibited in crossing the junction to occupy the lattice bonds available in the *p*-type material. In the *p*-type material, at higher temperatures, the electrons from the intrinsic material may also break the homopolar bonds and "drop" into the unoccupied site or hole, leaving a net positive charge behind as well as a hole which may then be filled by some other wandering electron. Because of the presence of the holes in the *p*-type material, it is difficult for an electron to cross the junction from the *p* to the *n* region, whereas it is relatively easy for this to occur in the opposite direction. As a result, while electrons drift across the junction in both directions, a net flow exists from the *n*- to the *p*-type material. This condition cannot continue indefinitely, since the *n*-type material, with a deficiency of electrons, develops a positive charge, while the *p*-type becomes negatively charged. A potential develops across the junction, then, as shown in Fig. 2-19. Here the plus signs refer to charges caused by electron-deficient atoms and the negative signs indicate the presence of excess electrons. In the absence of an external potential, an equilibrium condition exists in which a small potential exists across the junction and conduction across the junction is equally easy for electrons approaching it from either side.

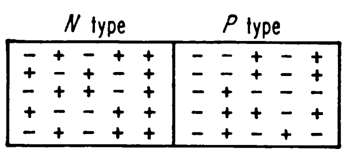

FIG. 2-19. Symbolic representation of an *N*-*P* junction illustrating the development of junction potential.

If an external potential is applied to the device with the p region positive and the n region negative, as shown in Fig. 2-20, electrons will be attracted toward the p region, progressing in a random fashion by dropping into holes vacated by other electrons. The holes, then, tend to migrate to the negative cathode and the electrons to the positive anode. The magnitude of this current flow will be a function of the amount of each impurity present, the temperature, and the magnitude of the applied potential. These relationships can be expressed by Eq. (2-3), in which I_0 is dependent on the intrinsic material and the impurities.[26]

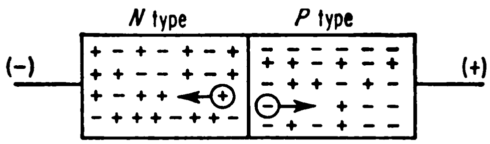

FIG. 2-20. Symbolic representation of an N-P junction illustrating the migration of holes and electrons under the influence of an external potential.

$$I_f = I_0[\exp (eV/kT) - 1] \quad (2\text{-}3)$$

In this equation, e is the charge of an electron, V is the developed junction potential, k is the Boltzmann constant, and T is the junction temperature in the Kelvin scale.

If the applied potential is reversed, as in Fig. 2-21, holes will again tend to migrate to the negative cathode and electrons to the positive anode. However, since the majority of the weakly bound electrons are in the n region and the majority of the holes exist in the p region, after a short time no weakly bound electrons exist in the p region and no holes in the n region. There is, then, no current across the junction. The absence of current carriers in the region of the junction creates a "depletion layer" which develops a charge opposite and equal to the applied potential. As occasional holes appear in the n region or unbound electrons in the p region (due to thermal agitation), they cross the junction and are swept out. This current I_r is extremely small in comparison with I_f of Eq. (2-3) at room temperature and voltages above ½ volt. I_r can be expressed as

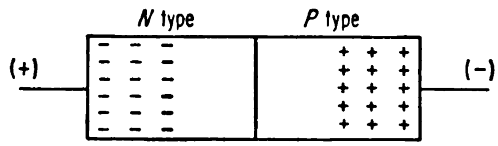

FIG. 2-21. Symbolic representation of an N-P junction illustrating the behavior of holes and electrons in the presence of a reverse potential.

$$I_r = I_0\,[1 - \exp (eV/kT)] \quad (2\text{-}4)$$

A typical static current-voltage characteristic is shown in Fig. 2-22 for a silicon junction diode at room temperature. This static characteristic is obtained by varying a d-c voltage in small increments.

The forward portion of the characteristic is seen not to agree with the exponential form of Eq. (2-3). This is because V of Eq. (2-3) is the junction potential, whereas the abscissa of Fig. 2-22 represents the applied voltage. The diode has a certain bulk resistance which adds a linear component to the exponential relationship and which limits the current at higher applied voltages. In fact, the characteristic at higher voltages is essentially dependent only on the bulk resistance, the exponential portion representing essentially only a constant voltage.

The reverse characteristic, on the other hand, differs from the form of Eq. (2-4) only after the breakdown voltage is reached. In this region, conduction takes place in a fashion not fully understood at the present time. It is believed that the sudden increase in current is a function of both "electron avalanche," which involves electron removal by electrons accelerated by the barrier potential, and "Zener breakdown," which is

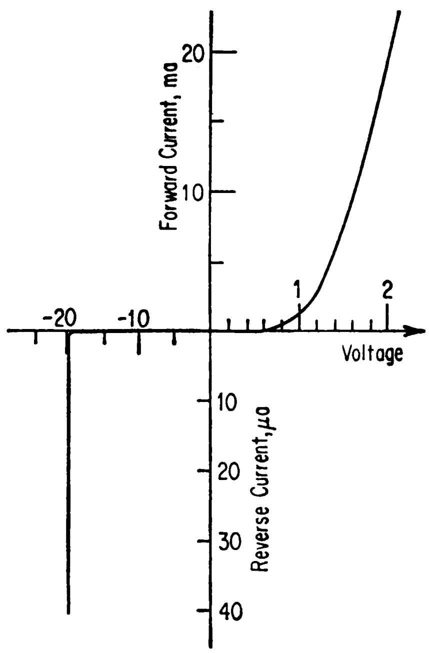

FIG. 2-22. Static current-voltage characteristic of a silicon diode.

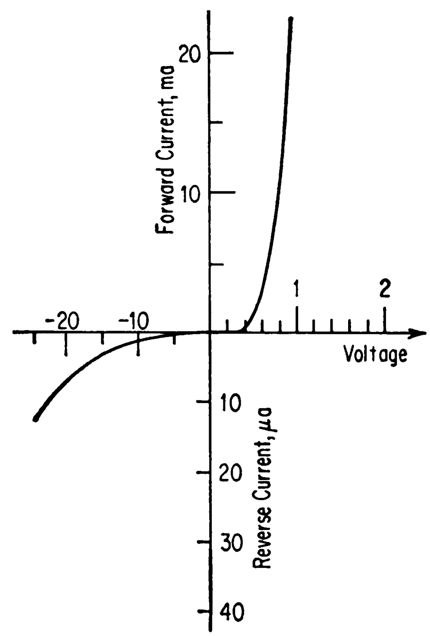

FIG. 2-23. Static current-voltage characteristic of a selenium cell.

caused by electrostatic rupture of the covalent bonds. The "nearly but not quite" vertical region makes the device extremely useful as a voltage reference, but adds little to its usefulness as a rectifier.

Plate Rectifiers. There have been three types of plate rectifiers in reasonably common use. These three types, copper (sometimes termed cuprous) oxide, selenium, and magnesium copper sulfide all display somewhat similar phenomena. Of the three, the copper oxide rectifier has been in commercial production for the longest time. The selenium rectifier gained tremendous popularity in the years immediately following World War II and is probably used almost exclusively now where plate rectifiers are required for self-saturating magnetic amplifiers. The magnesium copper sulfide rectifier is relatively unknown in magnetic-amplifier application. Because magnetic-amplifier designers show a marked preference for selenium when junction rectifiers are unsuitable, the discussion will be restricted to this material.

The precise mechanics of rectification at a metal-semiconductor interface are not entirely understood. It is postulated that a barrier (either chemical or physical, or a mixture) exists which corresponds to the junction in the single-crystal silicon rectifier already discussed. The manner in which the electrons cross the barrier is attributed variously to a diffusion effect, a thin barrier effect, or a quantum-mechanical tunnel penetration effect. The deficiencies of the various theories in accurately predicting behavior of a commercially produced cell (as one plate of a plate rectifier is called) in combination with the widely different methods of manufacture among processors have forced the applications engineer into a large measure of empiricism.

If, for instance, a particular circuit requires an inverse voltage of 38 volts, standard practice would be to use two cells in series, since cells processed to withstand 26 volts, or even 33 volts, in the inverse direction are common. A cell manufacturer may, however, produce a cell capable of withstanding 40 volts in the inverse direction by adding thallium in minute percentages to the counterelectrode in contact with the selenium. This results, unfortunately, in a cell with inferior aging characteristics.[27]

Another factor affecting cell characteristics is the forming process. It is characteristic of plate rectifiers that they do not display an asymmetric current-voltage function in the "as-manufactured" condition. They must be subjected to a reverse voltage for a certain length of time, during which the reverse current gradually decreases. The operating current-voltage characteristic of the cell is highly dependent on this forming operation. The characteristic is also a function of the previous history of the cell. There is a strong tendency to unform during shelf storage and a brief re-forming interval is discernible when voltage is applied to a cell which has not been subjected to a reverse voltage for a long period of time.

Another phenomenon associated with plate rectifiers is aging. With time, the forward resistance of a selenium rectifier tends to increase. At room temperature and nominal currents, a cell processed to withstand an inverse voltage of 26 volts may suffer a 30 per cent increase in forward resistance after 10,000 hr of operation. A cell processed to withstand an inverse voltage of 40 volts might suffer the same increase in forward resistance after only 500 hr of operation. The phenomenon of aging is a function of forward current and ambient temperature as well as of time.[28]

A typical static current-voltage characteristic for a small-area selenium cell is displayed in Fig. 2-23. This characteristic may be compared with the equivalent silicon characteristic in Fig. 2-22. The major advantage of silicon is shown more clearly in Fig. 2-24, where the reverse characteristics are plotted to the same scale. Unlike silicon, which can be processed for a wide range of inverse voltages (from 4 to 600 volts) in a single cell, selenium rectifiers have a narrow range of inverse voltages (18 to 40 volts) per cell. For applications where the inverse voltage exceeds the rating of the cells available, the cells may be connected in series. This presents a matching problem, as illustrated in Fig. 2-25, where the inverse characteristics of two selenium cells are shown. It is evident that, since the current through the two series elements must be the same, the two cells will not divide the voltage evenly, but REC_2 will experience an inverse voltage E_2 while REC_1 will see only E_1. It is

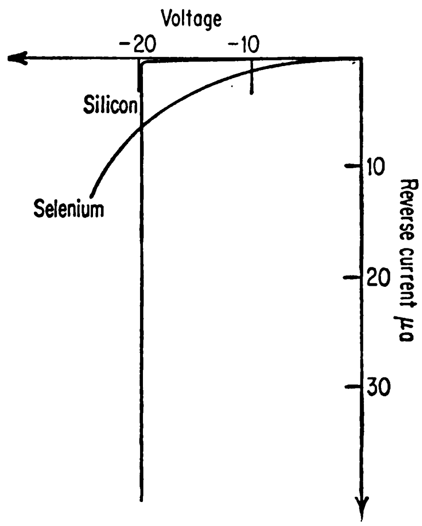

Fig. 2-24. Comparison of inverse characteristics of a selenium cell and a silicon diode.

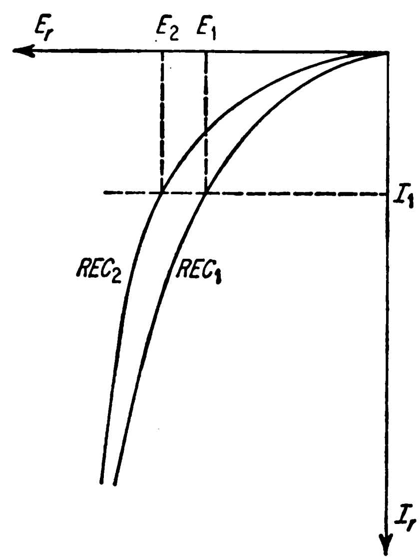

Fig. 2-25. Comparison of inverse characteristics of two selenium cells.

necessary, therefore, to ensure that the characteristics are sufficiently similar so that the inverse rating of one cell will not be exceeded before the other cell assumes a reasonable portion of the load. The same problem will exist if it is necessary to connect silicon diodes in series, but the necessity for this seldom comes up in magnetic-amplifier practice because of the wide range of inverse voltages available.

Parallel connection of plate rectifiers to increase the permissible forward current presents a current-sharing problem at a constant voltage in contrast to the previous case of voltage sharing at constant current. Matching of cells again provides the solution. In this area, plate rectifiers are, in general, superior to silicon diodes, particularly where a wide range of temperatures must be encountered. Because the forward characteristic of modern silicon diodes is so nearly vertical, a small differential change between the characteristics of two units during a temperature variation may result in a large change in the percentage of total current each will carry. As a result, the unit which tends to hog the current may experience a forward current in excess of its rating and be destroyed. Since the other will now be forced to carry all the current, it, too, will be destroyed. Silicon units, then, should be matched over the desired temperature range, not just at room temperature.

Dynamic Characteristics. The dynamic characteristics of silicon and selenium rectifiers are also widely different. When subjected to alternating currents, the reactive nature of the nonlinear impedances must be considered. Because of the presence of the junction, or barrier, the rectifier may be considered to be a pair of conducting volumes separated by a dielectric. This results in a capacitive reactance. In silicon rectifiers, the comparatively small area results in a capacitance of the order of 10–100 $\mu\mu$f. For selenium the capacitance varies with the magnitude and frequency of the applied voltage. A nominal figure of 0.10 μf/in.^{2} of rectifying surface at 15 volts and 400 cps is at least indicative of the magnitude of this phenomenon. The phenomenon of recovery time of a rectifier following a step change from heavy forward conduction to a blocking condition is seldom met in magnetic-amplifier applications and will not be discussed here.[29]

2-12. EQUIVALENT CIRCUITS

In considering the behavior of rectifiers in electrical circuits it is often convenient to represent them by an equivalent circuit as ideal diodes in combination with other components. The most common simple equivalent circuit is shown in Fig. 2-26. In this figure, C represents the capacitance, R_r the reverse resistance and R_f the forward resistance. All of these are nonlinear with respect to applied voltage, and the capacitance, at least, is a function of frequency.

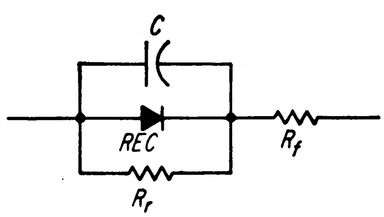

FIG. 2-26. Equivalent circuit of a rectifier.

For most purposes in magnetic-amplifier applications, the capacitance associated with a silicon diode may be neglected. Similarly, for small-area silicon diodes, the inverse resistance is sufficiently high for it usually to be considered infinite. When these factors may properly be ignored, the equivalent circuit becomes an ideal diode in series with a nonlinear resistance. Since silicon diodes are characterized by a quite sharp threshold voltage, it is often sufficient to construct an equivalent circuit consisting of an

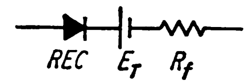

FIG. 2-27. Simplified equivalent circuit for a silicon diode.

ideal diode, a linear resistance R_f, and an ideal battery E_T, as shown in Fig. 2-27.

2-13. TEMPERATURE EFFECTS

Only seldom is a magnetic amplifier applied in an environment where the temperature is held constant. At best, there is usually a 30–40°F change with the seasons of the year. At worst, some military applications require an operating environment which varies from -55°C to $+100$ or even $+500$°C.

Manufacturers of semiconductor devices have made excellent progress in improving their products to function under extreme ambient temperatures. At present, germanium devices operate from -60°C to about 85°C, selenium to about 125°C, and silicon to about 200°C. A new development in growing junction silicon carbide crystals holds promise of a material which may operate up to 600°C.

These limits are a rough definition of the range over which present devices will operate. This is not to say that they operate as well at one point as at another. The forward drop of a silicon diode, for instance, for a constant current might be 0.6 volt at 150°C, 0.8 volt at room temperature, and 0.95 volt at -55°C, a change of over 50 per cent from one extreme to the other. The leakage current at rated voltage may vary from less than 0.001 μa at -55°C to 0.02 μa at room temperature to 20 μa at 150°C.

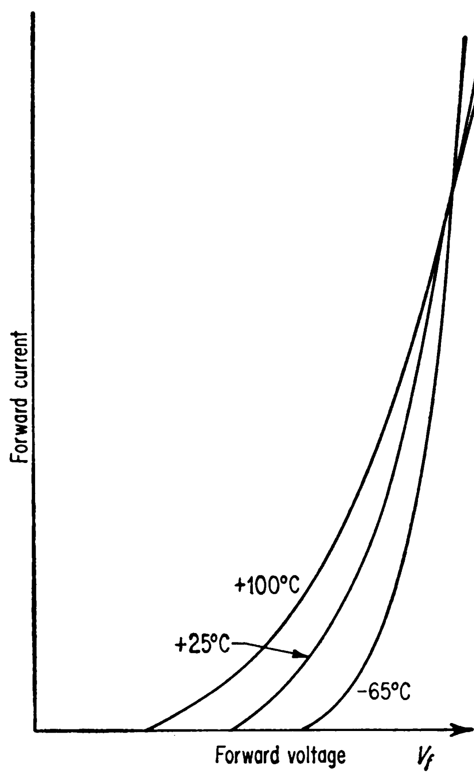

FIG. 2-28. Forward characteristic of a silicon diode at three temperatures.

The change in forward characteristics with temperature in silicon diodes is somewhat unusual. A set of characteristics obtained from a popular diode is shown in Fig. 2-28. The crossover point, which indicates a point of constant resistance with temperature, is quite significant. As mentioned earlier in the subsection on P-N junction diodes, the applied voltage can be considered as having two components, a component which is the voltage drop due to current through the bulk resistance and a component due to the junction potential. At low currents, the junction potential dominates and, for a constant current, the voltage decreases as temperature increases. At higher currents, the bulk resistance (which has a positive temperature coefficient) is dominant and voltage increases as temperature increases. Consequently, a current exists at which these opposite effects are of equal magnitude and voltage is independent of temperature.

In Fig. 2-29, the variation of the forward characteristic of selenium is shown with temperature as a parameter. Because of the large area of the specimen, the crossover point, if one exists, is far beyond the current rating of the rectifier. The variation in the reverse characteristic of

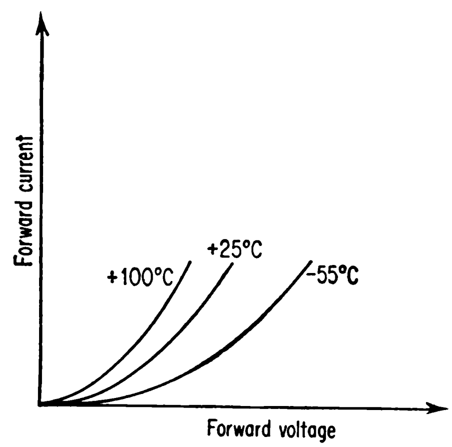

FIG. 2-29. Forward characteristic of a selenium cell at three temperatures.

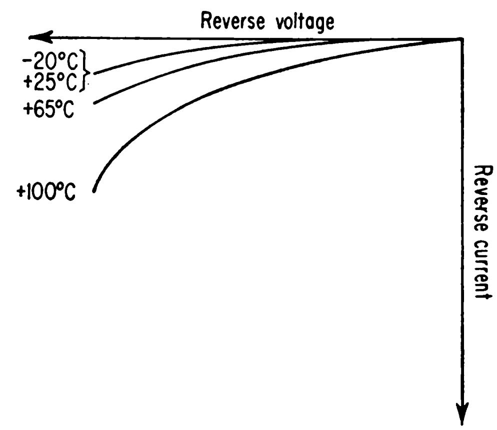

FIG. 2-30. Inverse characteristic of a selenium cell at four temperatures.

selenium as temperature is varied is shown in Fig. 2-30. As can be seen in this illustration, the performance is relatively unaffected at low temperatures but suffers severe degradation at high temperatures. Typical reverse current values at 26 volts would be 5 ma at room temperature and below, 13 ma at +65°C, and 25 ma at +100°C.

2-14. NUCLEAR RADIATION EFFECTS IN SEMICONDUCTORS

A modern requirement for electronic equipment in some specific applications is an ability to function adequately in an environment which subjects the equipment to severe nuclear radiation. This radiation consists, generally, of neutron, alpha-particle, beta-particle, and gamma-ray bombardment. Materials vary quite widely in ability to withstand one form or another of this type of radiation. Neutrons and gamma rays are the two types of radiation which have been used to determine radiation effects. Semiconductors, dependent upon molecular, atomic, and subatomic reactions for their useful properties, are particularly susceptible to degradation by nuclear radiation of both types. A formidable body of literature has appeared on the subject since 1955. It has been established that the rate of radiation, the duration of radiation exposure, and the total radiation all contribute to the final damage. Relative susceptibility to damage, threshold levels, and other qualitative and quantitative conclusions of particular authors seem to be in conflict.

The type of damage done to semiconductors and whether this damage is permanent, self-healing, or repairable (for instance, by annealing) seem to be a function of the three radiation factors quoted in the preceding paragraph. The existence of a threshold level of rate of irradiation seems quite firmly established. Below this level radiation does not seem to affect the properties of the component regardless of the length of time of exposure. Above this level damage may occur.

In general, silicon diodes seem to be less affected than germanium diodes by gamma radiation of the order of 10^6 roentgens/hr. At this level, the forward characteristic is relatively unaffected while the reverse current increases 10 per cent for silicon and 100 per cent for germanium. In a combined irradiation experiment at levels of 1.5×10^{13} fast neutrons/cm^2 and 2.5×10^{15} photons/cm^2, the reverse current of a germanium diode increased 2,000 per cent. In the same environment the reverse current of a selenium cell decreased 50 per cent.[30] Again, the forward characteristics remained relatively constant.

At present, it does not seem possible to generalize very much from the data available. As more data are amassed in statistically designed experiments it should be possible to define limits within which certain phenomena will probably occur. Since results may be affected by lack of insulation on lead wires, by temperature and humidity, by encapsulation and packaging, and by other factors, the only way to get a firm answer at the present state of the art is to test the desired component in the expected environment.

REFERENCES

1. Born, Max: "Atomic Physics," 6th ed., Hafner Publishing Company, New York, 1957.
2. Van Vleck, J. H.: Models of Exchange Coupling in Ferromagnetic Media, *Revs. Modern Phys.*, vol. 25, pp. 220–227, January, 1953.
3. Slater, J. C.: Ferromagnetism and the Band Theory, *Revs. Modern Phys.*, vol. 25, pp. 199–210, January, 1953.
4. Wohlfarth, E. P.: The Theoretical and Experimental Status of the Collective Electron Theory of Ferromagnetism, *Revs. Modern Phys.*, vol. 25, pp. 211–219, January, 1953.
5. Zener, C., and R. R. Heikes: Exchange Interactions, *Revs. Modern Phys.*, vol. 25, pp. 191–198, January, 1953.
6. Bozorth, R. M.: "Ferromagnetism," pp. 477–546, D. Van Nostrand Company, Inc., New York, 1951.

7. Bloch, F.: Theory of the Exchange Problem and of Remanence in Ferromagnetics, *Z. Physik*, vol. 74, pp. 295–335, 1932.
8. Williams, H. J., R. M. Bozorth, and W. Shockley: Magnetic Domain Patterns on Single Crystals of Silicon Iron, *Phys. Rev.*, vol. 75, pp. 155–178, January, 1949.
9. Phillips, F. C.: "An Introduction to Crystallography," p. 41, Longmans, Green and Co., New York, 1956.
10. Bozorth, R. M.: "Ferromagnetism," p. 481, D. Van Nostrand Company, Inc. New York, 1951.
11. Bean, C., and D. Rodbell: Kinetics of Magnetization in Some Square-loop Magnetic Tapes, *J. Appl. Phys.*, vol. 26, pp. 124–125, January, 1955.
12. Friedlaender, F. J.: Flux Reversal in Magnetic Amplifier Cores, *Trans. AIEE*, vol. 75, part I, pp. 268–276, 1956.
13. Savitski, M. J.: Effects of Composition and Processing Variables on the Magnetic Properties of the 50% Nickel-Iron Alloy, *J. Appl. Phys.*, vol. 29, pp. 353–355, March, 1958.
14. Lauriente, M.: Magnesium Oxide Films as Magnetic Tape Insulation, *Insulation*, vol. 2, pp. 21-24, Nov. 1959.
15. Roberts, R. W., and R. I. Van Nice: Influence of ID/OD Ratio on Static and Dynamic Magnetic Properties of Toroidal Cores, *Trans. AIEE*, vol. 74, part I, pp. 599–607, 1955.
16. Harris, F. K.: "Electrical Measurements," pp. 362–370, John Wiley & Sons, Inc., New York, 1952.
17. Stewart, K. H.: "Ferromagnetic Domains," pp. 165–168, Cambridge University Press, Cambridge, England, 1954.
18. Cioffi, P. P.: A Recording Fluxmeter of High Accuracy and Sensitivity, *Review of Scientific Instruments*, vol. 21, pp. 624–668, 1950.
19. Both, E.: Static and Dynamic Magnetization Characteristics of Magnetic Amplifier Core Materials, T-78, AIEE Conference on Magnetism and Magnetic Materials, 1955.
20. Bozorth, R. M.: "Ferromagnetism," pp. 427–430, D. Van Nostrand Company, Inc., New York, 1951.
21. Gould, H. L. B., and D. H. Wenny: Supermendur, *Electrical Engineering*, vol. 76, pp. 208–211, 1957.
22. Maxwell, L. R.: What Is Ferrimagnetism? *Electrical Engineering*, vol. 73, pp. 804–806, 1954.
23. Williams, H. J., R. C. Sherwood, M. Goertz, and F. J. Schnettler: Stressed Ferrites Having Rectangular Hysteresis Loops, *Trans. AIEE*, vol. 72, pp. 531–536, 1953.
24. Sery, R. S., R. E. Fischell, and D. I. Gordon: Effects of Nuclear Irradiation on Magnetic Properties of Core materials, *NAVORD Rept.* 4381, 1956.
25. Hunter, L. P.: "Handbook of Semiconductor Electronics," p. 3-3, McGraw-Hill Book Company, Inc., New York, 1956.
26. Dekker, A. J.: "Solid State Physics," p. 348, Prentice-Hall, Inc., Englewood Cliffs, N.J., 1957.
27. Henisch, H.: "Metal Rectifiers," Clarendon Press, Oxford, 1949.
28. Gramels, J.: Problems to Consider in Applying Selenium Rectifiers, *Trans. AIEE*, vol. 72, part I, pp. 488–492, 1953.
29. McPherson, L. G.: Recovery Time of Switching Transients in Silicon Diodes, CP No. 58-941, AIEE Summer General Meeting, 1958.
30. Miglicco, P. S.: Radiation Effects on Electronic Components, *Electronic Equipment*, July, 1957.

3

Mechanics of Operation of Self-saturating Magnetic Amplifiers

As sections of the previous chapter indicated, it is difficult to predict accurately the average rate of change of flux in ferromagnetic materials under other than very restricted conditions. However, it is precisely this function which is most basic to magnetic-amplifier operation. To achieve an engineering approximation to this characteristic, attempts to relate it to either control current only or control voltage only have been made. In this chapter, it will be shown that except in extreme cases, either of these approaches alone is unsatisfactory, but that an amalgamation of the two yields reasonable answers.[1]

The single-core amplifier, while useful in gaining a first understanding of the mechanics of operation of magnetic amplifiers, is not commonly employed in actual practice. It can be considered as the basic building block for more complicated circuits, but such use almost invariably alters the operation in some manner. An understanding of the more complicated circuits, however, is much more easily gained if one is already familiar with the operation of single-core amplifiers. For that reason, the simplest circuit will be discussed before proceeding to more practical but more complicated core arrangements.

As the phenomena which occur in the circuits are treated in this chapter, the explanations will be descriptive to a large extent. The waveshapes of currents and voltages and a few generally governing equations will be used as aids in understanding the discussion only when they are at least reasonably rigorous. Although mathematical treatments are more easily understood by most engineers, experience has shown that an attempt to employ this method exclusively for magnetic amplifiers results ultimately in greater confusion because several of the assumptions necessary to allow a mathematical presentation are not justifiable. It is, therefore, felt that qualitative descriptions will result in fewer erroneous concepts and lead more directly to the mature use of measured quantities and the appreciation of advanced circuit behavior which constitute the "design know-how" so important to the worker in this field.

3-1. SINGLE-CORE MAGNETIC AMPLIFIER WITH A-C SIGNAL

The simplest type of self-saturating magnetic amplifier to describe is the single-core half-wave circuit patented by F. G. Logan in the 1930s.[2] While there are several variations of even this simple circuit, the configuration shown in Fig. 3-1*a* serves as an excellent vehicle for explaining the mechanics of operation.

The circuit of Fig. 3-1*a* contains two nonlinear elements, the reactor L_1 and the rectifier *REC*. To avoid introducing two nonlinearities at the same time in the discussion, switch Sw_3 has been included in the circuit. Circuit operation will be explained first with Sw_3 closed and Sw_1 open. The circuit is then reduced to a marked resemblance to the transformer primary circuit introduced in Chap. 1. One essential difference is that

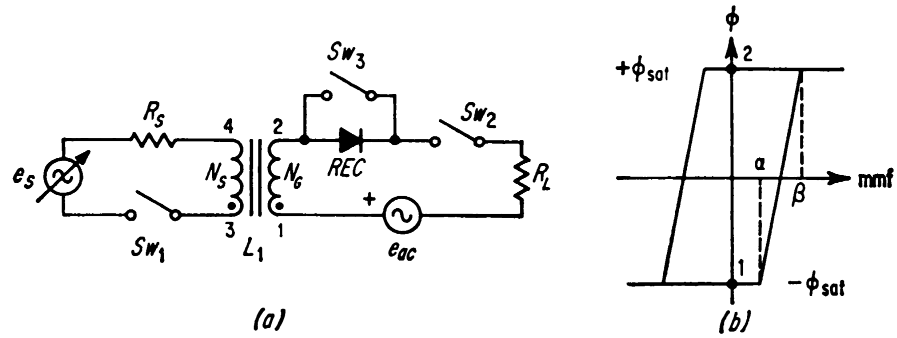

FIG. 3-1. Single-core magnetic amplifier. (*a*) Circuit diagram of a Logan amplifier; (*b*) assumed flux-mmf characteristic when Sw_2 and Sw_3 are closed.

the core material will now be allowed to saturate, a condition excluded from consideration in Chap. 1. The equations of operation will be written and discussed. Switch Sw_3 will then be opened and the effect of the unilateral properties of the diode examined. When the operation of the gating circuit has been explained, switch Sw_1 will be closed and the interaction of the signal and gating circuits will be discussed for the case in which the signal voltage e_S is zero and in which it is nonzero.

Signal Circuit Open. Consider the circuit of Fig. 3-1*a* with switch Sw_1 open and switches Sw_2 and Sw_3 closed. The applied voltage e_{ac} is assumed to be of the form $E_m \sin \omega t$.

The following equation may be written

$$e_{ac} = N_G\, d\phi/dt + iR_L \tag{3-1}$$

It is apparent that something must be known about the relationship between flux and current before anything further can be done with this equation. It will be assumed that laboratory measurements reveal that in this circuit the flux-mmf characteristic may be represented as in Fig. 3-1*b*. Before the piecewise linear technique can be applied, the time correspondence of the flux must be established. Lacking any further information concerning the relationship, one can use a rapidly converging cut and try method by postulating that, with Sw_3 closed, Sw_2 will be closed at the time that e_{ac} is zero, going from negative to positive. By choosing extreme values of ϕ and proceeding through the necessary number of half-cycles in each case, steady-state operation can be predicted.

It will first be assumed that flux is at point 1 on the flux-mmf characteristic at the time that Sw_2 is closed. The characteristic indicates that a threshold mmf equal to α must be established before flux starts to change. If α is in ampere-turns, the current which must flow to establish the required threshold mmf is given by

$$i_{L1} = \frac{\alpha}{N_G}$$

But if no flux is changing until $i_L = i_{L1}$, then from time zero until some unspecified time, Eq. (3-1) reduces to

$$e_{ac} = i_L R_L \tag{3-2}$$

Since e_{ac} is sinusoidal,

$$i_L = \frac{E_m}{R_L} \sin \omega t$$

and

$$i_{L1} = \frac{E_m}{R_L} \sin \omega t_1$$

Knowing the value of i_{L1} is α/N_G,

$$t_1 = \frac{1}{\omega} \sin^{-1} \frac{\alpha R_L}{N_G E_m} \tag{3-3}$$

After time t_1, flux bears a linear relationship to current,

$$\phi = k i_L - \frac{\alpha + \beta}{2}$$

and Eq. (3-1) becomes

$$E_m \sin \omega t = k N_G \frac{di_L}{dt} + i_L R_L$$

Solution of this differential equation yields

$$i_L(t) = \frac{1}{kN_G} \left\{ \frac{E_m}{(R_L/kN_G)^2 + \omega^2} \left[\exp\left(-R_L t/kN_G\right) - \cos \omega t + \frac{R_L}{k\omega N_G} \sin \omega t \right] + kN_G i_{L1} \exp\left(-R_L t N_G\right) \right\} \tag{3-4}$$

This expression can be awkward unless the assumption is made that kN_G is so large with respect to R_L that R_L/kN_G is very close to zero and exp (R_Lt/kN_G) may therefore be considered as unity. If this assumption is valid, then, for all reasonable power frequencies, $(R_L/kN_G)^2$ will certainly be negligible with respect to ω^2. Equation (3-4) may then be written as

$$i_L(t) = \frac{E_m}{kN_G^2}(1 - \cos \omega t) + i_{L1} \tag{3-5}$$

This equation will be valid until saturation is reached or the half-cycle of the applied voltage under consideration ends. The latter case is seldom purposely achieved in practical operation of self-saturating magnetic amplifiers since it frequently gives rise to a discontinuous transfer characteristic, as discussed in Chap. 8. Therefore, Eq. (3-5) will cease to be valid at some time t_2 when the flux reaches ϕ_{sat}, which determines i_{L2} as equal to β/N_G. To determine t_2

$$t_2 = \frac{1}{\omega}\cos^{-1}\left[1 - \frac{(\alpha - \beta)k\omega}{E_m}\right] \tag{3-6}$$

After saturation, Eq. (3-2) is valid once again until the half-cycle has ended and until flux starts to change in the negative direction. Since the flux-mmf characteristic is symmetrical, the same equations are valid in equivalent time intervals in the negative half-cycle and, at the beginning of the next positive half-cycle, flux is again at point 1 of Fig. 3-1*b*. Thus it is seen that, in two half-cycles, steady-state operation has been achieved, since the initial conditions for each successive cycle will be the same.

Had the initial condition of flux been at point 2 of the flux-mmf characteristic at the beginning of the first positive half-cycle, Eq. (3-2) would have been valid throughout the half-cycle, since there could have been no flux change. For the first negative half-cycle, however, conditions would still have been the same as in the first case, since the final value of current in the first positive half-cycle is a function of Eq. (3-2) regardless of the initial value of flux. Steady-state conditions will, therefore, be the same for both conditions. It is, then, obvious that if the flux has some intermediate initial value, the output during the first positive half-cycle will be a function of the initial value, but output after the termination of the first half-cycle will be unaffected by the initial flux condition. It can also be shown in an analogous manner that steady-state conditions are similarly independent of the time at which switch Sw_2 is closed.

The linearizations assumed are reasonable approximations to an actual material characteristic, except that no material can have a slope of zero in the saturated condition. A more accurate representation would be as shown in Fig. 3-2*a*. The inclusion of this practicality yields an equation similar in form to Eq. (3-4) for the initial and final periods. However, for most practical materials, the value of k valid in these periods is so low (about 0.0001 k used for the middle interval) that the time constant is extremely small and the phase shift between the zero crossings of voltage and current ($\Delta\theta$ in Fig. 3-2*b*) may be considered negligible for most computations. There is no doubt that neglect of this term can sometimes lead to erroneous results, but the complexity arising from its inclusion is definitely not compensated for by an appreciable increase in accuracy in the vast majority of the cases. For this reason it will be ignored throughout the remainder of this text. It is left to the practitioner to decide when it must be included.

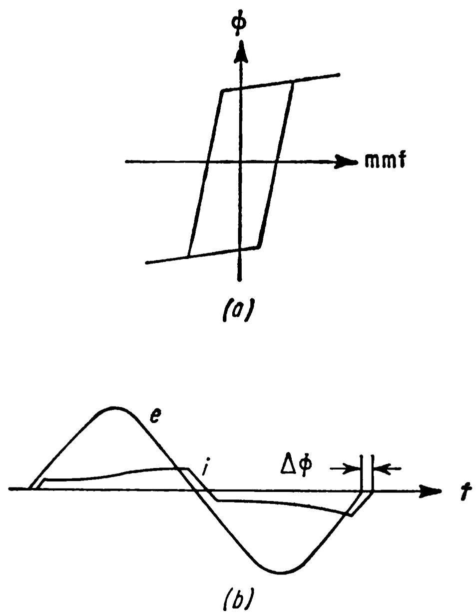

FIG. 3-2. Operation with less idealized material. (*a*) Assumed flux-mmf characteristic; (*b*) waveshapes of voltage and current.

The next step in analyzing magnetic-amplifier operation is to open switch Sw_3 of Fig. 3-1*a*. For the moment it will be assumed that the diode is ideal (zero forward resistance and infinite reverse resistance). If Sw_3 is opened during a positive half-cycle (that is, when the diode is conducting), opening the switch will have no effect until the half-cycle comes to an end. Throughout the negative half-cycle, the applied voltage appears across the diode and there is no flux change in the core during this period of time, since there is no negative mmf applied to the reactor. The beginning of the next positive half-cycle of applied voltage finds the flux at point 2 of the flux-mmf characteristic of Fig. 3-1*b* and all of the applied voltage appears across load resistor R_L since no flux change can occur in the core. The amplifier is often described as "in saturation" when these conditions are satisfied. Except under extreme signal conditions, the load voltage cannot be increased beyond the value it has at saturation. This is also the source of the term self-saturating magnetic-amplifier—with no signal applied, the load voltage is at its saturated condition. This establishes a steady-state condition for a single-core magnetic amplifier with the control or signal circuit open.

If the rectifier characteristic were assumed to be other than ideal, the results would be only somewhat different. If the forward resistance is other than zero, the rectifier and the load will share the applied voltage as the ratios of their resistances. That is,

$$e_{REC} = \frac{R_{REC}}{R_{REC} + R_L} e_{ac}$$

and

$$e_L = \frac{R_L}{R_{REC} + R_L} e_{ac}$$

As discussed in Chap. 2, the resistance of a suitable rectifier should not affect the load voltage appreciably except in extremely high-power low-voltage applications.

If silicon diodes having a virtual threshold are used, the threshold voltage must be much less than E_m or the threshold must be subtracted from e_{ac} before calculations are made. To avoid needless complications, it will be assumed here that E_m is much larger than the threshold. Particular cases where this assumption is not valid will be treated in appropriate sections later.

If the reverse resistance of the rectifier is not infinite, a "leakage" current will flow through the gate winding during the negative, or reset, half-cycle. Two cases may be distinguished when this condition exists. The first case occurs if the product of the instantaneous magnitude of this current and N_G (number of turns of the gate winding) exceeds the threshold mmf of the d-c hysteresis loop of the core material for some interval during the half-cycle. For this case, a flux change will occur in the reset half-cycle and a steady-state condition will exist, with the control circuit open, in which the amplifier is not quite saturated. Obviously, if the rectifying action is nearly nonexistent, the steady-state condition will approximate operation with Sw_3 closed. For most practical rectifiers, the amount of flux reset occurring without signal seldom exceeds 10 per cent of twice ϕ_{sat}. The second of the two cases is obtained if the product of the instantaneous magnitude of the leakage current and N_G does not exceed the threshold mmf of the d-c hysteresis loop. In this case, no flux change is obtained during the reset half-cycle in the absence of signal, and no-signal operation is essentially the same as for the case in which an ideal rectifier is used. The existence of such a small leakage current will, however, affect operation when the control circuit is closed and signal is applied. Modern rectifiers have such high reverse resistance that the leakage currents may properly be ignored in the present analysis. In the discussions that follow in the present chapter, therefore, rectifier leakage will be discussed only where such discussion is appropriate. A more complete discussion of rectifier leakage will be reserved for Chap. 8.

Signal Circuit Closed. If switch Sw_1 is closed, with e_S zero, no change in circuit operation is observed if leakage current of the rectifier is negligible. During the gating half-cycle, a voltage will appear across terminals 3 and 4 of the reactor in the period during which flux in the core is changing back to positive saturation. This voltage will be $e_{ac}N_S/N_G$ (the voltage drop across R_L due to magnetizing current will be assumed negligible with respect to E_m). A current will flow in the control circuit, $e_{ac}N_S/N_GR_S$, and this, in turn, will add to the magnetizing current of the gate circuit an amount $(N_S/N_G)^2e_{ac}/R_S$. During periods of flux change either in the positive or negative half-cycle, the operation is identical with operation of the nonideal transformer described in Sec. 1-3. It must be borne in mind, however, that while during the positive half-cycle the circuit behaves like a transformer with a low primary resistance, during the negative half-cycle the primary resistance (which now includes the reverse resistance of the rectifier) is much larger than the magnetizing impedance. Any finite secondary impedance, therefore, decreases the voltage across the primary terminals and thus limits the amount of flux reset during the negative half-cycle. The important point at this state of analysis, however, is not so much the quantitative effects of control-circuit resistance (although these will be shown to be quite important in a later section) as the fact that the control and gate circuits are coupled *only* during periods of flux change in the core. If flux is not changing, the two circuits cannot interact. This may seem obvious but it is surprising how often this truism is forgotten in a complicated analysis, particularly in its converse sense that, if interaction exists, flux must be changing.

Before considering circuit operation when e_S is not zero, it may be profitable to perform a mental exercise and consider a transformer with zero primary and secondary resistance, a primary voltage source e_1, and a secondary voltage source N_2e_1/N_1. If the core material has a rectangular characteristic as discussed in Chap. 1 in connection with Figs. 1-1*b* and 1-3, what will the secondary and primary currents be if the core material is not allowed to saturate? If the secondary circuit were open, the primary current would be a function of N_1. To reduce the amount of thought required in these mental gymnastics let it be assumed that the primary current under these conditions can be represented by an expression p/N_1. Then, if the primary circuit were open but the secondary circuit closed, the secondary current would be p/N_2. If the two voltage sources are of exactly the same phase and frequency and if the two circuits are closed at exactly the same time, will each of the two circuits provide one-half of the mmf required to change flux in the core or will one provide all the mmf and the other none? Obviously, the current in the primary cannot be p/N_1 and the current in the secondary

p/N_2 since this would provide twice the mmf enforced by the flux-mmf characteristic. The problem as stated is somewhat analogous to the venerable postulate of the irresistible force and the immovable object or, perhaps, the relative precedence of the chicken and the egg.

To reduce the problem to a more tractable condition, let it be assumed that some resistance exists in each circuit. If resistance is present, there must be some time in the cycle of supply voltage when the two circuits are decoupled because no flux is changing. The equivalent circuit for the decoupled condition is shown in Fig. 3-3*a* and that for the coupled condition in Fig. 3-3*b*.

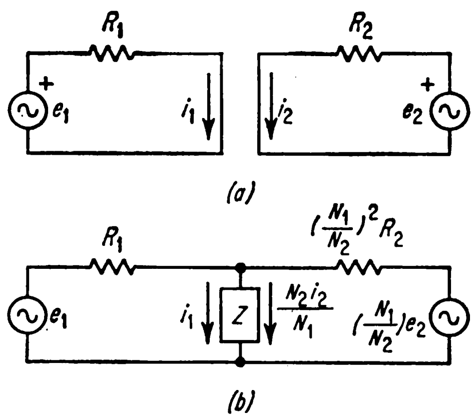

FIG. 3-3. Equivalent circuits for transformer with two active sources. (*a*) Primary and secondary decoupled; (*b*) primary and secondary coupled.

For Fig. 3-3*a*, the limiting condition is that the circuits become coupled when $i_1N_1 + i_2N_2 = p$, the threshold mmf of the core material. At this instant, the following equations may be written:

$$e_1 = i_1R_1 \qquad e_2 = i_2R_2$$

and, at the threshold,

$$i_1N_1 + i_2N_2 = p$$

From these equations and the assumption that the voltages are sinusoidal, the time t_1 at which coupling starts can be found:

$$t_1 = \frac{1}{\omega} \sin^{-1} \frac{pR_1R_2}{N_2E_{2m}R_1 + N_1E_{1m}R_2} \tag{3-7}$$

where E_{2m} is the maximum instantaneous value of e_2 and E_{1m} is the maximum instantaneous value of e_1. After t_1, $e_1 = (N_1/N_2)(e_2 - i_2R_2) + i_1R_1$ and, using the mmf equation,

$$i_1 = \frac{e_1 - e_2(N_1/N_2) + (N_1/N_2)(p/N_2)R_2}{R_1 + (N_1/N_2)^2R_2} \tag{3-8}$$

Equation (3-8) confirms the indeterminacy of currents when R_1 and R_2 are both zero. If $e_1 = N_1e_2/N_2$ in the resistanceless case, both numerator and denominator are zero. If $e_1 \neq N_1e_2/N_2$, both currents become infinite. This, of course, is a trivial case, but it is often comforting to know that an equation can be made to confirm intuitive conceptions in a limiting case. If $e_1 = e_2N_1/N_2$ and R_1 and R_2 are not zero, i_1 is a function of resistance and number of turns only. If R_2 were zero in this case, i_1 would also be zero. This means, simply, that e_2 would then supply all of the magnetizing current. The more general (and much more significant) case when $e_1 \neq N_1e_2/N_2$ and R_2 is nonzero is also more difficult of analytic reasoning. It can be shown that conditions may be set up to cause either current to reverse direction after time t_1, in which case the source supplying the negative current is absorbing energy rather than delivering it. The expression for i_1, however, is a function of too many variables to allow much generalization.

Returning, now, to the circuit of Fig. 3-1*a*, assume that e_S has some small nonzero value and let switch Sw_1 be closed at the time that e_{ac} is just starting a positive half-cycle after steady state has been established with the control circuit open. For simplicity, it will be assumed that e_S and e_{ac} are of the same frequency and phase. In this case, e_S will also be starting a positive half-cycle at the time that Sw_1 is closed. In a Logan circuit as usually applied, R_S will be greater than R_L, N_G greater than N_S, and it has already been assumed that e_S is much less than $e_{ac}N_S/N_G$. All three of these conditions tend to increase the percentage of the magnetizing current supplied by e_{ac}. This is not important in the first cycle after Sw_1 is closed, since the initial condition of flux is at positive ϕ_{sat}, but it becomes important in the ensuing positive half-cycles. Considering the first positive half-cycle, flux is initially at positive ϕ_{sat} and the control and gating circuits are decoupled. During this time, therefore, $i_S = e_S/R_S$ and $i_L = e_{ac}/R_L$. At the end of the first positive half-cycle, flux is still at positive ϕ_{sat} and both currents are zero. As the negative half-cycle starts, the rectifier prevents the flow of load current i_L, and current starts to flow in the control circuit. If the signal voltage is large enough, a point will be reached during this half-cycle when e_SN_S/R_S exceeds the threshold ampere-turns and flux will start to change. Flux will continue changing until i_SN_S falls below the ampere-turns required to maintain flux change. After the time that this occurs, i_S is once again equal to e_S/R_S.

If the threshold ampere-turns are exceeded only during a short interval in the neighborhood of $\pi/2$ radians in the negative half-cycle, the total flux change must be relatively small

$$\Delta\phi = \frac{1}{\omega N_S} \int_{\omega t=\pi/2^-}^{\omega t=\pi/2^+} (e_S - i_SR_S)\, d\omega t \tag{3-9}$$

Not only does flux change for only a short time, but the difference between e_S and i_SR_S is small, the combination of both conditions resulting in a very small flux change. It is important to note that, since e_S is less than $e_{ac}N_S/N_G$, as specified previously, the voltage appearing across the gate-winding terminals as a result of e_S must be less than e_{ac} and, therefore, it cannot cause current to flow in the gate circuit.

During the next positive half-cycle, the threshold ampere-turns will be established (largely as a function of e_{ac} as previously explained) and flux will begin to change. Since R_L is fairly small, the component of voltage drop $i_L R_L$ due to the magnetizing current component of i_L will be small and the voltage transformed into the control circuit will be nearly $e_{ac} N_S/N_G$. Since this value is larger than e_S, a negative current will flow in the control circuit with a value, from Eq. (3-8)

$$i_S = \frac{e_S - e_{ac}(N_S/N_G) + (N_S/N_G)R_L i_{mG}}{R_S + (N_S/N_G)^2 R_L} \tag{3-10}$$

The expression p/N_2 of Eq. (3-8) has been replaced by i_{mG}, the magnetizing current referred to the gate winding, since the equation was derived for a vertical-sided loop and the material of Fig. 3-1*b* has a finite slope. The rigor of the derivation is unaffected, but an additional variable has been introduced. The additional component of current, due to the current induced into the control winding, will cause an additional voltage drop across R_L. However, when R_L and R_S have practical values, this is only a second-order effect. It is now apparent why it was previously stated that, in a Logan circuit as usually applied, R_S will be greater than R_L and N_G greater than N_S. These conditions are imposed simply to limit the power dissipated while flux is changing. It will be shown later how this condition affects the control of load power by the signal.

Since the flux change during reset in the negative half-cycle was small, flux will change for only a very short time in the positive half-cycle before ϕ_{sat} is reached and the circuits become decoupled. The reactor is said to have "fired" at this time. (The term "fired" will be recognized as one borrowed from the field of thyratrons. The output waveshape of a half-wave magnetic amplifier bears a strong resemblance to that of the thyratron.) All of the voltage e_{ac} will now appear across R_L. When ϕ_{sat} is reached and the circuits are decoupled, the signal circuit current becomes positive once again and stays positive until the end of the half-cycle.

If e_S is now increased, all other independent parameters remaining constant, the current required to establish the threshold ampere-turns is reached earlier in the negative, or reset, half-cycle. The time interval during which flux is changing in a negative direction, therefore, is becoming longer and, at the same time, the magnitude of the voltage difference, $e_S - i_S R_S$, is increasing. Both effects contribute to a larger amount of flux reset. A larger flux reset causes e_{ac} to take longer to drive flux back to positive ϕ_{sat} in the gating half-cycle and delays the firing of the reactor and the appearance of e_{ac} across R_L, resulting in a smaller average load voltage. Thus it is seen that the average load voltage E_L is a function of the magnitude of the signal voltage e_S. Ideally, e_S could be increased sufficiently to reset the flux completely to negative ϕ_{sat}, and E_L would then approach a minimum value. Before this minimum is reached, however, a change in operating conditions occurs. The waveshapes of e_{ac}, e_{NG}, and e_{REC} are shown in Fig. 3-4 for the type of operation just discussed.

It is almost (but not entirely) invariant practice to design the gate winding of a magnetic amplifier according to the criterion

$$N_G = \frac{E_{ac}}{4.44 f \phi_{sat}} \tag{3-11}$$

where E_{ac} is the effective value of e_{ac} (if e_{ac} is sinusoidal) in volts and f is the frequency of e_{ac} in cycles per second. Equation (3-11) imposes the

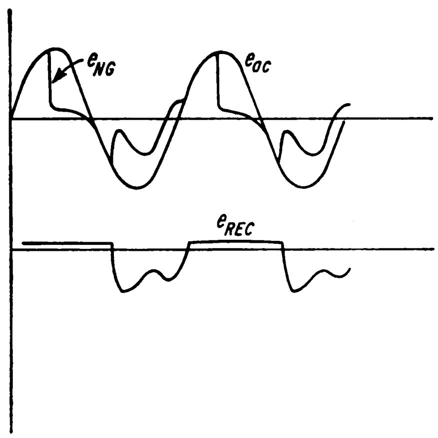

FIG. 3-4. Waveshapes in a-c controlled Logan amplifier.

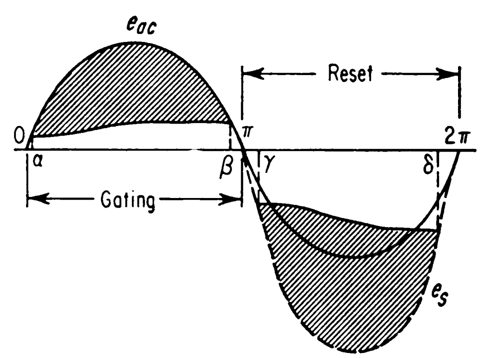

FIG. 3-5. Idealized volt-second areas in a-c controlled Logan amplifier.

restriction that, if flux is at $-\phi_{sat}$ at the beginning of a positive half-cycle, flux will just reach $+\phi_{sat}$ as the half-cycle ends. This may be expressed another way:

$$2\phi_{sat} = \frac{1}{\omega N_G} \int_{\omega t=0}^{\omega t=\pi} E_m \sin \omega t \, d\omega t$$

If this restriction is observed, a maximum volts/turn ratio is established. If e_S is increased until e_S/N_S exceeds the gate-circuit volts/turn ratio so established, the signal source may supply energy to the gate circuit during the reset half-cycle. Consider the conditions of Fig. 3-5. It will be assumed that e_S has been raised to the point where it is capable of resetting flux to $-\phi_{sat}$. During the gating half-cycle the flux starts to change at the angle α and reaches $+\phi_{sat}$ at the angle β. Both α and β are assumed negligibly close to zero and π, respectively.

This flux change required the application of a volt-second area, shown shaded in the figure. In the negative half-cycle, flux will not start to change until the angle γ is reached. Because N_S is less than N_G, the magnetizing current is larger than would be required in the gate circuit and, additionally, R_S is larger than R_L. These two conditions combine to make $(\gamma - \pi)$ greater than α. The same conditions will also cause

$(2\pi - \delta)$ to be greater than $(\pi - \beta)$. It is seen then that, if the time during which flux may change is reduced, the volts/turn applied must be increased to arrive at equal volt-seconds/turn areas and equal flux changes. But, if the volts/turn applied by e_S during reset exceeds e_{ac}/N_G, this implies that current must flow in the gate circuit during the reset half-cycle. Conduction of the rectifier in the reset half-cycle, when it would appear from examination of the gate circuit only that the rectifier should block current flow, is often termed "backfiring." The waveshapes of e_{ac}, e_{NG}, and e_{REC} are shown in Fig. 3-6 for the condition of pronounced backfiring.

When backfiring occurs, additional current flows in the control circuit to supply the energy now being dissipated in the gate circuit. This causes an increased voltage drop across the control-circuit resistance,

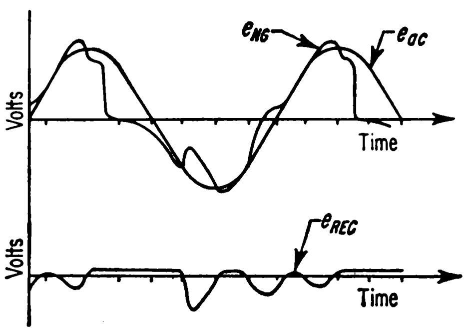

FIG. 3-6. Waveshapes in a-c controlled Logan amplifier with pronounced backfiring.

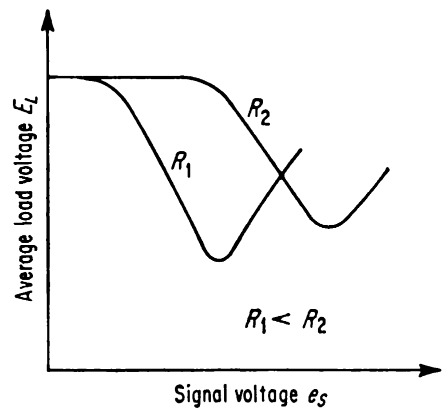

FIG. 3-7. Control characteristic of an a-c controlled Logan amplifier for two values of R_S.

resulting in a decreased efficiency in transforming the volt-seconds available at the signal-source terminals into flux change. In addition to this efficiency decrease, flow of load current during the reset half-cycle raises the average value of the load voltage. This occurs at the time that the signal voltage is being raised in order to decrease the average load voltage. Normally, it is possible to continue decreasing the average load voltage as e_S is raised for some time after backfiring first appears. Eventually, though, output voltage will start to rise with continued increase in signal voltage. Figure 3-7 presents the variation of average load voltage as a function of the effective value of e_S for two typical values of R_S. Such a presentation is called a "control characteristic."

3-2. SINGLE-CORE MAGNETIC AMPLIFIER WITH D-C SIGNAL

The operation of the Logan circuit with d-c control differs in some respects from operation with control by an a-c signal of supply frequency and phase. It must be recognized that the term "d-c signal" is somewhat a misnomer. If by d-c one means a *constant* current, then the expression "d-c signal" is a contradiction. Use of the term "signal" implies that information is to be transmitted. But a constant parameter can contain no information. The information is contained in the changes of the parameter which may then be constant between changes. In the case of d-c signal this is really what is meant. The term usually implies a slowly varying or a step-change unidirectional voltage or current. If step changes are allowed, they usually have a low repetition rate. When a static-control characteristic is spoken of, the term refers to the locus of the output magnitude as the input function is varied in steps, the output being read after steady state is established following each change in input. The same reasoning really applies to the case of an a-c signal of supply frequency and phase. The information in this case is in the form of a modulation impressed upon what is essentially a carrier. The sinusoidal variation of the signal voltage at supply frequency transmits no information.

With this point clarified, consider the circuit of Fig. 3-8*a*. The only changes made from Fig. 3-1*a* are in the control circuit. Here a d-c source replaces the previous a-c source and the positive direction of current has been reversed. If E_S is zero, the operation of the circuit is identical with the operation previously described for the condition of e_S zero. However, let E_S have some small, nonzero magnitude (large enough that E_SN_S/R_S exceeds the threshold mmf of the core) and let the initial flux condition be at $-\phi_{sat}$. The material characteristic of Fig. 3-1*b* will be assumed to apply here also. If switch Sw_1 is closed as e_{ac} begins a positive half-cycle, $t = t_0$ in Fig. 3-8*b*, the control current i_S will jump instantaneously to its steady-state value, E_S/R_S. The load current will also have its steady-state value, e_{ac}/R_L, but e_{ac} is zero at the time Sw_1 is closed. Instantaneously, then, the mmf on the core is $-N_SE_S/R_S$. Since flux was assumed at $-\phi_{sat}$, it cannot change in the negative direction, regardless of the magnitude of the negative mmf. As time progresses, e_{ac} increases in the positive sense and i_L increases also. At some time, if the magnitudes of E_S, R_S, e_{ac}, R_L, and threshold ampere-turns allow, i_L will produce sufficient mmf to exceed the sum of threshold ampere-turns and N_SE_S/R_S. At this time t_1, flux will begin to change toward $+\phi_{sat}$.

As flux changes, i_S increases to $(E_S/R_S) + N_S(e_{ac} - i_LR_L)/N_GR_S$, which is larger than its steady-state value. If the magnitude of e_{ac} is sufficient, e_{ac} will supply the losses in R_L and still drive the flux from negative to positive saturation by the end of the gating half-cycle. At some time t_2 before the positive half-cycle ends, by proper choice of the magnitude of e_{ac}, flux will reach $+\phi_{sat}$ at the time that e_{ac}/R_L equals

β/N_G plus $N_S E_S/N_G R_S$. After this time, flux can no longer change and the two circuits are decoupled, the two currents assuming their respective steady-state values. As the load current decreases, it will eventually have a value equal to $N_S E_S/N_G R_S$. At this instant of time, the mmf of the core is zero. Further decrease of i_L results in an increasing negative mmf which will, before the half-cycle ends, exceed the threshold mmf

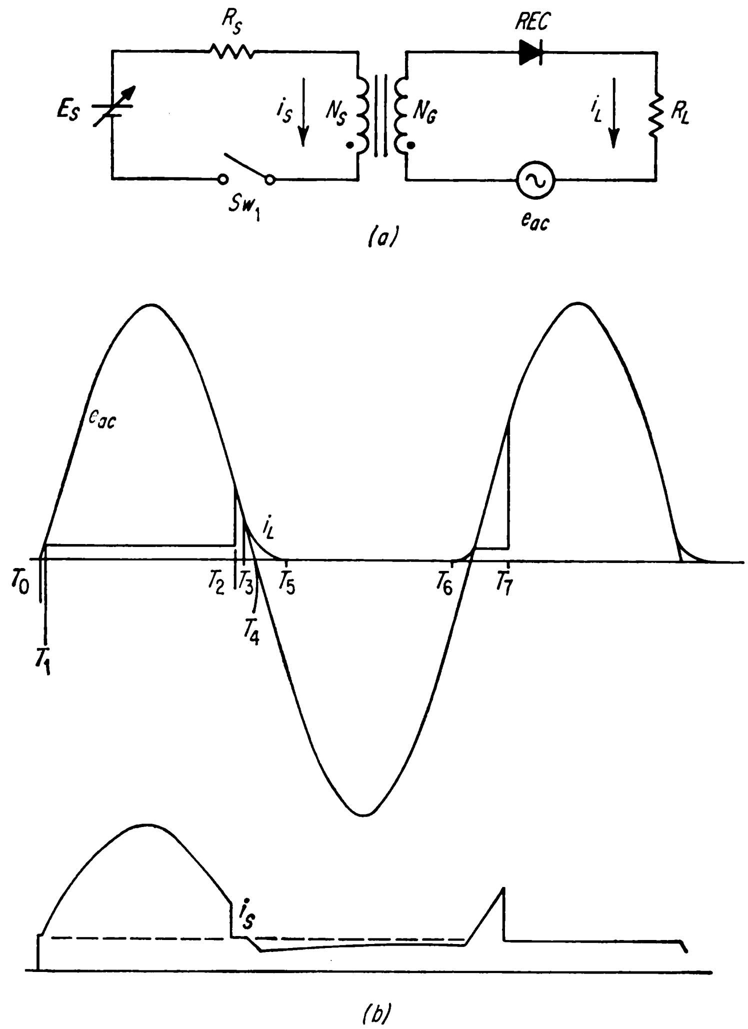

FIG. 3-8. D-c controlled Logan amplifier. (*a*) Circuit diagram; (*b*) waveforms.

of the core. At this time t_3, flux starts to change in a negative direction, resulting in a voltage appearing across the gate-circuit terminals of the reactor in a direction to increase i_L. The corresponding voltage appearing at the control-circuit terminals of the reactor is in a direction to decrease i_S. These conditions are maintained as e_{ac} passes through zero, time t_4, and starts to increase in the negative direction. The appearances of the waveshapes in this interval are considerably influenced by the squareness (B_r/B_m ratio) of the actual core material used.

Since i_L is still flowing at the start of the reset half-cycle, backfiring exists and will continue until e_{ac} exceeds the voltage at the gate-circuit terminals of the reactor. The voltage appearing at the reactor terminals will be primarily a function of the amount by which $E_S N_S/R_S$ exceeds the threshold mmf and, secondarily, since the rectifier is backfiring, a function of R_S and R_L. Since E_S was initially assumed small, the reactor-terminal voltage may be assumed small and it can be concluded that e_{ac} will be larger than the reactor-terminal voltage within a few tenths of a radian after the beginning of the reset half-cycle. Backfiring ceases at this time t_5, i_L is zero, and attention can be concentrated on events occurring in the signal circuit.

It was previously stated that the voltage appearing across the signal-circuit reactor terminals because of flux change is in a direction to decrease i_S. It will be recognized that this decrease cannot result in an i_S less than that required to cause flux to change since the reactor-terminal voltage is required to keep i_S below the value of $N_S E_S/R_S$. Since the voltage is proportional to the rate of change of flux and this quantity, in turn, is a function of the difference between the actual mmf (or "exciting" mmf) and the threshold mmf, the current tends to remain constant. This results from the initial assumption that E_S is a d-c voltage. If the reactor-terminal voltage tends to decrease because of a decrease in the rate of change of flux, the current tends to rise, causing an increased rate of change of flux and restoring the reactor-terminal voltage toward its previous value.

Since E_S was assumed small, the total change of flux during the reset half-cycle will be considerably less than twice ϕ_{sat}. Since the core does not saturate, the conditions outlined above (that is, a reasonably constant current causing a reasonably constant rate of change of flux) will be maintained until the reset half-cycle is nearly ended. Just before the end of the half-cycle, t_6, the instantaneous magnitude of e_{ac} will be less than the voltage appearing at the gate-circuit reactor terminals and backfiring will occur.[3] Because of the additional current appearing in the control circuit (which, since the additional negative ampere-turns are negated by a corresponding positive mmf in the gate circuit, does not increase $d\phi/dt$), the voltage drop across R_S increases and the rate of change of flux decreases. Eventually, e_{ac} passes through zero and attains a magnitude sufficient to cause an mmf in excess of the value of mmf required to cause a flux change in the positive direction.

The operation after this point in time is identical with the operation described for the first positive half-cycle while flux is changing. However, it was assumed for heuristic reasons that the flux condition was

$-\phi_{sat}$ at the time that Sw_1 was closed. It is seen that this is not a steady-state condition, since the next gating half-cycle starts with flux much closer to $+\phi_{sat}$. Since the flux change permitted ($+\phi_{sat} - \phi_i$, where ϕ_i is the flux level at the start of a gating half-cycle) is much less than twice ϕ_{sat}, the flux will reach $+\phi_{sat}$ quite early in this gating half-cycle, time t_7, and i_L will attain its steady-state value of e_{ac}/R_L and will maintain it until, almost at the end of the gating half-cycle, flux starts to change in the negative direction as previously described. Now a steady-state operating condition has been established, since events will repeat themselves with a period equivalent to one cycle of the supply frequency.

If E_S is increased, a new value of E_S/R_S is established, the difference between exciting and threshold mmf is increased, and a new value of $d\phi/dt$ is achieved during the reset half-cycle. The total flux change occurring in the reset half-cycle is, therefore, larger and, correspondingly, e_{ac} will appear across R_L later in the gating half-cycle. Since E_S is now larger than previously, the time during which backfiring occurs will be longer than the few tenths of a radian previously postulated. Let it be assumed, now, that E_S is increased until flux just achieves the level of $-\phi_{sat}$ before it starts to change in the positive direction. If reasonable values have been chosen for the various circuit and core parameters, flux will start to change in the positive direction quite soon after the start of a gating half-cycle and will not start to change in the negative direction until very late in the gating half-cycle. These restrictions limit the time interval during which flux can change in the negative direction to a period very nearly equivalent to that of a half-cycle of supply frequency. This means that the *average* rate of change of flux during reset must be very close to the *average* rate of change of flux during gating. But it has been seen that backfiring tends to limit the rate of change of flux during reset to an instantaneous value not much in excess of that which would result from application of e_{ac} to the gate terminals. Since e_{ac} causes flux change during gating and limits the rate of flux change during reset, it can be assumed that the flux-mmf characteristic traversed when E_S has the exact value required to completely reset flux is nearly identical with the characteristic which would be obtained by applying e_{ac} to the gate winding with the control circuit open and the rectifier shorted. This, if the value of R_L is reasonable, is equivalent to the so-called sine-flux hysteresis loop.

This equivalence, in years past, led to the assumption that the gain of a magnetic amplifier could be predicted by measuring the width of the sine-flux hysteresis loop taken at the supply frequency. The subject of bias will be discussed fully in a later section of this chapter but it will be introduced briefly here to point out the fallacy of such an assumption. It has been shown that no reset can occur unless the value of E_S is sufficient to make $E_S N_S/R_S$ larger than the threshold ampere-turns. If this value of signal voltage could be supplied from some other source, then the amplifier would be "biased" to some point called the "knee" of the control characteristic. The maximum signal voltage required in this case would be the difference between the amount found necessary to just drive flux to $-\phi_{sat}$ during reset and the amount necessary to just exceed the threshold mmf when bias is absent. Thus, the gain of an amplifier with d-c signal is found to be some function of the maximum half-width of a sine-flux hysteresis loop and the threshold mmf.

3-3. SINGLE-CORE MAGNETIC AMPLIFIER WITH RESET SOURCE IN SIGNAL CIRCUIT

Another single-core magnetic-amplifier circuit was disclosed by R. A. Ramey in 1951.[4] The basic circuit is shown in Fig. 3-9. The gate circuit is identical with that of the Logan circuit but the control circuit differs by the addition of voltage source e_r and rectifier REC_2. The primary functional difference between the two circuits is that whereas in the Logan circuit a signal voltage supplied the power necessary for reset of core flux, in the Ramey circuit a signal parameter (not necessarily a voltage) controls the reset power supplied by the source e_r.

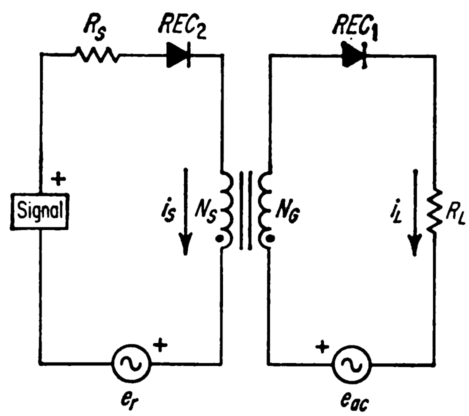

FIG. 3-9. Circuit diagram of single-core amplifier with reset source in signal circuit.

When the signal of Fig. 3-9 is zero, operation is identical with the a-c signal Logan circuit when signal to the latter is large enough to produce nearly complete reset. That is, the magnitude of e_r is nearly equal to $N_S e_{ac}/N_G$. It is desirable in the Ramey circuit to have R_S as small as possible when the signal is zero. If R_S is small and e_r is nearly equal to $N_S e_{ac}/N_G$, the current in the control circuit i_S will be small in the gating half-cycle, since it will be $(e_r - N_S e_{ac}/N_G)/R_S$. On the reset half-cycle, i_S will be the magnetizing current of the signal winding.

The signal source of Fig. 3-9 is shown as a block because it can take various forms. It can, for instance, be a d-c voltage, an a-c voltage, or a variable impedance. Suppose, for example, that the signal is a resistance, variable continuously between zero ohms and many megohms. When the resistance is zero, the reactor is almost completely reset each half-cycle. When the resistance is extremely high, the threshold ampere-turns cannot be supplied by e_r and no reset takes place. Obviously, for some intermediate value of resistance, partial reset may occur. If the variable resistance is a potentiometer, then the value of load voltage is a function of the potentiometer shaft position. In this case the input power is simply the power necessary to turn the shaft.

In most applications, however, the input is not mechanical position. If the input is an a-c signal 180° out of phase with e_r, operation reduces to the Logan circuit with a-c signal and low control-circuit resistance, but with one difference. This difference can be illustrated by considering a reset-inhibiting signal sufficient to cause the reactor to fire at an angle of $\pi/2$ in the gating half-cycle. During the gating half-cycle, while the circuits are coupled, the control current can be approximated by

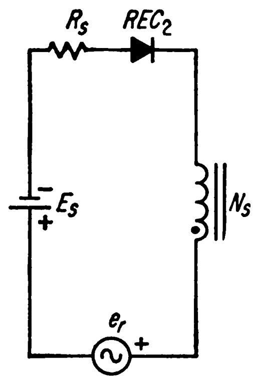

FIG. 3-10. Signal-circuit diagram for d-c controlled Ramey amplifier.

$$i_S = \frac{e_S - e_r + N_S e_{ac}/N_G}{R_S} \tag{3-12}$$

if the voltage drop across R_L is neglected. Since e_r is nearly equal to $N_S e_{ac}/N_G$, the current becomes, to a close approximation,

$$i_S = \frac{e_S}{R_S}$$

After firing, however, the circuits are decoupled and

$$i_S = \frac{e_S - e_r}{R_S}$$

Since e_r is greater than e_S, i_S would be negative if it were not for the presence of the rectifier REC_2. This rectifier prevents the flow of current in the negative direction. The rectifier is usually shown in Ramey-type circuits, but is a practical requirement only in the case of a d-c signal.

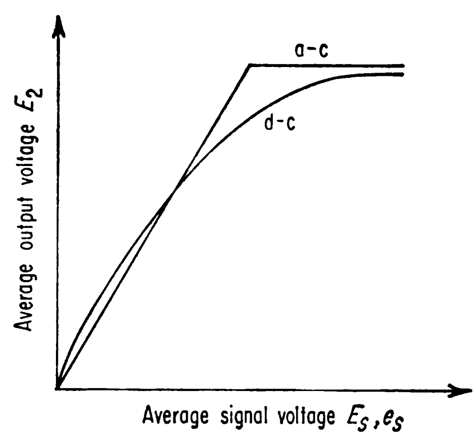

FIG. 3-11. Comparison of d-c signal and a-c signal control characteristics for Ramey amplifier.

When the signal is d-c, the control circuit is as shown in Fig. 3-10, with the polarities indicated for the gating half-cycle. The two voltages, E_S and e_r, now add, rather than subtract as in the a-c case, and the current could assume quite large negative values were it not for the rectifier. The use of a d-c signal also presents a difficulty in achieving an output which varies linearly with signal magnitude. If R_S is small, essentially all of the volt-seconds contained in e_r are available to reset flux with zero signal. As signal is increased, however, reset will occur only during the interval that e_r exceeds E_S. Since E_S is essentially constant over a half-cycle of e_r, and e_r is assumed sinusoidal, equal increments of E_S will not result in equal decrements of flux change. A unit change of E_S will be most effective in inhibiting reset at low values of E_S and least effective as the maximum value E_{rm} of e_r is approached. The resulting control characteristic is shown in Fig. 3-11 and is compared with the characteristic obtained with a modulated a-c signal. The linearity of the d-c characteristic is seen to be inferior to that obtained with an a-c signal.

3-4. COMPARISON OF LOGAN AND RAMEY SINGLE-CORE CIRCUITS

One of the implications made in the discussion of the Logan circuit was that the resistance of the control circuit, R_S, should be large. It was stated in discussing the Ramey circuit that R_S should be as small as possible. The effects of control-circuit resistance in both types of circuit will now be discussed in somewhat more detail.

Consider the circuit of Fig. 3-8. If $R_S(N_G/N_S)^2 = R_L$, then during the time that flux is changing in the gating half-cycle, i_L will equal $i_{mG} + e_{ac}/2R_L$. But, after firing, $i_L = e_{ac}/R_L$, or what may be termed the resistance-limited condition. If the reactor never fires, therefore, the average load voltage, neglecting exciting current, is

$$\begin{aligned} E_L &= \frac{1}{2\pi} \int_{t=0}^{t=\pi/\omega} i_L R_L \, dt = \frac{1}{2\pi} \int_{t=0}^{t=\pi/\omega} \frac{e_{ac} R_L}{2R_L} \, dt \\ &= \frac{E_m}{\pi} \end{aligned}$$

This is the minimum value of E_L which can be obtained, regardless of the value of E_S, and is one-half the maximum possible output. Variation of E_S, then, can only vary E_L from its maximum value to one-half its maximum. With R_S infinite, however, E_L may be varied from its maximum value to zero if exciting current is neglected. If R_S is zero, no variation in E_L is possible, regardless of the value of E_S. The effect of R_S is illustrated in Fig. 3-12 for a d-c signal circuit. Reducing R_S from R_2 to R_1 decreases the total variation in load voltage from ΔE_{L2} to ΔE_{L1}. Comparison of the curves of Fig. 3-12 with those of Fig. 3-7, which were obtained with the Logan circuit using an a-c signal, reveals that the effect of a variation in R_S has an opposite effect on ΔE_L in the two cases. However, while ΔE_L approaches zero at an increasing rate as R_S approaches zero for the case of the Ramey circuit with d-c signal,

ΔE_L approaches zero at a decreasing rate as R_S approaches infinity in the case of the Logan circuit with a-c signal.

It was found that, except for the current limiting action of the rectifier, the mechanics of operation of the Ramey circuit with a-c signal was equivalent to that of the Logan circuit with a-c signal. It is seen, then, that to obtain a reasonable range of output voltage, R_S must be small. However, where the signal is obtained from a practical signal source, the output impedance of the source must be included in R_S. A low output impedance implies a large power-handling capability. In most cases in which an amplifier is employed, the power-handling capability of the source is limited, from which it may be inferred that the output impedance is not low. It is not possible to set down hard and fast rules governing the efficient use of a Ramey-type amplifier with a-c signal, but it should be pointed out that while a range of conditions exists where the circuit has sufficient advantage to justify the additional complexity of e_r and REC_2, use of the circuit should not be made indiscriminately. Consideration must be given to the effect of source impedance and the possibility, if the source has sufficient output power, of obtaining the required voltage or current gain with a transformer rather than an amplifier.

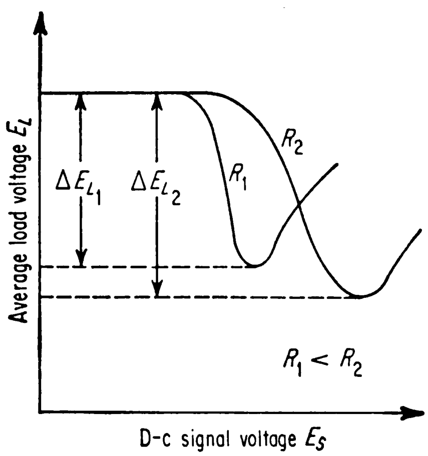

FIG. 3-12. Control characteristic of a d-c controlled Ramey amplifier for two values of R_S.

When a d-c signal is used, the two circuits are less similar. The maximum average signal current which can flow in a Logan circuit is simply $E_{S_{\max}}/R_S$. This maximum will occur, obviously, when E_S is maximum. In a Ramey circuit, assuming $e_r = N_S e_{ac}/N_G$ and R_S small, the maximum average signal current will be one-half of the average reset current. This maximum current, in contrast with the Logan circuit, will occur when E_S is zero. It should be clear that, since no signal-circuit rectifier is present in the Logan circuit, and since a reactor winding cannot sustain a steady-state d-c voltage, the d-c, or average, current must be E_S/R_S. In the Ramey circuit, no such concise statement can be made. Both reset and gating half-cycles must be considered separately. The polarities existing in the signal circuit for three distinct time periods are shown in Fig. 3-13 with the corresponding voltage waveforms. The polarities existing during the gating half-cycle prior to the firing of the reactor are shown in Fig. 3-13a, while the postfiring period is shown in Fig. 3-13b. The gating half-cycle is treated as one period rather than two to clarify the waveshapes existing during this time, as shown in Fig. 3-13*d* to *g*. The waveshapes during the reset half-cycle are shown in Fig. 3-13*h* to *k*. The current in the signal circuit must be the voltage across the signal-circuit resistance divided by the value of the resistance, e_{RS}/R_S. The magnitude of e_{RS}/R_S must be zero during the gating half-cycle and

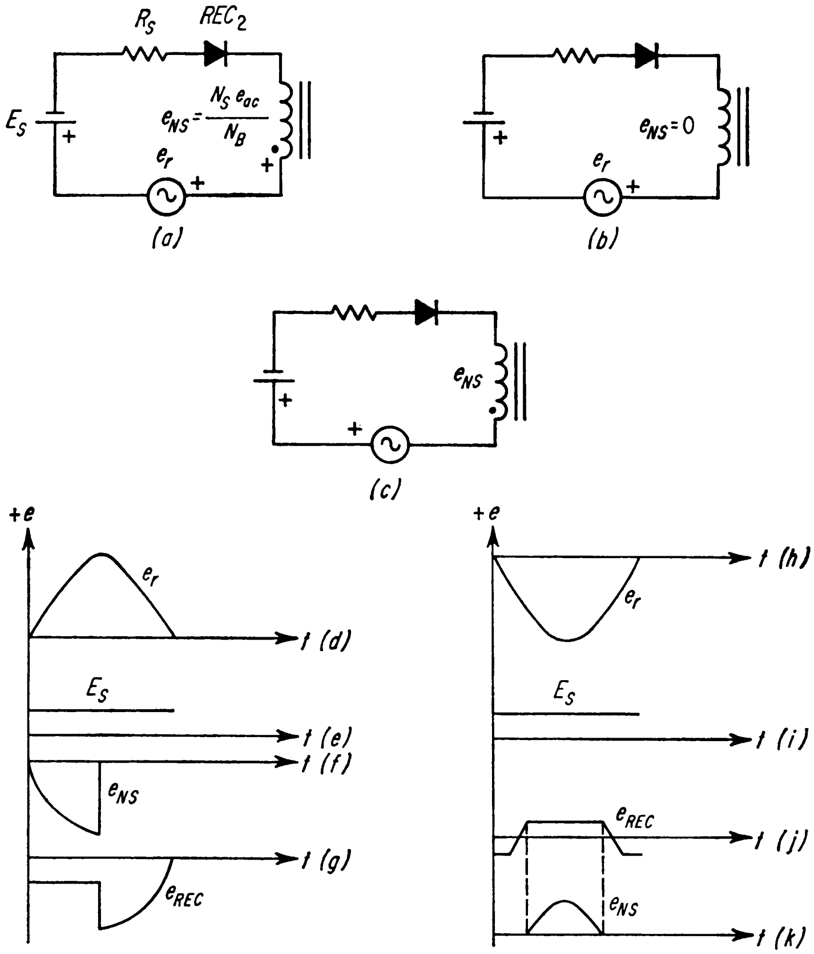

FIG. 3-13. Voltage polarities and waveforms for a d-c controlled Ramey amplifier. (*a*) Prefiring signal-circuit polarities; (*b*) postfiring signal-circuit polarities; (*c*) resetting polarities in signal circuit; (*d*) waveform of e_r during gating; (*e*) E_S during gating; (*f*) waveform of e_{NS} during gating; (*g*) waveform of e_{REC} during gating; (*h*) e_r during reset; (*i*) E_S during reset; (*j*) e_{REC} during reset; (*k*) e_{NS} during reset.

must be equal to the magnetizing current during the time that flux is resetting in the reset half-cycle.

3-5. APPLICATION OF BIAS

It has been seen in the illustrative control characteristics presented in previous sections that for the Logan circuit the variation of output is extremely nonlinear with respect to the input quantity. Reference to Fig. 3-7 or 3-12, for instance, shows that, because of the existence of threshold ampere-turns, the output is insensitive to changes in the input voltage over an appreciable region for small values of input. Somewhat larger values of input result in operation at the knee of the characteristic and still larger inputs bring the operation into a region described as the "linear region." It is desirable, in most cases, to operate at one end or the other of this linear region at zero signal. In some other cases, operation in the middle of the linear region at zero signal is to be preferred. To achieve operation for any of these conditions, some form of biasing is required.

It was seen, in the discussion of the Ramey circuit, that the presence of e_r biased the amplifier to minimum output and that the application of signal then increased output. For a d-c signal, this circuit was seen to distort the linearity of the basic amplifier because of the summation of d-c and a-c voltages.

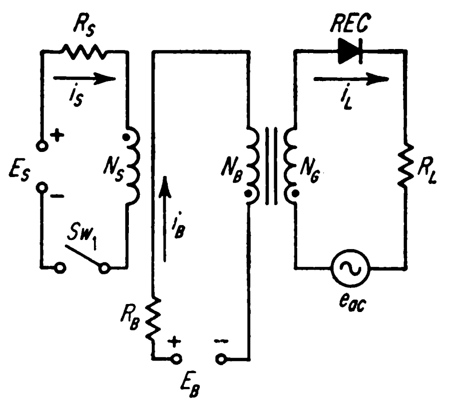

FIG. 3-14. Circuit diagram of single-core amplifier with bias.

Once it is recognized that very few practical applications allow use of single-core circuits and that, as will be seen, multicore circuits may be most efficiently biased by use of a separate bias winding, discussion of the operation of single-core circuits when biasing is done by means of a separate winding logically follows. The circuit of Fig. 3-14 will be used as a vehicle for discussion. E_S and E_B represent d-c voltages of the polarity indicated. It is to be noted that, with respect to the applied voltages in the respective circuits, the windings N_S and N_B are of opposite polarity.

If switch Sw_1 is open, the circuit reduces to that of Fig. 3-8, the operation of which was described in Sec. 3-2 and typical control characteristics for which were given in Fig. 3-12. Let it be assumed that the magnitude of E_B is just sufficient for flux to be reset halfway from $+\phi_{sat}$ to $-\phi_{sat}$ during the reset half-cycle. In this case, the average output voltage will be midway in the linear region.

For the most part, the description of operation of various circuits has been made with reference to threshold mmf, exciting mmf, and "mmf necessary to maintain flux change," but with only limited reference to "effective operating flux-mmf characteristics." The development of the subject of bias, however, requires a closer consideration of the detailed flux, current, and time relationships and these will now be considered.

If the operating flux-current loop for the circuit and conditions under consideration is displayed on an oscilloscope, a loop similar to that shown in Fig. 3-15*a* is obtained. The asymmetry of this loop arises from the condition that the positive flux excursion is produced by a sinusoidal source acting through a relatively low impedance, whereas the negative flux excursion results from the action of a d-c source through a relatively high resistance. The approximate constancy of the left side of the loop for a particular amount of reset was explained in Sec. 3-4. If E_B is varied in steps and the steady-state loop photographed at each step, a composite similar to that shown in Fig. 3-15*b* will be obtained. It is observed that the successive "left flanks" are displaced from each other, each being characterized by a different value of exciting ampere-turns.[5] A control characteristic, then, is obtained by reading the respective input and output voltages associated with each loop.

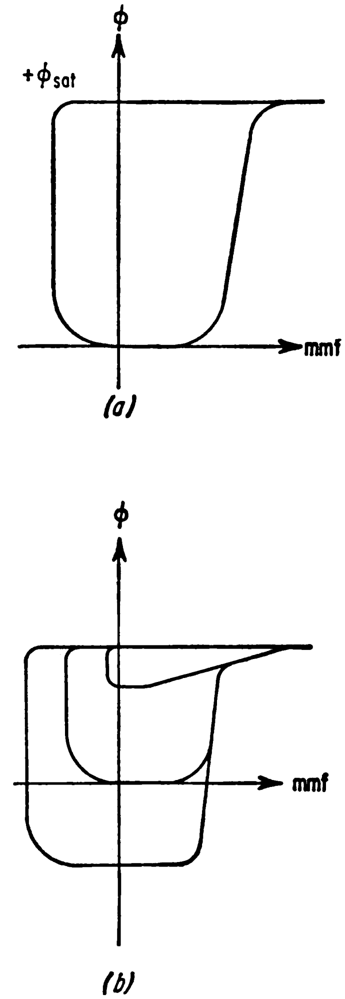

FIG. 3-15. Flux-mmf characteristics for circuit of Fig. 3-14. (*a*) Biased to $\Delta\phi = \varphi_{sat}$; (*b*) biased to successive levels of $\Delta\phi$.

With E_S zero, let switch Sw_1 be closed as e_{ac} starts a gating half-cycle. As flux changes prior to firing, currents are induced in both signal and bias circuits, delaying the firing angle of the core beyond the angle at which it fired when Sw_1 was open. The current in the gate circuit was increased during the prefiring interval, tending to raise the output voltage, but the firing was delayed, tending to decrease output voltage. The net result (since initial flux value is unchanged and, therefore, the volt-second area absorbed by the reactor is unchanged) is that, for this first half-cycle, the output voltage has the same average value as it had before Sw_1 was closed. During the reset half-cycle, the voltage appearing across the reactor terminals in the signal circuit due to the flux resetting under the action of the bias circuit results in a signal current flowing. This current decreases the exciting ampere-turns seen by the core, resulting in less flux reset during the reset half-cycle.

During the next gating half-cycle, the reactor will absorb a smaller volt-second area prior to firing and the output voltage, averaged over this and each succeeding gating half-cycle, will be increased. It is seen, then, that closing the signal circuit has changed the bias point from mid-range to a somewhat higher value of output voltage. A more subtle result is that the minimum output voltage which can be achieved has also been increased. This is caused by the increased drop across R_L during the prefiring interval. At cutoff (the point on the static-control characteristic at which the reactor just never fires) the output voltage is a function of prefiring gate current only and so is higher when Sw_1 is closed than when it is open.

If E_S is not zero when Sw_1 is closed and if Sw_1 is closed during the gating half-cycle when flux is at $+\phi_{sat}$, the three circuits are decoupled and all currents are resistance-limited. The net mmf acting on the core is now a function of three currents rather than two. Previously, operation was described with two currents causing opposing mmfs. Operation now is similar, except that the mmf due to the signal current adds to the mmf of the load current, and the sum of these two mmfs is opposed by the mmf of the bias current. If $(E_BN_B/R_B) - (E_SN_S/R_S)$ is greater than the threshold ampere-turns, flux will start to change in the negative direction. The voltage appearing at the reactor terminals will cause signal current to increase and bias current to decrease. Operation will now be the same as described for the case when E_S was zero except that, since $(E_BN_B/R_B) - (E_SN_S/R_S)$ is less when E_S is nonzero, the exciting ampere-turns are less than in the previous case, resulting in less flux change during the reset half-cycle.

Had the polarity of the signal source been reversed, the mmfs of the signal and bias circuits would add, resulting in a larger exciting mmf and, thus, in a greater flux change than in the case of the bias acting alone. It is found experimentally that when R_S and R_B have reasonably high values, the amount of flux reset is the same as if one source or the other had provided all of the net mmf. That is, the control characteristic, plotted as a function of the summation of mmfs, is identical with what would have been obtained had one source been left at zero and the control characteristic obtained by varying the other source to obtain a plot of output against control mmf.

3-6. TWO-CORE MAGNETIC AMPLIFIER

In proceeding to a discussion of the operation of more complex circuit configurations, an attempt will be made to follow a logical pedagogical pattern rather than to discuss circuits in order of comparative practical importance. Where no benefit is derived from the order of discussion, the configuration most likely to be encountered in practice will be discussed first. In discussing two-core circuits, the choice lies between a discussion of either so-called "fast-response" amplifiers or amplifiers which display an approximately exponential change in average output in response to a step change in input. The latter, for want of a more descriptive term, have been called "doublet" amplifiers.[1] While it may be argued that the name "doublet" may be confused with the term "doubler," which is often used to describe a specific circuit configuration, the word is already in the literature and will be used in this text as a general name for amplifiers which, because of the method of coupling used in the control circuits, display an approximately exponential change in output following a step change in input. Circuit configurations which give rise to essentially a step change in output at a discrete interval of time following a step change in input will be referred to as fast-response amplifiers.

Because doublet amplifiers have enjoyed far greater popularity than fast-response amplifiers both in the literature and in practice, this type will be discussed first. Fast-response amplifiers, particularly since the appearance of Ramey's papers on the subject, have been steadily gaining in popularity as a review of the literature will attest. However, doublet amplifiers possess several advantages and incorporate some peculiar features which make them a logical next step in treating self-saturating magnetic amplifiers.

3-7. TWO-CORE MAGNETIC AMPLIFIER WITH TIME DELAY

Of the three most popular doublet amplifiers, the two most commonly used (the doubler and the center-tapped circuits) have, in addition to the control-circuit coupling mentioned in the last section, a load-circuit coupling which tends to make explanation of their behavior somewhat more complicated than a similar description of the less commonly used bridge circuit. The basic operation of a doublet amplifier will, then, be explained using the bridge circuit as a model. Following this, some of the major differences between the bridge circuit and the doubler will be examined.

It has been shown in previous sections that single-core amplifiers which use the materials previously described exhibit a dead time in their response. That is, the output does not respond instantaneously to an input change. The change in the output is delayed until the next gating half-cycle. A gradual change in output involving several successive gating half-cycles cannot occur unless an external feedback circuit is provided. The dead time may, when the signal change occurs after a reset half-cycle has commenced, take two gating half-cycles to achieve a complete change. But, in view of the integrating action which occurs during the reset half-cycle, it *does* respond fully in the next gating half-cycle to the integral of the input change, integrated over the period from the start of the reset half-cycle to its end.

In order to obtain a time delay in addition to a dead time, two reactors must be combined in such a way that the gate-circuit source e_{ac} contributes to the reset mechanism. The bridge circuit chosen to illustrate the nature of this contribution is shown in Fig. 3-16. It will be observed that, if negligible rectifier leakage is assumed, the gate circuit really consists of two loops, one operative during positive half-cycles, the other during negative half-cycles of e_{ac}. During positive half-cycles, current will flow through N_{G1}, REC_1, R_L, and REC_3. During negative half-cycles, the loop is REC_2, R_L, REC_4, and N_{G2}. The voltage appearing across R_L, then, never changes direction and the output will consist of unidirectional pulses with an average value dependent upon the initial value of core flux at the beginning of each half-cycle.

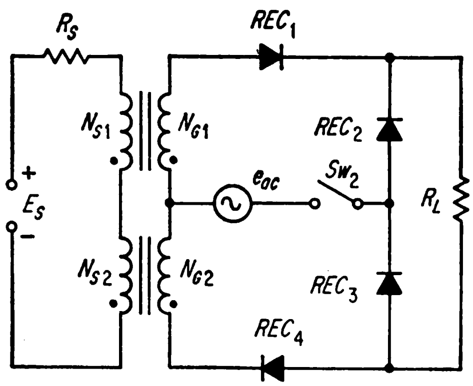

FIG. 3-16. Circuit diagram of bridge amplifier.

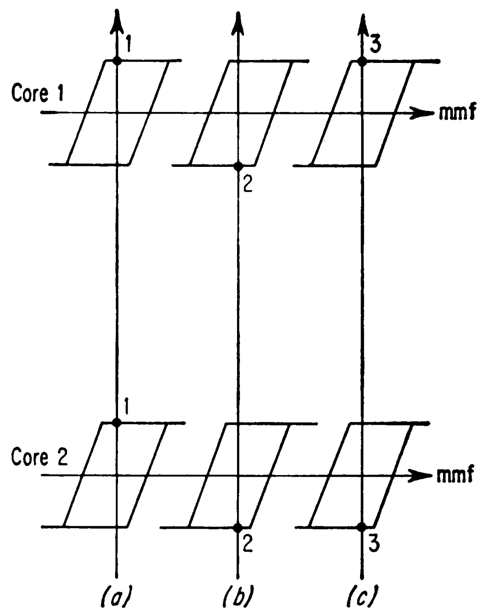

FIG. 3-17. Initial flux conditions. (a) Both cores at $+\phi_r$; (b) both cores at $-\phi_r$; (c) core 1 at $+\phi_r$, core 2 at $-\phi_r$.

Let it be assumed that E_S is zero and that R_S is a finite, nonzero resistance. The initial core flux conditions existing in the cores at the time that Sw_2 is closed fall into three general categories, illustrated in Fig. 3-17. If the initial flux condition is as illustrated in Fig. 3-17a, let Sw_2 be closed when e_{ac} is zero and going positive. The loop for this half-cycle includes reactor L_1 but, since flux in this core is already at positive saturation, no flux change occurs, e_{ac} appears immediately across R_L, and the output voltage is a complete half-cycle of e_{ac}. When the polarity of e_{ac} reverses, commencing a reset half-cycle of reactor L_1 and a gating half-cycle of reactor L_2, the same condition is repeated for L_2 and another complete half-cycle of e_{ac} appears across R_L. Since E_S is zero and no flux changed in reactor L_2, no voltage was present in the control circuit and no reset of flux in core 1 occurred. The initial flux condition for the next positive half-cycle, therefore, is the same as for the previous one and steady state has been established.

If the initial flux condition is as illustrated in Fig. 3-17*b* let Sw_2 be closed when e_{ac} is zero and going positive. After e_{ac} has attained a magnitude sufficient to establish the threshold ampere-turns, flux in core 1 will begin to change in the positive direction. The flux change will cause a voltage to appear in the control circuit. This voltage is of a polarity to change flux in core 2 in a negative direction, but since the flux in core 2 is already at $-\phi_{sat}$, no flux change can occur in core 2 and the current in the control circuit is limited by resistance R_S. This current, reflected into the gating circuit, increases the load current as discussed for the Logan circuit. Assuming a reasonable design, the flux in core 1 will just reach $+\phi_{sat}$ as $e_{ac}N_{G1}/R_L$ has decreased to the ampere-turns required to maintain flux change. At the beginning of the negative half-cycle, then, core 1 is at $+\phi_{sat}$ and core 2 at $-\phi_{sat}$. After the threshold ampere-turns have been established in the loop containing N_{G2}, flux will begin to change in core 2. The voltage appearing across N_{S2} because of this flux change is of the polarity to change flux in core 1 in a negative direction. The current in the signal circuit, therefore, is limited by the magnetizing current of the signal winding of core 1 rather than by R_S as was true in the previous half-cycle. The flux in core 2 proceeds to $+\phi_{sat}$ due to the action of e_{ac} and, because of the coupling between cores in the signal circuit, flux in core 1 is reset away from $+\phi_{sat}$.

It is appropriate to note here that, if the signal circuit resistance could have been made zero as this negative half-cycle had started, reactor L_2 would have transferred to reactor L_1 through the signal circuit the same volt-seconds/turn which L_2 received from e_{ac}. For this condition, the flux in core 1 would have arrived at $-\phi_{sat}$ at the same time that the flux in core 2 arrived at $+\phi_{sat}$. The initial conditions for the next positive half-cycle, then, would have been the converse of the conditions existing at the start of the negative half-cycle under consideration, and the cores would continue alternating the transfer of volt-seconds/turn indefinitely.[6] The load voltage would never achieve the value it had for the initial conditions assumed in Fig. 3-17*a*.

It has already been assumed, however, that R_S is not zero. For any nonzero finite resistance, a certain portion of the volt-seconds/turn delivered to reactor L_2 by e_{ac} will be lost across the signal-circuit resistance because of the magnetizing current requirement of reactor L_1. For this reason, the flux in core 1 can never be driven all the way to $-\phi_{sat}$ by the voltage appearing across N_{S2} during the gating of reactor L_2. The initial flux conditions for the next positive half-cycle, then, will be that flux in core 2 is at $+\phi_{sat}$ and flux in core 1 is somewhere between $+\phi_{sat}$ and

$-\phi_{sat}$. Since the flux change from the initial condition to $+\phi_{sat}$ is less in this positive half-cycle than it was for the first positive half-cycle, reactor L_1 will fire before the end of the half-cycle and the voltage appearing across N_{S1} will go to zero. The volt-seconds/turn appearing across N_{S1} in this half-cycle will be less than the volt-seconds/turn appearing across N_{S2} in the previous negative half-cycle and will suffer a similar transfer loss across R_S. The final value of flux in core 2 at the end of this positive half-cycle, then, will be closer to $+\phi_{sat}$ than the final value of flux in core 1 in the preceding negative half-cycle. In each succeeding half-cycle there will be less and less flux change in the resetting core and, correspondingly, a larger and larger output voltage appearing across R_L. This "ratcheting" process will continue until in some half-cycle the volt-second area appearing across the terminals of the signal winding of the gating reactor is less than or equal to the losses due to the signal-circuit resistance. When this condition is reached, no flux is changed in the resetting core and the final state is abruptly achieved. Operation after this time is the same as considered for the conditions associated with Fig. 3-17*a*.

It is seen, then, that steady state need not be achieved within one or two half-cycles after Sw_2 is closed. If R_S is very small or N_S very large, time periods exceeding several seconds may elapse before steady state is reached. This type of response was obviously impossible in the single-core circuits discussed earlier.

The initial flux conditions represented by Fig. 3-17*c* are recognized as identical with the conditions encountered at the end of the first half-cycle in the discussion of Fig. 3-17*b*. One core is at $+\phi_{sat}$; the other at $-\phi_{sat}$. Operation after closing Sw_2 for this condition will be identical with the previous case except that, if Sw_2 is closed at an equivalent time (i.e., e_{ac} zero and going positive), the output voltage will be a maximum for the first half-cycle, will abruptly drop to a low value in the next, and will then ratchet back to its minimum value.

If the doublet amplifier is to be biased to some point on the control characteristic other than the maximum output point, the circuit of Fig. 3-18 will be considered. If e_{ac} has been applied (Sw_2 closed) at some previous time and steady-state operation exists, let switch Sw_1 be closed with e_{ac} zero and going positive. E_B, R_B, and N_B will be assumed to have finite, nonzero values. It was previously shown that, in the absence of a control voltage, steady-state operation of a doublet amplifier requires that both cores remain at $+\phi_{sat}$. Therefore, when Sw_1 is closed, flux will not change in core 1 and no voltage will appear in the bias circuit across N_{B1}. If, however, E_B/R_B is greater than the threshold ampere-turns, some reset will occur in core 2 in this first half-cycle. At the start of the next negative half-cycle, the flux in core 2 is no longer at $+\phi_{sat}$ but at some lower value. During some portion of the negative half-cycle, a voltage will appear across N_{B2} as e_{ac} drives flux back to $+\phi_{sat}$. This voltage will aid E_B in producing reset in core 1 and, at the beginning of the second positive half-cycle, the value of flux will be less than the value of flux in core 2 was at the beginning of the first negative half-cycle. The voltage appearing across N_{B1} during the second positive half-cycle will aid E_B in resetting core 2 and the amount of reset will exceed the reset of core 1 in the preceding half-cycle.

It would appear that this process must continue until each core is completely reset during the appropriate half-cycle. However, it was

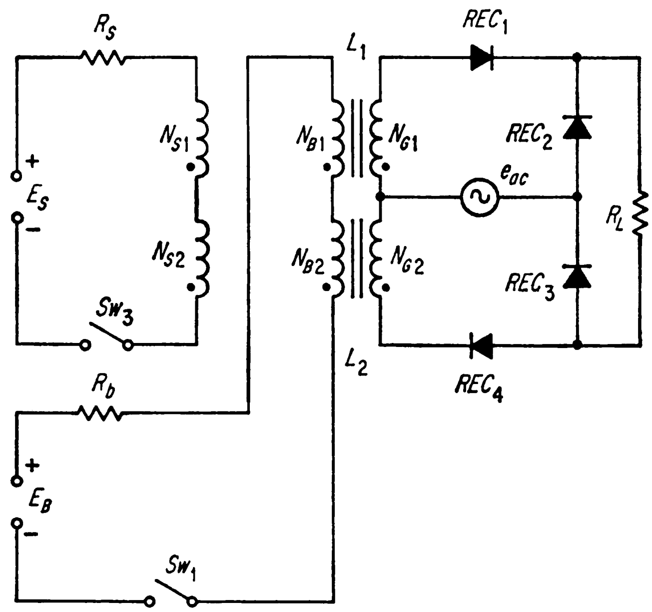

FIG. 3-18. Bridge amplifier with bias.

seen in Sec. 3-5 that a larger amount of mmf was required to achieve a larger amount of reset in the same interval of time for the Logan circuit, and the same mechanism can be shown to be true for the doublet amplifier. That is, for given finite, nonzero values of N_B and R_B, a range of values of E_B can always be found within which the output varies smoothly from full on to full off. The lower limit of E_B results in a full-on condition and the upper limit in a full-off condition. Intermediate values of output are achieved with intermediate values of E_B.

The dynamic properties of the volt-seconds/turn transfer process on successive half-cycles by the two energy sources E_B and e_{ac} as opposed by R_B determine the number of half-cycles required to achieve any desired steady-state output condition. A time constant can be related to this characteristic number of half-cycles. For bias circuits designed for high E_B, high R_B, and low N_B, steady state will be reached in a very few half-cycles after Sw_1 is closed. In the limiting case, in fact, the new steady state will be established in the next half-cycle after the closing of Sw_1.

If a steady-state condition is assumed for which the output is one-half its maximum possible value, let Sw_3 be closed when the flux in core 1 is at $+\phi_{sat}$. The current in the signal circuit will not jump immediately to its E_S/R_S value as was true for the single-core circuit. Even though core 1 is at $+\phi_{sat}$, the flux in core 2 is changing under the influence of E_B and a voltage is present across N_{S2} in a direction to oppose E_S. If R_S is sufficiently high, the loading effect on E_B and the contribution of the possible transfer of volt-seconds in the signal circuit will be negligible. The relationship among the turns on the control windings, the resistances of the control circuits, and the characteristic response time of the amplifier will be developed more fully in Chaps. 4 and 5.

3-8. COMPARISON OF BRIDGE AND DOUBLER CIRCUITS

The output circuits of the bridge and doubler circuits are shown in Fig. 3-19a and b, respectively. The two have been drawn in a manner to emphasize the principal difference in operation. The doubler circuit as drawn has an a-c output while the output of the bridge is d-c. The essential difference in operation, however, is that when one core of the doubler is saturated, the gate winding of the other core is essentially short-circuited.[7,8] This is in distinct contrast to operation in the bridge circuit, where the resetting core always has the voltage due to reset opposed by a voltage very nearly equal to the magnitude of e_{ac}. The effect of the dependence of gate-circuit impedance as seen by the resetting core on the firing angle of the gating core is to introduce an additional form of positive feedback into the circuit. It was for this reason that the bridge circuit was chosen to illustrate the basic operation of doublet amplifiers. In the bridge circuit the resetting core always has e_{ac} appear-

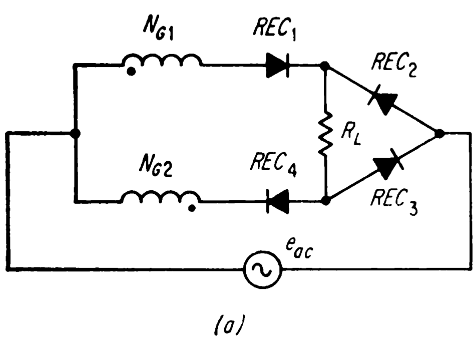

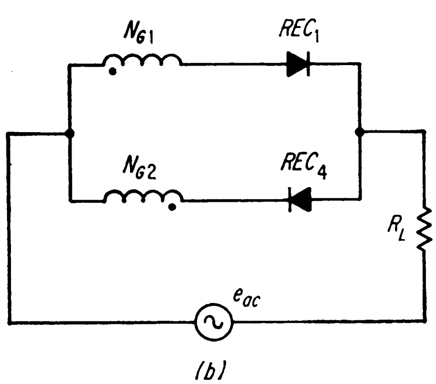

FIG. 3-19. Comparison of doublet amplifiers. (a) Bridge; (b) doubler.

ing across the load resistor or across the gating core, but, in either case, the voltage is in series with the gate winding of the resetting core and has a polarity which opposes backfiring of the rectifier associated with the resetting core.

3-9. TWO-CORE MAGNETIC AMPLIFIER WITHOUT TIME DELAY

In order to avoid the introduction of time delay, single-core building blocks must be combined in such a way that e_{ac} cannot cause the appearance of volt-seconds in a control circuit to reset the nongating core. The

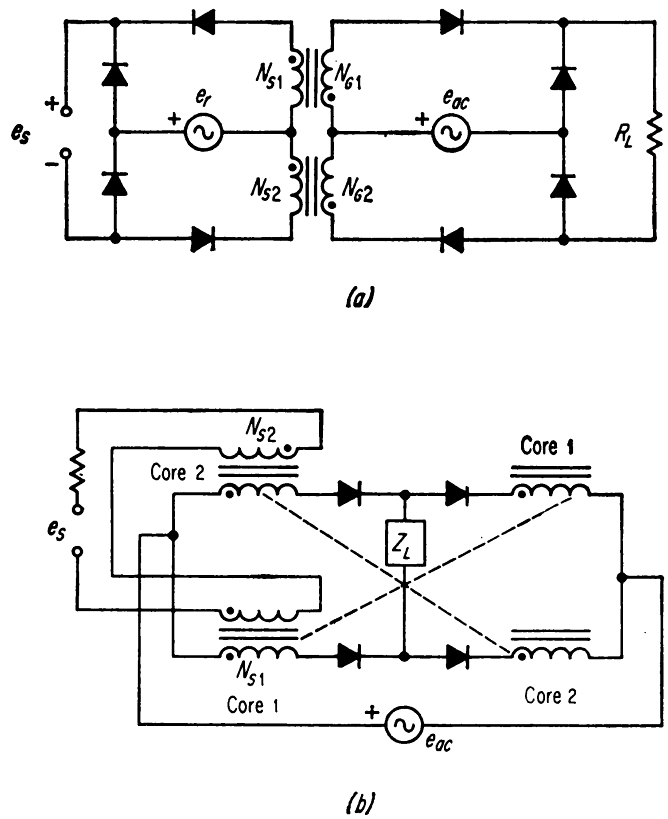

FIG. 3-20. Fast-response amplifiers. (a) Use of signal-circuit rectifiers; (b) two cores gating in same half-cycle.

two circuits illustrating methods of accomplishing this decoupling with two cores are shown in Fig. 3-20. In the circuit of Fig. 3-20a, the required decoupling is obtained by bypassing the gate-circuit volt-seconds around the resetting core by means of a bridge arrangement of rectifiers in the control circuit. This method retains full wave output at the expense of an increased number of rectifying elements. In Fig. 3-20b,[9] this decoupling is obtained simply by having both reactors gate on the same half-cycle and, therefore, never introducing any volt-seconds from the gate circuit into the control circuit on the reset half-cycle. This type of circuit will be discussed in greater detail in Chap. 7.

REFERENCES

1. Pula, T. J., and F. G. Timmel: A New Approach to Self-saturating Magnetic Amplifiers, *Proc. Natl. Electronics Conf.*, vol. 12, pp. 425–443, 1957.
2. Logan, F. G.: Electric Controlling Apparatus, U.S. Patent 1,977,179, Apr. 19, 1935.
3. Huhta, H.: Flux Resetting Characteristics of Several Magnetic Materials, *Trans. AIEE*, vol. 73, part I, pp. 111–114, 1954.
4. Ramey, R. A.: On the Mechanics of Magnetic Amplifier Operation, *Trans. AIEE*, vol. 70, part II, pp. 1214–1222, 1951.
5. Lord, H. W.: Dynamic Hysteresis Loops of Several Core Materials Employed in Magnetic Amplifiers, *Trans. AIEE*, vol. 72, part I, p. 86, Fig. 3B, 1953.
6. Scorgie, D. G.: Fast Response with Magnetic Amplifiers, *Trans. AIEE*, vol. 72, part I, pp. 741–749, 1953.
7. Pittman, G. F., Jr.: Notes on the Control Mechanism of Self-saturating Magnetic Amplifiers, Conference Paper, AIEE Summer General Meeting, 1953.
8. Lord, H. W.: The Influence of Magnetic Amplifier Circuits upon the Operating-hysteresis Loops, *Trans. AIEE*, vol. 72, part I, pp. 721–728, 1953.
9. Lufcy, C. W., P. W. Barnhart, and A. E. Schmid: An Improved Magnetic-servo Amplifier, *Trans. AIEE*, vol. 71, part I, pp. 281–289, 1952.

4

Volt-second Transfer Efficiency

It is known directly from the integral form of Faraday's law that the time integral of the voltage across the terminals of a magnetic reactor divided by the number of reactor turns is equal to the flux change in the reactor. Furthermore, since in self-saturating magnetic amplifiers reset of flux is always initiated from what is essentially positive saturation, the amount of flux change during a reset half-cycle determines the initial flux level at the beginning of the next gating half-cycle. For any practical design, this initial flux level is basic in determining the firing angle in the gating half-cycle. Therefore, a basic quantity in magnetic-amplifier control is this volt-second integral. Such reasoning provided the basis for considering self-saturating magnetic amplifiers as volt-second controlled devices.[1]

The principal pitfall in applying this approach to control arises in the indiscriminate identification of the signal voltage with the reactor voltage during reset. Because a finite nonzero field (and consequently a finite nonzero signal-circuit current) is required to reset the flux in a core within the allowed time interval, the signal voltage and the reactor resetting voltage will be significantly different whenever there is appreciable signal-circuit impedance. The dual requirements of providing power gain and suppressing excessive circulation currents in the signal circuit due to the gate-circuit voltage make an appreciable signal-circuit impedance the rule rather than the exception, particularly for a preamplifier or the initial stage of a cascaded stage design.

The advantage of thinking in terms of volt-second control is that the reactor flux change and the consequent firing angle are more easily understood. If this conceptual advantage is to be retained, however, it is necessary to develop a usable means of distinguishing between the volt-seconds which cause a change in reactor flux level and the value of volt-seconds which is obtained merely by substituting the known signal voltage into Faraday's law. In other words, it is necessary to investigate the efficiency of the transfer of volt-seconds from the signal source to the terminals of a resetting reactor for cases involving realistic signal-circuit impedances and reactor-core materials, instead of optimistically assuming that this transfer is 100 per cent efficient.[2]

This chapter, therefore, will be devoted to a discussion of measurements of the efficiency of the transfer of volt-seconds from a signal source to a resetting reactor through an appreciable signal-circuit resistance for biased and unbiased reactors. In the process of this discussion, the signal-circuit parameter N_S^2/R_S will be considered in some detail and an attempt made to show the complementary relationships which exist between volt-seconds and ampere-turns in the control of physically realizable self-saturating magnetic amplifiers.

4-1. GENERAL CONTROL-CIRCUIT CONSIDERATIONS

In Sec. 1-4, the distinction was drawn between voltage, current, and power gains. Following the conclusions of that section, a magnetic device will be considered to possess amplification only if it provides power gain. A consideration of power gain immediately requires knowledge of the power drawn from the signal source and in most practical design problems this leads inevitably to calculations involving the internal impedance of the signal device. Introduction of the concept of finite nonzero source impedances requires that the idealizations of voltage sources be abandoned. When these practical considerations are introduced with flux-current loops with nonvertical sides, the mechanics of control become very complex indeed. However, these are the normal design conditions and this is the type of problem which must be attacked.

Practitioners in the field of magnetics, in general, are only too well aware of the fact that they must often ignore conclusions drawn from previously useful approximations which do not happen to be justifiable assumptions with respect to the problem at hand. The field of self-saturating magnetic amplifiers, unfortunately, is no exception to this generalization. In the design of magnetic amplifiers, it is recognized as an indispensable part of the art that certain measured quantities on both magnetic and rectifier materials must be incorporated somehow into any specific design. It is also recognized that in assessing the dynamic response of a magnetic amplifier, the analytical procedures employed are, at best, useful approximations. These design measurements and procedures form the content of following chapters. It is of the utmost importance, therefore, to be able to find a few guideposts which can form the basis for these systematic, if empirical, design procedures. The main thesis of this chapter is to provide one such guidepost in the concept of volt-second transfer efficiency. In consequence, the term N^2/R will emerge as a control-circuit parameter useful in amplifier design.

To provide a satisfactory explanation of the distinction between fast-response and doublet circuits or to show that, for different amounts of reset, the sides of the operating flux-current loops for an amplifier cannot be coincident, requires only a qualitative description of the mechanics of operation, as was made in Chap. 3. However, quantitative information is necessary for attacking a problem involving power gain. It will be shown in Chap. 5 that, once the flux change occurring in a resetting reactor in the nth half-cycle during steady-state operation is known, the amount of output during the $(n + 1)$th half-cycle can be predicted. The basic problem then centers around determination of the amount of flux change which will occur in a particular reset half-cycle as a consequence of the application of a given amount of signal power into a control circuit consisting of a reactor in series with a passive impedance element. The problem logically separates into two parts: (1) reset energy is provided in one reset half-cycle (fast-response amplifiers); (2) reset energy is provided gradually over a succession of reset half-cycles (doublet amplifiers). The process of transfer of volt-seconds from a source to a resetting reactor through a linear resistance will now be considered in detail and the basic nature of N^2/R as a control-circuit parameter will be developed for both fast-response and doublet amplifiers.

4-2. CONCEPTS OF VOLT-SECOND TRANSFER EFFICIENCY

In order to begin the quantitative consideration of the transfer of volt-seconds from a source to a resetting reactor through a linear resistance, measurements on the Logan circuit will be examined under the conditions of square-wave excitation and zero bias. Square-wave excitation has been selected to minimize backfiring and bias has been eliminated initially to avoid the complications associated with coupling between control circuits.

For this simple circuit, measurements of the average value of the voltage appearing at the reactor terminals for various voltages applied by the signal source will be considered for various values of signal-circuit voltage, turns, and resistance. Figure 4-1 provides a functional block diagram of the circuit used to obtain these measurements. The circuit consists essentially of a half-wave single-core self-saturating magnetic amplifier (discussed qualitatively as the Logan circuit in Chap. 3). The gate-circuit square-wave supply is introduced through a step-down transformer to provide low source impedance and a high-quality silicon diode is used to make the resetting magnetic potential due to the diode leakage current a negligible factor. The reactor voltage waveshape during reset appears across a single-turn pickup winding and is amplified to a reasonable level through circuitry approaching zero N^2/R in a manner quite similar to that used in the constant current flux reset tester to be described in detail in Chap. 6. The average value of this voltage is the quantity measured. In the control circuit of Fig. 4-1, the series arrangement of a variable amplitude d-c supply and a decade box resistor provides for application of any desired combination of E_S and R_S for selected values of signal turns wound on the reactor under study.

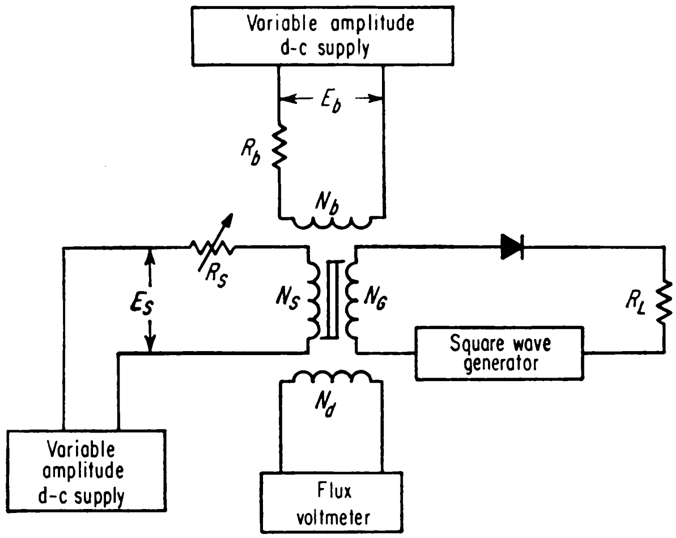

FIG. 4-1. Block diagram of circuit used to obtain volt-second transfer efficiency measurements.

If the voltage appearing at the terminals of a signal source were 100 per cent efficient in resetting flux in a reactor, then Eq. (4-1) would be applicable

$$\frac{1}{N_S}\int_0^{t=\pi/\omega_G} e_S\,dt = \Delta\phi = \frac{1}{N_d}\int_0^{t=\pi/\omega_G} e_d\,dt \tag{4-1}$$

where N_S represents the signal turns, e_S the signal voltage, t time, $\Delta\phi$ the flux change occurring in the time period, N_d pickup turns, e_d the voltage appearing across the pickup winding, and ω_G the repetition rate of the gating voltage. If the signal source is not 100 per cent efficient, the left-hand equation of Eq. (4-1) would no longer be true, but the right-hand equation would still hold. A measure of efficiency can be formed, therefore, by dividing the right-hand equation by the left-hand equation as in Eq. (4-2).

$$\text{Efficiency (\%)} = \frac{\dfrac{1}{N_d}\displaystyle\int_{t=0}^{t=\pi/\omega_G} e_d\,dt}{\dfrac{1}{N_S}\displaystyle\int_{t=0}^{t=\pi/\omega_G} e_S\,dt} \times 100 \tag{4-2}$$

Since, in the circuit under consideration, the flux change in the resetting half-cycle is equal to the flux change in the gating half-cycle, the upper

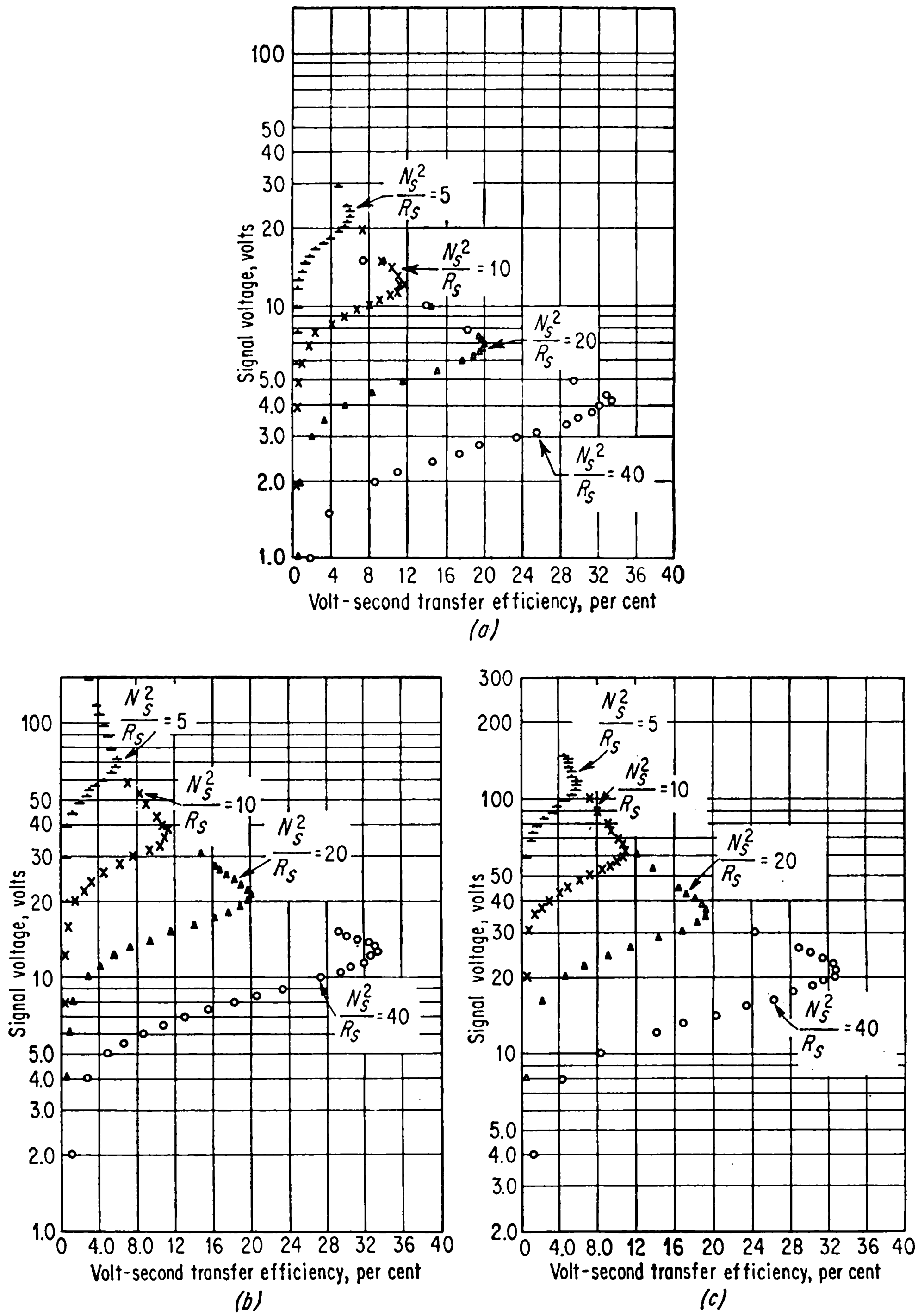

Fig. 4-2. Volt-second transfer efficiency as a function of signal voltage (N^2/R as a parameter). (*a*) $N_S = 100$ turns; (*b*) $N_S = 300$ turns; (*c*) $N_S = 500$ turns.

limit of integration in Eq. (4-2) can be changed from π/ω_G to $2\pi/\omega_G$ in both the numerator and denominator if a d-c signal voltage is assumed. The denominator is reduced to E_S/N_S and, since the pickup winding is a single turn, the numerator is reduced to E_d. The volt-second transfer efficiency, therefore, is simply $E_d/(E_S/N_S)$.

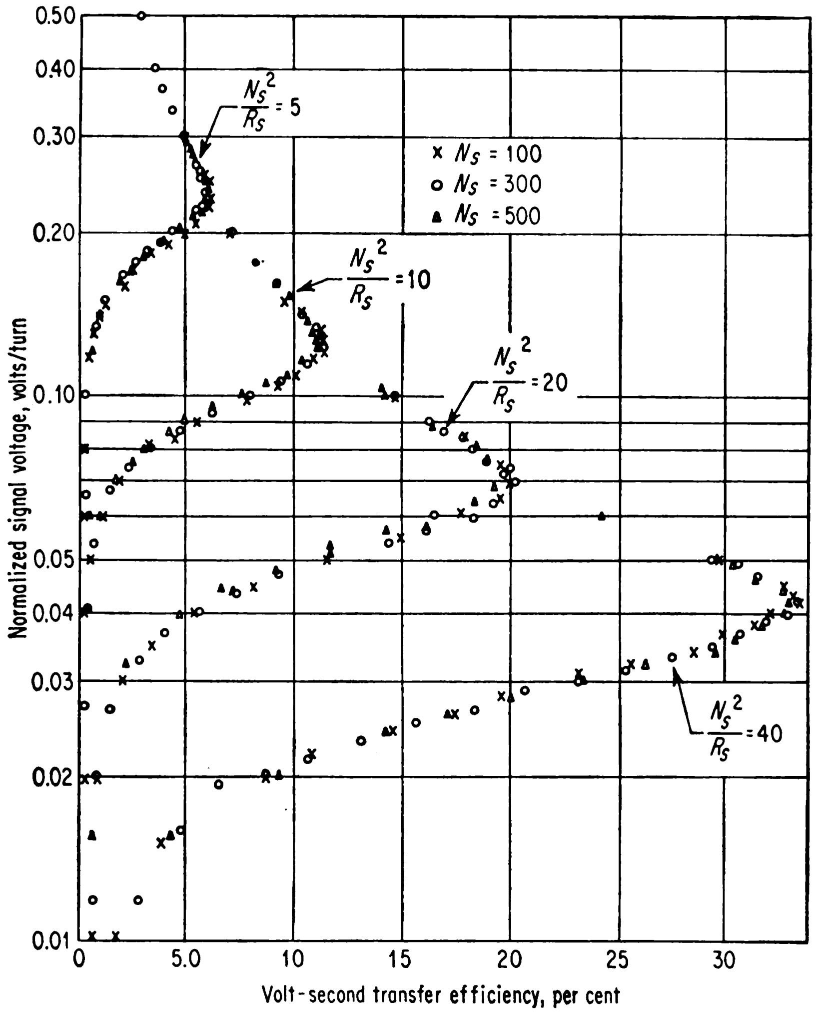

FIG. 4-3. Volt-second transfer efficiency as a function of signal volts/turn (50 per cent nickel-iron).

A family of curves obtained for a typical square-loop material (50 per cent nickel-iron) is shown in Fig. 4-2a. Signal voltage is the independent variable and reactor voltage divided by signal voltage is the dependent variable for various values of N_S and R_S with the quantity N^2/R as a parameter. When volt-second transfer efficiency curves of this type are compared for equal values of $N_S{}^2/R_S$ but have been obtained by using different values of N_S and R_S, it is found that the peak volt-second transfer efficiency values are equal but the peaks occur at a value of voltage which is higher in direct proportion to the number of signal turns used. This can be verified by comparing Fig. 4-2*a*, *b*, and *c*. This result means that the accompanying values of the average ampere-turns are equal.

When these curves for equal values of N_S^2/R_S are replotted not as volt-second transfer versus signal voltage, but as volt-second transfer

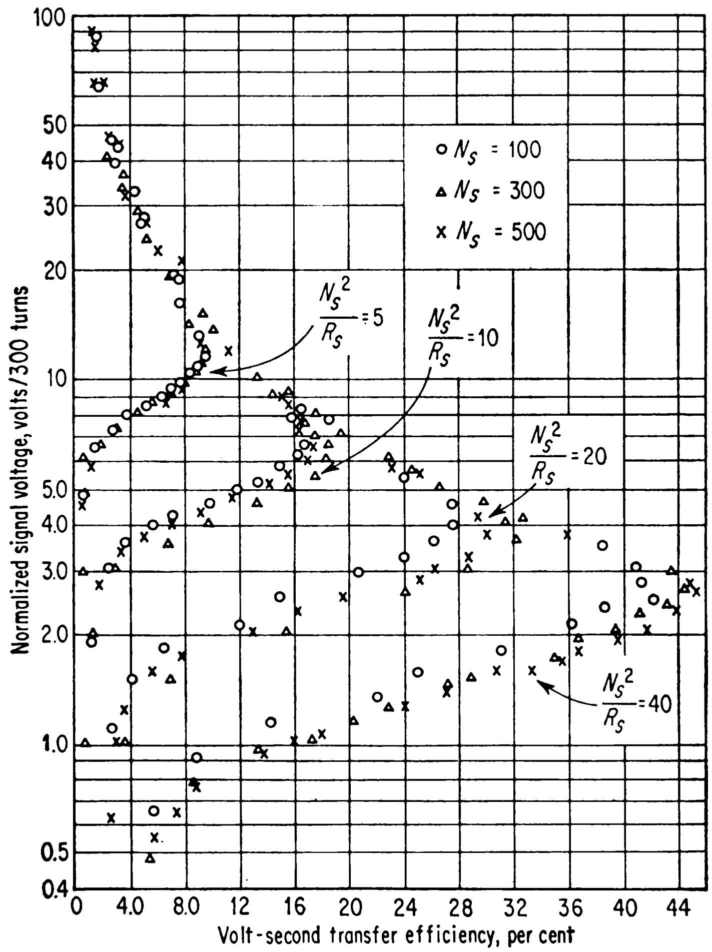

FIG. 4-4. Volt-second transfer efficiency as a function of signal volts/turn (4 per cent molybdenum-79 per cent nickel). (*From Ref. 2, by permission of AIEE.*)

versus volts/turn applied by the signal source as shown in Fig. 4-3, it can be seen that the complete curves for equal N_S^2/R_S values practically coincide throughout their quite irregular shape. Similar results obtained for a 4 per cent molybdenum-79 per cent nickel material are shown in Fig. 4-4.

It has been demonstrated, then, that for square-loop materials, N^2/R remains a basic reactor parameter. It should also be noted from this "normalization" of the signal voltage that the quantity E_S/N_S has the units of flux change if considered in terms of the average reactor voltage (from $\Delta\phi = 1/N \int e\, dt$). From this it can be seen that the obtained change of flux (i.e., the value obtained by relating flux change to reactor-terminal voltage) for each particular E_S is a constant percentage of the impressed change of flux (i.e., the value which would have been obtained if the control-circuit impedance were zero) for various combinations of N_S and R_S as long as the N^2/R values are equal. It is only when R_S approaches zero or the flux-current loop is considered to be ideal that a flux change is obtained which corresponds to the value which would be calculated from the normalized value of applied voltage.

4-3. N^2/R AS A CONTROL-CIRCUIT PARAMETER

The emergence of N^2/R as a fundamental parameter in the volt-second transfer efficiency characteristics of the Logan circuit during reset allows a very interesting observation concerning the respective roles of voltage and current in control of magnetic amplifiers.

By manipulating Faraday's law

$$\begin{aligned} e &= N \frac{d\phi}{dt} \\ &= AN \frac{d(\mu H)}{dt} \\ &= AN \frac{d(\mu N i/l)}{dt} \\ &= \frac{A}{l} N^2 \frac{d(\mu i)}{dt} \\ &= \frac{A}{l} N^2 \mu \frac{di}{dt} + \frac{A}{l} N^2 i \frac{d\mu}{dt} \end{aligned} \tag{4-3}$$

In Eq. (4-3), even though the terms $\mu\, di/dt$ and $i\, d\mu/dt$ cannot be evaluated, the coefficient of each of the terms equated to e contains the factor N^2. This, of course, follows directly from the transformer approach. However, it is only when this expression is divided through by $R \neq 0$ that N^2/R appears in the coefficient. And in this case it is related to e/R, a "core current" expression. Therefore, as soon as the determinate volt-second control idealization is abandoned, the emergence of N^2/R as a basic parameter equivalently expresses the fact that the current accompanying reset also becomes basic.

Having established that N^2/R constitutes a basic reactor parameter in terms of volt-second transfer efficiency for the Logan circuit, it is instructive at this point to investigate the variation of the incremental V/NI gain versus N^2/R for the bridge circuit considered qualitatively in Chap. 3

as a representative doublet amplifier. Incremental gain is here defined as the gain for biased reactors.

Typical curves of output voltage as a function of signal ampere-turns for a bridge circuit using the same two magnetic materials used for the Logan circuit are shown in Figs. 4-5 and 4-6. As has already been mentioned in Chap. 3, the current flowing in the control circuit on each half-cycle contributes to the flux change in the resetting core. This is true whether the energy source supplying this current is primarily E_S (as is

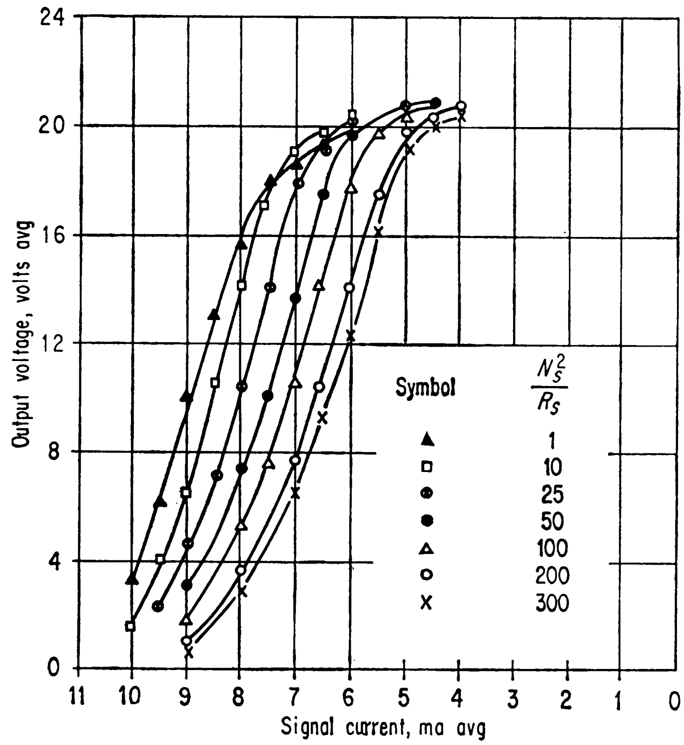

FIG. 4-5. Output voltage as a function of signal current for a bridge circuit using 50 per cent nickel-iron (N_S^2/R_S as a parameter).

the case with low N^2/R) or primarily e_{ac} (as is the case with high N^2/R). If the values of incremental volts/ampere-turn gain are calculated from Figs. 4-5 and 4-6 and these values plotted versus N^2/R for both core materials, the curves of Fig. 4-7 are obtained. The approximate constancy of the incremental ampere-turns over a wide range of N^2/R as seen from Fig. 4-7 suggests that $\Delta N_S I_S$ is a basic characteristic of the material for equivalent flux change in a given time. Furthermore, because of the change in resetting voltage waveshape with N^2/R in the bridge circuit, this approximate constancy suggests that $\Delta N_S I_S$ is a basic characteristic regardless of the detailed waveshape of the energy source producing this $\Delta\phi$ through a finite resistance. It should be emphasized in this regard that average control ampere-turns cannot be directly related to resetting

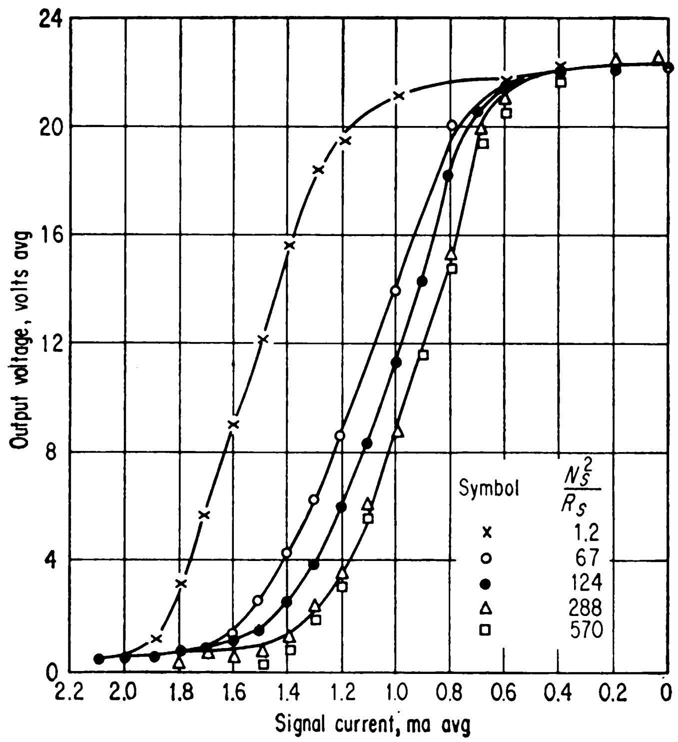

FIG. 4-6. Output voltage as a function of signal current for a bridge circuit using 4 per cent molybdenum-79 per cent nickel (N_S^2/R_S as a parameter).

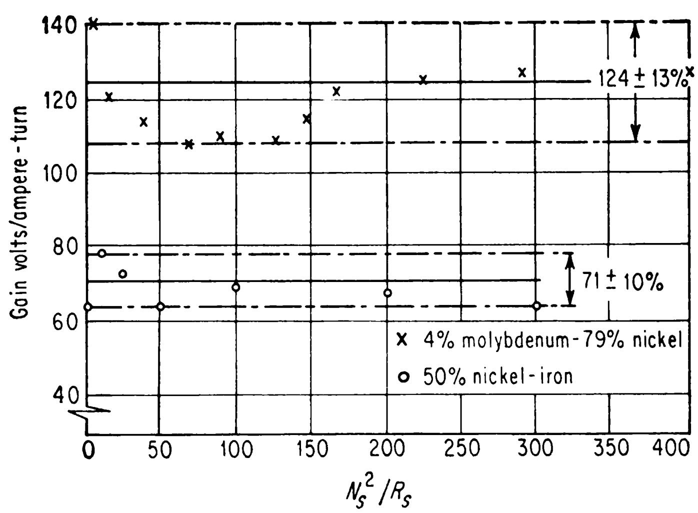

FIG. 4-7. Volts/ampere-turn gain of a bridge circuit as a function of N_S^2/R_S for two materials.

ampere-turns in half-cycle amplifiers such as the Logan circuit. The marked dependence of gain on N^2/R in a Logan circuit is shown in Fig. 4-8; however, this gives no information on variation of resetting ampere-turns since the voltage induced from e_{ac} does not produce any core reset.

It is interesting to attempt to extend these ideas on the approximate constancy of resetting ampere-turns for the complete flux change in a given time to the Logan circuit. For this purpose, consider the governing equations of the Logan circuit during a reset half-cycle; from Kirchhoff's voltage law:

$$E_S = i_S R_S + e_{NS}$$

Now by basic magnetic-amplifier design, for complete reset

$$E_{NS} = \frac{N_S}{N_G} E_{NG}$$

Therefore, in terms of average values this expression becomes

$$\bar{\imath}_S = \frac{E_S - (N_S/N_G)E_{NG}}{R_S}$$

Multiplying through by N_S,

$$N_S\bar{\imath}_S = \frac{N_S E_S - (N_S^2/N_G)E_{NG}}{R_S}$$

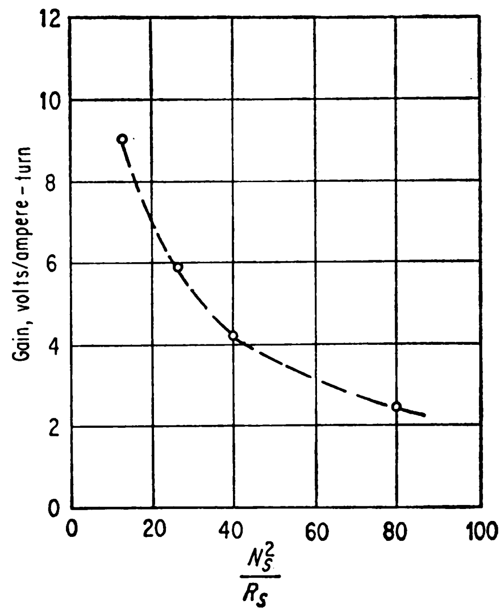

FIG. 4-8. Volts/ampere-turn gain of a Logan circuit as a function of N_S^2/R_S (50 per cent nickel-iron material).

Note carefully here that $\bar{\imath}_S$ is *not* the average control current but the average control current *during reset.* The average control current in steady state, of course, is E_S/R_S and the above expression for current could be interpreted to show that the average resetting ampere-turns are equal to the observed average ampere-turns minus the average loss ampere-turns. Since E_S/R_S is all that can be measured in steady state, equating all other quantities to $N_S E_S/R_S$ and operating on this expression yields

$$N_S I_S = N_S\bar{\imath}_S + \frac{N_S^2}{R_S}\frac{E_{NG}}{N_G}$$

Now, the volts/ampere-turn gain is expressed as

$$G_{v/NI} = \frac{E_L}{N_S I_S}$$

or here, from the above, as

$$G_{v/NI} = \frac{E_L}{N_S \bar{\imath}_S + \dfrac{N_S{}^2}{R_S}\dfrac{E_{NG}}{N_G}}$$

Converting this to volts/volt gain

$$G_{v/v} = \frac{E_L}{N_S \bar{\imath}_S + N_S{}^2 E_{NG}/R_S N_G} \frac{N_S}{R_S}$$

or

$$G_{v/v} = \frac{E_L N_S}{N_S \bar{\imath}_S R_S + N_S{}^2 E_{NG}/N_G}$$

It is convenient to operate on $G_{v/v}/E_L$ and consider the "normalized" gain. In any already designed gate circuit, E_{NG}/N_G = constant; call it constant a. And pursuing the conclusion from the bridge circuit, assume $N_S \bar{\imath}_S$ is constant b. The normalized expression then becomes

$$\frac{G_{v/v}}{E_L} = \frac{N_S}{bR_S + aN_S{}^2}$$

Taking the partial derivative of the expression with respect to N_S for R_S fixed $\neq 0$, this becomes, upon equating to zero,

$$0 = (bR_S + aN_S{}^2)(1) - N_S(2aN_S)$$

or

$$aN_S{}^2 = bR_S$$
$$\frac{N_S{}^2}{R_S} = \frac{b}{a}$$

This then represents the value for $N_S{}^2/R_S$ which will maximize the volts/volt gain. Substituting this value back for $N_S{}^2/R_S$

$$G_{v/NI} = \frac{E_L}{b + (b/a)a} = \frac{E_L}{2b}$$

But for $N^2/R = 0$, the $G_{v/NI}$ expression reduces to

$$(G_{v/NI})_0 = \frac{E_L}{b}$$

For maximum volts/volt gain with R_S fixed $\neq 0$, a value of N^2/R which makes the v/NI gain equal to $\frac{1}{2}(G_{v/NI})_0$ should be chosen.

Interpreting this result in terms of incremental volt-second transfer efficiency, the $N_S{}^2/R_S$ which gives $G_{v/NI} = \frac{1}{2}(G_{v/NI})_0$ gives maximum $G_{v/v}$ when N is varied for fixed $R_S \neq 0$. But the product $(N_S \bar{\imath}_S)$ has been assumed to be a constant for a given material configuration and frequency for full linear ΔE_L. Therefore, for maximum $G_{v/v}$ for fixed R_S this is equivalent to letting $I_S = 2\bar{\imath}_S$. And in steady state, $I_S = E_S/R_S$. Therefore, $\bar{\imath}_S = E_S/2R_S$. In other words, maximum $G_{v/v}$ is obtained for fixed $R_S \neq 0$ when, in terms of average values, half the voltage during reset appears across R_S.[3,4] But this is just what is obtained with an incremental volt-second transfer efficiency of 50 per cent.

It is instructive to attack this same derivation in terms of electromagnetic rather than circuit quantities. Applying directly the observation for doublets that the average $(d\phi/dt)$ must be equal for all N^2/R values and attempting to extend this to the Logan circuit, the governing equations for the Logan circuit during reset are:

$$E_S = i_S R_S + N_S \frac{d\phi}{dt}$$

Multiplying through by N_S/R_S this becomes:

$$\frac{N_S}{R_S} E_S = N_S i_S + \frac{N_S{}^2}{R_S} \frac{d\phi}{dt}$$

Rearranging to isolate the resetting mmf yields

$$N_S i_S = \frac{N_S}{R_S} E_S - \frac{N_S{}^2}{R_S} \frac{d\phi}{dt}$$

Now consider the value of N_S which will maximize this mmf for complete reset. For constant $R_S \neq 0$, by partial differentiation with respect to N_S:

$$\frac{\partial(N_S i_S)}{\partial N_S} = \frac{E_S}{R_S} - \frac{2N_S}{R_S} \frac{d\phi}{dt} - \frac{N_S{}^2}{R_S} \frac{\partial(d\phi/dt)}{\partial N_S}$$

Equating this expression to zero, therefore, gives the condition for maximum $N_S i_S$ as

$$\frac{E_S}{R_S} - \frac{2N_S}{R_S} \frac{d\phi}{dt} - \frac{N_S{}^2}{R_S} \frac{\partial(d\phi/dt)}{\partial N_S} = 0$$

Considering this expression in terms of average values and tentatively extending the conclusion from doublets, i.e., $(\overline{d\phi}/dt)$ is a constant, the expression becomes:

$$\frac{E_S}{R_S} = \frac{2N_S}{R_S} \left(\frac{\overline{d\phi}}{dt}\right)$$

or

$$E_S = 2N_S \left(\frac{\overline{d\phi}}{dt}\right)$$

For constant $R_S \neq 0$, the average net mmf during reset is maximized by choosing N_S such that

$$\frac{N_S(\overline{d\phi/dt})}{E_S} = 0.50$$

But this is equivalent to obtaining a volt-second transfer ratio of 50 per cent, since

$$VSTR = \frac{\int_{t=0}^{t=\pi/\omega} e_{NS}\,dt}{E_S\,\pi/\omega}$$

or

$$VSTR = \frac{1}{E_S}\,\frac{\int_{t=0}^{t=\pi/\omega} e_{NS}\,dt}{\pi/\omega}$$

$$= E_{NS}\,\frac{1}{E_S}$$

and

$$E_{NS} = N_S\left(\frac{\overline{d\phi}}{dt}\right)$$

Therefore, the ampere-turn control approach assumption of $N_S\bar{\imath}_S$ = constant for complete reset and the volt-second control approach assumption of $(\overline{d\phi/dt})$ = constant for complete reset both yield the same result of adjusting N_S, for fixed $R_S \neq 0$, to obtain a volt-second transfer ratio of 50 per cent.

Apart from the usefulness of this conclusion in optimizing the volts/volt gain of certain types of self-saturating magnetic amplifiers, the correspondence of both ampere-turn and volt-second approaches sheds considerable light on the fundamental physical processes in control.

In the first place, analyses using practical core materials cannot neglect the incremental ampere-turns required to produce a change of flux level and, contrariwise, the choice of parameters which maximizes the average resetting mmf at the same time produces the optimum magnitude of this $(\overline{d\phi/dt})$ and, consequently, the maximum reset with the associated maximum volts/volt gain.

If these complementary assumptions [i.e., $N_S\bar{\imath}_S$ = constant and $(\overline{d\phi/dt})$ = constant] are considered in terms of modern domain theory, they are quite reasonable, because they imply that for a given average incremental H field (proportional to $N_S\bar{\imath}_S$) the same average domain-wall velocity (proportional to $\overline{d\phi/dt}$) is obtained regardless of how this configuration was produced in the circuit. And it has been shown that this proportionality constitutes one of the basic relationships in domain-wall dynamics.[5]

In the following section the significance of these conclusions in terms of incremental volt-second transfer efficiency measurements will be investigated.

4-4. INCREMENTAL VOLT-SECOND TRANSFER EFFICIENCY

An examination of the volt-second transfer efficiency curves discussed in Sec. 4-2 shows that the relationship between the efficiency and the

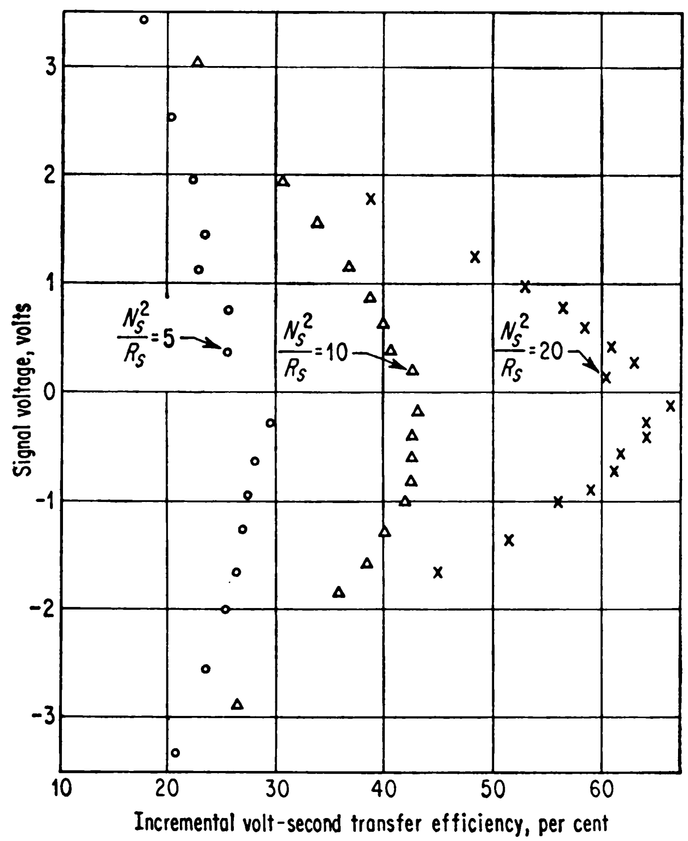

FIG. 4-9. Incremental volt-second transfer efficiency as a function of signal voltage for a 50 per cent nickel-iron material (N^2/R as a parameter). (*From Ref. 2, by permission of AIEE*).

volts/turn applied is quite variable. It is reasonable to expect this to produce quite a nonlinear volts/volt amplifier gain curve. For this reason it is general design practice to provide some sort of bias in order to shift the operating point of the reactor to a more nearly linear portion. In terms of volt-second transfer concepts, this means that information concerning the incremental volt-second transfer efficiency of resetting reactors must be obtained. This can be done by biasing the Logan circuit to half of maximum volt-second transfer with a separate winding having a negligible N^2/R. For the measurements obtained with the special test circuit of Fig. 4-1, the N^2/R of the bias circuit was adjusted to

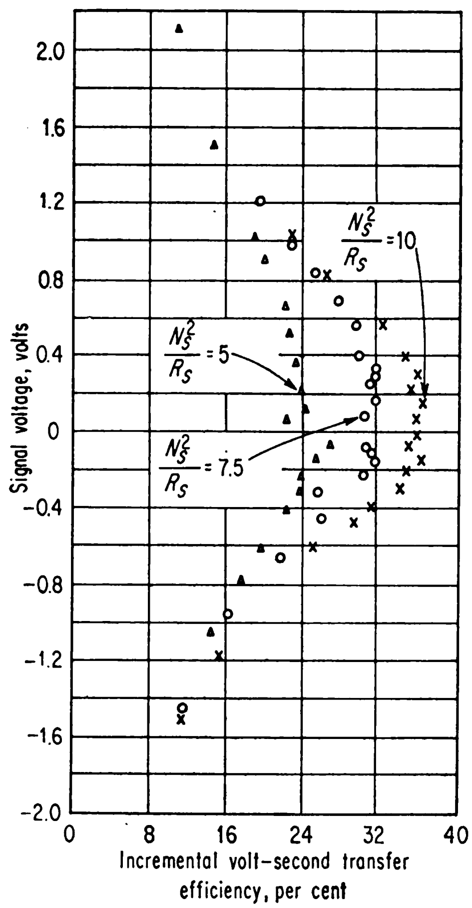

FIG. 4-10. Incremental volt-second transfer efficiency as a function of signal voltage for a 4 per cent molybdenum-79 per cent nickel material (N^2/R as a parameter).

approximately 0.30. The fundamental nature of N^2/R as a parameter is not jeopardized by this procedure. Nor is the character of volts/turn as a normalized signal. When measurements of incremental volt-second transfer efficiency versus signal voltage are plotted, the curves are symmetrical and considerably more vertical than without bias for both square-loop magnetic materials. Typical curves are shown in Fig. 4-9 for 50 per cent nickel-iron and in Fig. 4-10 for 4 per cent molybdenum-79 per cent nickel. Furthermore, when these curves are replotted versus volts/turn applied, as shown in Figs. 4-11 and 4-12, the curves for a particular N^2/R show strong correlation. This means that the incremental volt-second transfer efficiency remains substantially constant over a considerable swing of the input signal and that an incremental efficiency can be associated with each N^2/R. This material characteristic is really the

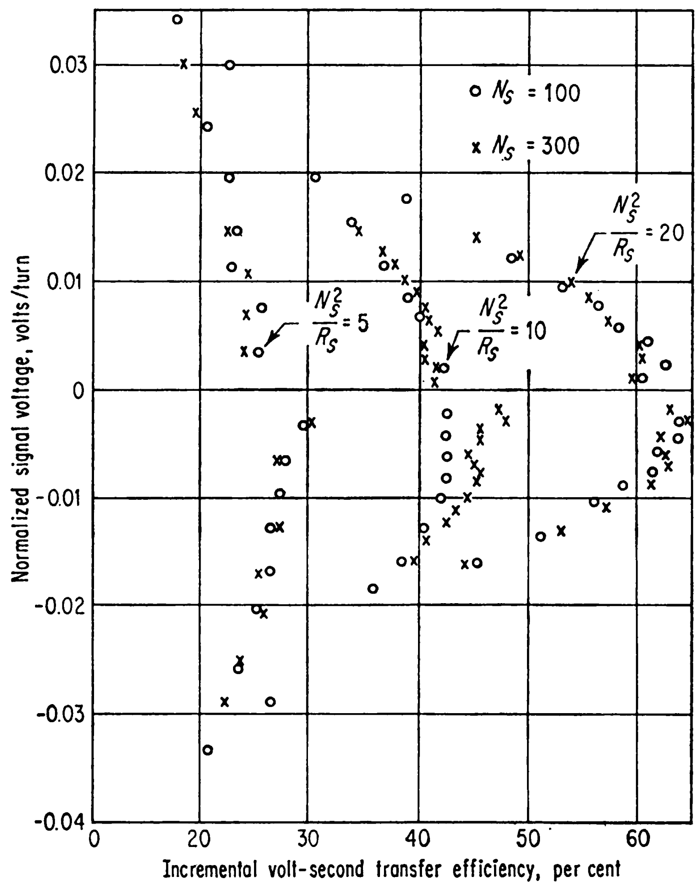

FIG. 4-11. Incremental volt-second transfer efficiency as a function of signal voltage for a 4 per cent molybdenum-79 per cent nickel material (N^2/R as a parameter).

source of the "linear" portion of the volts/volt or volts/incremental ampere-turn gain curve of self-saturating magnetic amplifiers.

As a series of curves of incremental volt-second transfer efficiency versus volts/turn applied is obtained, the curves show a shift in percentage with N^2/R. A fundamental characteristic of a particular core configuration at a given frequency is then the N^2/R value corresponding to a particular incremental volt-second transfer efficiency percentage. The application of these measurements to the design of fast-response amplifiers will be considered in Chap. 7.

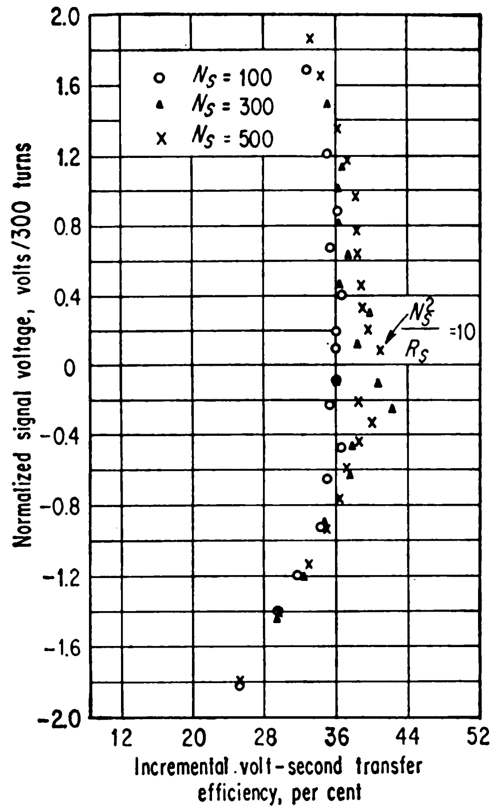

FIG. 4-12. Incremental volt-second transfer efficiency as a function of signal volts/turn for a 4 per cent molybdenum-79 per cent nickel material (N^2/R as a parameter). (*From Ref. 2, by permission of AIEE*).

REFERENCES

1. Ramey, R. A.: On the Control of Magnetic Amplifiers, *Trans. AIEE*, vol. 70, part II, pp. 2124–2128, 1951.
2. Pula, T. J.: Volt-second Transfer Efficiency in Fast Response Magnetic Amplifiers, Part I. N^2/R and Control, *Trans. AIEE*, vol. 77, part I, pp. 861–866, 1958.
3. Hughes, G. E., and H. A. Miller: Fast Response Magnetic Amplifiers, *Trans. AIEE*, vol. 73, part I, pp. 69–75, 1954.
4. Kikuchi, T., and K. Murakami: On the Input Power of the Half-wave Magnetic Amplifier Circuit, *Trans. AIEE*, vol. 76, part I, pp. 10–14, 1957.
5. Sixtus, K. J., and L. Tonks: Propagation of Large Barkhausen Discontinuities, *Phys. Rev.*, vol. 37, pp. 930–959, 1931.

5

Dynamic Response

In the preceding chapters, concerned for the most part with phenomenological analyses, transient conditions were discussed only where the elapsed time required for the completion of a specific operation was essential to an understanding of the mechanics of the operation. Once an appreciation of steady-state conditions is acquired, however, it is essential that the dynamic response as well as the static characteristics be examined. In this chapter, therefore, the dynamic response of magnetic amplifiers will be considered in detail. The treatment will be mathematical where the governing equations may be manipulated in a direct fashion, and phenomenological where the mathematics becomes untractable. The frequency-domain operations prevalent in automatic-control technology will be used principally, but a direct treatment of transient response of a doublet amplifier in the time domain is included to prove the equivalence of the two methods when applied to magnetic amplifiers.

5-1. FEEDBACK-CONTROL NOTATION AND METHODS

In all but the simplest cases involving transient conditions, a mathematical treatment is usually easier to manipulate if a transformation is made which converts time functions into complex frequency functions. After the manipulations have been made, an inverse transformation is used to provide an answer in the time domain. While several transformations have been suggested, some of which are superior in special cases, the most popular transformation is the Laplace transform, derived in a quite rigorous fashion from consideration of the Fourier integral.

The Laplace transform has been found so convenient that numerous specialized derivations have been made from it, such as the two-sided Laplace transform, the starred transform, the z transform, etc.[1] Obviously, a treatment of these topics is beyond the scope of a book of this nature. It is hoped that the reader is already acquainted with transformational calculus. For the reader whose formal education ended before the use of these techniques became widespread (and that wasn't very long ago) a very brief description of the Laplace technique follows.

While the following mathematical treatment is rigorous regardless of the nature of the variables involved, it will be assumed that the two domains to be considered are time and frequency. If a function of time, denoted by $f(t)$ is sectionally continuous (finite number of finite discontinuities) for all positive values of t and is of exponential order as t tends to infinity, a function of complex frequency, denoted by $F(s)$, may be formed

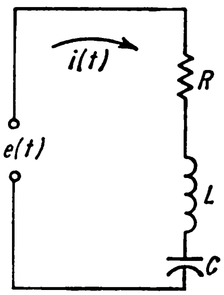

FIG. 5-1. Simple series R, L, C circuit.

$$F(s) = \int_{t=0}^{t=\infty} f(t)\epsilon^{-st}\,dt \tag{5-1}$$

where it is usually understood that $s = \sigma + j\omega$. The inverse transformation, required to return to the time domain, is

$$f(t) = \frac{1}{2\pi j}\int_{s=c-j\infty}^{s=c+j\infty} F(s)\epsilon^{ts}\,ds \qquad t > 0 \tag{5-2}$$

The value of the transformation technique lies in the fact that differentiation in the time domain becomes multiplication in the frequency domain. Difficult differential equations in the time domain, therefore, become comparatively simple algebraic manipulations in the frequency domain.

For example, consider the simple R,L,C circuit of Fig. 5-1. If $e(t)$ is assumed to be $E_m \sin \omega t$, the differential equation may be written as

$$e(t) = E_m \sin \omega t = L\frac{di}{dt} + Ri + \frac{1}{C}\int i\,dt \tag{5-3}$$

If initial conditions are assumed quiescent and it is desired to solve Eq. (5-3) for the current, the following transformation is made

$$E(s) = \frac{E_m\omega_0}{s^2 + \omega_0^2} = LsI(s) + RI(s) + \frac{I(s)}{Cs} \tag{5-4}$$

By manipulating Eq. (5-4)

$$\begin{aligned} I(s) &= \frac{E_m\omega_0 s/L}{\left(s^2 + \dfrac{Rs}{L} + \dfrac{1}{LC}\right)(s^2 + \omega_0^2)} \\ &= \frac{E_m\omega_0}{L}\,\frac{s}{[(s + R/2L)^2 - (R/2L)^2 + 1/LC](s^2 + \omega_0^2)} \end{aligned} \tag{5-5}$$

Equation (5-5) is in a form which can be found in most tables of inverse Laplace transforms.[2] From the tables

$$\begin{aligned} i(t) = {} & \frac{E_m\omega_0 C}{[(1 - LC\omega_0^2)^2 + (RC\omega_0)^2]^{1/2}}\left\{\sin\left(\omega_0 t - \tan^{-1}\frac{RC\omega_0}{1 - LC\omega_0^2}\right)\right. \\ & \left. + \left(\frac{4L}{4L - R^2C}\right)^{1/2} \exp\,(-RT/2L)\,\sin\left[\left(\frac{4L - R^2C}{4L^2C}\right)^{1/2} t + \psi\right]\right\} \end{aligned} \tag{5-6}$$

where

$$\psi = \tan^{-1}\left[-\left(\frac{4L - R^2C}{R^2C}\right)^{1/2}\right] - \tan^{-1}\frac{R(4LC - R^2C^2)^{1/2}}{2L - R^2C - 2\omega_0^2L^2C}$$

In feedback-control systems, interest lies in the output obtained for a given input to a system, subsystem, or component. In Fig. 5-2, a block diagram is shown for the simplest form. The output $C(s)$ is obtained from the input $R(s)$ operated on by the block represented by its transfer function $G(s)$. If the block were the circuit of Fig. 5-1, with an input $e(t)$, and an output which was the voltage across the resistor,

$$C(s) = RI(s) = \frac{RE(s)}{sL + R + 1/Cs} \tag{5-7}$$

Forming the output-input ratio from Eq. (5-7),

$$\frac{C(s)}{E(s)} = \frac{Rs/L}{s^2 + (Rs/L) + 1/LC} = G(s) \tag{5-8}$$

Equation (5-8) expresses the "transfer function" of the circuit of Fig. 5-1 when the input and output quantities are as stated.

Returning to Fig. 5-2, the block shown might represent any configuration which has a transfer function which can be expressed as a Laplace

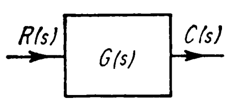

FIG. 5-2. Block diagram of a simple system.

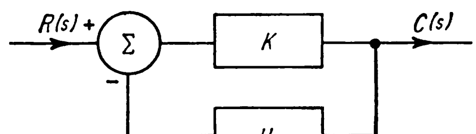

FIG. 5-3. Block diagram of a system containing a feedback loop.

transform. It might, for instance, be a simplified representation of the more complicated structure shown in Fig. 5-3. Here k represents a pure gain (although it could easily be some function of frequency) in the forward loop and H represents the gain of the feedback loop (which is also frequently a function of frequency). Since the output is a function of itself as well as of the input (by virtue of the feedback loop and the summation point), the following may be written

$$C(s) = kR(s) - kHC(s) \tag{5-9}$$

By suitable algebraic manipulation, the following set of equations may be obtained from Eq. (5-9) and the definition that $G(s) = C(s)/R(s)$

$$\frac{C(s)}{R(s)} = \frac{k}{1 + kH} = G(s) \tag{5-10}$$

If, for example, the forward loop transfer function is $(s + a)/(s + b)$

$(s + c)$ and it is desired that the closed loop be a simple time delay of the form $1/(s + d)$, it can be shown that the feedback path should contain

$$\frac{(a + d - b - c)s + ad - bc}{s + a}$$

In a doublet magnetic amplifier without external feedback or output filtering, the approximation has often been made that the output increases exponentially in response to a step increase in control voltage. This response is similar to that obtained when the switch is closed on a d-c circuit containing only resistance and inductance. Since the quantity L/R has the dimensions of time, an approximation frequently seen in the literature is that, for a doublet magnetic amplifier with low control-circuit resistance,[3]

$$G(s) = \frac{k}{1 + Ts} \tag{5-11}$$

where T is equal to L/R. It will be shown that this approximation is a useful one only when the condition of low control-circuit resistance is met, and the signal frequency is at least an order of magnitude smaller than the supply frequency.

5-2. IMPLICATIONS OF DEAD TIME

The phenomenon of dead time, sometimes called transportation lag or ideal time lag, can best be categorized as a lack of change in output for a specific interval of time following a change in input.[4] This is illustrated in Fig. 5-4. A step change in input at time $t = 0$ results in a step change of output at time $t = T_T$. The dead time, then, is T_T. The time function of such an output is generally represented as $u(t - T_T)$. The Laplace transform

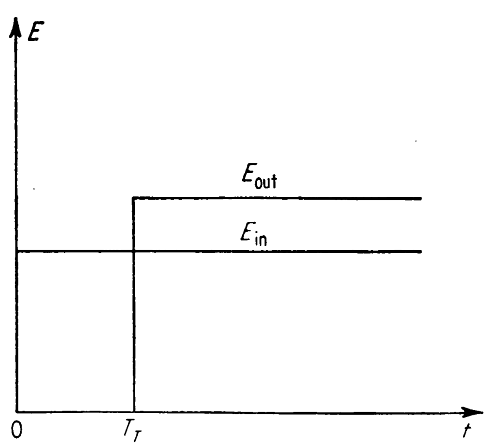

FIG. 5-4. Response of a system containing dead time.

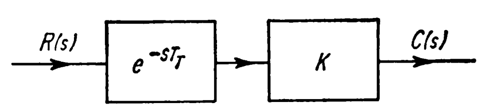

FIG. 5-5. Block diagram for system with response of Fig. 5-4.

of such a transfer function is exp $(-sT_T)$. The block diagram of this system, shown in Fig. 5-5, can be expressed mathematically as

$$C(s) = kR(s) \exp(-sT_T)$$

If feedback is put around this system as in Fig. 5-6, the transfer function becomes

$$G(s) = \frac{k \exp(-sT_T)}{1 + k \exp(-sT_T)} \tag{5-12}$$

It can be shown that $G(s)$ has an infinite number of poles and the system will be unstable for any gain constant k greater than unity.

As was demonstrated in Chap. 3, the output of a magnetic amplifier of the Logan type occurs only on positive half-cycles. The input is effective only during the alternate half-cycles. For this reason there is a lag between the time of any change of input and the time at which the input change becomes apparent at the output. It has been suggested, therefore, that the transfer function of such a magnetic-amplifier circuit can be represented as $k \exp(-sT_T)$ where T_T is the time interval between a step change of input and the corresponding change in output.[5] The validity of such a representation can be demonstrated experimentally. The experimental results do not differ markedly from calculated results until the signal frequency approaches values in the neighborhood of one-fifth to one-fourth of the power-supply frequency.

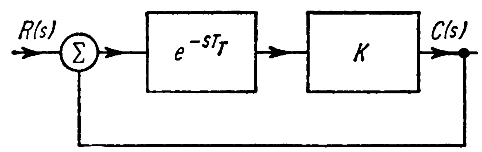

FIG. 5-6. Block diagram of a dead-time system with feedback.

This postulate, that $G(s) = k \exp(-sT_T)$, must be only an approximation, since it does not explain transient behavior at signal frequencies approaching the supply frequency. The disparity in results arises in part from the fact that T_T is not necessarily a constant but varies from a minimum of ½ cycle to a maximum of 1½ cycles. This variation in T_T is explained by considering a magnetic amplifier as a form of sampled-data system. The voltage appearing at the terminals of the reactor during a reset half-cycle is integrated over this period of time, and the output in the following half-cycle reflects the value of this integrated function. The input is not sampled, and, therefore, is not effective, during the gating half-cycle.

A further factor influencing the form of the exact transfer function is the method used to describe the output of the amplifier.[6] The instantaneous magnitude of output voltage is never the function of interest. The useful output may be the average value, the rms value, or even the magnitude of the supply-frequency component of the Fourier series representation. The unresolved question is, "When can the output quantity be said to have changed?" In a given amplifier, the angle at which a core fires in a given half-cycle may be said to define the output which will be obtained during that half-cycle, regardless of how the output is measured. However, since none of the three most common descriptions of output is linearly related to firing angle, it cannot be said that the time at which a core fires defines the time at which a change in useful output is obtained.

While rigorous, reasonably simple methods have been devised to handle sampled-data systems (for example, the z transform method), the assumption must be made that the interval over which sampling occurs is negligible with respect to the interval between sampling instants.[7] This restriction is obviously not met in a magnetic amplifier. A more complicated method, the pulse-width transform, removes the restriction on sample width, but is not applicable to analysis within closed loops.[8] A magnetic amplifier, therefore, cannot be rigorously treated as a sampled-data system with dead time since it is not a true sampled-data system nor does it have a constant dead time. While the concepts associated with sampled-data systems may occasionally be used with reasonable success in specific problems,[9] their indiscriminate use should be avoided.

Despite the deficiencies of the representations discussed, they are useful under restricted conditions and are the chief tools of the designer of magnetic amplifiers. A short apprenticeship usually suffices to acquaint a beginner with the major pitfalls associated with the various techniques. When properly applied, these techniques have proven to be valuable guides in arriving at satisfactory results.

5-3. THE TIME CONSTANT OF A DOUBLET AMPLIFIER

The gradual, half-cycle by half-cycle, change of average output voltage of a doublet amplifier in response to application of signal was described in Chap. 3. A more detailed mathematical analysis will be explained in this section, using the difference-differential equations which arise from the coupling of the cores through the control circuit.

Attempts were made in the early 1950s to represent the magnetic amplifier by a block diagram and it was then recognized that a positive feedback mechanism occurs in doublet amplifiers as a result of control-circuit coupling between the cores. Acting upon this premise, Johannessen in 1954 developed the governing difference-differential equations of a doubler circuit in terms of a vertical flux-mmf characteristic with zero area for the core material and the assumption of a finite nonzero reverse resistance for the rectifier.[10] As discussed in Chap. 3, the assumption of a vertical flux-mmf characteristic of zero area is untenable in the analysis of self-saturating magnetic amplifiers. Also, use of silicon diodes with a reverse resistance of the order of 10^{10} ohms approaches a nonfinite reverse resistance. However, the method developed by Johannessen has had wide influence on the analysis of magnetic-amplifier circuitry regardless of any specific inaccuracies in its application in a particular case.[11,12]

Consider, for instance, the bridge circuit shown in Fig. 5-7*a*. As explained in Chap. 3, reactor L_1 is reset during negative half-cycles of e_{ac} and reactor L_2 is reset during positive half-cycles. This circuit can be considered as two parallel forward paths, conducting on alternate half-cycles, and two parallel feedback paths, conducting on alternate half-cycles. By merging the parallel paths, the block diagram shown in Fig. 5-7*b* may be obtained. Before considering the block diagram, however, the operation of the circuit of Fig. 5-7*a* will be considered in the time domain.

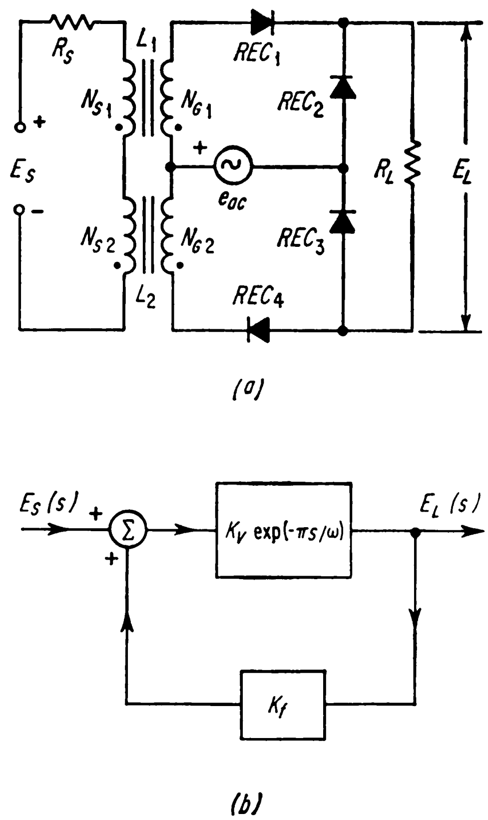

Fig. 5-7. Bridge magnetic amplifier. (*a*) Circuit diagram; (*b*) block diagram.

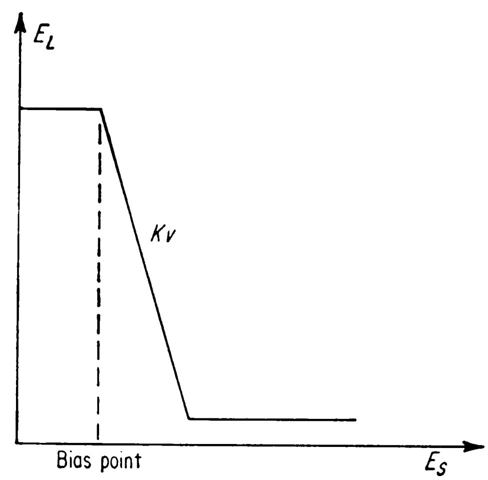

Fig. 5-8. Idealized static transfer characteristic of bridge circuit showing bias point.

To avoid unnecessary complication in the notation it will be assumed that both reactors are identical and that the static-transfer characteristic of one of the reactors (obtained, for instance, by opening either REC_1 or REC_4, varying E_S, and observing E_L) is of the form shown in Fig. 5-8. It will also be assumed that, with E_S zero, the amplifier is biased to the upper knee of the curve as shown in Fig. 5-8. If a step input, E_S, is applied at the instant of time when reactor L_1 is starting its reset half-cycle, no change in output voltage will appear for one half-cycle of the supply voltage. Before application of E_S, both cores were in a saturated condition. Reactor L_2 is starting a gating half-cycle at the time of application of E_S and will be unaffected by the presence of signal. At positive saturation at this time, no flux will change in reactor L_2 and, hence, no voltage will appear across the windings of L_2. Under the influence of E_S, however, flux will change in reactor L_1 during this zeroth half-cycle in exactly the same fashion as would occur in a Logan circuit. At the beginning of the following half-cycle, therefore, the flux in reactor L_1 will not be at positive saturation and the average output voltage during this first half-cycle will be less than during the previous half-cycle. The change in output voltage, which is equivalent to the volt-second area which was absorbed by the reactor prior to firing, is reflected into the control circuit and some portion of it adds to E_S in producing reset of reactor L_2. For this first half-cycle (the first in which an output change is observed)

$$\Delta E_{L(1)} = K_v E_S \tag{5-13}$$

where K_v is the slope of the characteristic of Fig. 5-8 and $\Delta E_{L(1)}$ is the change of output voltage in the first half-cycle in which such a change is observed. Since this change in output voltage was reflected into the control circuit prior to firing of reactor L_1, the reset occurring in reactor L_2 during this first half-cycle will be greater than the reset which occurred in reactor L_1 during the zeroth half-cycle. If K_f is the efficiency of the transfer of volt-seconds from one reactor to the other through the control circuit, the cumulative change in output voltage in the next half-cycle may be written

$$\Delta E_{L(2)} = K_v(E_S + K_f\, \Delta E_{L(1)}) \tag{5-14}$$

By substituting Eq. (5-13) into Eq. (5-14)

$$\Delta E_{L(2)} = K_v(E_S + K_f K_v E_S) = K_v E_S(1 + K_f K_v) \tag{5-15}$$

The cumulative change in output during the third half-cycle may be written

$$\Delta E_{L(3)} = K_v(E_S + K_f\, \Delta E_{L(2)}) \tag{5-16}$$

since the volt-second area transferred from the gating core during the previous half-cycle is proportional to the change in output voltage during the second half-cycle. By substituting Eq. (5-15) into Eq. (5-16)

$$\begin{aligned}\Delta E_{L(3)} &= K_v[E_S + K_f K_v E_S(1 + K_f K_v)] = K_v E_S[1 + K_f K_v(1 + K_f K_v)] \\ &= K_v E_S(1 + K_f K_v + K_f{}^2 K_v{}^2) \end{aligned} \tag{5-17}$$

By induction, then,

$$\Delta E_{L(n)} = K_v E_S(1 + K_f K_v + K_f{}^2 K_v{}^2 + \cdots + K_f{}^{(n-1)} K_v{}^{(n-1)}) \tag{5-18}$$

If a new gain constant K_c is defined as

$$K_c = \frac{K_v}{1 - K_v K_f}$$

this can be rearranged as

$$K_v K_f = 1 - \frac{K_v}{K_c} \tag{5-19}$$

By substituting Eq. (5-19) into Eq. (5-18)

$$\Delta E_{L(n)} = K_v E_S[1 + (1 - K_v/K_c) + (1 - K_v/K_c)^2 + \cdots + (1 - K_v/K_c)^{(n-1)}] \tag{5-20}$$

Equation (5-20) may be written as

$$\Delta E_{L(n)} = K_v E_S \sum_{r=0}^{(n-1)} (1 - K_v/K_c)^r \tag{5-21}$$

If both sides of Eq. (5-21) are multiplied by $(1 - K_v/K_c)$, the result subtracted from Eq. (5-21), and the difference simplified

$$\Delta E_{L(n)} = K_c E_S[1 - (1 - K_v/K_c)^n] \tag{5-22}$$

The symbol n, it should be recalled, represents the number of half-cycles which have elapsed since the beginning of the first half-cycle in which a change in output voltage was observed. Since π/ω is the time duration of a half-cycle, it can be seen that

$$n = \frac{t\omega}{\pi}$$

where t is time measured from the beginning of the first half-cycle in which an output voltage change was observed, not time measured from the step change of signal voltage. Substituting the time function for the half-cycle function, Eq. (5-22) becomes:

$$\Delta E_L = K_c E_S \left[1 - \left(1 - \frac{K_v}{K_c}\right)^{t\omega/\pi}\right] \tag{5-23}$$

Equation (5-23) may be manipulated to form

$$1 - \frac{\Delta E_L}{K_c E_S} = \left(1 - \frac{K_v}{K_c}\right)^{t\omega/\pi} \tag{5-24}$$

By taking the natural logarithm of both sides of Eq. (5-24)

$$\ln\left(1 - \frac{\Delta E_L}{K_c E_S}\right) = \frac{t\omega}{\pi} \ln\left(1 - \frac{K_v}{K_c}\right) \tag{5-25}$$

If a new symbol α is introduced

$$\alpha = -\frac{\omega}{\pi} \ln\left(1 - \frac{K_v}{K_c}\right)$$

and the antilogarithm of both sides of Eq. (5-25) is taken

$$1 - \frac{\Delta E_L}{K_c E_S} = \epsilon^{-\alpha t} \tag{5-26}$$

By one more manipulation

$$\frac{\Delta E_L}{E_S} = K_c(1 - \epsilon^{-\alpha t}) \tag{5-27}$$

Equation (5-27) is the exponential frequently employed to represent the time delay of magnetic amplifiers. Because of the definition of zero time, however, this expression is not exact since zero time is usually taken as the time of the step input. Such a correction would add an interval equal to π/ω to Eq. (5-27) with the result

$$\frac{\Delta E_L}{E_S} = K_c \left\{ 1 - \exp\left[-\alpha t - \ln\left(1 - \frac{K_v}{K_c}\right)\right]\right\}$$

which may be written, using Eq. (5-19)

$$\frac{\Delta E_L}{E_S} = K_c\left(1 - \frac{\epsilon^{-\alpha t}}{K_v K_f}\right) \tag{5-28}$$

It must be borne in mind that Eq. (5-28) has meaning only at instants of time when $t\omega/\pi$ has an integral value, since time was introduced as a variable to replace n which can have only integral values. The proper representation of such an output, then, is a series of steps constantly decreasing in step magnitude, as shown in Fig. 5-9.

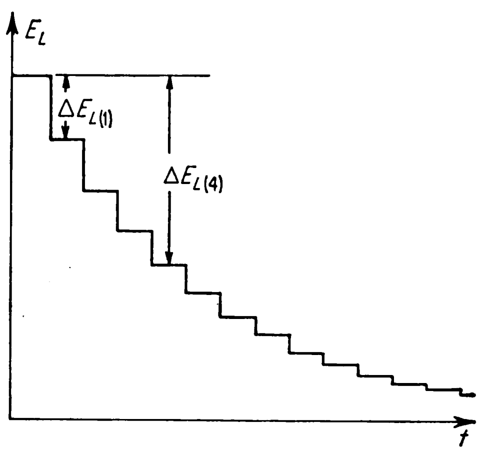

FIG. 5-9. Time response represented by Eq. (5-28) when $t\omega/\pi$ has only integral values.

An assumption made at the beginning of the preceding derivation was that the step change in E_S was initiated at the start of a reset half-cycle of reactor L_1. Had this step change been delayed, for example by a quarter-cycle, the output representation of Fig. 5-9 would be altered. The change in output voltage $\Delta E_{L(1)}$ would have been decreased to half the value shown. The difference $(\Delta E_{L(2)} - \Delta E_{L(1)})$ will be greater for the second case, however, and the steps will gradually approach the same value in both cases as time progresses. This dependence of output magnitude on the time in the supply-voltage cycle at which a signal change is initiated makes an exact analysis as a true dead-time system impossible.

If the assumption is made, however, that the block diagram of Fig. 5-7*b* is at worst a fair approximation to the circuit of Fig. 5-7*a*, an analysis in the frequency domain can be made. From the block diagram it is seen that

$$E_L(s) = K_v\epsilon^{-\pi s/\omega}[E_S(s) + K_fE_L(s)]$$

which can be written

$$E_L(s)(1 - K_vK_f\epsilon^{-\pi s/\omega}) = K_v\epsilon^{-\pi s/\omega}E_S(s)$$

or

$$\frac{E_L(s)}{E_S(s)} = \frac{K_v\epsilon^{-\pi s/\omega}}{1 - K_vK_f\epsilon^{-\pi s/\omega}} \tag{5-29}$$

The equivalence of Eqs. (5-29) and (5-28) can be demonstrated by use of the z transform technique if it is assumed that the input function is a unit step. Obviously, in view of the discussions in this and the preceding section, the equations developed must be applied with caution. They will, however, yield answers which are usually sufficiently accurate for most purposes up to signal frequencies in the range of one-fifth to one-fourth of the supply-voltage frequency.

5-4. LIMITATIONS OF PRESENT DYNAMIC THEORIES

The present theories of the dynamic response of magnetic amplifiers, including those of the previous section, may be grouped, generally, into two classes: those that require a large amount of empiricism (such as a measurement of open- and/or closed-loop gains) or those based on highly idealized representations of the core-material characteristics. None takes into account, directly, the mechanics of the core material in changing from one minor hysteresis loop to another. It is obvious from the discussion in Chap. 4 that circuit arrangement is a major factor in determining the transient response of a self-saturating magnetic amplifier and that a Logan circuit will have a half-cycle response regardless of the quality of the core material. In amplifier circuits in which coupling between cores is possible, however, the properties of the core material determine the dynamic response of a given configuration.

In addition to a rigorous mathematical method which will make tractable the nonlinearities and discontinuities involved in magnetic-amplifier operation, therefore, an exact analysis of magnetic-amplifier behavior will require a more detailed knowledge of the dynamic properties of core materials. The first deficiency is only serious when an attempt is made to predict performance at signal frequencies approaching one-fourth of the supply frequency. Because the phase shift is so large at these frequencies, this region is not often of more than academic interest, but in the few applications in which such prediction is required, laboratory measurement of the particular configuration considered is the only way to get accurate information. With accurate knowledge of the effects of the dynamic core properties (obtained, perhaps, by measuring open- and closed-loop gains) the block diagram technique will yield reasonable predictions at the lower frequencies.

The dynamic properties of the core material are of more concern than the lack of mathematical rigor at all frequencies when coupling between cores exists. Hubbard has suggested the input impedance of the reactors as the parameter which should be evaluated to obtain a constant which is representative of the core material for use in block diagram analysis or synthesis.[12] Such an evaluation would be more difficult to make than the gain measurements used in the preceding section, but should yield a quantity of more general usefulness than the simple gain measurements. Unfortunately, even this parameter is not nearly sufficiently constant to

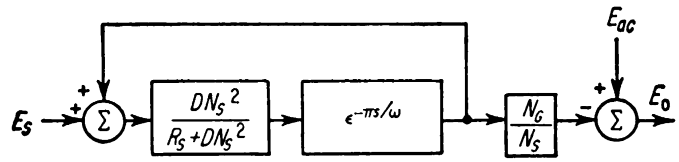

Fig. 5-10. Expanded block diagram of a bridge circuit.

yield really accurate results (within the region of reasonable accuracy of the mathematical representation) over a range of core sizes, winding turns, etc. While probably the best technique available today, it still falls short of the ideal solution.

Finzi and Critchlow have attacked the dynamic material characteristics directly for amplifiers in which the control-circuit impedance can be considered infinite.[13] By assuming that the rate of change of flux is uniquely determined by a given mmf (assumed to be nearly constant over reasonably long periods of time) and a given level of flux, they have demonstrated that, for core materials with quite square operating loops, a control characteristic can be predicted with reasonable accuracy using data from dynamic core tests. Within the circumscribed region of their investigation, the assumptions seem justified and they have advanced an excellent description of core flux behavior during the process of "triggering," a subject which will be discussed in Chap. 8. These authors concede, however, that the state of the art precludes formulation of the criteria into a quantitative analysis at the present time.

Admitting the inadequacies of present methods in certain regions of operation, a great deal can still be learned by application of these techniques. For example, an expanded block diagram of a bridge-type amplifier is shown in Fig. 5-10. It can be demonstrated that proper manipulation will make this diagram equivalent to that shown in Fig.

5-7b. By expanding the diagram, however, it is possible to illustrate the effects of changing parameters more clearly than the simpler diagram allows.

To construct the diagram of Fig. 5-10, it is necessary to assign notation to the voltage-current relationship of the signal winding during reset. This relationship will be designated as DN_S^2 for the purposes of this discussion. The significance and derivation of the notation will be discussed in Chap. 7. The forward gain of the portion of the diagram containing the feedback loop is $DN_S^2 \exp(-\pi s/\omega)/(R_S + DN_S^2)$. The feedback gain is unity. The closed-loop response is

$$G_1 = \frac{DN_S^2 \exp(-\pi s/\omega)/(R_S + DN_S^2)}{1 - DN_S^2 \exp(-\pi s/\omega)/(R_S + DN_S^2)} \tag{5-30}$$

As R_S is varied, the zero frequency magnitude of G_1 will vary and will approach zero as R_S approaches infinity (N^2/R approaches zero). It is common practice in automatic control systems synthesis or analysis to present a Bode diagram of the transfer function.[14] The Bode diagram is a plot of the phase-shift characteristic of the system as a function of signal frequency and a plot of the attenuation characteristic as a function of signal frequency. These plots are normally presented together on a common frequency axis. To illustrate the variation of the characteristics when R_S is varied parametrically, however, the complete Bode diagram of the G_1 of Eq. (5-30) is shown in two illustrations, Figs. 5-11 and 5-12. In Fig. 5-11, the attenuation is shown as a function of frequency for several magnitudes of the gain factor $DN_S^2/(R_S + DN_S^2)$. This gain factor approaches zero as R_S approaches infinity and approaches unity as R_S approaches zero. It can be seen from the denominator of Eq. (5-30) that the system becomes marginally unstable when the gain factor reaches unity. The gain factor, then, can only have values between zero and unity. Neither of these limiting conditions can be shown on the attenuation diagram since they imply zero frequency attenuations of positive and negative infinity. A limiting phase-shift characteristic is shown in Fig. 5-12, however, since a finite limit of phase shift exists for the condition of $DN_S^2/(R_S + DN_S^2) = 0$. The phase-shift characteristic for the condition when the gain factor is equal to unity cannot be shown on a logarithmic scale.

To illustrate the error introduced when the approximation of Eq. (5-11) is used [i.e., $G(s) = k/(1 + Ts)$], the phase-shift characteristic is plotted in Fig. 5-12 for three values of T. The three dotted curves show that, while the approximation is reasonably accurate when the corner frequency (defined as the 45° phase-shift point) is 0.10 cps, there is appreciable error when the phase shift of 45° occurs at 12 cps, and considerably more when the 45° phase-shift point occurs at 100 cps.

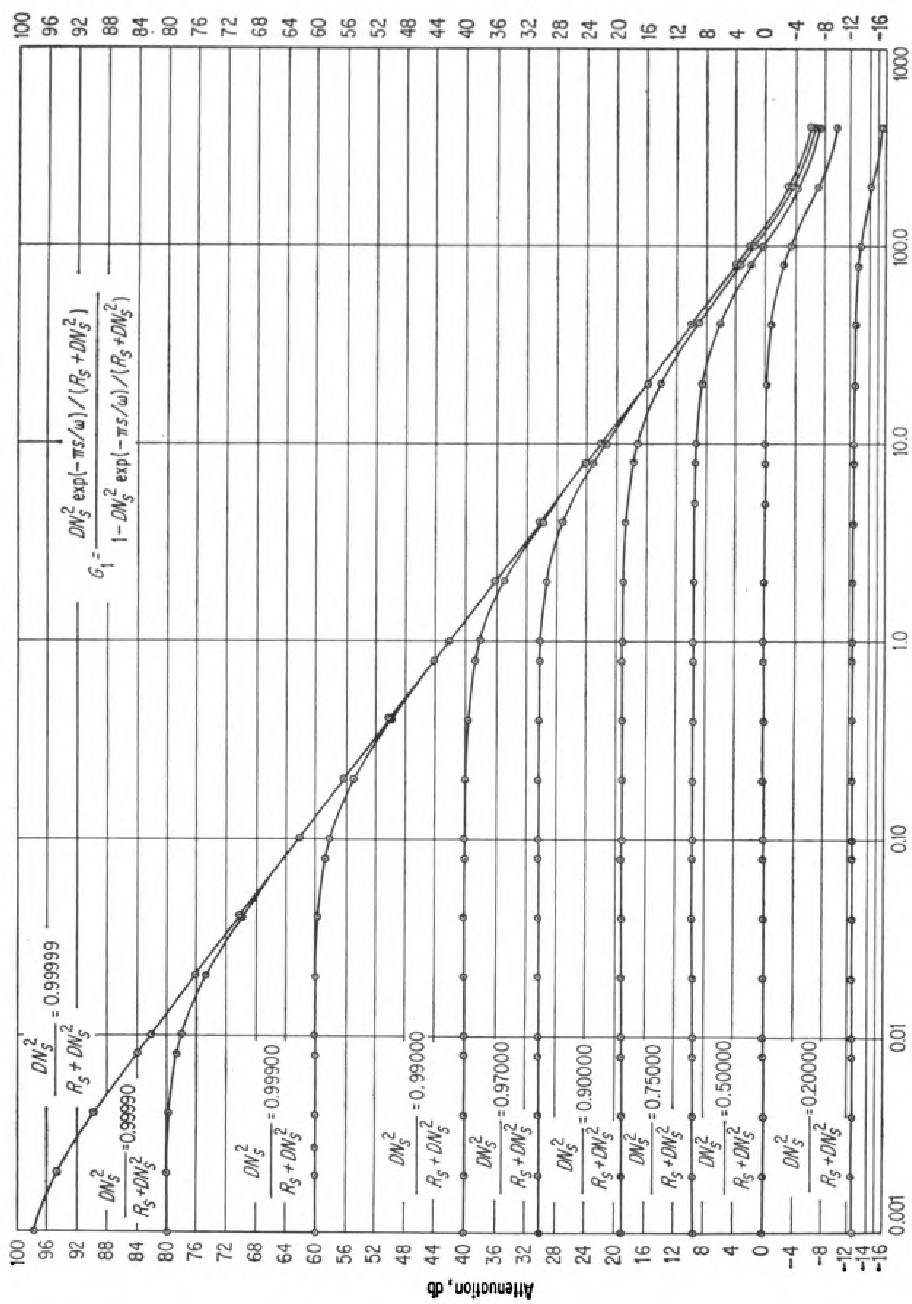

FIG. 5-11. Attenuation of a bridge amplifier as a function of signal frequency.

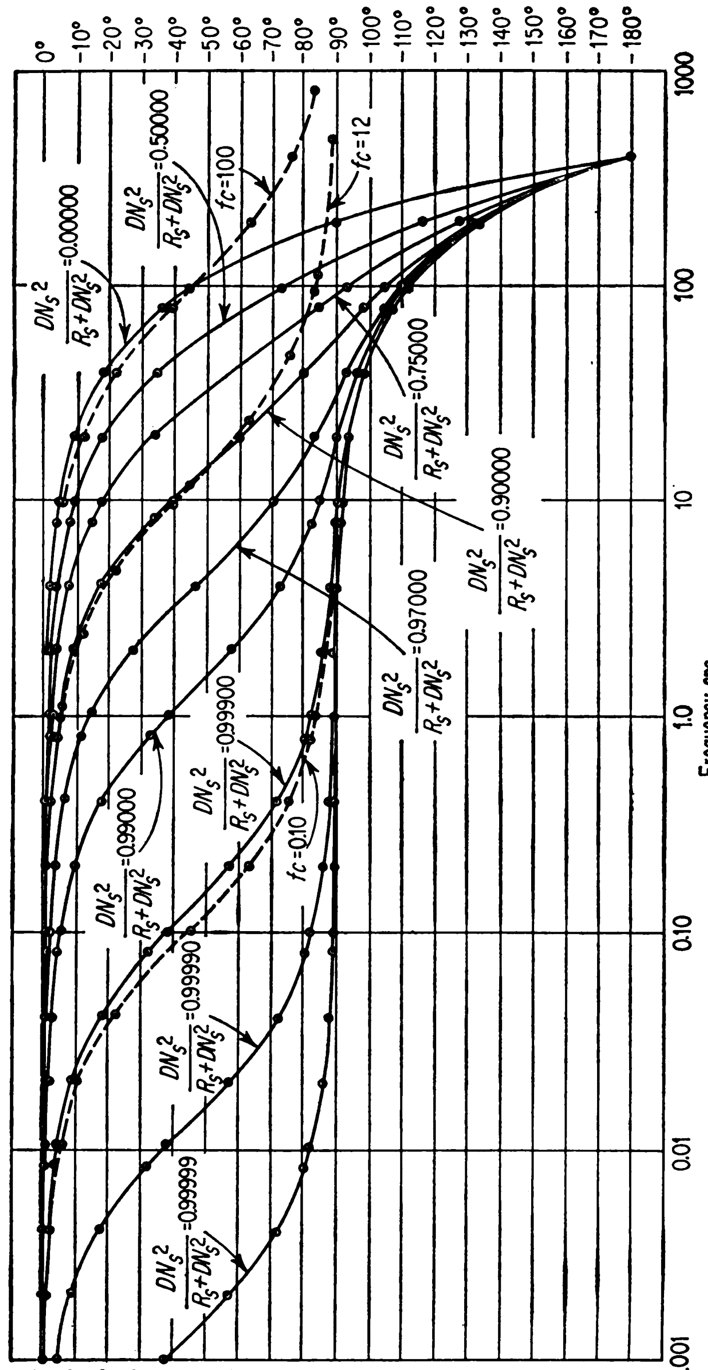

FIG. 5-12. Phase shift across a bridge amplifier as a function of signal frequency.

It should now be reasonably clear to the reader that the concept of control-circuit inductance which was advanced in the early history of magnetic amplifiers to explain the exponential change in output in response to a step change of signal has no basis in fact. The time constant observed results from the positive feedback mechanism, as demonstrated in Eq. (5-28) or Eq. (5-29), and not from the storage of energy in an inductance, as would be implied by Eq. (5-11).

5-5. APPLICATION OF FEEDBACK NETWORKS

Despite the inadequacies of present theories in explaining the dynamic response of magnetic amplifiers, a great deal has been accomplished in applying feedback networks to synthesize desired responses.[15] The bulk of this work has been concentrated in regions where the available approximations to amplifier response are valid. An appreciable amount, nonetheless, has been done empirically to synthesize responses in regions where present theories are grossly inadequate.

The use of feedback in magnetic amplifiers predates the introduction of self-saturation and serves to increase the gain of simple saturable reactor circuits. This use of feedback destroys the symmetrical response to positive and negative signals characteristic of saturable reactor circuits and results in an output at zero signal larger than that which can be accounted for by the magnetizing current of the cores. In short, the altered static characteristic resembles the characteristic later obtained through use of the self-saturating technique, and this resemblance led to the description of self-saturation as 100 per cent feedback.

With the introduction of improved methods of explaining amplifier operation and the use of more standardized terminology from the field of automatic control, the term feedback is usually now reserved for external networks added to an amplifier to improve or alter its basic characteristics or to explain behavior arising from coupling between reactors. While external feedback is frequently employed to stabilize the static characteristics of an amplifier, for example to improve linearity, decrease environmental sensitivity, minimize changes in static gain, etc., its principal use is to alter the dynamic response of an amplifier.

5-6. TYPES OF REACTOR COUPLING RESULTING IN TIME DELAY

In the introductory paragraph of Sec. 3-7, it was intimated that, of the popular doublet amplifier circuits, only in the bridge circuit were the reactors coupled through the control circuits alone. In the doubler and center-tapped circuits, the reactors are coupled through the load circuit as well. A brief comparison of the bridge and doubler circuits was made in Sec. 3-8, mentioning the load coupling. A more complete treatment will be given here as well as a treatment of the load circuit idiosyncracies of the center-tapped circuit.

Load-circuit Coupling. The circuit diagram of a simple typical doubler circuit is illustrated in Fig. 5-13. Let it be assumed that E_S is initially zero and that a step change of E_S is initiated at a time when e_{ac} is zero and going positive. The flux in reactor L_1 will be unaffected by the change in E_S during the first half-cycle and load current i_1 will flow throughout the half-cycle. The voltage appearing across points a and b of Fig. 5-13 under these conditions will be the sum of the iR drop in the winding N_{G1} and the forward drop of the rectifier REC_1. During this first half-cycle, the signal voltage E_S is causing a flux change in reactor L_2. The direction of flux change is such that the voltage appearing across the gate winding N_{G2} is positive at terminal 2 of reactor L_2 and negative at terminal 1. If the magnitude of the voltage appearing across terminals 1 and 2 exceeds the sum of the voltage across points a and b and the threshold voltage of rectifier REC_2, backfiring of rectifier REC_2 occurs and current i_2 will flow during this reset half-cycle of reactor L_2. In this first half-cycle, both the voltage across points a and b and the threshold voltage of rectifier REC_2 are essentially independent of the magnitude of E_S. This implies that the magnitude of E_S will determine whether or not backfiring will occur in this half-cycle. If E_S is sufficiently small, $N_{G2}\, d\phi_2/dt$ will never exceed the sum of the threshold voltage and the voltage at points a and b. If such a case is assumed, flux in reactor L_2 will be reset a small amount during this first half-cycle and will still be changing when reset is interrupted at the end of the reset half-cycle. At the start of the next half-cycle, flux in reactor L_2 will not be at positive saturation and a voltage will appear in the control circuit across terminals 3 and 4 of reactor L_2. The polarity of this voltage, as explained in Chap. 3 in connection with the bridge circuit, will be in a direction to aid E_S in resetting reactor L_1. Until flux in reactor L_2 reaches positive saturation, the voltage across points a and b will be the supply voltage e_{ac}, and backfiring of rectifier REC_1 will not occur unless $N_{G1}\, d\phi_1/dt$ exceeds e_{ac}. If R_S is assumed very large, the effect of control-circuit coupling between reactors may be neglected and the flux change taking place in reactor L_1 may be considered as occurring under the influence of E_S alone. Since

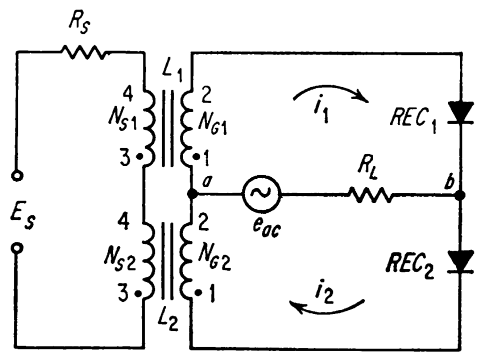

FIG. 5-13. Circuit diagram of a doubler amplifier.

E_S did not cause backfiring in the previous half-cycle, when the voltage across points a and b was small, backfiring cannot occur in this half-cycle either. Under the conditions postulated, then, the possibility of load-circuit coupling has had no effect on dynamic operation and half-cycle response is attained.

If a larger value of E_S is assumed, however, such that backfiring does occur on the first half-cycle, the effect of load-circuit coupling becomes apparent. If the magnitude of E_S causes backfiring of rectifier REC_2 during essentially all of the first half-cycle, some reset will occur in reactor L_2. The amount of reset will be given by

$$\Delta\phi_2 = \frac{1}{N_{G2}} \int_{t=0}^{t=\pi/\omega} (e_{a-b} + e_{REC_2})\, dt \tag{5-31}$$

During the second half-cycle the voltage across points a and b will be e_{ac} until reactor L_2 fires at an angle α_2. The amount of reset in reactor L_1 during the interval between π and α_2 will be greater than the amount of reset in reactor L_2 during an equal interval in the previous half-cycle and, therefore, the total amount of reset in reactor L_1 will exceed the magnitude of reset flux expressed in Eq. (5-31) if it is assumed that backfiring will reoccur after reactor L_2 fires. This assumption seems reasonable since, as explained in Sec. 2-7, the tendency is for $d\phi/dt$ to increase with time under the influence of a constant magnetic potential, at least when the mmf is reasonably small and the interval of time considered is not too long. At this point, no equation similar to Eq. (5-31) can be written for this half-cycle as was done for the first half-cycle because nothing has yet been said about backfiring before reactor L_2 fires. If backfiring does occur prior to firing of reactor L_2, Eq. (5-31) is valid. If backfiring does not occur for the duration of the interval from π to α_2, the voltage across terminals 3 and 4 cannot be expressed as a function of load-circuit parameters and may be considered indeterminate for the purposes of this discussion. For magnitudes of E_S which cause total flux changes of between one-quarter and three-quarters of the total possible flux change ($2\phi_{sat}$), backfiring will probably occur during the entire first half-cycle, but will not occur for the full interval from π to α_2 in the second half-cycle. The voltage across terminals 3 and 4 of reactor L_1 is, therefore, indeterminate, although it is known to be less than e_{ac} but greater than the voltage across reactor L_2 in the first half-cycle. The flux reset occurring in reactor L_1 during this second half-cycle, then, while not exactly predictable, is known to be greater than the reset of reactor L_2 in the first half-cycle. In the third half-cycle, therefore, the angle α_3 at which reactor L_1 fires will be greater than α_2. Reset of reactor L_2 in the interval from 2π to α_3 will be greater than the reset of reactor L_1 from π to α_2 because the voltage across points a and b will be equal to e_{ac} for a longer time in the third half-cycle than in the second. This process continues until the change in firing angle from one half-cycle to the next is so small that the additional amount of reset is negligible.

If a certain voltage across points a and b is assumed and added to an assumed rectifier threshold voltage, a volt-second area can be postulated for the first half-cycle, shown shaded in Fig. 5-14 as $e_{a-b} + e_{REC}$. The voltage which might appear across terminals 1 and 2 in the absence of backfiring is shown as e_{fr}. The supply voltage e_{ac} is shown for reference. Reactor L_2 is reset by an amount proportional to the volt-second area

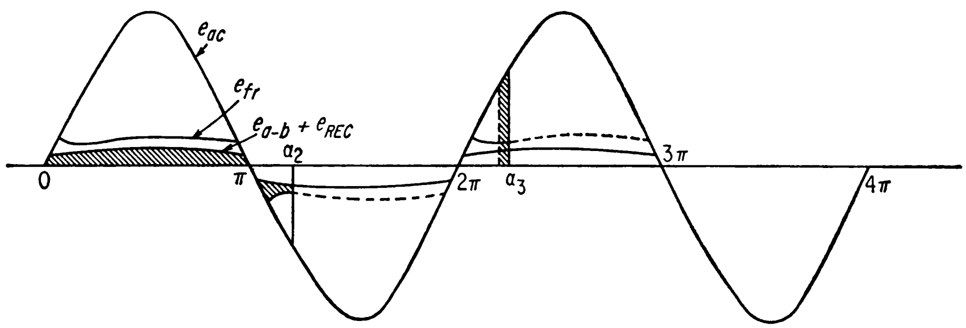

FIG. 5-14. Waveshapes illustrating the effect of load coupling on the response of a doubler amplifier.

under $e_{a-b} + e_{REC}$ during the first half-cycle. During the second half-cycle, reactor L_2 fires at α_2, where

$$\int_{t=0}^{t=\pi/\omega} (e_{a-b} + e_{REC})\, dt = \int_{t=\pi/\omega}^{t=\alpha_2/\omega} e_{ac}\, dt$$

The amount of reset in reactor L_1 during this half-cycle will exceed the amount of reset in reactor L_2 during the first half-cycle by an amount proportional to the volt-second area difference between $e_{a-b} + e_{REC}$ and e_{fr} from π to α_2. This volt-second area difference is shown shaded in Fig. 5-14. In the third half-cycle, $(\alpha_3 - 2\pi)$ differs from $(\alpha_2 - \pi)$ by an angle which causes the shaded area in the third half-cycle to equal the shaded area in the second half-cycle. The incremental reset of reactor L_2 becomes proportional to the solid area shown in the third half-cycle. This solid area is obviously much less than the shaded area and the sequence will converge rapidly to steady-state conditions.

It has been demonstrated that when the N^2/R parameter of a doubler circuit approaches zero, the transient response is affected by load-circuit coupling if backfiring occurs. If the N^2/R parameter approaches infinity, load-circuit coupling may be ignored. A high N^2/R parameter implies a large amount of positive feedback and a resulting high gain. The small signal voltages required (even to achieve complete reset) would probably not be large enough to cause backfiring to occur in the first half-cycle following a step change in signal voltage. Additionally, the large time delay introduced by a high N^2/R parameter would tend to make the contribution of load-circuit coupling negligible assuming some might exist, since the effects of load coupling were seen to cause rapid convergence of the series.

A typical center-tapped circuit diagram is shown in Fig. 5-15. It can be seen by inspection that the voltage across a resetting core in the center-tapped circuit must exceed the *sum* of e_{ac} and the voltage across the load resistor in addition to the threshold voltage of the rectifier before backfiring can occur.

$$E_{NG} > e_{ac} + e_L + e_{REC}$$

In the doubler circuit, it was only necessary for the resetting voltage to exceed the *difference* between e_{ac} and the voltage across the load resistor in addition to the threshold voltage of the rectifier for backfiring to occur.

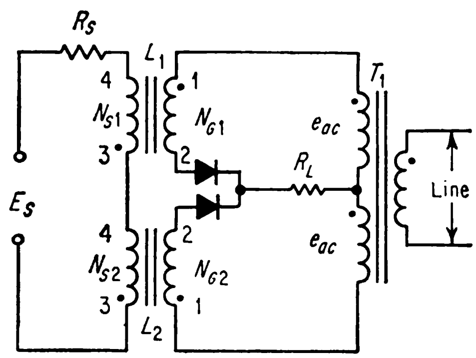

Fig. 5-15. Circuit diagram of a center-tapped amplifier.

$$E_{NG} > e_{ac} - e_L + e_{REC}$$

As a result of the much higher reset voltages allowed before backfiring occurs, backfiring is less of a problem in the center-tapped circuit than in the doubler circuit. The possibility of load-circuit coupling is still present in the center-tapped circuit, however, since the voltage across the load resistor is a function of the firing angle of the gating core. It is the presence of the load resistor in the circuit through which backfiring current must flow which results in load-circuit coupling and which marks the difference between the bridge circuit in which there is no such coupling and the doubler or center-tapped circuits in which coupling occurs.

Interstage Coupling. Another form of coupling which gives rise to time delay occurs when two or more amplifiers which would normally display fast-response are cascaded. In Fig. 5-16 two half-wave amplifiers are connected in cascade. If driven individually, each amplifier would exhibit half-cycle response and it could be assumed that, in cascade, the system would exhibit one-cycle response. It is possible, however, that appropriate design of the interstage circuit (composed of e_1, N_{G1}, R_1, REC_1, and N_{S2}) would result in a system exhibiting time delay in addition to dead time. An explanation of this phenomenon requires first a discussion of the desired operating characteristics of the circuit.

In a half-wave circuit, the volume of the core determines the power (energy/cycle) required of the signal source to obtain a given per cent reset of flux. In most applications it is desirable that a change in signal from zero to maximum be capable of changing the amount of reset from 0 to 100 per cent. Core volume also determines the amount of power which can be delivered to the load; and if the load power specified for a design requires a core volume which, for 100 per cent reset, calls for a signal power in excess of what is available, two stages of amplification must be used. For space and weight (and occasionally accuracy) reasons, it is frequently necessary to design the signal source as small as possible, resulting in low available signal power. When the response time of the amplifier must be of the order of 1 or 2 cycles of supply frequency, fast-response amplifiers must be utilized. Practical considerations place a lower limit on the volume of a core for use in a half-wave magnetic amplifier and, therefore, on the minimum signal power which

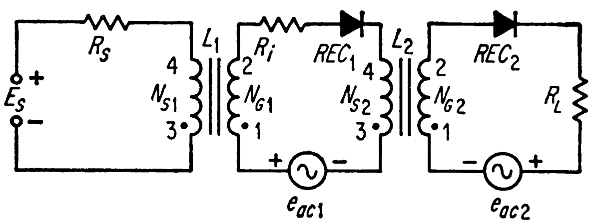

FIG. 5-16. Circuit diagram of cascaded fast-response amplifiers.

will completely reset the core. This minimum signal power, incidentally, is several orders of magnitude larger for the fast-response half-wave amplifier than for a doublet amplifier, since the latter has a much greater response time.

In Fig. 5-16, then, reactor L_2 has a reasonably large volume core capable of controlling the desired load power when reset is varied from 0 to 100 per cent.[16] Reactor L_1 has a minimum volume core the reset of which can be varied from 0 to 100 per cent by the signal source E_S at a minimum expenditure of power. When E_S is zero, the reset of reactor L_1 is zero and (assuming a core material in which $B_r/B_m = 1$) no volt-seconds from e_{ac1} are absorbed by reactor L_1 during a positive half-cycle of e_1. In the diagram, R_i represents the lumped interstage resistance including the winding resistances of N_{G1} and N_{S2} and the source resistance of e_{ac1}. Since reactor L_1 is saturated, e_{ac1} appears across R_i, REC_1, and N_{S2} throughout the half-cycle. If the magnetizing impedance of winding N_{S2} is assumed very large with respect to R_i, it may be assumed that the losses in R_i are negligible and that voltage which appears across terminals 3 and 4 of reactor L_2 will be the difference between e_{ac1} and the forward drop of REC_1. If the turns of winding N_{S2} are appropriately chosen, the voltage appearing across this winding may reset reactor L_2 completely in this half-cycle. Under these conditions, the load voltage will be essentially zero in steady state. It must be observed here that, if all the conditions imposed are met, e_{ac1} must be very nearly equal to $N_{S2}e_{ac2}/N_{G2}$ if the forward drop of REC_1 is assumed small with respect to e_{ac1}.[17]

Since e_{ac1} is very nearly equal to $N_{S2}e_{ac2}/N_{G2}$, on a reset half-cycle of reactor L_1 (concurrent with the gating half-cycle of reactor L_2), the following voltage equation may be written for the interstage circuit:

$$\frac{N_{S2}e_{ac2}}{N_{G2}} - e_{ac1} = 0 \tag{5-32}$$

If, at the beginning of a reset half-cycle of reactor L_1, a step change in E_S is assumed which will cause a voltage e_{NG1} to appear across the gate winding of reactor L_1, Eq. (5-32) will be modified to

$$e_{NG1} + \frac{N_{S2}e_{ac2}}{N_{G2}} - e_{ac1} = 0 \tag{5-33}$$

if the forward drop of the rectifier is neglected. Since the values of e_{ac2} and e_{ac1} have not changed, it would appear that e_{NG1} must be zero, which would indicate that no reset can take place in reactor L_1. However, since e_{ac1} was only approximately equal to $N_{S2}e_{ac2}/N_{G2}$, and since the forward drop of REC_1 has been neglected, e_{NG1} may have a small magnitude before backfiring of REC_1 occurs. If some reset does occur in this reset half-cycle of reactor L_1, then in the following gating half-cycle reactor L_2 will not be completely reset by e_{ac1} since some volt-seconds will be absorbed by reactor L_1 as flux is driven back to $+\phi_{sat}$. In the following reset half-cycle of reactor L_1, then, the term $N_{S2}e_{ac2}/N_{G2}$ will disappear from Eq. (5-33) before the end of the reset half-cycle, allowing voltage e_{NG1} to assume any magnitude less than e_{ac1}. This will allow a greater amount of reset than was allowed in the previous reset half-cycle. A greater reset of reactor L_1 results in less reset of reactor L_2 in the next half-cycle, resulting in an earlier firing angle of L_2 in its gating half-cycle. This causes the disappearance of the $N_{S2}e_{ac2}/N_{G2}$ term earlier in the reset half-cycle of reactor L_1 and so on. It is seen, then, that the fast-response characteristic is lost under the conditions assumed and that a transient build-up occurs which resembles the operation of the load-circuit coupling previously described.

By proper design of the interstage circuit, which includes recognition of the fact that R_i is not necessarily small with respect to the magnetizing impedance of N_{S2} and that, for a very small core in reactor L_1, the forward drop of the rectifier may be large with respect to the peak value of e_{ac1}, the increase in response time can be prevented. It is sufficient for the present discussion to emphasize that whenever two reactors are used in the same circuit, the possibility of coupling must be investigated before fast-response can be presumed.

REFERENCES

1. Truxal, J. G.: "Automatic Feedback Control System Synthesis," McGraw-Hill Book Company, Inc., New York, 1955.
2. Goldman, Stanford: "Transformation Calculus and Electrical Transients," Prentice-Hall, Inc., Englewood Cliffs, N.J., 1949.
3. Storm, H. F.: "Magnetic Amplifiers," p. 272, John Wiley & Sons, Inc., New York, 1955.
4. Truxal, J. G.: "Automatic Feedback Control System Synthesis," pp. 546–557, McGraw-Hill Book Company, Inc., New York, 1955.
5. Baker, F. A., and F. G. Timmel: Magamps Applied to Aircraft Control Problems, *Aeronaut. Eng. Rev.*, vol. 13, pp. 46–49 and 66, November, 1954.
6. Barker, R. C., and G. M. Northrop: Some Frequency Response Measurements on Magnetic Amplifiers, *Proc. Natl. Electronics Conf.*, vol. 12, pp. 444–453, 1957.
7. Ragazzini, J. R., and L. A. Zadeh: The Analysis of Sampled-data Systems, *Trans. AIEE*, vol. 71, part II, pp. 225–232, 1952.
8. Longuemare, R. N.: Critical History of Sampled-data System Analysis, M.S. Thesis, The Johns Hopkins University, Baltimore, Md., 1958.
9. Kadota, T. T., and H. C. Bourne: Operational Magnetic Amplifiers with Multiple Control Windings, *Trans. AIEE*, vol. 76, part I, pp. 515–520, 1957.
10. Johannessen, P. R.: Analysis of Magnetic Amplifiers by the Use of Difference Equations, *Trans. AIEE*, vol. 73, part I, pp. 700–711, 1954.
11. Lynn, G. E.: A Fast-response Full-wave Magnetic Amplifier, *Trans. AIEE*, vol. 77, part I, pp. 37–41, 1958.
12. Hubbard, R. M.: Magnetic Amplifier Analysis and Application Using Block-diagram Techniques, *Trans. AIEE*, vol. 76, part I, pp. 578–588, 1957.
13. Finzi, L. A., and D. L. Critchlow: Dynamic Core Behavior and Magnetic Amplifier Performance, *Trans. AIEE*, vol. 76, part I, pp. 229–240, 1957.
14. Chestnut, Harold, and R. W. Mayer: "Servomechanisms and Regulating System Design," pp. 297–318, John Wiley & Sons, Inc., New York, 1951.
15. Decker, R. O.: Alteration of the Dynamic Response of Magnetic Amplifiers by Feedback, *Trans. AIEE*, vol. 73, part I, pp. 658–664, 1954.
16. Voice, C. C.: Fast Response Multi-stage Magnetic Amplifiers, *Proc. Natl. Electronics Conf.*, vol. 12, p. 417, 1956.
17. Pula, T. J., G. E. Lynn, and J. F. Ringelman: Volt-second Transfer Efficiency in Fast Response Magnetic Amplifiers, Part II, N^2/R as a Design Parameter, *Trans. AIEE*, vol. 78, part I, p. 9, 1959.

6

Magnetic Material Evaluation

Accurate reliable test methods for evaluating those characteristics of a toroidal core which determine the performance of the core in a magnetic-amplifier circuit are required for economical mass production of high-performance magnetic amplifiers as well as for fast accurate design procedures for magnetic-amplifier circuits. At present no satisfactory single-test method exists which can evaluate cores for use in all magnetic-amplifier circuits. In 1959, the American Institute of Electrical Engineers published two test procedures for core matching and grading for use in industry.[1] Concurrent with the submission of these test procedures, the Institute sponsored a program to determine the amount of correlation existing between core performance in a magnetic-amplifier circuit and the core test parameters as measured in any test circuit. These activities indicate that deficiencies still exist in the present state of the art of core testing. Since the results of the Institute's programs, initiated to remedy the deficiencies, will not be available for two or three years, it is necessary to review both of the test procedures in their present form. Other test methods are in use for specialized purposes but space does not allow a description of all the methods which might be used. Before considering test methods, however, it is advisable to discuss the magnetic properties which are involved in magnetic-amplifier operation.

6-1. CORE-MATERIAL CHARACTERISTICS DETERMINING AMPLIFIER PERFORMANCE

The basic properties of ferromagnetic materials were discussed in Chap. 2. The static and dynamic operation of magnetic amplifiers employing these ferromagnetic materials was explained in Chaps. 3 and 5. In considering methods for testing materials to be used in magnetic amplifiers, it is worthwhile to devote a section to a review of the connection between certain magnetic properties and amplifier operation. It must be understood that such a discussion will be incomplete, since the present state of the art does not include a thorough understanding of all aspects of the problem.

Basically, operation of a magnetic amplifier involves a reset period and a gating period. The performance of the amplifier is a function of phenomena (both circuital and magnetic) which occur in one or the other of these two periods. During the gating period, four separate items may be considered:

1. The gate current which flows prior to the firing of a reactor
2. The volt-seconds absorbed by the reactor prior to firing
3. The time required for gate current to rise from the prefiring state to the postfiring state
4. The ratio of the amount of energy stored in the reactor during a gating period to the amount of energy dissipated in the core material during the gating period

During the reset period three factors are of primary interest:

1. The average signal current required to achieve a nonnegligible amount of flux reset
2. The average signal current required to reset the core completely
3. The manner in which the time rate of change of flux varies within the reset period

In general, all of these factors will have some influence on the performance of any self-saturating magnetic amplifier, although special cases may exist in which the influence of one or more factors may be negligible.

When those factors affecting amplifier performance during the gating period are considered, what core-material characteristics are found responsible for the phenomena observed? No general answers are available because each factor is influenced not only by core-material characteristics but also by circuit parameters. Certain specific assumptions must be made, then, concerning the amplifier circuit. The assumption that flux changes under the influence of a voltage rather than a current source during gating is probably least likely to be violated in practice.

With this assumption made, the core-material properties influencing the prefiring gate current (frequently called the magnetizing current) may be investigated. Except when the amplifier is operating at or near cutoff, the domain walls are never completely swept out during the reset period and so it is not generally necessary to nucleate domain walls at the beginning of a gating period. The prefiring gating current then, is not necessarily a function of the magnetic potential required for domain-wall nucleation, but approaches this value as an upper limit. The current (and hence the magnetic potential) will vary inversely with the time rate of change of flux toward positive saturation in a manner to maintain the voltage at the gate-winding terminals of the reactor just a little less than the voltage at the terminals of the voltage source. The magnitude of this magnetizing current, then, is a function of the magnetic potential required to keep the domain walls moving past the inclusions and imperfections in the core material at a rate consistent with the applied voltage. A magnetic term is already associated with this phenomenon: dynamic coercive force. The first factor listed above is shown, therefore, to be associated with the dynamic coercive force of the magnetic material.

The second factor, the volt-second area absorbed by the reactor prior to firing, is, of course, a direct function of the amount of reset taking place in the previous reset half-cycle, the number of turns of the gate winding, and the cross-sectional area of the core. For a given number of turns and a fixed core size, a practical upper limit to the volt-second area which can be absorbed exists, regardless of the amount of energy supplied during the reset half-cycle. This practical upper limit is imposed by the saturation flux density of the core material used.

The magnetic phenomena which determine the time required for gate current to rise from the prefiring to the postfiring state are less easy to define. Since practical core materials are polycrystalline substances, the transition is, at least in oriented materials, a function of how many grains have an easy direction of magnetization parallel to the applied field. In addition to the degree of grain orientation, the transition is a function of the energy required to rotate the magnetization vector away from the easy direction of magnetization into parallel alignment with the applied field. This energy is a function of the magnetic crystalline anisotropy constant of the material. In a nonoriented material, the transition is governed by phenomena not well understood. It is believed that a stress anisotropy resulting from stresses set up along slip lines in the crystallites of the polycrystalline material plays at least a contributory part. The energy required to rotate the magnetization vector away from the direction it would have in the absence of an external field is of importance in a nonoriented material as well as in an oriented one. In a nonoriented material, however, the energy is not necessarily a function of the magnetic crystalline anisotropy constant alone.

The ratio of the amount of energy stored in the reactor during a gating period to the amount of energy dissipated in the core material is a function of the ratio of the difference between the remanent flux density and the saturation flux density to the amount of reset occurring in the previous reset period. With zero reset, nearly all of the energy delivered to the reactor is stored energy.

In considering the factors of interest during the reset period, a further knowledge of amplifier circuitry is needed. As indicated in previous chapters, control-circuit resistance and reactor coupling play a dominant role in determining how reset takes place. A further complication is added when the possibility of backfiring is taken into consideration. Since the waveshape of the signal makes a significant contribution to amplifier performance, a d-c signal voltage will be assumed. This assumption makes it reasonable to treat the variation of mmf at the beginning of a reset period as a step change without too great a distortion of fact. As explained in Sec. 2-5, a step change in magnetic potential from a remanent condition will not result in a flux change unless the magnitude of the step is sufficiently large to nucleate domain walls. The average signal current required to achieve a nonnegligible amount of flux change, then, is a function of the magnetic potential required to nucleate domain walls in a specimen in its remanent state.

The average signal current required to reset the core completely is probably the most difficult parameter to assess with respect to a combination of magnetic characteristics of the core material. Certainly it is dependent on the third factor listed as affecting amplifier performance during reset, the manner in which $d\phi/dt$ varies with time. It is also a function of the waveshape of the voltage appearing at the reactor terminals, which in turn is a function of the signal waveshape, reactor coupling, and control-circuit resistance. After these dependencies are accounted for, however, the average signal current required to reset the core completely is a function of the magnetic potential required to nucleate domain walls and the potential required to cause them to move at a rate which results in complete reset at the end of the reset period.

6-2. BASIC TESTER CIRCUITS, WAVEFORMS, OPERATING LOOPS

The two test methods believed to give the best correlation in general between measured core characteristics and amplifier performance are the constant-current flux reset method and the sine-current excitation method. Other test methods are in use which are believed to give better correlation in particular cases for special amplifier circuits. Since these other methods are usually similar in many respects to the two methods adopted as standard by the AIEE Magnetic Amplifiers Committee, only the standard methods will be discussed in detail.

Constant-current Flux Reset Test. The constant-current flux reset test was published first by Conrath[2] and was generalized and expanded by Roberts.[3] The basic circuit for the test is shown diagrammatically in Fig. 6-1.

To determine the squareness of the effective hysteresis loop of a particular core one must measure the peak flux density to which the core is driven and its remanent flux density (or the equivalents of these properties). Squareness is a brief term frequently used to describe the ratio of remanent flux density to peak flux density and is related to characteristic 4 of the gating interval as discussed in Sec. 6-1. Characteristic 4 of the gating interval is the ratio of the amount of energy stored in a reactor during a gating period to the amount of energy dissipated in the core material during the gating period.

To obtain these ratios by use of the constant-current flux reset test, switch *Sw* of Fig. 6-1 is thrown to connect the half-wave sinusoidal current supply into the gating circuit. The variable d-c current supply is turned to zero. Under these conditions, the magnetic potential applied to the core is varied from zero to a large positive value every other half-cycle of the current-supply frequency. The peak magnetic potential is usually in excess of five times the dynamic coercive force of the material. With this type of operation, the flux in the core is varied from its positive remanent state to the flux level associated with the peak magnetic

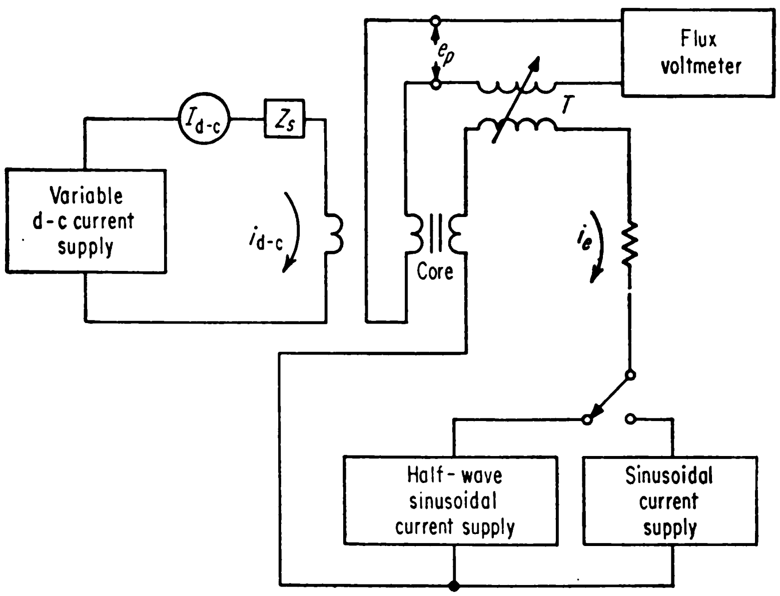

FIG. 6-1. Basic circuit for constant-current flux reset test.

potential. Since the peak magnetic potential is large, essentially all 180° domain walls have been swept out and the flux change observed is a result of rotation of the magnetization vector plus a small amount due to wall motion in the vicinity of crystal imperfections. The changing flux causes a voltage to appear across the winding associated with the flux voltmeter. The flux voltmeter measures the average or peak voltage (depending upon the circuit used) appearing across this winding and yields a reading which is calibrated to an equivalent flux density change. The flux density change thus obtained is $B_m - B_r$.

If the output of the variable d-c current supply of Fig. 6-1 is increased from zero, an I_{dc} can be found at which a nonnegligible amount of flux reset occurs. This additional flux change is evidenced by a corresponding increase in the reading of the flux voltmeter. Continuing to increase the output of the variable d-c current supply will result in a continuing increase in the reading of the flux voltmeter until the flux is cycling between $+\phi_m$ and $-\phi_m$. The reading of the flux voltmeter at this point is equivalent to a flux density change of $2B_m$. The ratio of B_r/B_m can now be formed from the first and last readings of the flux voltmeter by proper arithmetical manipulation.

If the readings of the flux voltmeter and the reset current meter are constantly monitored as the reset current is increased from zero, a reset characteristic can be obtained as shown in Fig. 6-2. In this figure, the readings of the flux voltmeter are shown as a function of reset current. In making comparisons between cores of the same material, it is difficult and time-consuming to plot the entire reset characteristic. To facilitate such comparisons, five standard test points have been recommended by a working group of the AIEE. In defining the standard test points, it was first necessary to define a standard maximum change of flux density for a given material under the conditions imposed by the proposed standard test methods. The five test points indicated on the curve of Fig. 6-2 were then determined as follows:[1]

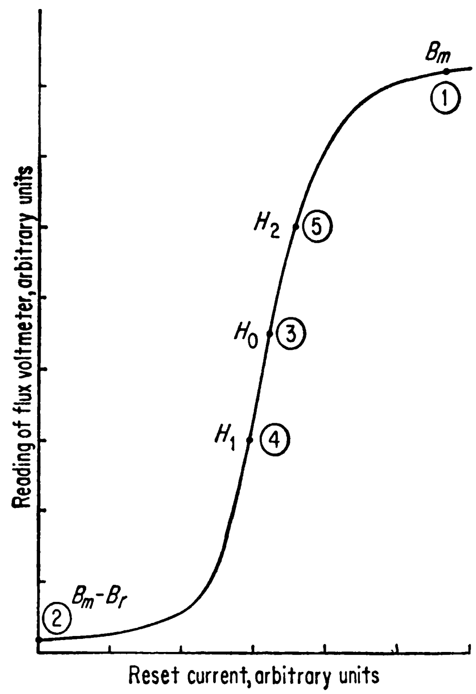

FIG. 6-2. Typical reset characteristic of a core, showing the standard test points.

1. B_m shall be measured at a peak magnetic field intensity (H_m) specified for a given material in the proposed standard.

2. $B_m - B_r$ shall be measured at zero reset magnetic field intensity.

3. H_0 is equivalent to the reset magnetic field intensity required to produce a cyclic change of induction (ΔB_0) equal to one-half the standard maximum flux density change specified for the core material.

4. H_1 is equivalent to the reset magnetic field intensity required to produce a cyclic change of induction (ΔB_1) equal to one-third the standard maximum flux density change specified for the core material.

5. H_2 is equivalent to the reset magnetic field intensity required to produce a cyclic change of induction (ΔB_2) equal to two-thirds the standard maximum flux density change specified for the core material.

These points can then be used to obtain information concerning the results to be expected from use of the cores in a magnetic-amplifier circuit. B_m, for example, gives the maximum induction directly. $B_m - B_r$ is a measure of squareness and can be utilized to determine a squareness ratio. Either H_0 or H_1 can be used to predict the amount of bias current required to bias the amplifier to a given operating point. The difference (ΔH) between H_1 and H_2 is a measure of the gain of the core.

The test method can also provide information concerning the comparative merits between two materials. A material gain G can be defined as $(\Delta B_2 - \Delta B_1)/\Delta H$. B_m and B_r/B_m afford comparisons of maximum flux density and squareness ratio, respectively.

With an appreciation of what measurements are made with the constant-current flux reset test, the circuitry may be discussed in somewhat

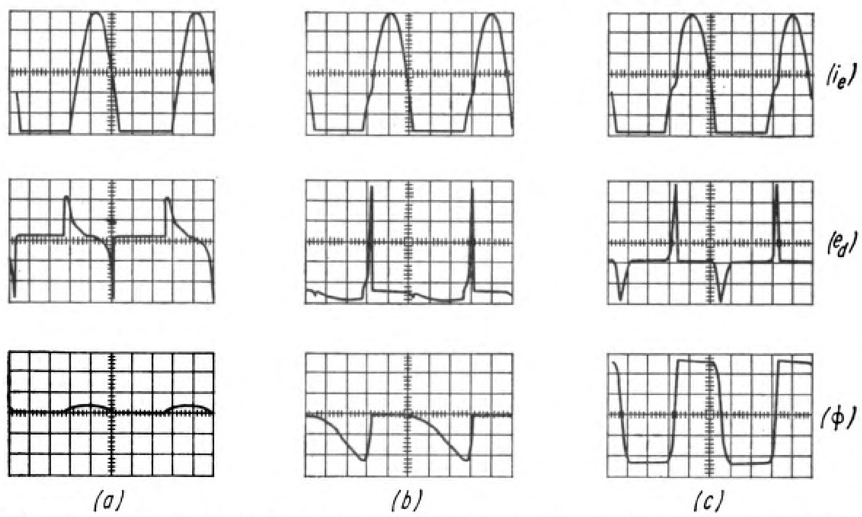

FIG. 6-3. Waveshapes of exciting current, pickup voltage, and flux for the constant-current flux reset test. (a) $\Delta\phi = \phi_m = \phi_r$; (b) $\Delta\phi = \phi_m$; (c) $\Delta\phi = 2\phi_m$.

more detail. The half-wave sinusoidal current supply of Fig. 6-1 is obtained by using a voltage source in series with a resistance and a diode. The rms amplitude of the voltage source is specified by the AIEE standard to be greater than 100 times the half-cycle average value of voltage induced in the excitation winding. This ensures a reasonable approximation to the desired sinusoidal current. The variable transformer T coupling the excitation circuit and the voltmeter circuit is an air-core transformer used to buck out the undesired induced voltages resulting from the unavoidable proximity of the two circuits. The purpose of the impedance Z_s in the control circuit is to reduce control current ripple to a minimum and to prevent the flow of induced currents which would tend to load the excitation circuit. A typical tester will have a total N^2/R of much less than 0.1.

The sinusoidal current supply which may be connected into the excitation circuit by means of switch Sw is used to obtain a more meaningful reading of B_m. As will be shown in the later discussion of waveshapes and operating loops, the use of a sinusoidal current for gating and a constant current for reset results in asymmetrical operating flux-current loops. The value of B_m obtainable under such conditions is usually not in agreement with the value of B_m found by other measurement techniques. For this reason a full-wave supply is used to obtain the $2B_m$ reading and the output of the variable d-c current supply is turned to zero.

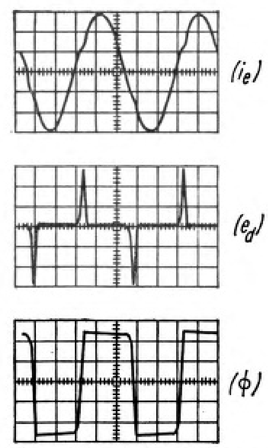

FIG. 6-4. Waveshapes resulting from use of full-wave supply.

Typical waveshapes of various parameters of interest are shown in Figs. 6-3 and 6-4 for a 50 per cent nickel-iron core. The waveshapes of i_e, e_d, and flux ϕ are shown in Fig. 6-3a for zero reset, in Fig. 6-3b for reset equivalent to B_m, and in Fig. 6-3c for full reset, nearly equivalent to $2B_m$. The waveshapes of i_e, e_d, and ϕ are shown in Fig. 6-4 for measurement of B_m using the full-wave sinusoidal current supply. The flux-current loops for operation corresponding to the conditions of Fig. 6-3 are shown in Fig. 6-5.

It will be recognized that the waveshapes and operating loops will vary somewhat as a function of the material tested. Graphs of flux change as a function of reset magnetizing force are shown in Fig. 6-6 for four different materials. Such a comparison allows a much better evaluation of the magnetic properties pertinent to magnetic-amplifier performance than do comparisons of such phenomena as d-c hysteresis loops, a-c hysteresis loops, or various permeabilities.

Sine-current Excitation Test. The origin of the sine-current excitation test lies in the dynamic sine-current hysteresis loop. The

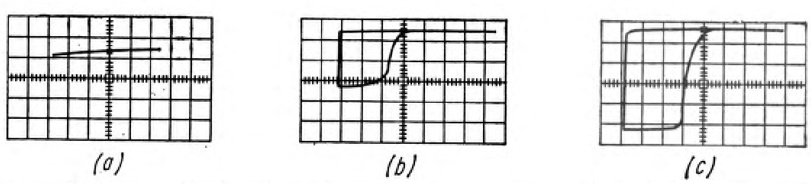

FIG. 6-5. *B-H* loops obtained during constant-current flux reset test. (*a*) $\Delta\phi = \phi_m - \phi_r$; (*b*) $\Delta\phi - \phi_m$; (*c*) $\Delta\phi = 2\phi_m$.

equipment required to display this loop was modified and added to by numerous people[4,5] and much of the circuitry used in the test as adopted by the AIEE was patented in 1957 by Patrick and Jansens.[6] The basic circuit for this test is shown in Fig. 6-7. Measurements of $B_m - B_r$ and B_m are identical with the methods described for the constant-current flux reset test. In fact, the originally developed tests were both modified to some degree at the time of standardization in order that the measurements of $B_m - B_r$ and B_m would show good correlation.

As Fig. 6-7 shows, the sine-current excitation test makes no provision for intermediate reset of the core. Measurement of $B_m - B_r$ is made with half-wave sinusoidal current excitation and all other measurements are made with full-wave or symmetrical sinusoidal current excitation. In addition to B_m and $B_m - B_r$, the sine-current excitation test measures the sine-current coercive force and the maximum differential permeability

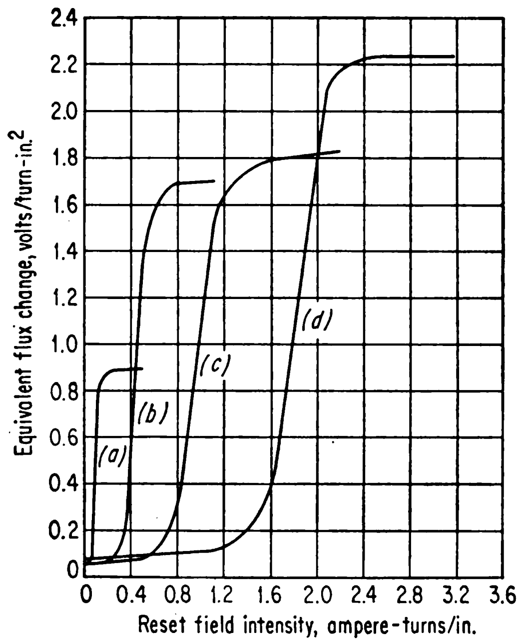

FIG. 6-6. Normalized reset characteristic for four materials. (*a*) 4 per cent molybdenum-79 per cent nickel; (*b*) 50 per cent nickel-iron; (*c*) 3 per cent silicon-iron; (*d*) 50 per cent colbalt-iron.

as defined by the maximum time rate of change of flux and the mmf at which it occurs. The latter two measurements are made with the aid of the long-persistence screen cathode ray oscilloscope shown in Fig. 6-7. The horizontal and vertical deflections of the oscilloscope are calibrated by means of the two d-c references V and V' shown.

With switch Sw_2 in position 1, the output voltage is connected to the vertical deflection plates of the oscilloscope and the excitation current drives the horizontal deflection plates. The resultant trace is shown in Fig. 6-8. The dynamic coercive force is defined for the purposes of this test as the magnetic field intensity at which $d\phi/dt$ and, hence, the voltage across the pickup winding, is a maximum. The value of the maximum differential permeability is a function of the value of the maximum voltage

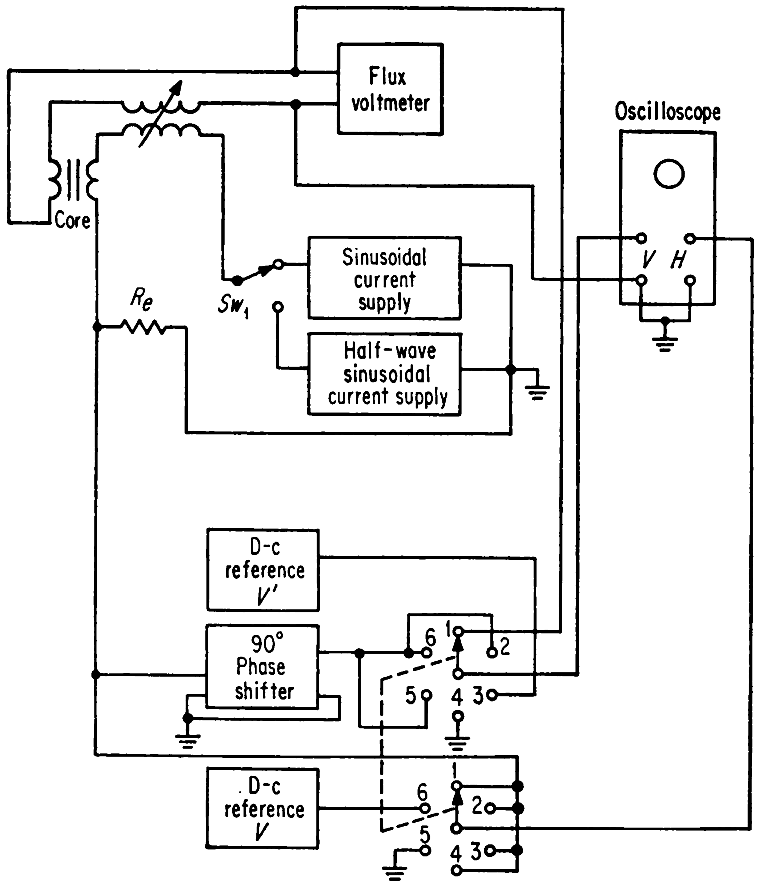

FIG. 6-7. Basic circuit for sine-current test.

across the pickup winding and the field intensity at which this maximum occurs.

The value of the maximum differential permeability can be determined from a properly calibrated ellipse, the trace of which is displayed by shifting the phase of the voltage appearing across R_e of Fig. 6-7 by 90° and applying the resulting phase-shifted voltage to the vertical deflection plates. This is done by placing switch Sw_2 in position 2. Calibration of the ellipse is obtained from the reference voltage V' which determines a level of the vertical deflection of the beam. This calibration is obtained with switch Sw_2 in position 3. The ellipse obtained in position 2 should be tangent to the horizontal line obtained in position 3. Positions 4 and 5

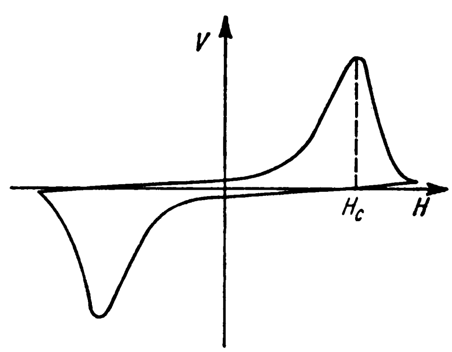

FIG. 6-8. Oscilloscope presentation of sine-current test.

of switch Sw_2 provide zero references for the vertical and horizontal deflections, respectively. Position 6 locates the point of maximum induced voltage with respect to a known horizontal deflection voltage, allowing calibration of the dynamic coercive force.

Normally, switch Sw_2 is a motor-driven two-gang six-position switch. The rate at which it is driven allows sufficient time for all of the various traces to be observed simultaneously on the long-persistence screen. Such a display eliminates problems associated with drift in the oscilloscope amplifiers and facilitates the required calibration procedures.

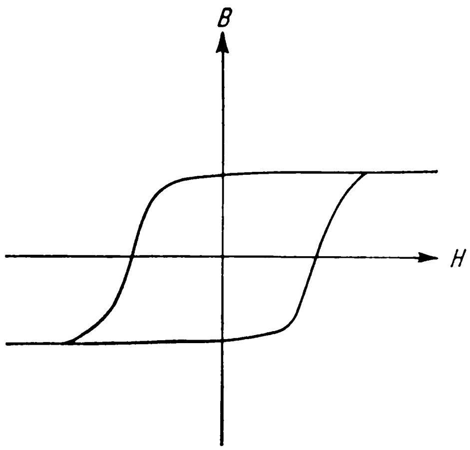

FIG. 6-9. Sine-current B-H loop.

The waveforms (with respect to time) of i_e and e_d are identical with the waveshapes shown in Fig. 6-4. These waveforms are, of course, obtained with switch Sw_1 in position to connect the full-wave sinusoidal current supply into the excitation circuit. Waveforms obtained with the half-wave sinusoidal current supply connected are identical with those of Fig. 6-3a. The operating loop is the sine-current hysteresis loop shown in Fig. 6-9.

The measurements of B_m and $B_m - B_r$ can be as readily related to circuit applications as the same measurements using the constant-current flux reset tester. The relationship between bias and coercive force and between gain and maximum differential permeability, however, is questionable.

From the descriptions given of the two types of core test methods, a few conclusions may be drawn concerning the usefulness of the methods with respect to measurement of those properties of a reactor which affect amplifier performance as listed in Sec. 6-1. Neither method, for example, yields any information about the prefiring gate current since both methods employ a current source rather than a voltage source to obtain the gating function. For the same reason, neither method yields information concerning the time required for gate current to rise from the prefiring to the postfiring state.

The two methods allow essentially equivalent conclusions to be drawn concerning the material squareness as well as the volt-second area absorbed by the reactor prior to firing. Actually, more information about this volt-second area can be gleaned from the constant-current flux reset method than from the sine-current method since the former provides for flux changes intermediate between B_r and $-B_m$.

Information concerning phenomena occurring during the reset half-cycle is almost completely lacking in the sine-current method, whereas the constant-current flux reset method provides information concerning the average signal current required to achieve nonnegligible reset as well as the average signal current required for complete reset. Neither method provides information concerning the manner in which the time rate of change of flux varies within the reset period.

6-3. LIMITATIONS IMPOSED BY COMPONENTS OF TESTERS

It must be recognized that the testers described have certain inherent limitations which prevent complete realization of the ideal measurements desired. As an example of these limitations, the implausibility of a sinusoidal current supply with a saturating core device as a load may be considered. Unless a ridiculous amount of sophistication is incorporated into the circuit, a sinusoidal voltage source cannot deliver a sinusoidal current to such a load unless some specified error is allowed. Another example is that the space factor of the core can never be known accurately. Other, not quite so obvious, instances might be cited. Some limitations imposed by nonideal components will be considered in this section.[7]

Broadband Amplifiers. The flux voltmeter portion of the circuits of Figs. 6-1 and 6-7 must include an amplifier of some sort. A casual glance at the e_d waveshapes of Fig. 6-3*a* or *c* is sufficient to indicate that the frequency spectra of such waveshapes are extremely broad. It has been estimated, for instance, that significant error can be introduced if the amplifiers are not flat within 1 per cent over nearly three decades. Such amplifiers can be built, but it is difficult to maintain such performance over long periods of time without excessive maintenance costs.

An alternative to amplification of the waveshapes of Fig. 6-3*a* and *c* is to integrate these waveshapes (usually through use of a Miller-type integration circuit) and to amplify the smoother waveshapes resulting from integration.[8] This second method is becoming more common in testers in use in industry, the problems associated with the construction and maintenance of an adequate integrating circuit being somewhat less formidable than those associated with an adequate broadband amplifier.

Noise. While other components introduce limitations peculiar to their kind (e.g., resistors can never be made truly noninductive, switches do not yield step changes with zero rise time), a principal problem arises from noise. Regardless of the circuitry used, the low-level signals available from the core are degraded to some extent by noise. The use of the bucking transformer T of Fig. 6-1 is a necessity if noise is not to obscure the signal voltage arising from the $B_m - B_r$ test almost totally. The amplifier or integrator fed directly by the pickup winding is a particularly susceptible component with respect to noise. It is common practice to shield this stage and its associated leads completely. Proper grounding is usually achieved only by tedious trial-and-error experimentation.

In addition to the usual radiation noise, very low frequency conducted noise is a major problem in testers. This type of noise, often called drift, is usually associated with the tubes and the voltage sources, power supplies and regulators used to supply the testing circuitry. The effect of the presence of this noise is to increase the variability of the tester, thus decreasing its precision.[9]

6-4. ACCURACY AND STANDARDIZATION

The successful application of proper engineering techniques to the problems associated with tester circuitry can be assessed only by evaluation of the accuracy and precision of a tester built to certain specifications. Unfortunately, no one standard exists against which the accuracy of a core tester can be measured.

Accuracy. What has been done in the absence of such a standard is to assign quite arbitrary percentage error values to unknown sources of error and to calculate percentage error values from the accuracy of individual components. Using such a technique, Jaquet estimated an error of 4.45 per cent in measuring $B_m - B_r$, 1.47 per cent in the measurement of H_1, 1.92 per cent in measuring ΔH, and 0.88 per cent in the measurement of B_m.[7] Empirically it has been determined that the average reading (averaged over four readings) obtained on a given core with a given tester may vary as much as 1.5 per cent over a six-month period for any test point. Since it is doubtful that the properties of the core have changed (although this is admittedly an outside possibility), the assumption must be made that the tester has changed. Careful measurements of the parameters of the components of the tester fail to reveal any significant difference from the same values measured six months earlier.

Experiences such as that outlined above indicate the dilemma facing the magnetic-amplifier designer. Either he must admit that he cannot measure the desired core properties much closer than 5 per cent or that, while he can measure them more closely than this at any given time, these measured properties may vary arbitrarily with time within the 5 per cent range. Since, as indicated previously, the probability of the magnetic properties of the core varying with time seems quite small, attention has been focused on the elimination of variation in the tester. Since the variations are erratic and of a long-term nature and since they are reasonably small, their elimination or reduction requires a long-term statistical approach. While some work is being done at various locations, insufficient data are available at the present time to judge if significant progress is being made.

Standardization. While it is impossible to say how accurate a given tester is, it is possible to determine how it reads with respect to other, similar testers. One method for achieving this in industry is to circulate a group of so-called "standard" cores. The test points on each core are measured four times within a period of days on a given tester. From the data obtained, a statistical analysis suitable for digital computer programming yields the comparative accuracy and the variability of the tester. The accuracy is as compared with results obtained with some other tester arbitrarily chosen as standard.[9]

In an attempt to make standardization a little less arbitrary, the cognizant AIEE committee has recommended that the flux voltmeter of a tester be calibrated in terms of the B_m of a Supermalloy core as measured by normal d-c loop methods. This brings the standardization of one of the test points a little closer. It must be admitted, however, that the measurements of the saturation flux density of a given core by d-c loop methods vary by a few per cent from one laboratory to another. A great deal of ingenuity will have to be exercised before standardization of testers becomes a science rather than an art.

6-5. EFFECTS OF TEMPERATURE ON CORE CHARACTERISTICS

The manner in which certain magnetic properties of a core material change with temperature was discussed briefly in Chap. 2. The influence of temperature on the operational characteristics of a complete amplifier is discussed in Chap. 8. However, since the manner in which the core characteristics vary with temperature is of particular interest to the amplifier designer, further information on temperature variation will be given as measured by the constant-current flux reset method.

The complete core characteristic of a typical 50 per cent nickel-iron core is shown in Fig. 6-10 at six different temperatures. Similar curves are shown in Fig. 6-11 for a 4 per cent molybdenum-79 per cent nickel core. Also shown are the flux voltmeter readings for the H_1 and H_2 points which define ΔH according to the standard test procedure. It can be seen that the points chosen to define the flux excursion over which the gain is measured are really not suitable for the entire temperature range over which the characteristics were obtained. For the 50 per cent nickel-iron material, use of the standard test points at high temperatures yields a gain figure considerably lower than the actual slope of the characteristic over the reasonably linear portion of the curve. Behavior of the high-nickel material is somewhat similar with respect to the H_2 point, although the difference between the slope of the curve and the standard gain measurement is considerably less. However, the H_1 point for this material is seen to fall on a nonlinear portion of the curve at very low temperatures. Because of this behavior, a certain amount of judgment must be exercised in interpreting core test data obtained with the standard test method over an extended temperature range.

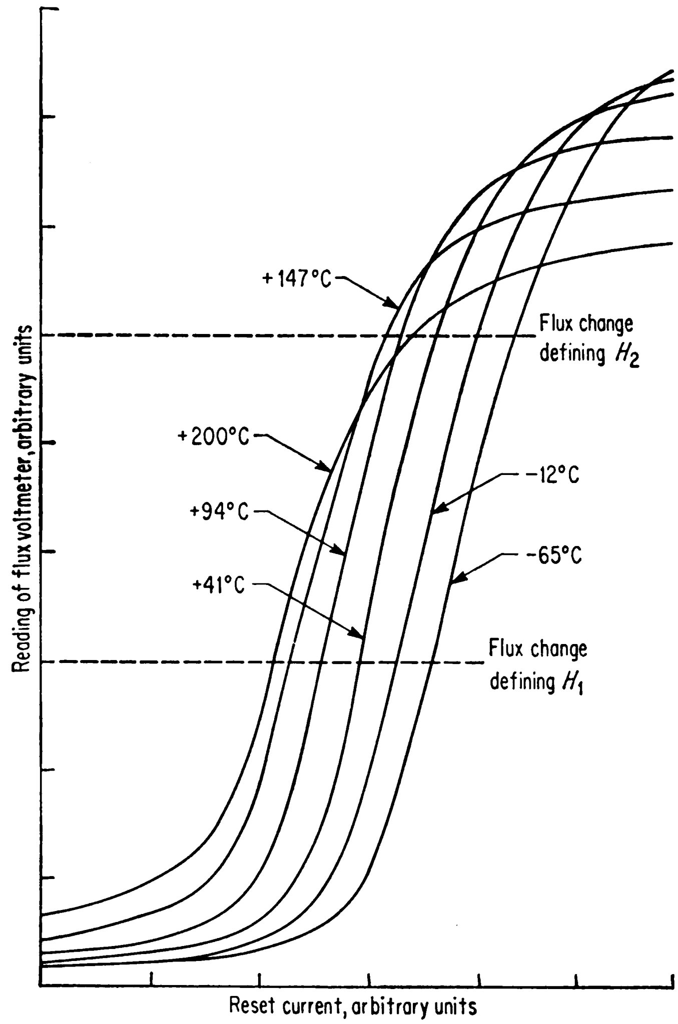

FIG. 6-10. Reset characteristic of 50 per cent nickel-iron at different temperatures.

Because the standard test method is defined, it is frequently used in presenting data obtained over an extended temperature range despite the deficiencies introduced by shifts in the position of the linear region of the total curve. Use of the standard test points makes it possible, for instance, to average the results obtained on several cores and present the averages in tabular or graphical form. Such a presentation is made in Fig. 6-12 where the average $B_m - B_r$ reading of 10 cores, each core read twice, is shown as a function of temperature. Two groups of 10 cores are represented, one group being of 50 per cent nickel-iron, the other

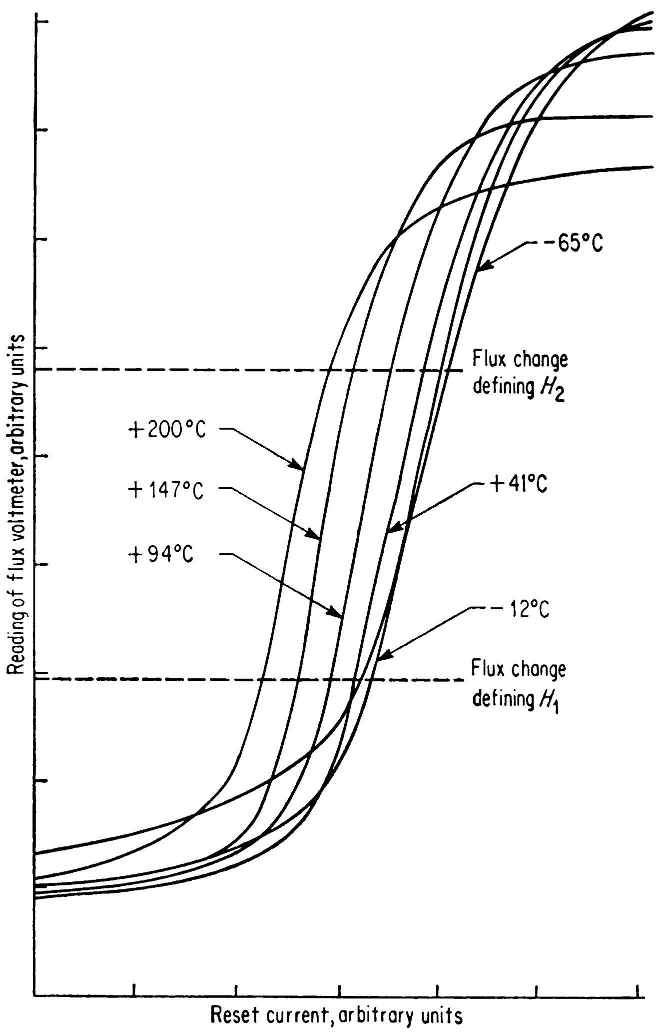

FIG. 6-11. Reset characteristic of 4 per cent molybdenum-79 per cent nickel at different temperatures.

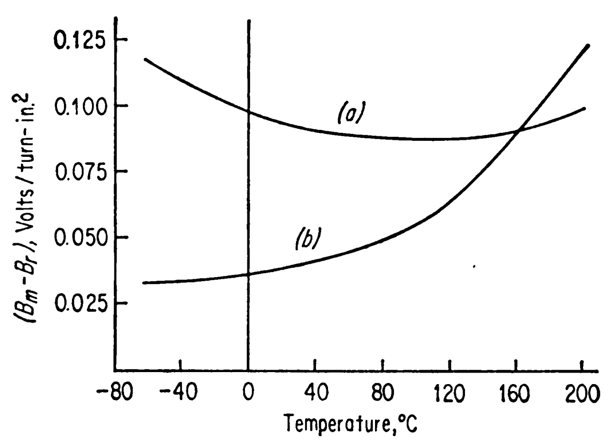

FIG. 6-12. $B_m - B_r$ as measured by the constant-current flux reset test as a function of temperature. (a) 4 per cent molybdenum-79 per cent nickel; (b) 50 per cent nickel-iron.

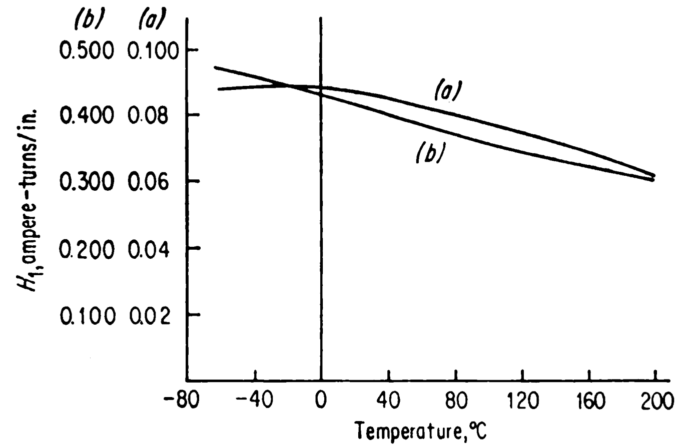

Fig. 6-13. H_1 as a function of temperature. (*a*) 4 per cent molybdenum-79 per cent nickel; (*b*) 50 per cent nickel-iron.

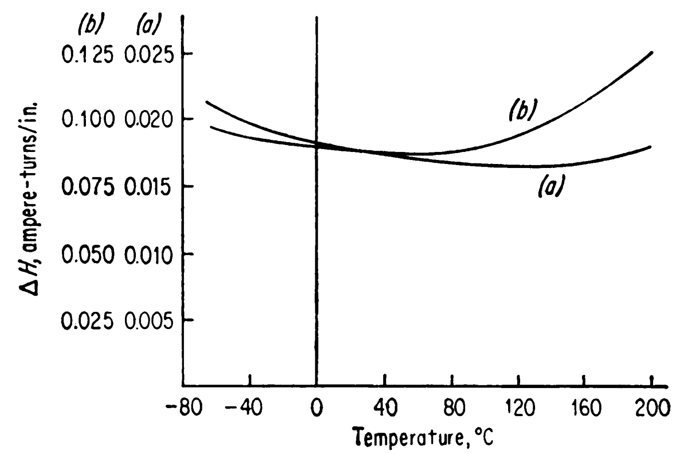

Fig. 6-14. ΔH as a function of temperature. (*a*) 4 per cent molybdenum-79 per cent nickel; (*b*) 50 per cent nickel-iron.

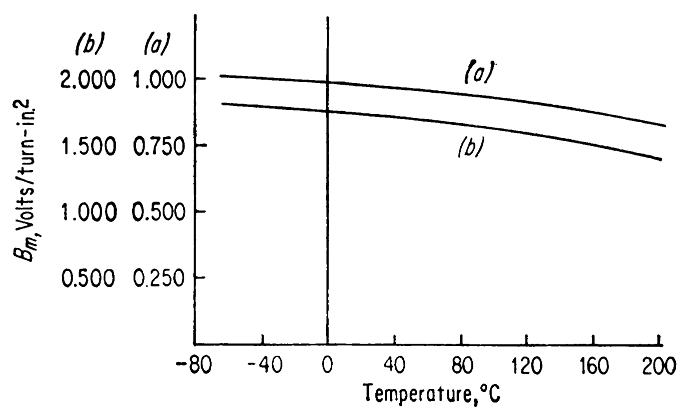

Fig. 6-15. B_m as measured by the constant-current flux reset test as a function of temperature. (*a*) 4 per cent molybdenum-79 per cent nickel; (*b*) 50 per cent nickel-iron.

a high-nickel material. Curves for H_1, ΔH, and B_m are shown in Figs. 6-13, 6-14, and 6-15, respectively. For each test point, each core displays approximately the same type of variation, although the percentage variation of the individual cores shows some diversity.

REFERENCES

1. Test Procedure for Toroidal Magnetic Amplifier Cores, *AIEE No.* 432, 1959.
2. Conrath, J. R.: Magnetic Amplifier Gapless-Core Tests, *Electronics*, pp. 119–121, November, 1952.
3. Roberts, R. W.: Magnetic Characteristics Pertinent to the Operation of Cores in Self-Saturating Magnetic Amplifiers, *Trans. AIEE*, vol. 73, part I, pp. 682–690, 1954.
4. Patrick, J. D.: A Method of Measuring Dynamic Magnetic Properties of Core Materials, *NAVORD Rept.* 940–1456, 1954.
5. Mitch, J. E., H. A. Lewis, and L. A. Parnell: Production Testing of Tape Core Materials, Conference Paper, AIEE Summer General Meeting, 1956.
6. Patrick, J. D., and A. Jansens: A-C Permeability and Hysteresis Analyzer, U.S. Patent 2,805,390, Sept. 3, 1957.
7. Jaquet, J. R.: Design Criteria for a Practical Flux-Reset Core Tester, T-86, *Proc. Spec. Tech. Conf. Magnetic Amplifiers, AIEE*, pp. 74–105, 1956.
8. Lord, H. W.: A Delta-B Indicator, *Electrical Engineering*, vol. 75, p. 1012, 1956.
9. Airth, H. B., and G. E. Lynn, A Statistical Determination of Correlation Between Constant Current Flux Reset Core Testers, T-116, *Proc. Spec. Tech. Conf. Nonlinear Magnetics and Magnetic Amplifiers, AIEE*, pp. 74–81, 1959.

7

Design Methods for Typical Circuits

In practice, every magnetic-amplifier design originates with an application. It is not surprising, therefore, that the method of design is influenced by the application for which it is intended. The design of vacuum-tube circuitry is almost always a matter of tailoring a circuit to utilize an existing tube design to perform a desired function. In designing magnetic-amplifier circuits, however, the amplifier as well as its associated circuitry is tailored to perform the given function. It is obviously impossible to describe design methods to cover all possible amplifiers in all possible associated circuits. What will be attempted here is to show how typical applications are analyzed to determine the characteristics desired from the amplifier. Then the basic design methods to produce the desired characteristics will be discussed. In this discussion, the general uses to which theory and measured data can be put will be pointed out.

7-1. REQUIRED DESIGN INFORMATION

The first major step in the design of a magnetic amplifier is to assemble information concerning the functional requirements demanded of the amplifier in the application for which it is intended and the available power sources. Failure to recognize the importance of this step makes any logical design impossible. Failure to complete the assembly of the information systematically may result in false starts with resulting rework as the limitations imposed by the particular application become apparent.

Functional Requirements. Information concerning the function of the amplifier can be gathered most conveniently if certain categories are assigned: for example, load circuit, signal circuit, amplifier performance, and environment. These requirements do not need detailed discussion; the mere recognition of their importance is practically sufficient. A typical set of requirements is listed here to illustrate what might be considered a check-off list which is followed explicitly or implicitly by an experienced designer when he considers a new application.

A. Load circuit

1. Power required to be delivered to the load
2. Type of load, static or active
3. Amplifier output impedance, static and dynamic
4. Type of output, d-c or a-c
5. Waveform of output
6. Grounded or isolated load
7. Duty cycle
8. Single-ended or push-pull
9. Maximum power which may safely be applied to load

B. Signal circuits

1. Number and type of signals
2. For each signal source
   a. Minimum input impedance amplifier may have
   b. Source impedance
   c. Maximum signal power available
   d. Grounded or isolated
   e. Possibility of grounding
   f. Sensitivity to variations in input impedance of amplifier
   g. Summation or discrimination
   h. D-c or modulated a-c
   i. If a-c, phase relationship with respect to amplifier gating voltage

C. Amplifier performance

1. Transfer function with respect to each signal
   a. Power gain
   b. Dynamic response
   c. Proportional, on-off, variable, nonlinear
2. Linearity required (if proportional)
3. Minimum environmental sensitivity required

D. Operating and storage environment

1. Temperature
2. Humidity
3. Shock
4. Vibration
5. Altitude
6. Salt spray
7. Sand and dust
8. Radiation level

Some of these requirements, naturally, will yield only the expected conditions when checked. In the experience of the authors, however, surprising answers are quite frequently received when some of the items listed are checked with the originator of the application. Particularly in view of the small amount of time required to make such a systematic check at the initiation of a design, it is felt quite strongly that it is worth doing thoroughly.

Available Power Sources. Another basic area of information which serves to tie down any particular design concerns the power sources which are available in the particular system. The following types of information should be obtained concerning such power sources at the initiation of a design.

A. Gate voltage source
1. Frequency and tolerance
2. Voltage and tolerance
3. Power capabilities
4. Source impedance
5. Waveshape, distortion, and noise
6. Single or multiple phase

B. Direct current
1. Voltage and tolerance
2. Ripple and noise
3. Power available
4. Source impedance

C. Sequence of energizing supplies
D. On and off transients (e.g., voltage surges)
E. Grounded or capable of being grounded

7-2. SELECTION OF TYPE OF AMPLIFIER

Once the required information has been listed, the next major step in the design of a magnetic amplifier for a specific application is to select, from a study of the functional requirements listed above, the type or types of configuration most suitable. An experienced designer follows a considerably detailed reasoning process which begins at the time of assembly of the information concerning the requirements of the particular application and which ends with the selection of an amplifier type which seems most suitable. Since this entire selection process is frequently thought through before a single written calculation is made, the inexperienced designer or the student trying to learn how and where to begin can easily underestimate the importance of this step. Or, if its importance is appreciated, the flow of thought involved is not understood, since it is not always easy to describe such a mental process explicitly. In an attempt to establish rough guide lines for the designer, a type of flow chart is shown in Table 7-1.

This chart is used in conjunction with the assembled information concerning the functional requirements and the power sources available for a specific application. To make the chart of manageable size, it is assumed that six types of circuit are sufficient to meet the designer's needs. These types are identified in the chart by the following symbols:

B – Bridge circuit	HW – Half-wave circuit
CT – Center-tapped circuit	$H3$ – Hybrid III circuit
D – Doubler circuit	$H4$ – Hybrid IV circuit

The preliminary choices of amplifier circuit types emerge at the bottom of the flow chart from systematic consideration of the functional requirements and power source information previously assembled. Enlarged charts can easily be devised to include other circuit types. The chart presented here, however, is adequate to illustrate the method used for selection of amplifier type.

Selection is begun by considering the type of output, since this may be considered the most fundamental basis for selection. When a selection of which path to follow (a-c or d-c output) has been made, the next requirement to be considered is the type of signal available. Again a selection of path is made according to the functional requirements. At each successive branch point, a multiplicity of paths is presented and successive decisions are made, based on the requirements of the particular design. The process is self-explanatory and will not be discussed further.

It should be recognized that there is some choice in the sequence chosen for selection and the details of the chart could certainly be presented in diverse forms. The important point to be conveyed is that this phase of a design study is quite basic and yet is often treated perfunctorily if at all in the literature and in verbal indoctrination of new engineers in the field. Most frequently the process is passed by as being in the realm of "design know-how."

Succeeding sections will present illustrative procedures for designing typical amplifiers. Since the preliminary design of single-ended doublet amplifiers is the same regardless of whether the bridge, center-tapped, or doubler configuration is to be used, the design of a bridge circuit only will be presented. Discussion of design methods for the fast-response amplifiers will be limited to the design of push-pull half-wave circuits and the Hybrid III circuit.

TABLE 7-1

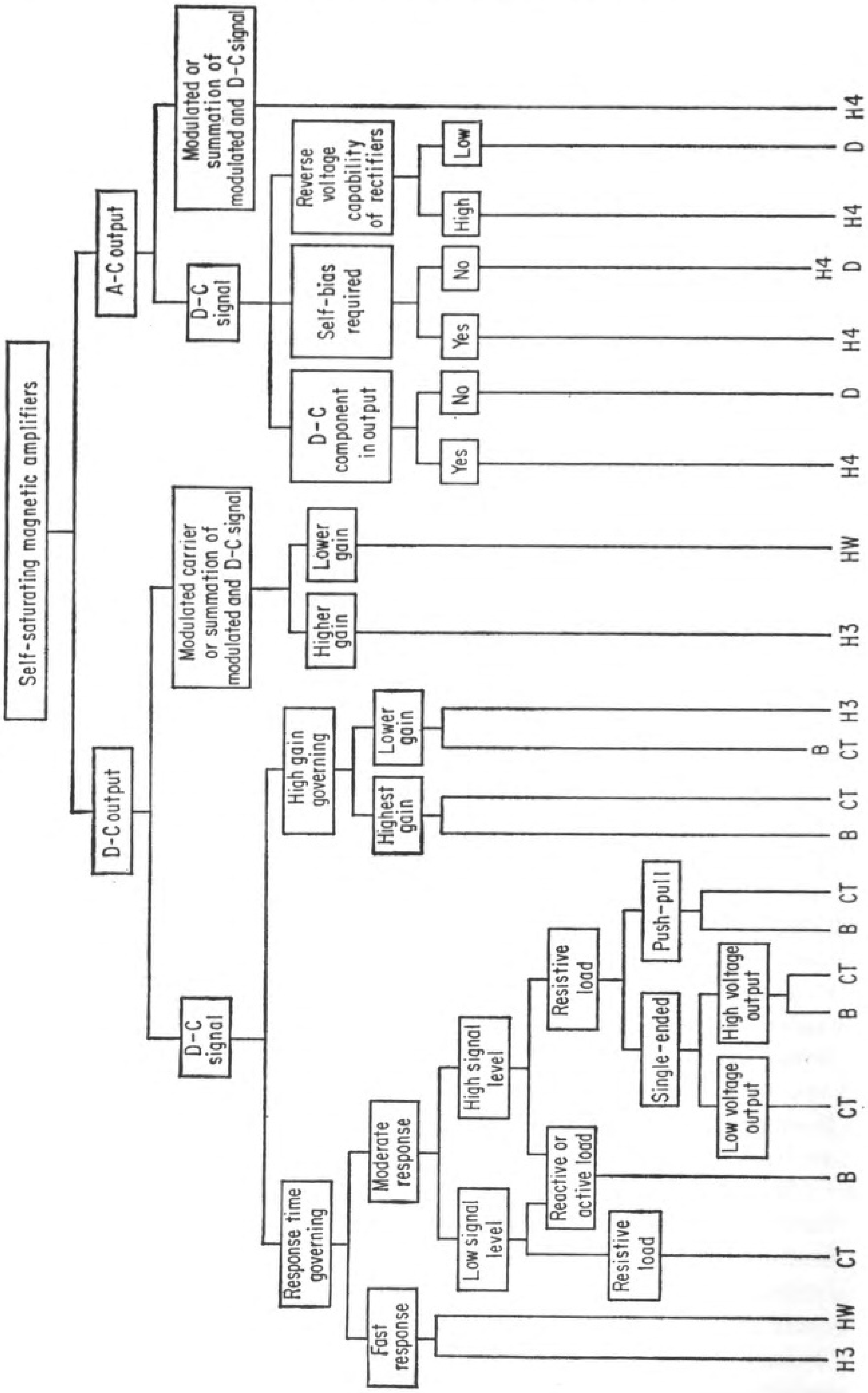
Self-saturating magnetic amplifiers
D-C output
A-C output
D-C signal
Modulated carrier or summation of modulated and D-C signal
D-C signal
Modulated or summation of modulated and D-C signal
Response time governing
High gain governing
Higher gain
Lower gain
D-C component in output
Self-bias required
Reverse voltage capability of rectifiers
Fast response
Moderate response
Highest gain
Lower gain
Yes
No
Yes
No
High
Low
Low signal level
High signal level
Resistive load
Reactive or active load
Resistive load
Single-ended
Push-pull
Low voltage output
High voltage output
H3
HW
CT
B
CT
B
CT
B
CT
B
CT
B
CT
H3
H3
HW
H4
D
H4
D
H4
D
H4

7-3. ILLUSTRATIVE DESIGN PROCEDURES FOR DOUBLET AMPLIFIERS

To illustrate the design methods discussed, it will be assumed that the following functional requirements have been specified for a particular application where the only gating source available has a frequency of 400 cps. The source impedance is much less than 1 ohm.

1. The output shall be d-c nonreversible polarity.
2. The d-c power delivered to the load shall be 4 watts into a 300-ohm resistor.
3. The signal source is d-c with a source impedance of 100 ohms.
4. The signal power available to drive the amplifier from cutoff to full output is 5×10^{-4} watts at a maximum signal voltage of 1 volt.
5. The phase shift of the amplifier shall not exceed 45° at a signal frequency of 4 cps.
6. Because of packaging considerations, it is desirable that this be a single-stage design.

From these specifications, it is seen that an amplifier with a d-c power gain of 8,000 and a corner frequency of 4 cps is required. Following Table 7-1, an amplifier with d-c output, d-c signal, response-time governing, moderate response, high signal level, resistive load, single-ended, leads to either the bridge or center-tapped circuits. Since the output voltage required (approximately 35 volts) is neither very high nor very low, the bridge circuit will be chosen.

With the choice of amplifier made, the next problem is to design such an amplifier. The design method to be described has been found to work reasonably well, but is certainly capable of being improved upon. Other design methods, some more or less explicit, exist in the literature.[1,2] Curves will be used for the major portions of the design work. These curves are intended for use at a 400 cps gating frequency. The derivations of these sets of curves are given in a later section of this chapter. Similar sets of curves can then be drawn for any gating frequency desired. Some curves are amenable to normalization with respect to frequency while others are not. No attempt has been made here to perform such normalization since it is not the intent to present a complete design handbook. In a field where a thorough understanding of basic design principles is required, handbook design usually results only in an inferior product. The intent of the curves presented is to provide a groundwork of general design rules which must then be supplemented or overruled by mature judgment.

Single-ended Amplifier Design. The illustrative curves which are presented have been developed from the block diagram of Fig. 5-10, shown again for reference as Fig. 7-1. From Fig. 7-1, the zero frequency voltage gain K_v can be shown to be

$$K_v = \frac{DN_S N_G}{R_S} \tag{7-1}$$

The values to be assigned to the parameter D and the manner in which this parameter was derived will be discussed in a following paragraph.

The choice of curves to be used and the order in which they are used will be a function of how the specifications for the particular application are presented. It is rarely true that the given specifications uniquely determine the final amplifier configuration. In most cases the designer must decide whether to minimize space and weight or to add additional safety factors to ensure satisfactory minimum performance more fully. Often the converse decision must be made of whether to exceed the space and weight specification or to sacrifice some performance criterion. Occasionally, even experience is an insufficient guide and the amplifier

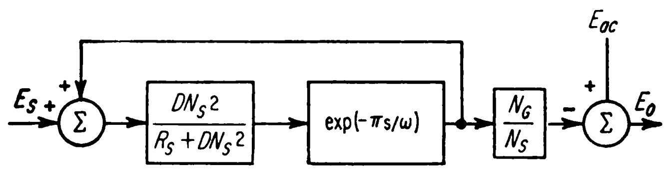

FIG. 7-1. Block diagram of Fig. 5-10.

produced is inferior to a possible alternative which was overlooked during the design.

The curves to be presented are based, of necessity, upon numerous compromises. For example, the number of turns of a given wire size which can be wound upon a given core are a function of:

1. The actual diameter of the wire used compared to the nominal diameter given in handbooks for the AWG number
2. The inside diameter of the core box compared to the guaranteed minimum box diameter
3. The size of the shuttle on the winding machine used
4. The type of winding machine used
5. The skill of the winding-machine operator
6. The amount of interwinding insulation used, if any

These variables are mentioned to point up the necessity for tempering handbook data with engineering judgment. A design method which tries to make allowance for the worst conditions which can occur will lead to such a conservative design that it cannot meet the competition. On the other hand, if the method is too optimistic, the final product probably cannot be manufactured in high volume at reasonable cost. All the curves presented for amplifier design are, therefore, a compromise between the conservative and the optimistic. Engineering judgment must then decide whether to tighten or loosen the design in certain places to improve performance or to ease manufacturing difficulties.

Returning to the design problem at hand, the first step in amplifier design is usually to select the core to be used. The characteristics of 10 typical cores of 50 per cent nickel-iron (B cores) and 5 typical cores of 4 per cent molybdenum-79 per cent nickel (A cores) are given in Table 7-2. These characteristics may be found in, or derived from, the manufacturer's published data.[3-5] The magnetic characteristics are those measured by the constant-current flux reset method. The last column, ohms/turn^2, is a measure of the effective resistance of a reactor made from the particular core. This parameter has been assigned the symbol D. The significance of this parameter is shown in Fig. 7-1. The value of this parameter was chosen by dividing the ϕ_m (in average volts/turn) of the core by three times the Δmmf (in ampere-turns) of the core. This gives a rough measure of the parameter desired.

To determine what core should be used, any one of the amplifier specification criteria could be applied first to eliminate those cores which will not satisfy the criterion selected. In the given sample problem, for example, it might be decided first to eliminate those cores which are not capable of controlling 4 watts of d-c output power in the two-core single-stage amplifier selected. It should be noted that in many magnetic-amplifier applications, the specifications require a given average current to be supplied at a given average voltage. The product of these average values may be referred to as d-c power. It will be noted that a half-wave rectified current and voltage will provide only one-fourth the d-c power of a full-wave rectified current and voltage, but will provide one-half the true power (product of rms current and voltage). For this reason, a core in a half-wave circuit is considered to be capable of controlling only one-fourth the d-c power that two cores in a full-wave circuit can control. The d-c output power controlling capabilities of each core (in a half-wave circuit) are presented in Fig. 7-2 as a function of the percentage of the total available winding area occupied by the gate winding. These curves are based on certain circuit-loss assumptions described in Sec. 7-5. For this sample problem it will be presumed that these assumptions are justified.

Since 4 watts is the required d-c load power in the sample problem, dividing by 4 to obtain half-wave per-core power shows that 5 of the 15 cores plotted on Fig. 7-2 can be eliminated as being incapable of controlling 1.0 watt. The minimum signal power required to drive each core is plotted in Fig. 7-3 as a function of the percentage of total available winding area occupied by the signal winding. It is seen that any of the 15 cores can satisfy the specification that the maximum signal available, 5×10^{-4} watt, should control the amplifier from cutoff to full output.

TABLE 7-2

Core No.	Nominal core size, in.			Nominal active core area, meters²	Nominal mean core length, meters	Box Dimensions, in.			A_W, max, in.²
	ID	OD	Height			Min ID	Max OD	Max Height	
A1	⅜	½	⅛	4.03×10^{-6}	0.0348	0.310	0.579	0.235	0.0675
A2	½	⅝	⅛	4.03×10^{-6}	0.0449	0.435	0.704	0.235	0.141
A3	½	⅝	¼	8.06×10^{-6}	0.0449	0.440	0.715	0.366	0.121
A4	¾	1	¼	1.61×10^{-5}	0.0697	0.630	1.115	0.378	0.240
A5	1	1⅜	¼	2.42×10^{-5}	0.0946	0.915	1.478	0.374	0.562
B1	7/16	9/16	⅛	4.03×10^{-6}	0.0398	0.372	0.638	0.235	0.101
B2	½	¾	⅛	8.06×10^{-6}	0.0497	0.435	0.829	0.235	0.141
B3	½	¾	¼	1.61×10^{-5}	0.0497	0.435	0.829	0.355	0.117
B4	¾	1	¼	1.61×10^{-5}	0.0697	0.630	1.115	0.378	0.240
B5	⅝	1	⅜	3.61×10^{-5}	0.0648	0.540	1.085	0.500	0.133
B6	1	1⅜	¼	2.42×10^{-5}	0.0946	0.915	1.478	0.374	0.562
B7	1	1½	¼	3.22×10^{-5}	0.0997	0.901	1.644	0.376	0.540
B8	1	1½	⅜	4.83×10^{-5}	0.0997	0.901	1.644	0.501	0.540
B9	1¼	1¾	½	6.44×10^{-5}	0.1198	1.080	1.910	0.675	0.824
B10	1½	2	½	6.44×10^{-5}	0.1398	1.401	2.149	0.674	1.450

Core No.	Nominal core characteristics $\phi_m - \phi_r$		mmf_0, ampere-turns	Δmmf, ampere-turns	ϕ_m		D, ohms/turn²
	Webers	Volts/turn rms			Webers	Volts/turn rms	
A1	8.95×10^{-7}	0.00075	0.1260	0.0237	3.34×10^{-6}	0.00594	0.0752
A2	8.95×10^{-7}	0.00075	0.1628	0.0306	3.34×10^{-6}	0.00594	0.0531
A3	1.79×10^{-6}	0.0015	0.1628	0.0306	6.7×10^{-6}	0.0119	0.1167
A4	3.58×10^{-6}	0.003	0.2530	0.0475	1.34×10^{-5}	0.0238	0.1500
A5	5.37×10^{-6}	0.0045	0.3431	0.0700	2.06×10^{-5}	0.0366	0.1570
B1	5.62×10^{-7}	0.0005	0.643	0.115	5.96×10^{-6}	0.0106	0.0276
B2	1.17×10^{-6}	0.001	0.803	0.190	1.19×10^{-5}	0.0212	0.0335
B3	2.25×10^{-6}	0.002	0.803	0.190	2.39×10^{-5}	0.0425	0.0671
B4	2.25×10^{-6}	0.002	1.127	0.200	2.39×10^{-5}	0.0425	0.0637
B5	5.12×10^{-6}	0.00448	1.045	0.280	5.35×10^{-5}	0.0950	0.1018
B6	3.36×10^{-6}	0.003	1.525	0.298	3.58×10^{-5}	0.0637	0.0642
B7	4.5×10^{-6}	0.004	1.611	0.381	4.78×10^{-5}	0.0850	0.0670
B8	6.75×10^{-6}	0.006	1.611	0.381	7.15×10^{-5}	0.127	0.100
B9	9.0×10^{-6}	0.008	1.931	0.396	9.55×10^{-5}	0.170	0.129
B10	9.0×10^{-6}	0.008	2.255	0.401	9.55×10^{-5}	0.170	0.127

Figure 7-4 presents the corner frequency obtainable with a given core as a function of the signal power available. It is seen that only 7 of the 15 cores have the specified minimum frequency response for the specified maximum signal power. Of those 7, 5 had previously been eliminated because of output power considerations. Thus it is seen that if the required amplifier can be built in one stage, it must use either A4 or A5 cores. It will be observed from Fig. 7-4 that core A5 requires 2.25×10^{-4}

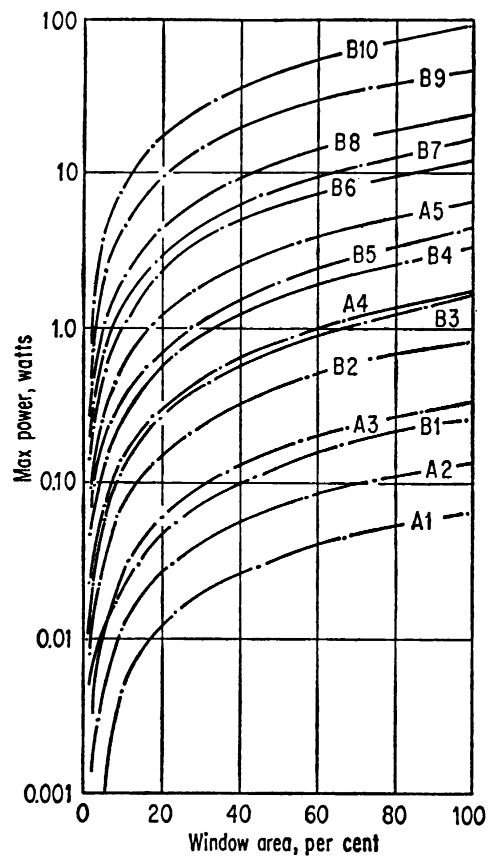

FIG. 7-2. Maximum controlled power per core as a function of percentage of window area occupied to gate winding.

watt to achieve the specified corner frequency while core A4 requires only 10^{-4} watt. This fact may be used to advantage later, should both cores prove satisfactory from all other considerations.

Figure 7-5 presents the N^2/R value for each core which will result in a given corner frequency. Cores A4 and A5 are quite similar with respect to this characteristic and require an N^2/R of approximately 200 at a corner frequency of 4 cps. Where a choice of cores allows an amplifier design which has gain and response-time parameters well in excess of the values specified, it is advantageous to design that amplifier which requires the least power for the specified frequency response. Therefore, if a

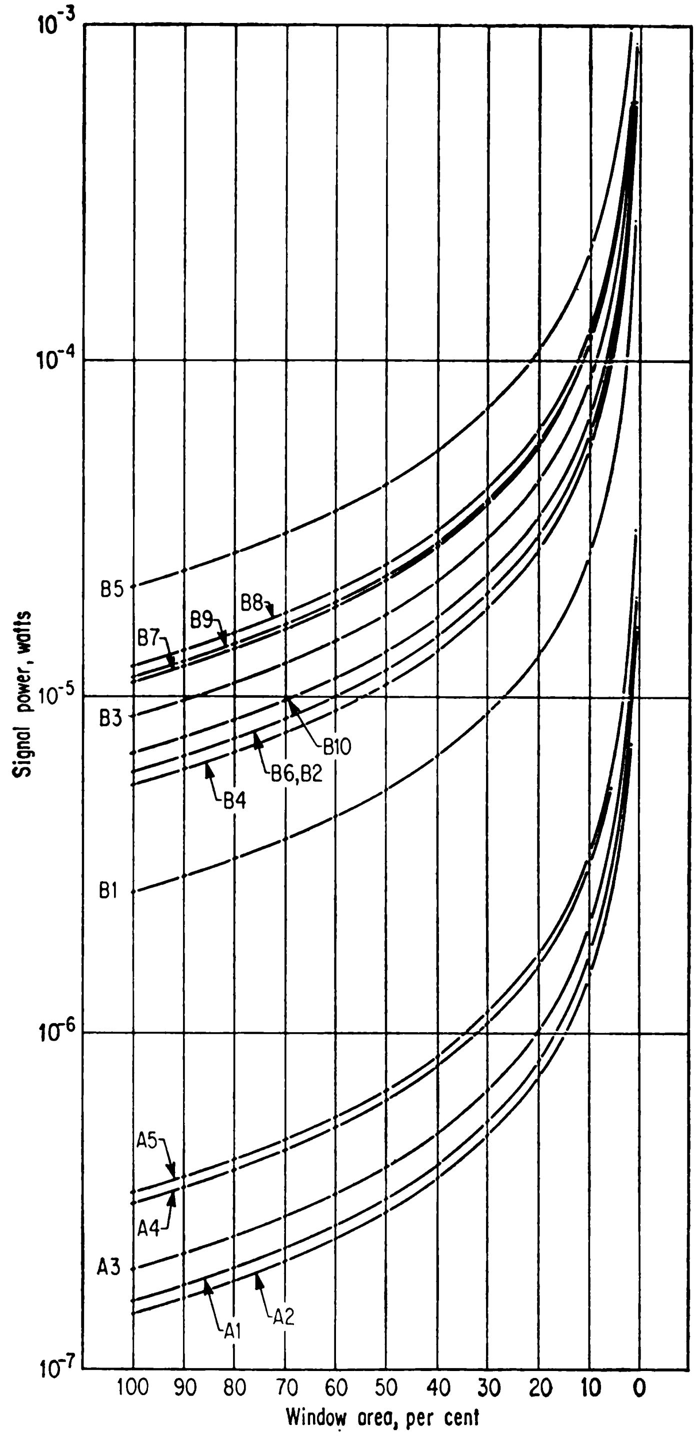

FIG. 7-3. Minimum signal power required for complete reset as a function of percentage of window area occupied by signal winding.

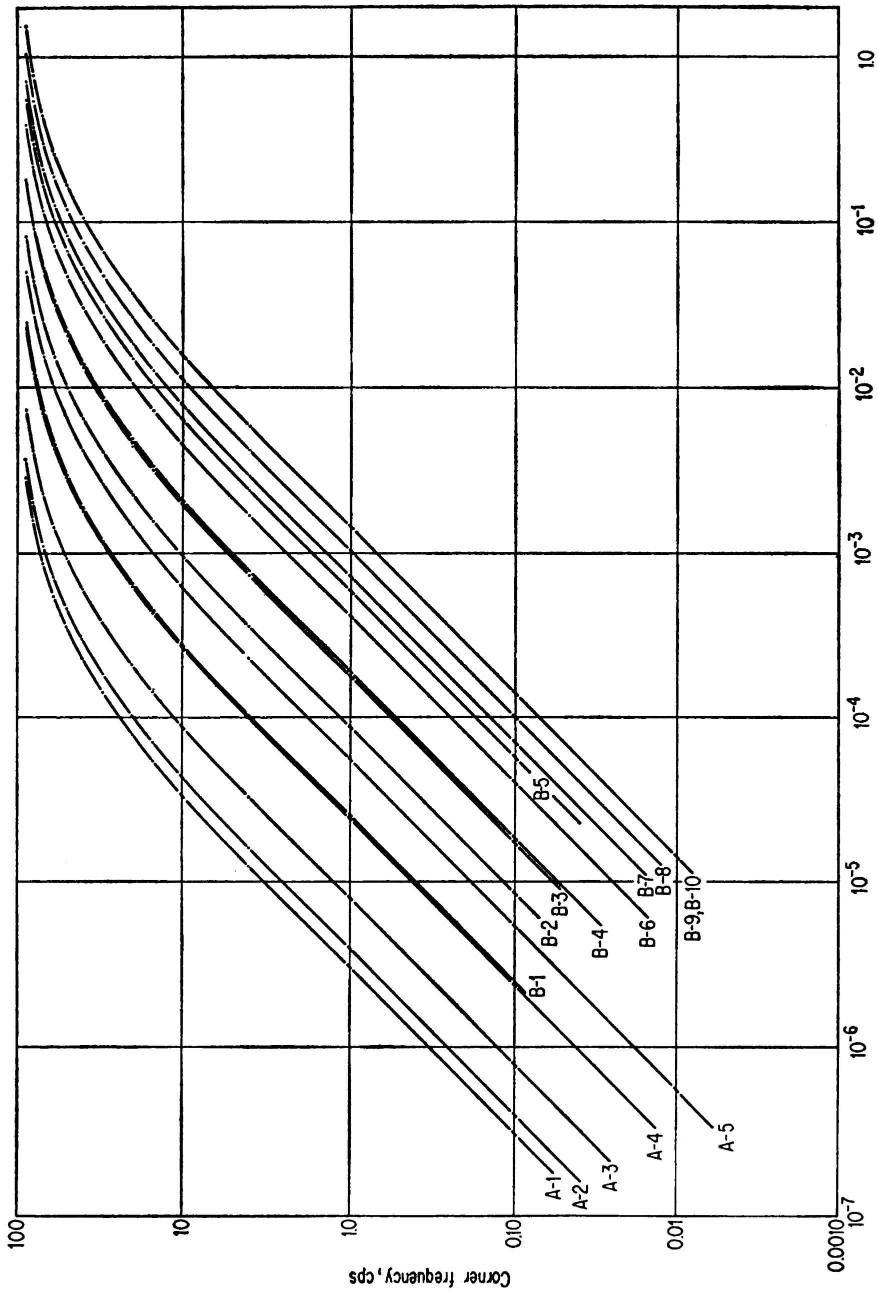

FIG. 7-4. Corner frequency of a bridge amplifier as a function of signal power available for full reset.

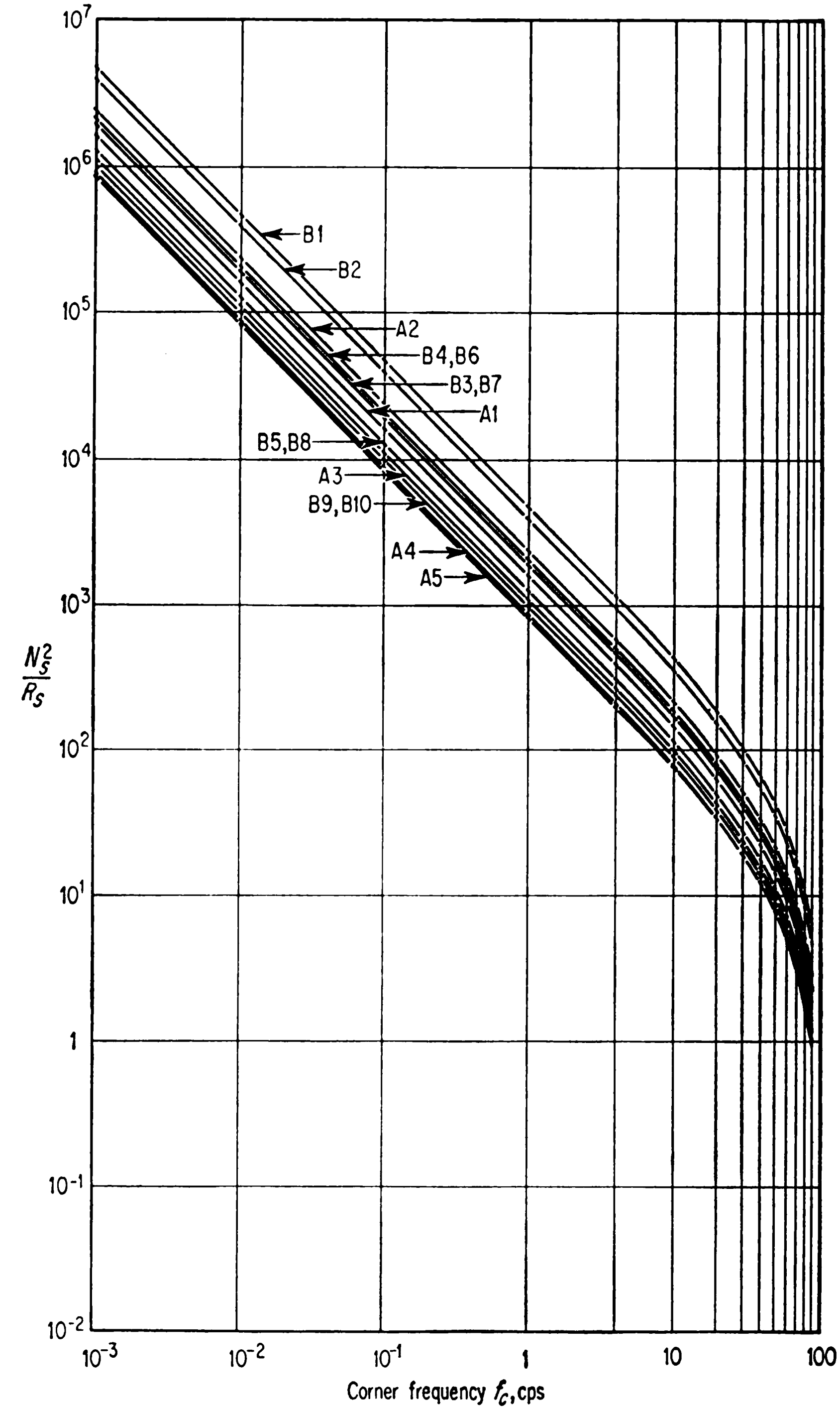

FIG. 7-5. N^2/R as a function of the required corner frequency.

type A4 core is used in this design, full output can be achieved with an input of only 10^{-4} watt. In order to take full advantage of this, the full power output of the signal source should be utilized in designing the signal circuit, however. The signal-circuit resistance R_S, then, is determined by the signal power available and the signal voltage specified, or $\frac{1}{5} \times 10^{-4}$, or 2,000 ohms. The number of signal turns N_S is equal to the square root of the product of R_S and the N^2/R read from the curve, or 632 turns.

The output voltage required can be determined from the load power and load resistance specifications. Thus, the d-c load voltage is the square root of the product of the d-c power specified and the load resistance. For the example under consideration, the required d-c load voltage is about 34.6 volts. Converting this to an effective value, the load voltage will be approximately 38.4 volts rms. Allowing for 10 per cent voltage losses in the gate circuit, the gate voltage should be about 42.2 volts rms. If the A4 core is examined first (since its use will result in a smaller amplifier than use of an A5 core), it is found from Table 7-2 that the ϕ_m (in volts/turn) of an A4 core is 0.0238, and the number of turns required is 42.2/0.0238 or 1,780.

Some applicable properties of commonly available magnet wire are given in Table 7-3. The load current the wire must carry can be calculated from the d-c load voltage and the load resistance. Since each core carries one-half of this current (which must be converted to an rms value by dividing by 0.636), the wire must handle 0.091 amp rms. From Table 7-3, this current requires No. 33 wire. In Fig. 7-6 a turns density chart presents the approximate area occupied by a winding as a function of number of turns with wire size as a parameter. In preparing the curves, it has been assumed that three types of production winding machines are available, that the machine operators are quite skilled, that the guaranteed minimum box inner diameter will be held, that the shuttle used will be the smallest which can be used for a given wire size, and that the wire has the nominal diameter and thickness of insulation. Where these assumptions are optimistic, the next larger size core will be required to allow for greater winding area. Where the assumptions are pessimistic, the next smaller size core may be chosen. This, in turn, will influence minimum control power, maximum output power, temperature rise, and a host of other parameters. Fortunately, so many factors influence the best possible design that a statistical averaging tends to occur, minimizing the influence of any one factor.

From Fig. 7-6, it is found that 1,780 turns of No. 33 wire occupies 0.147 in.^{2}. From Table 7-2, core A4 has a total available winding area of 0.240 in.^{2}. Thus, it is seen that the gate winding would occupy 61 per cent of the available winding area. From Fig. 7-2, it is seen that an

TABLE 7-3. TABULATED DATA FOR AWG WIRE SIZES

AWG wire No.	Copper diam, in.	Circular mils	Area, in.^{2}	Nominal resistance per 1,000 ft at 25°C, ohms	Diam for single enamel, in.	Current, amp (based on 500 cm per amp)
42	0.0025	6.219	0.000004884	1,701	0.0030	0.0126
41	0.0028	7.840	0.000006158	1,349	0.0033	0.0157
40	0.0031	9.888	0.000007766	1,069	0.0037	0.0198
39	0.0035	12.47	0.000009793	848.1	0.0041	0.0249
38	0.0040	15.72	0.00001235	672.6	0.0047	0.0314
37	0.0045	19.83	0.00001557	533.4	0.0052	0.0397
36	0.0050	25.00	0.00001964	423.0	0.0058	0.0500
35	0.0056	31.52	0.00002476	335.5	0.0064	0.0630
34	0.0063	39.75	0.00003122	266.0	0.0072	0.0795
33	0.0071	50.13	0.00003937	211.0	0.0080	0.1003
32	0.0080	63.21	0.00004964	167.3	0.0091	0.1264
31	0.0089	79.70	0.00006260	132.7	0.0100	0.1594
30	0.0100	100.5	0.00007894	105.2	0.0113	0.2010
29	0.0113	126.7	0.00009953	83.44	0.0126	0.2534
28	0.0126	159.8	0.0001255	66.17	0.0142	0.3196
27	0.0142	201.5	0.0001583	52.48	0.0158	0.4030
26	0.0159	254.1	0.0001996	41.62	0.0175	0.5082
25	0.0179	320.4	0.0002517	33.00	0.0197	0.6408
24	0.0201	404.0	0.0003173	26.17	0.0219	0.8080
23	0.0226	509.5	0.0004002	20.76	0.0244	1.0190
22	0.0254	642.4	0.0005046	16.46	0.0274	1.2848
21	0.0285	810.1	0.0006363	13.05	0.0306	1.6202
20	0.032	1022	0.0008023	10.35	0.0341	2.044
19	0.036	1288	0.001012	8.210	0.0382	2.576
18	0.040	1624	0.001276	6.510	0.0427	3.248
17	0.045	2048	0.001609	5.163	0.0477	4.096
16	0.051	2583	0.002028	4.094	0.0533	5.166
15	0.057	3257	0.002558	3.247	0.0601	6.514
14	0.064	4107	0.003225	2.575	0.0672	8.214
13	0.072	5178	0.004067	2.042	0.0752	10.356
12	0.081	6530	0.005129	1.619	0.0841	13.060
11	0.091	8234	0.006467	1.284	0.0941	16.468

A4 core will supply 1.0 watt when 60 per cent of the winding area is allotted to the gate winding. The area left for all control windings, signal, bias and, if necessary, feedback, is 0.093 in.^{2}. Since it can be seen from Fig. 7-3 that the available signal power will drive an A4 core with negligible area occupied by the signal winding, it is only necessary to choose a wire which will carry the signal current and which will not present winding problems. The signal current is less than 1 ma, so any

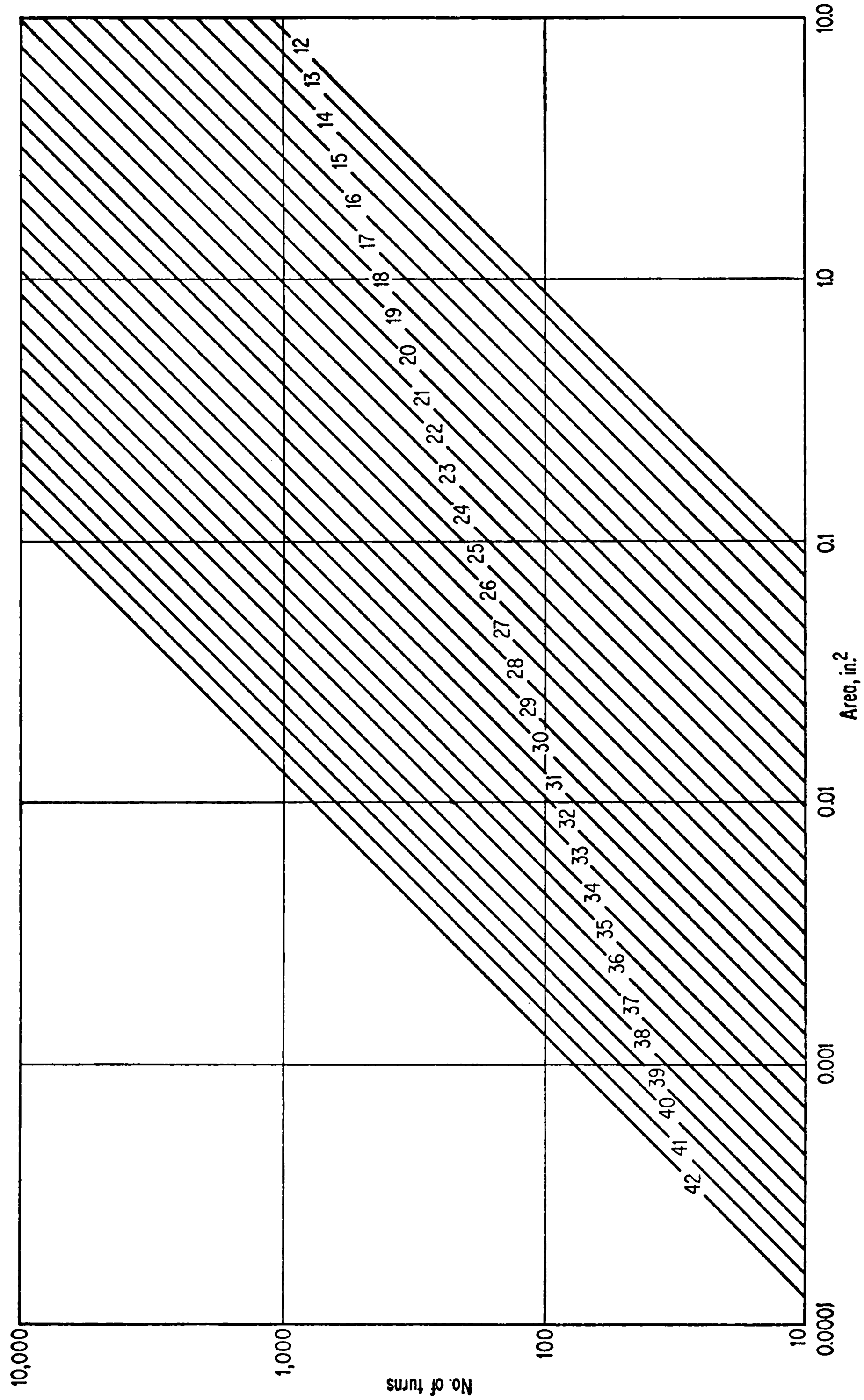

Fig. 7-6. Turns density chart for single-enamel wire.

easily wound wire will suffice. From Fig. 7-6, 632 turns of No. 40 wire will occupy less than 0.013 in.^{2}, leaving 0.08 in.^{2} for bias and feedback windings and for any interwinding insulation which may be required. An approximate value of mmf required to bias a nominal A4 core to cutoff in this single-ended amplifier can be obtained by summing the mmf$_0$ of Table 7-2 with one and a half times the Δmmf. This is approximately 0.325 ampere-turn. If it is assumed that a 50-turn bias winding will be used, a bias current of about 6 ma is necessary. If a rectified 115-volt line voltage is used to supply bias current, a bias resistor of over 17,000 ohms will be used. The N^2/R of the bias winding, therefore, is much less than unity, and will have negligible effect on the dynamic response of the amplifier since the N^2/R of the signal winding is 200. If No. 40 wire is used for the bias winding, the winding will occupy 0.001 in.^{2}.

The initial design of the amplifier is now complete. On paper, this amplifier should deliver the required power to the specified load with one-fifth of the specified signal power and have the specified corner frequency. Since not all the available signal power is used to drive the amplifier from knee to knee of its curve, the amplifier will reach full output at 0.447 volt of signal, and any further increase of signal voltage would be wasted. This allows feedback to be put around the amplifier to minimize environmental sensitivity and gain change. Use of feedback will also extend the corner frequency, allowing a healthy factor for last minute changes in system requirements. It will be observed that had core A5 been chosen, not only would a larger amplifier have resulted, but the allowable percentage of feedback would have been much smaller. As a general rule, which like most general rules may be subject to occasional exceptions, choice of the smallest core which will satisfy the requirements will result in the optimum design.

It must be emphasized that this design method is based on assumptions which are only rough approximations. The method does take into account most of the properties of an amplifier which are mathematically tractable. However, second-order effects and nonlinearities of the so-called linear portion of the transfer characteristic are not accounted for. It is often found after laboratory operation of a prototype model that small variations in the calculated parameters improve amplifier performance. When specifications are extremely tight, considerable design modifications of this type must often be incorporated in the final design on the basis of such laboratory results. However, use of the method does result in a nearly optimum amplifier in a large number of cases. In summary, the method eliminates those cores which are obviously unsuitable from a look at the curves of Figs. 7-2, 7-3, and 7-4. Thereafter, the method takes the smallest of the candidate cores and continues the design until either a successful design results or the smallest candidate core is eliminated and the investigation of the next smallest begun. This second step would probably have been necessary in the sample problem if, for instance, the d-c load power had been specified as 6 watts instead of 4. In that case, probably only core A5 would have met the requirements for a single-stage amplifier.

The subject of interwinding insulation has been mentioned as affecting the utilization of the available winding area. For low-voltage applications, the normal wire insulation is normally sufficient. When, however, the design results in voltages in excess of the dielectric strength of the wire insulation (the dielectric strength left after the insulation has suffered through the winding operation) appearing across adjacent layers or turns, interwinding layer insulation is required. Normal transformer practice in this regard is usually sufficient although the voltages may be somewhat lower for magnetic amplifiers because of the rougher treatment given the insulation by toroidal rather than layer-type winding machines. The use of layer insulation results in less window area available for wire.

Push-pull Amplifier Design. In many servo applications, it is necessary to amplify signals which reverse polarity or phase. The output of the amplifier, in these cases, should change polarity or phase accordingly. It is necessary under these conditions to design a push-pull, or double-ended, amplifier. A push-pull bridge circuit is shown in Fig. 7-7, and the approximately equivalent block diagram in Fig. 7-8.

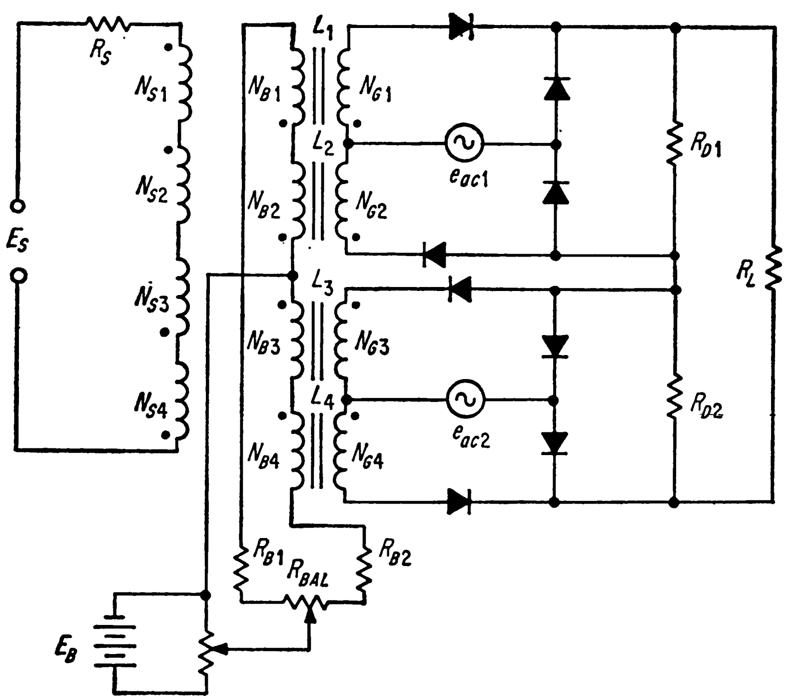

FIG. 7-7. Circuit diagram for push-pull bridge amplifier.

From the block diagram, it can be demonstrated that the zero frequency volts/volt gain can be expressed as

$$K_v = \frac{2DN_SN_G}{R_S} \tag{7-2}$$

A comparison of Eqs. (7-2) and (7-1) reveals that the volts/volt gain of the push-pull circuit is twice the gain of the single-ended circuit. These equations are based on the block diagrams of Figs. 7-1 and 7-8 and assume that the cores of the push-pull amplifier are biased to a firing angle of 90°. It will be shown later that the method of loading the push-pull amplifier almost invariably requires the addition of another block to the block diagram and results in a lower gain than that shown in Eq. (7-2).

The curves of Fig. 7-5 can be applied to push-pull amplifiers if the N^2/R values of the illustration are divided by two. That is, a given

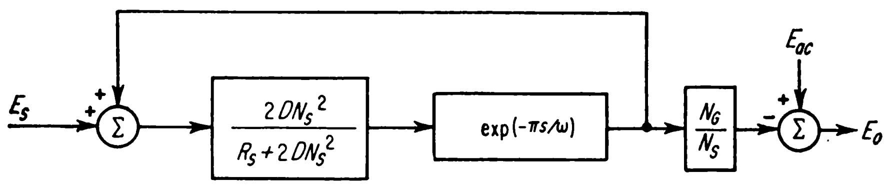

FIG. 7-8. Block diagram for circuit of Fig. 7-7.

core type used in the push-pull configuration has the same corner frequency as the same core type in the single-ended configuration when the latter has twice the N^2/R of the former. The curves of Fig. 7-3 apply to the push-pull configuration if the signal-power values of the illustration are divided by two; that is, if the cores are biased to a quiescent firing angle of 90°, the signal power required to drive the amplifier to full output is one-half the power required to drive a single-ended amplifier from cutoff to full output. It must be remembered that these curves are indicative of the power required only if the winding resistance is the only resistance in the signal circuit. The curves of Fig. 7-4 may be applied to the push-pull configuration by multiplying the signal-power values of the illustration by two.

7-4. ILLUSTRATIVE DESIGN PROCEDURES FOR FAST-RESPONSE AMPLIFIERS

Fast-response amplifiers, as a class, are characterized by a relatively high signal-power requirement. In some applications, however, this disadvantage is more than outweighed by the relative insensitivity of the phase shift of the amplifier to signal frequency. As shown in Chap. 5, in amplifiers in which the inherent positive feedback of doublet amplifiers is made negligible [$DN_S^2/(R_S + DN_S^2)$ approaches zero] the corner frequency becomes one-quarter of the gating frequency. The minimum signal power required to drive a biased reactor in the Logan circuit from cutoff to full output is a function of N^2/R and occurs, as would be expected from the discussion in Chap. 4, when the incremental volt-second transfer efficiency is 50 per cent. For a single-ended Logan circuit, this minimum signal power is approximately $10.8B_m \Delta H$ watts. Few applications allow use of the single-ended Logan circuit, however, and detailed illustrative design methods for the fast-response class of amplifiers will be limited to the push-pull Logan amplifier and the Hybrid III type of amplifier. Design of the Hybrid IV amplifier is quite similar to that of the Hybrid III and the former will be discussed only briefly.

Push-pull Logan Amplifier. The circuit to be considered is shown in Fig. 7-9. The minimum signal power for this circuit is approximately $5.4B_m \Delta H$ watts. The curves of Fig. 7-2 relating controlled load power

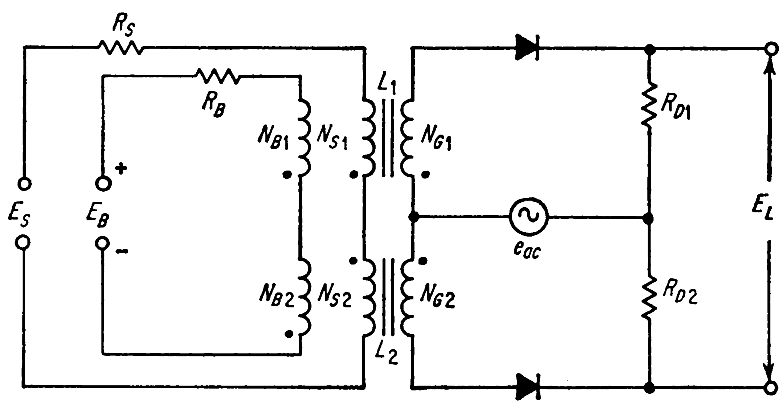

FIG. 7-9. Circuit diagram for a push-pull Logan amplifier.

to percentage of winding area apply directly to this circuit, provided that the power considered is the power delivered to R_D. The effect of a differential load of finite resistance is discussed in Sec. 8-3. It can be shown that to obtain a given load power with minimum total dissipation, $R_L = 1.414R_D$ and the total d-c power dissipated is $(3 + 2\sqrt{2})$ times the d-c load power. Thus, the curves of Fig. 7-2 can be made to apply if the desired load power is multiplied by roughly six. Since the maximum output power and the minimum signal power are constants, the maximum power gain of a core type in this class of amplifier is fixed. Given a signal source and the impedance of this source, the maximum power which can be obtained from the source is obtained when the total signal-circuit resistance (including the source resistance) is made equal to the reactor impedance during reset (this reactor impedance being resistive for square-loop reactors). These ideas were developed fully in Chap. 4. To obtain maximum gain when modulated carrier sources with a linear internal inductance are used, the inductive reactance should be matched with an external series capacitive reactance and R_S should then be matched to the reactor impedance. If the inductive reactance is small with respect to the circuit resistance, this refinement is unnecessary. Where the allowable power drain on the signal source is less than would be delivered by such matching, of course, R_S must be increased to limit the signal power to the maximum specified. The power delivered to the amplifier is then multiplied by the power gain of the largest core which

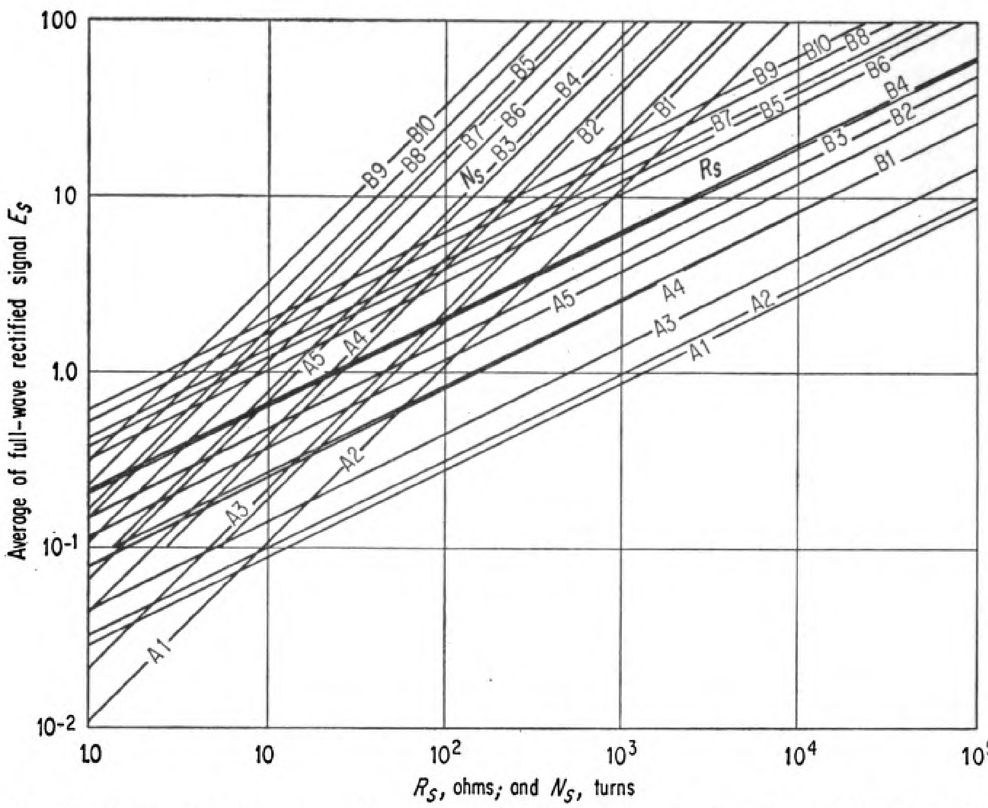

FIG. 7-10. Signal voltage required for complete reset as a function of signal-circuit turns and resistance.

can be driven by the available signal power. If the result exceeds the output power required of the core by the specifications, the required amplifier can be built. If the available core output power so determined is less than the required core output power, a multistage design or a doublet amplifier must be used.

The constant input power lines of the cores of Table 7-2 are plotted in Fig. 7-10 as functions of E_S, R_S, and N_S. A maximum efficiency amplifier can be designed from this set of curves. With a d-c signal voltage of, for instance, 2 volts and a source resistance of 2,000 ohms, the intersection of these values on the graph of Fig. 7-10 shows that three core types may be driven satisfactorily with this amount of signal.

Assuming that the signal current is limited, not by the dissipating ability of the source, but only by its internal resistance, an A3 core would normally be chosen, since it has superior power-controlling capabilities. From Fig. 7-2, an A3 core can control 0.34 watt if 100 per cent of the winding area is allocated to the gate winding. An A3 core, then, could supply $0.34/(2 + 3\sqrt{2})$ watt to an optimum differential load in this type of circuit. Since the signal source dissipates $4/(2 \times 10^3)$ or 2 milliwatts, the power gain of such an amplifier would only be about 30. The signal turns required are found from Fig. 7-10 to be 90. Since the signal current is 1 ma, the wire used for the signal winding may be extremely small and the winding area occupied by 90 turns of this wire may be considered negligible. Therefore, the core is shown to be capable of controlling the 0.058-watt load power originally assumed from the 100 per cent gate winding point of the curve of Fig. 7-2.

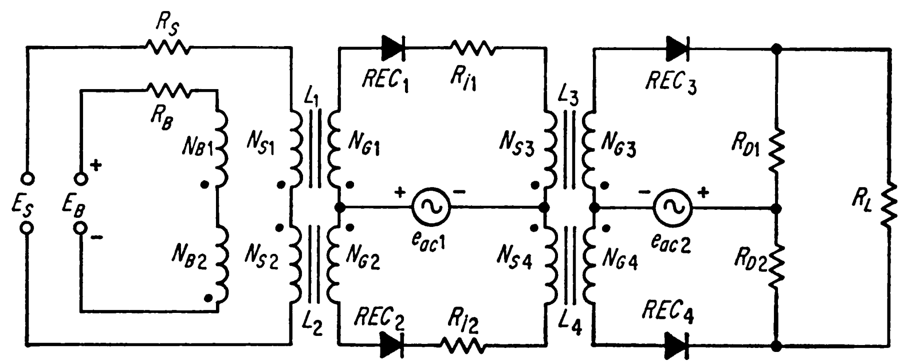

FIG. 7-11. Circuit diagram for a Hybrid III amplifier.

Hybrid III Amplifier. The circuit to be considered is shown in Fig. 7-11.[6] It will be recognized that the first stage of this two-stage amplifier is identical with the circuit of Fig. 7-9 except that the resistors R_{D1} and R_{D2} of the latter circuit have been replaced by the signal windings of a second stage. In complementary fashion, the second stage resembles the circuit of Fig. 7-9 except that the bias circuit has been eliminated and a three-terminal signal source replaces the two-terminal signal source of the push-pull Logan circuit. Since the design of the push-pull Logan circuit was seen to be extremely tractable, it would seem that the design of an amplifier which cascades two stages bearing a marked resemblance to the push-pull Logan circuit should not pose any insoluble problems. Unfortunately, the operation of the interstage circuit which couples the first stage gate windings and second stage signal windings involves principles which are not fully understood at present. If the circuit did not have the advantages of high gain and fast response, it would probably not be considered practical. With these advantages, however, the circuit is used frequently and the problems associated with the interstage circuit are solved on a cut and try basis, often through use of an additional voltage source.[7]

The circuit is most frequently used in applications in which the available signal power is moderate, the required output power is reasonably large, and a corner frequency in the neighborhood of 50 cps is mandatory. It can be seen from Fig. 7-10 that of the 15 cores whose properties are tabulated in Table 7-2, the Al-type core requires the least signal power when used in a push-pull Logan circuit. This signal power is seen to be approximately 7.7×10^{-4} watt. The design of the signal circuit of the Hybrid III is in all respects similar to the push-pull Logan circuit and this signal-power requirement may be considered as close to the present state of the art requirement for this class of amplifier operating at a 400-cps gating frequency.

If the assumption is made that amplifiers of the Hybrid III class are always designed to require an absolute minimum power from the signal source, a logical design procedure can be justified. Such a requirement implies that the first-stage core must be a type Al. If this restriction is removed, however, the design procedure to be discussed breaks down and the design becomes largely a laboratory technique. Large numbers of amplifiers can be produced economically from such a laboratory design, but the development costs are considerably higher than for an amplifier which an engineer can design at his desk with a reasonable degree of accuracy.

For the discussion to follow, then, it will be assumed that the cores for the first stage will be of type Al from Table 7-2. The signal circuit can then be designed from the information in Fig. 7-10. The load-circuit design and the second-stage cores can be designed in the same way as for the push-pull Logan circuit.

It has been found empirically that a Hybrid III amplifier using type Al cores in the first stage will work reasonably well if, after firing of the first-stage reactor, the sum of the average voltage drops represented by the iR drop and the forward voltage across the rectifier is about equal to the average voltage appearing across the second-stage signal winding during the gating half-cycle of the first stage. That is,

$$\int_{t=\alpha/\omega}^{t=\pi/\omega} iR_{i1}\,dt + \int_{t=\alpha/\omega}^{t=\pi/\omega} e_{REC}\,dt = \frac{1}{N_{S3}}\int_{t=\alpha/\omega}^{t=\pi/\omega} e_{S3}\,dt = \frac{1}{2}\int_{t=\alpha/\omega}^{t=\pi/\omega} e_{ac}\,dt \tag{7-3}$$

where R_{i1} is the lumped resistance of the interstage circuit and e_{S3} is the voltage appearing across the signal winding of reactor L_3. The relationships enforced by Eq. (7-3) have rather far-reaching consequences. The most important of these is that an upper bound is placed on the size of core used in the reactor of the second stage. This results from the fact that, even when $\alpha = 0$, the energy which can be used for reset of reactor

L_3 is limited by the magnitude of interstage circuit resistance and the forward drop of the diode. It has been found that the rms magnitude of e_{ac1} should be of the order of 2 to 5 volts.

Within the framework of these restrictions, the designer can determine the number of turns required for N_{S3} for a given core size by using the mmf_0 data of Table 7-2 and the resistance of a typical gate winding for a type Al core. An experienced designer can usually achieve a satisfactory design on the first trial while a designer not familiar with this type of circuit but using the design aids discussed here may require several trials.

Hybrid IV Amplifier. The Hybrid IV type of amplifier is included at this point principally because of the similarity of the methods used in its design to those of the Hybrid III type. As reference to the circuit diagram of Fig. 7-12 shows, the two first-stage cores of the Hybrid IV

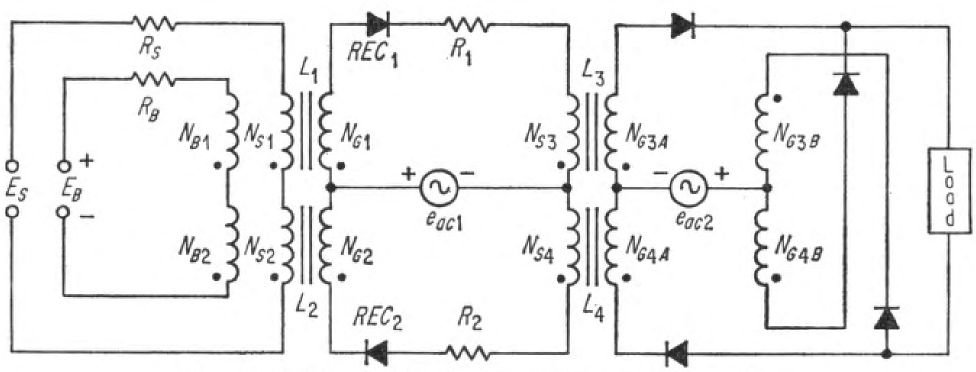

FIG. 7-12. Circuit diagram for a Hybrid IV amplifier.

amplifier gate on alternate half-cycles, resulting in loss of the fast-response feature as a consequence of the control-circuit coupling. The configuration of the circuit of Fig. 7-12 accepts a phase-reversible a-c signal and provides a phase-reversible a-c output. The output will contain a variable d-c component often desirable for damping in dynamic control applications. The feedback resulting from the signal-circuit coupling is asymmetric with respect to the sense of the applied signal, as can be deduced from consideration of the circuit. The transfer function of this type of circuit has not been very thoroughly investigated other than experimentally. Apart from the dynamic characteristics, the design of this amplifier proceeds along lines very similar to those followed for the Hybrid III amplifier. The second-stage configuration is very similar to that first described by Geyger.[8]

7-5. DERIVATION OF DESIGN CURVES

The design curves used in the preceding sections of this chapter were based on the assumption of a 400-cps gating frequency. To enable the interested designer to derive the curves for other gating frequencies and to give the student a clearer insight into the approximations made in deriving the displayed curves, a detailed derivation of each of the sets of curves will be made in this section. The sets of curves will be discussed in the order in which they appear in the chapter, except for Fig. 7-5, which must be derived prior to discussion of Fig. 7-4.

The maximum d-c power-controlling capability of the 15 cores of Table 7-2 was shown in Fig. 7-2 as a function of the percentage of the available window area occupied by the gate winding. In compiling the data for Fig. 7-2, it was assumed that the ratio of conductor cross-sectional area to the area of conductor and insulation is independent of wire size and that the winding space factors are the same for all wire sizes. If such an assumption is made, it can be shown that the turns-current product and, therefore, the voltage-current product, is independent of wire size. To obtain the curves displayed in Fig. 7-2, then, it is only necessary to compute the controllable power for several percentages of window area occupied by the gate winding and draw a smooth curve through the points so obtained.

A typical computation would be made as follows. For an A4 core, for example, obtain the nominal ϕ_m in volts/turn (0.0238) from Table 7-2. A convenient number of gate winding turns is assumed, in this case 1,000 turns, which defines a gating voltage of 23.8 volts rms. If No. 30 wire is assumed, 1,000 turns occupies, from Fig. 7-6, an area of 0.16 in.^{2}, which is two-thirds of the total available area (obtained from Table 7-2). For a mean length of turn of 1.4 in. as given in Fig. 7-13, and using the data of Table 7-3, 1,000 turns of No. 30 wire will have a resistance of 12.27 ohms. The load resistance can be determined from the expression

$$R_L = \frac{(0.45 \times \text{gating volts, rms}) - 0.35}{0.636 \times \text{rated current of wire, rms}} - R_{NG}$$

The gating voltage is determined by ϕ_m and the number of turns chosen, the rated current of the chosen wire can be obtained from Table 7-3, and 0.35 is the average forward drop of a typical silicon diode averaged over a complete cycle. For the example under consideration,

$$R_L = \frac{(0.45 \times 23.8) - 0.35}{0.636 \times 0.201} - 12.27 = 68.5 \text{ ohms}$$

The d-c power can be expressed as the product of the load resistance and the square of the average current,

$$P_L = I_L{}^2 R_L = (0.636 \times 0.201)^2 68.5 = 1.12 \text{ watts}$$

By repeating this procedure often enough for all core sizes of interest, a reasonably accurate set of curves can be drawn for any gating frequency.

Since ϕ_m does not vary appreciably with frequency, it is possible to draw a normalized set of curves in which power/cycle is plotted against winding area. Since most designers work with only one or two nominal gating frequencies, however, it is usually more convenient to plot power directly for a fixed gating frequency.

In Fig. 7-3, the minimum signal power is plotted against percentage of available window area occupied by the signal winding. To obtain such a set of curves, a quite rough approximation must be made. It is necessary to assume that the volts/ampere-turn gain obtained on a constant-current flux reset tester is invariant with N^2/R. The magnitude of the error involved in such an assumption for doublet amplifiers can be estimated from the curves of Fig. 4-7. The approximation seems justifiable, however, in view of the convenience offered in reaching a design decision rapidly.

With the assumption of the invariance of the volts/ampere-turn gain, the minimum signal power can be derived quite easily. The average signal voltage must be equal to the product of the signal-circuit resistance and the average signal current

$$E_S = I_S R_S$$

But the average signal current required to control the amplifier from cutoff to full output can be approximated as three times the Δmmf of Table 7-2 divided by the number of signal turns,

$$I_S = \frac{3\Delta\text{mmf}}{N_S}$$

From the two foregoing equations,

$$E_S I_S = \frac{9(\Delta\text{mmf})^2 R_S}{N_S^2} = P_S \tag{7-4}$$

and this is the d-c signal power. Minimum power to control an amplifier from cutoff to full output will be delivered by the signal source when there is no resistance external to the amplifier and the total resistance is in the reactor windings. Calculations have been made which indicate that, for a given core size, the power dissipated in the signal winding for a given number of ampere-turns varies by a factor of about 50 per cent as the wire size is varied from No. 12 to No. 40. Since choice of wire size is complicated by external factors such as signal-source voltage level, capability of available winding machines, stacking factor achieved by a given winding machine in putting wire into a given circular area, and others, the decision was made to assume that the area assigned to the signal winding would be fully utilized when No. 20 wire was used. As indicated previously, the actual minimum power required will vary with wire size chosen.

The assumption of No. 20 wire is made purely for the sake of convenience to arrive at a meaningful comparison of the minimum signal powers required by different cores.

The computations are based on the power determined from Eq. (7-4), recognizing that R_S, in view of the assumptions made, consists only of the winding resistance of the two reactors in series. The resistance of the signal winding is computed from the number of turns of No. 20 wire required to fill the desired percentage of total window area, the resistance of No. 20 wire, and the mean length of turn. The total available window

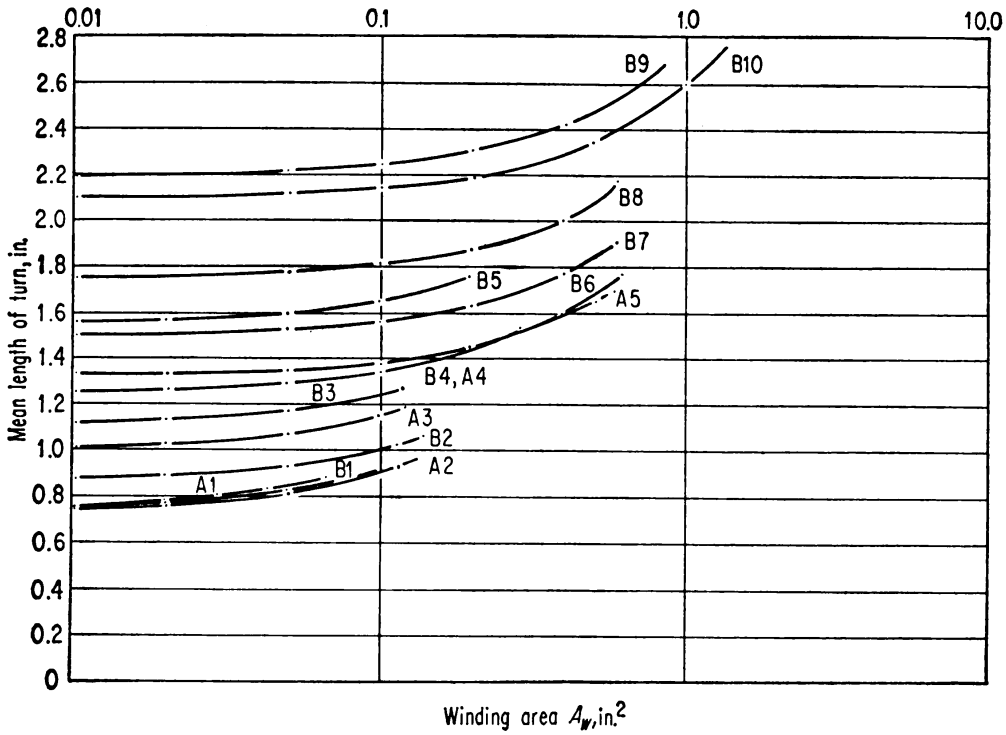

FIG. 7-13. Mean length of turn as a function of window area occupied by winding.

area is given in Table 7-2, the winding density in Fig. 7-6, the wire resistance in Table 7-3, and the mean length of turn in Fig. 7-13. It must be recognized that this minimum signal power can seldom be achieved in actual practice but is, rather, a lower bound for use in arriving at a reasonable choice of core for a particular design.

In Fig. 7-4, the corner frequency which can be expected with a doublet amplifier using a given core size is plotted as a function of the signal power available with the assumption made that the amplifier is to be driven from cutoff to full output. These curves are obtained in practice by manipulation of the data presented in Fig. 7-5. The curves of Fig. 7-5, in turn, result from consideration of the data of Fig. 5-12 in which the phase shift of a doublet amplifier is plotted as a function of frequency for various values of $DN_S^2/(R_S + DN_S^2)$. From the data of Fig. 5-12, a calculation can be made of the value of DN_S^2/R_S which results in a 45° phase shift at a given frequency. For example, if $DN_S^2/(R_S + DN_S^2)$ has a value of 0.97, DN_S^2/R_S will equal 32.33 and the corner frequency is 3.75 cps. From several such calculations, a curve such as is shown

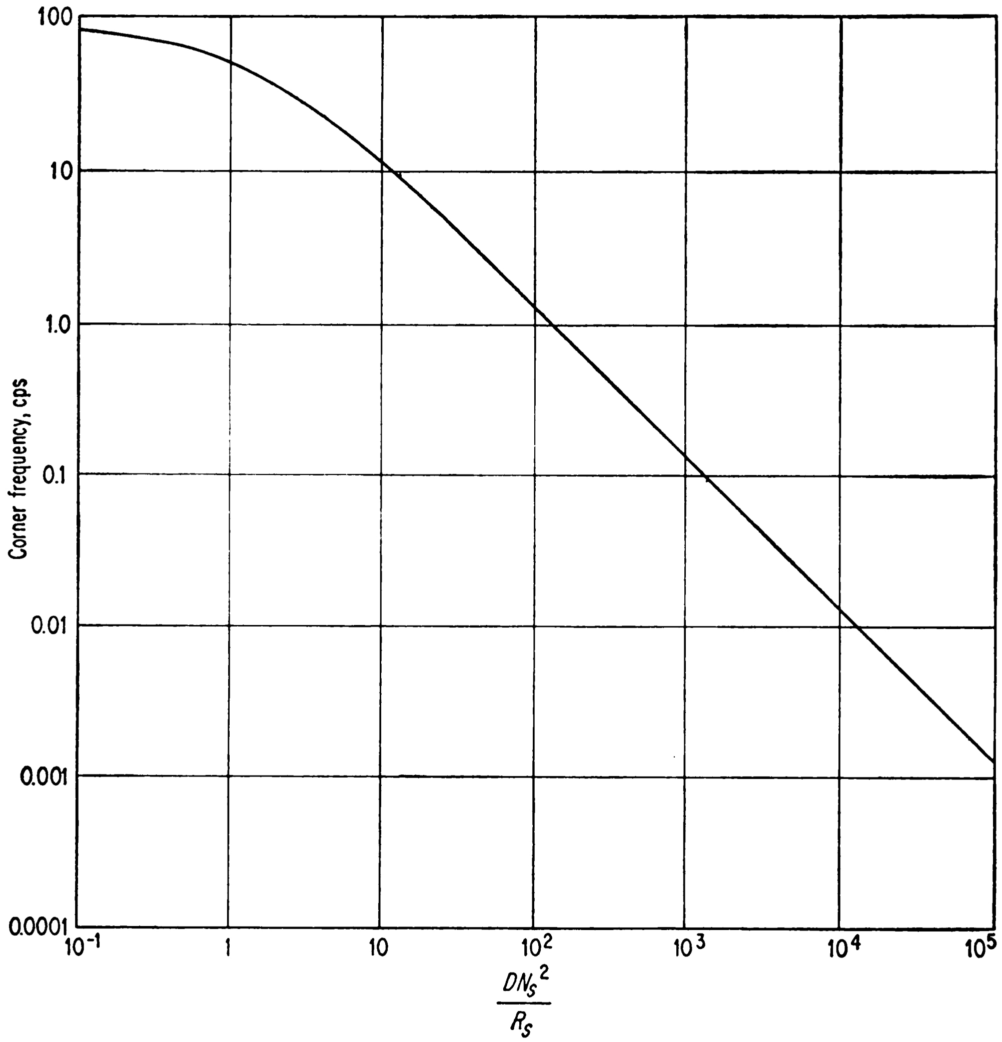

FIG. 7-14. Corner frequency as a function of the parameter DN_S^2/R_S.

in Fig. 7-14 can be plotted, relating corner frequency to DN_S^2/R_S. Using the values of D for a given core type given in Table 7-2, the curves of Fig. 7-5 can be calculated from the curve of Fig. 7-14. Using the curves of Fig. 7-5 and Eq. (7-4), the signal power P_S can be plotted as a function of corner frequency.

From the derivations of this section, it is possible to construct a set of design curves for any gating frequency. It is necessary, of course, to have the constant-current flux reset data measured at the frequency of interest. It must be emphasized that these curves are for design aids only. The lack of rigor in the assumptions made, particularly with respect to the linearity of many of the magnetic properties as measured by the constant-current flux reset test, as well as the wide variation in properties between cores of a given size, makes it impossible to achieve a really accurate design without a certain amount of cut and try in the laboratory. It is believed, however, that the method outlined reduces the amount of empiricism to a minimum.

REFERENCES

1. Hubbard, R. M., and M. M. Bishop: A Comprehensive Study of Magnetic Amplifier Design, *Trans. AIEE*, vol. 77, part I, pp. 562–580, 1958.
2. Anderson, R. E.: Magnetic-amplifier Design, *Trans. AIEE*, vol. 77, part I, pp. 160–176, 1958.
3. Hipermag Cores, *Bulletin DB* 44-750, Westinghouse Electric Corp., 1956.
4. Precision-made Tape-wound Cores, *Bulletin TB*-105, G-L Electronics Co., Inc.
5. Performance-guaranteed Tape Wound Cores, *Catalog TWC*-200, Magnetics, Inc., 1957.
6. Pula, T. J., G. E. Lynn, and J. F. Ringelman: Volt-second Transfer Efficiency in Fast Response Magnetic Amplifiers, Part II, N^2/R as a Design Parameter, *Trans. AIEE*, vol. 78, part II, pp. 8–11, 1959.
7. Patton, H. W.: The Pulse Stretch Coupling Circuit, *Trans. AIEE*, vol. 75, part I, pp. 377–379, 1956.
8 Geyger, W. A.: "Magnetic Amplifier Circuits," p. 181, McGraw-Hill Book Company, Inc., New York, 1954.

8

Special Design Problems

The evolution of magnetic-amplifier design theory has been quite slow and the theory is often based in large measure on necessary but unrealistic assumptions, particularly with respect to the idealization of components. An example of such logical but unrealistic assumptions is the postulate that the reactors in a doublet amplifier are identical. As a consequence of such departures from the ideal, second-order effects arise to plague the designer. Such effects are evidenced by phenomena such as environmental sensitivity, often called drift, by discontinuities and nonlinearities, by gain changes, and by other undesirable qualities. These important design problems, arising frequently from use of nonideal components and materials, will be discussed qualitatively. Few, if any, quantitative data are known to exist. What is presented in this chapter, then, can serve only as a guide to alert the designer to the existence of these effects and to present a few "fixes" which in the past have minimized the undesired characteristics when they have become impossible to endure.

A discussion of the effects of choice of gating frequency will also be included in this chapter since it can be a specific design problem.[1] In a large majority of cases, of course, the choice of gating frequency is dictated by the line frequency available. In those cases where it is possible to include a separate supply, however, the question frequently arises as to what frequency to choose in consideration of particular specifications of signal power available, minimum space and weight, amplification, and transient response. These questions will be discussed qualitatively and an attempt will be made to establish approximate guideposts for design.

8-1. ENVIRONMENTAL SENSITIVITY

Among terms and definitions proposed in February, 1958, as standard in the magnetic-amplifier field by the cognizant AIEE subcommittee are environmental sensitivity and drift.[2] Drift is defined as "a change in the control characteristic due to unassignable causes over a specified time interval." Environmental sensitivity is defined as "the change in the control characteristic due to specified changes in environmental conditions. These include changes in ambient temperature, supply voltage, supply frequency, and other specified changes." Additional committee work is in progress to improve upon or add to these definitions. A particular criticism of both is that neither allows easy assignment of quantitative values to the phenomenon under discussion. Pending an improved standard definition, the environmental sensitivity will be defined in this text as a change in quiescent operating point, rather than a change in the entire control characteristic.

A typical change in quiescent operating point is shown in Fig. 8-1 for a single-ended amplifier subjected to a substantial increase in ambient temperature. In Fig. 8-2 is shown the effect of an increase in ambient temperature on the characteristics of a push-pull amplifier. Assuming a given control input (e.g., a bias current), the quiescent operating point has shifted from point A to point B of Fig. 8-1. The gain of the amplifier remains essentially unchanged, however. If two such amplifiers are connected push-pull and biased to the mid-point of the linear range, the room-temperature characteristics of each half and of the push-pull arrangement are as shown by solid lines in Fig. 8-2. When subjected to an increase in ambient temperature, the characteristics shift to those

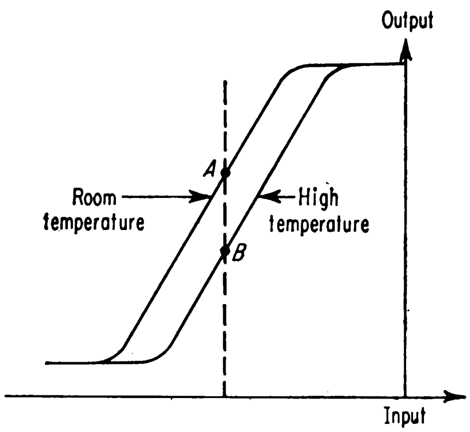

FIG. 8-1. Control characteristic of a single-ended bridge amplifier at two ambient temperatures illustrating the change in quiescent operating point.

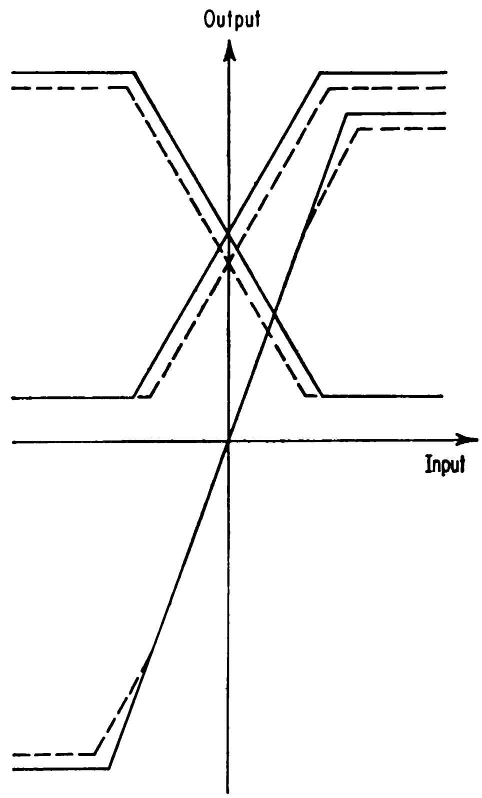

FIG. 8-2. Control characteristics of a push-pull bridge amplifier at two ambient temperatures, illustrating the constancy of the quiescent operating point.

shown by dotted lines in Fig. 8-2. The characteristic of each half is the same as that shown for the high-temperature condition in Fig. 8-1. It is seen, however, that there is no change in the quiescent operating point of the push-pull output. Over a large portion of the range, the characteristic is unaffected by the temperature change. As saturation is approached, however, the gain changes abruptly to one-half the value obtained in the neighborhood of the quiescent point and this decreased gain remains constant until saturation is reached, resulting in a severe nonlinearity.

A comparison of Figs. 8-1 and 8-2 reveals that the environmental sensitivity of the push-pull circuit is zero while the sensitivity of the single-ended circuit is quite large (defining environmental sensitivity with respect to the quiescent operating point). It will also be observed, though, that the gain of the single-ended circuit is shown as unaffected by temperature, while the gain of the push-pull circuit has become quite nonlinear near the extremes of the operating region even though the gain of the individual amplifiers has not changed.

It will be recognized that the examples shown are quite idealized. Some change in gain will usually be observed in a single-ended circuit if the ambient temperature is changed in large increments. More important, two amplifiers connected in a push-pull configuration will almost never change in identical ways to yield zero environmental sensitivity. The important feature to be noted is that the push-pull configuration inherently minimizes environmental sensitivity.

In addition to the inherent lack of sensitivity to most environmental changes (it can be demonstrated that the push-pull configuration minimizes changes in quiescent operating point caused by supply voltage and frequency variations as well as those of ambient temperature), most push-pull configurations lend themselves naturally to circuitry which further reduces sensitivity. Such circuitry is frequently required not only to reduce the change in quiescent operating point to an absolute minimum, but to minimize the nonlinearity observable in Fig. 8-2. These improvements in environmental sensitivity and linearity are usually accomplished by the addition of a self-bias circuit such as the typical configuration shown in Fig. 8-3.[3] Basically, the circuit shown consists of two single-ended bridge amplifiers with a common load resistor, the signal windings connected in series opposition, and bias windings connected in parallel. The bias-circuit current is a function of the sum of the individual load currents.

The operation of the self-biased amplifier can best be explained by assuming three levels of resistance for resistor R_{BL} and displaying (1) the voltages across resistors R_{D1} and R_{D2} as a function of signal current, (2) the net output voltage appearing across the load, and (3) the current

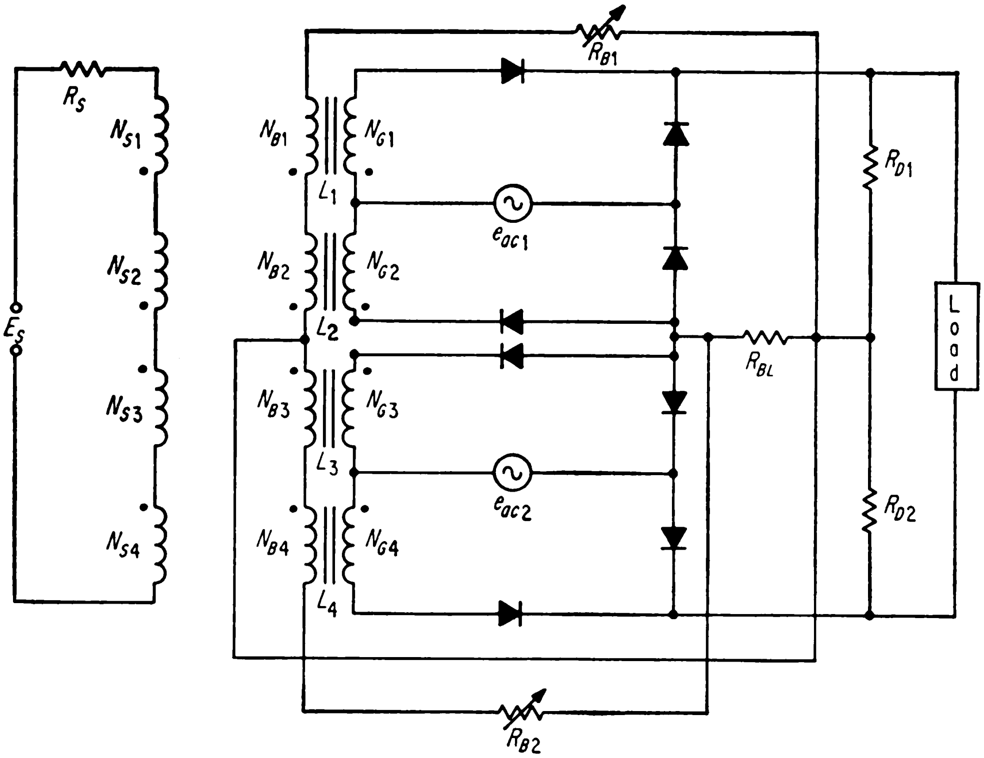

FIG. 8-3. Circuit diagram of a push-pull bridge amplifier with self-bias.

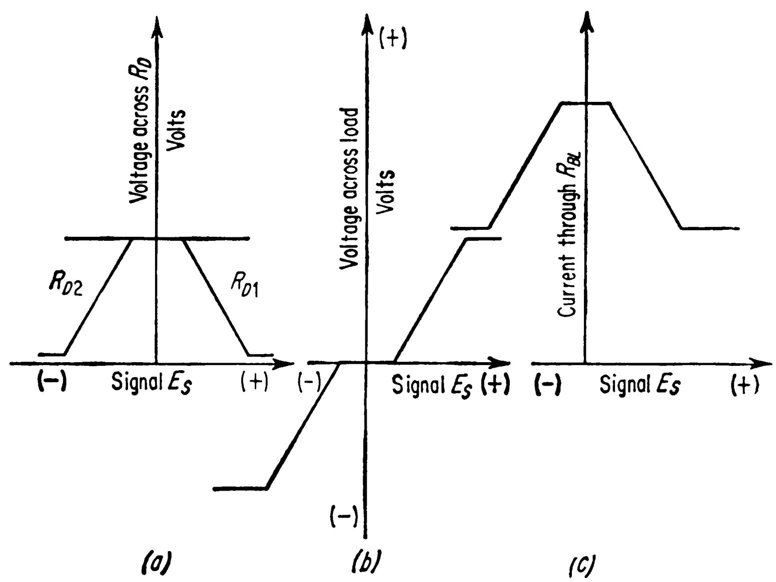

FIG. 8-4. Voltages in circuit of Fig. 8-3 as a function of signal voltage when quiescent firing angle is zero.

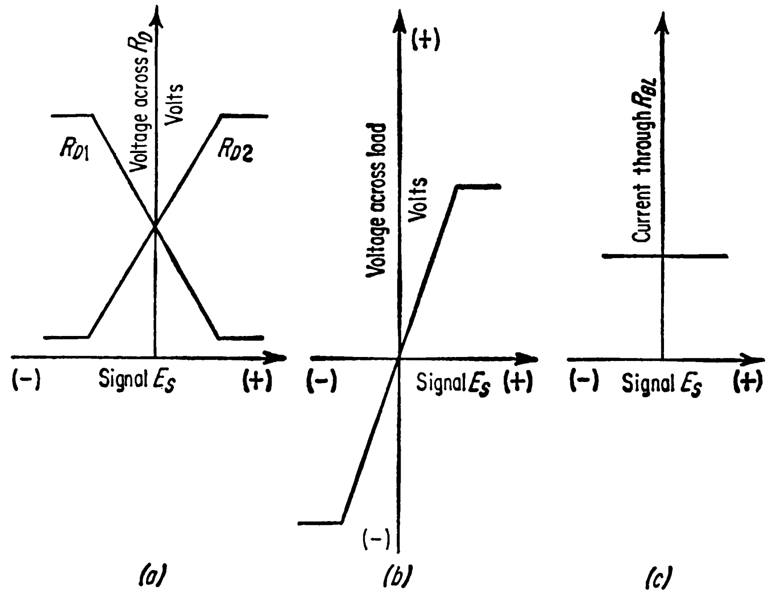

FIG. 8-5. Voltages in circuit of Fig. 8-3 as a function of signal voltage when quiescent firing angle is 90°.

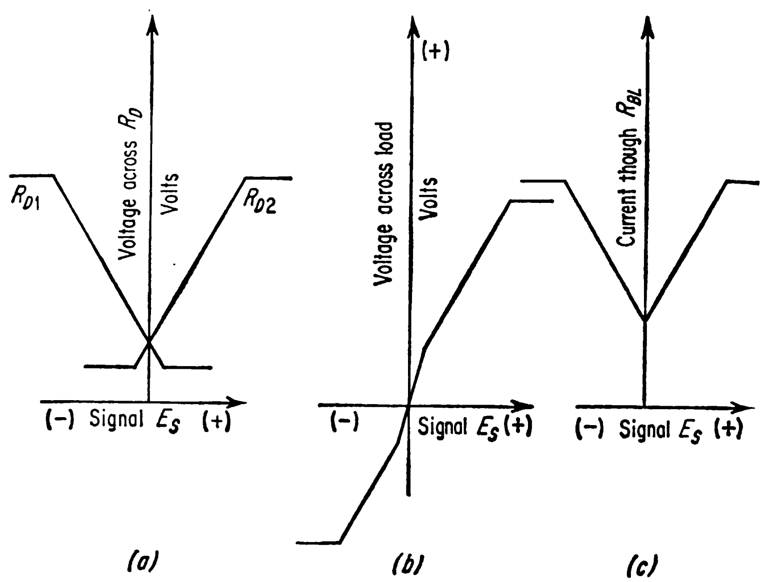

FIG. 8-6. Voltages in circuit of Fig. 8-3 as a function of signal voltage when quiescent firing angle is nearly equal to 180°.

flowing through resistor R_{BL}. These three parameters are displayed in Fig. 8-4 for the condition in which R_{BL} is zero, in Fig. 8-5 for the condition in which R_{BL} has a value which, for proper values of R_{B1} and R_{B2}, results in a firing angle of 90° for each amplifier, and, finally, in Fig. 8-6 for the condition in which R_{BL} has a value which, for proper values of R_{B1} and

R_{B2}, results in each amplifier operating almost at the cutoff point. These figures illustrate that, to obtain a reasonable range of linear high-gain output, it is necessary to bias the cores to a firing angle near 90°.

It has already been seen in Fig. 8-2 that, with a source of fixed bias, a change in environment resulted in a nonlinearity toward the extremes of the operating range. With the self-bias circuit of Fig. 8-3, it is possible to minimize the extent of the nonlinearity with respect to the operating range of the amplifier. A bias diagram can be constructed as shown in Fig. 8-7 for one-half of the amplifier to determine the improvement to be expected from the use of self-bias. An amplifier subject to conditions which alter the characteristic of each half from curve 1 to curve 2 of Fig. 8-7 would suffer a change in quiescent voltage from E_Q to E_2 under the condition of fixed bias. Identical conditions for an amplifier employing self-bias would cause a change in quiescent voltage from E_Q to E_1. The benefits of self-bias are self-evident.

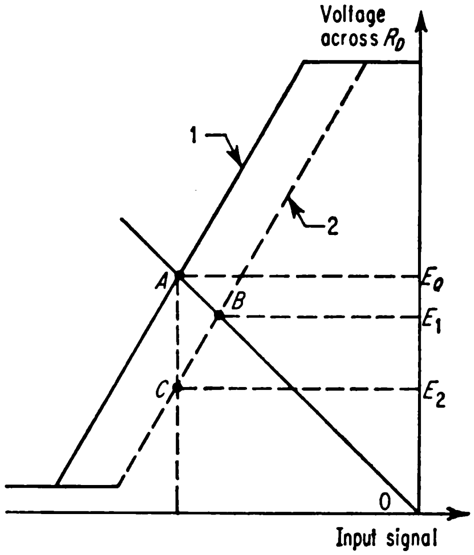

FIG. 8-7. Bias diagram illustrating improvement due to self-bias.

An extension of this concept is feasible when additional power for the self-bias circuit can be utilized without interference with the performance

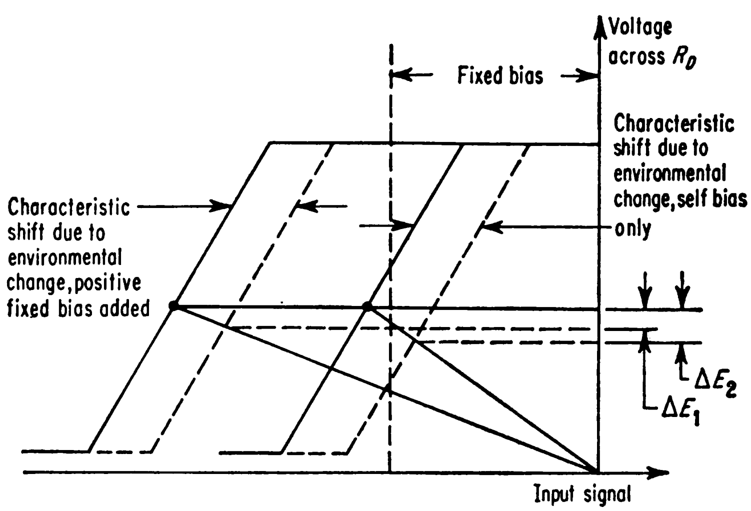

FIG. 8-8. Bias diagram illustrating use of combined fixed and self-bias.

of the load circuit. This involves the use of a positive fixed bias which effectively extends the upper knee of the amplifier characteristic, as shown in Fig. 8-8. In this figure, an extended and a nonextended characteristic are shown with equal characteristic changes caused by an environmental change. The effect of the extension of the knee can be seen by a comparison between ΔE_1, the change in quiescent voltage with positive fixed bias added, and ΔE_2, the change in quiescent voltage with the same self-bias as in Fig. 8-7. This minimizing of the effects of characteristic shifts is extremely important in most servo applications, where a change in quiescent operating point is reflected as an error.

8-2. GAIN CHANGE

In the previous section, the effect of an environmental change on the transfer characteristic was assumed to be equivalent to a simple shift of the vertical axis. This idealization was made to simplify the explanation of environmental sensitivity and self-bias and to reserve for this section the subject of gain change. In addition to the displacement of the vertical axis as a result of an environmental change, the slope or gain of the transfer characteristic is also affected. The self-biasing technique of Sec. 8-1 does nothing to reduce this effect. In applications where the gain of the stage is required to remain within close limits over a range of various environmental conditions, the principal method used to achieve the requirements is the application of negative feedback around the stage.

The gain of an amplifier is affected by many variables and is probably the most sensitive parameter with respect to environmental changes. Use of high-grade oriented materials makes the core sensitive to changes in pressure which, as a result of differential expansion of materials, frequently accompany changes in ambient temperature. A change in temperature also directly affects the saturation flux density, the resistivity, and the relaxation losses of the core material. Aside from changes in the core parameters, the gain of an amplifier is affected by changes in the resistance of the windings, in the characteristics of rectifiers, and in circuit components such as resistors, capacitors, etc. Measurements made on several presumably identical amplifiers indicate that not only is the magnitude of a gain change impossible to predict accurately with respect to a given environmental change, but even the algebraic sign of the change is subject to variation. That is, while the gain of 90 per cent of the amplifiers in a given sample may decrease in response to a given environmental change, the gain of the other 10 per cent may be either unaffected or increased. The application of basic feedback control principles shows that such gain changes can be minimized by the use of negative feedback. The transfer function C/R of the block diagram of Fig. 8-9, for example, can be derived quite simply.

$$
\begin{aligned}
C &= G(R - CH) = GR - GHC \\
C(1 + GH) &= GR \\
\frac{C}{R} &= \frac{G}{1 + GH}
\end{aligned}
\tag{8-1}
$$

If, in Eq. (8-1), the product of G and H can be made very large with respect to unity, so that the denominator can be considered only as GH, C/R reduces to $1/H$. The amplification of the system, then, is independent of changes in G so long as GH remains very large with respect to unity. Unfortunately, the forward gain of a magnetic amplifier is seldom large enough that the GH product can be made very large with respect to unity and still obtain a useful closed-loop gain. However, even though the closed-loop gain of a magnetic amplifier with feedback can seldom be made totally insensitive to changes in the forward gain, a considerable improvement is possible through the addition of feedback. In addition to reducing the magnitude of the change in gain with respect to a change in environment, negative feedback will reduce the change in quiescent operating point which is observed in a given amplifier.

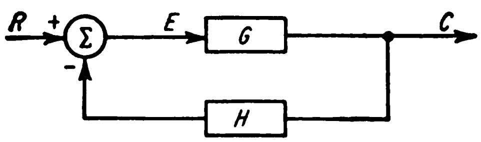

FIG. 8-9. Simple block diagram of an amplifier.

8-3. NONLINEARITIES

One cause of a nonlinearity in the transfer characteristic of a magnetic amplifier was shown in Sec. 8-1 to be the lateral shift of the characteristics of the two halves of a push-pull amplifier. The most common cause of a nonlinearity, however, is the inherently nonlinear relationship between the amount of reset flux obtained and the signal parameter. Most commonly used core materials, when used in a half-wave amplifier with very low N^2/R, will display a reasonably large range in which reset and signal have a tolerably linear relationship. In magnetic-amplifier design methods, this range is usually assumed to be exactly linear and to extend from cutoff to full output. For a reasonably high N^2/R, these approximations are not in good agreement with experimental evidence, as shown in Fig. 8-10. In this figure, a transfer characteristic measured on a half-wave amplifier with moderately high N^2/R (about 500) is displayed and compared to a highest-gain linear approximation. It is obvious that extreme linearity is obtained over only a small range of operation.

While the curve of Fig. 8-10 may not be quite typical of useful half-wave circuits (which usually operate at a lower value of N^2/R), the only phenomenon which is exaggerated by the increase in N^2/R is the magnitude of the nonlinearity; the nonlinear operation itself is fundamental. It appears, then, that in specifying the operating range of a magnetic

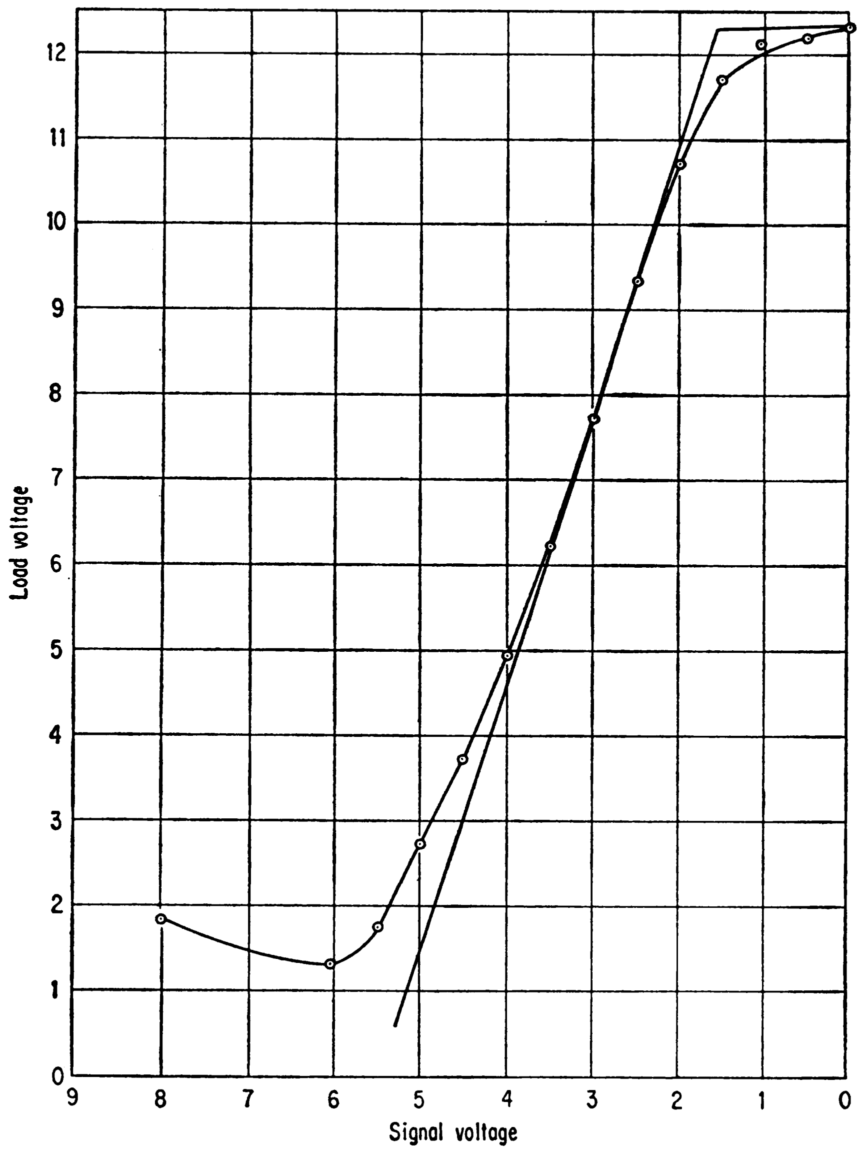

FIG. 8-10. Transfer characteristic of a Logan circuit with high N^2/R compared with a straight line.

amplifier, the percentage of deviation from linearity that may be tolerated must be specified. The nonlinearity which may be observed in a given bridge circuit is shown in Fig. 8-11. For the particular amplifier on which the data for Fig. 8-11 were obtained, the linear range for a given percentage of deviation from linearity is appreciably greater than the range for the same percentage of deviation for the amplifier of Fig. 8-10.

Nonlinearities caused by the nature of the core material or by choice of bias point in push-pull amplifiers are common to most magnetic amplifiers. However, two causes of nonlinearity exist which, if not peculiar to, at

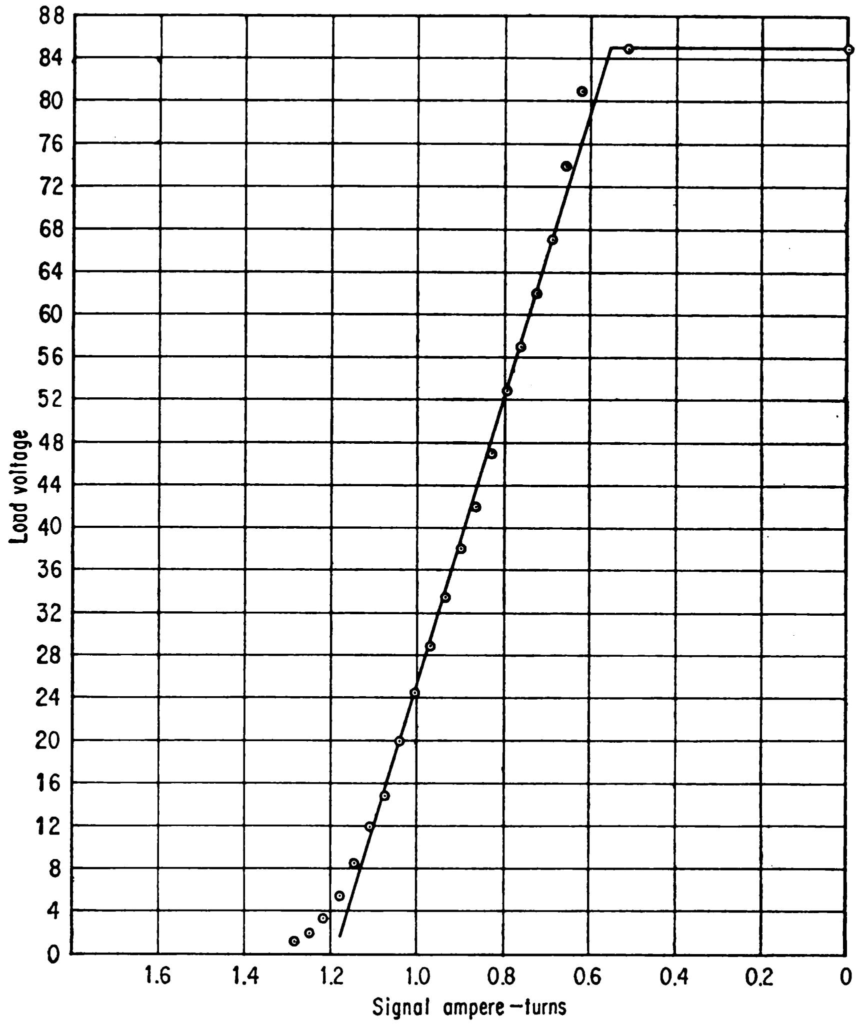

FIG. 8-11. Transfer characteristic illustrating the nonlinear characteristic of a bridge circuit.

least are exaggerated in, the two-stage fast-response amplifier discussed in Chap. 7. These two nonlinearities will be developed in considerable detail to illustrate the quantitative arguments which can be presented if suitable approximations are carefully made. For convenience, the salient points of such a circuit are presented again in Fig. 8-12.

Let it be assumed, to emphasize only the important points, that the characteristics of the first-stage cores are perfectly linear, that is, that the average voltage across the gate windings of the first-stage cores is proportional to the signal voltage and can be expressed as

$$E_{NG1} = kE_S \tag{8-2}$$

If it is assumed that the voltage losses in the interstage circuit prior to firing of the first-stage cores are chiefly a function of the diode threshold

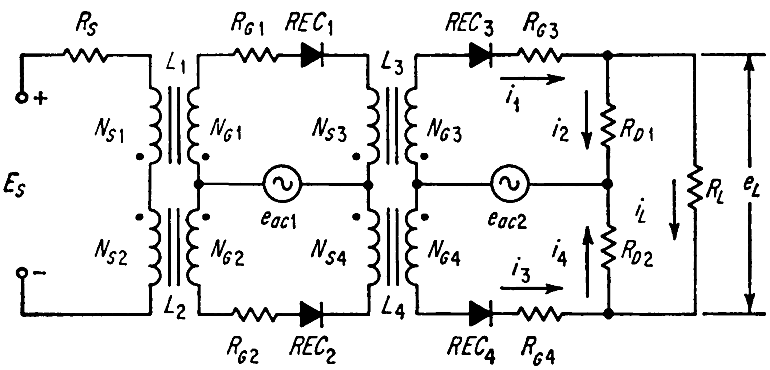

FIG. 8-12. Circuit diagram of a Hybrid III amplifier.

voltage E_T, another equation for E_{NG1} can be written. Defining e_{ac1} as $E_{1m} \sin \omega t$,

$$\begin{aligned} E_{NG1} &= \frac{\omega}{\pi} \int_{t=0}^{t=\alpha/\omega} (E_{1m} \sin \omega t - E_T)\, dt \\ &= \frac{1}{\pi} [E_{1m}(1 - \cos \alpha) - E_T\alpha] \end{aligned} \tag{8-3}$$

Equating the right-hand sides of Eqs. (8-2) and (8-3) and solving for $\cos \alpha$

$$\cos \alpha = 1 - \frac{E_T\alpha}{E_{1m}} - \frac{\pi k E_S}{E_{1m}} \tag{8-4}$$

After firing of the first-stage cores, the interstage circuit voltage losses will increase because of the large difference in magnetizing currents required for the first- and second-stage cores. If this new loss level is designated as E_i, the average voltage across the signal windings of the second-stage cores can be written

$$\begin{aligned} E_{NS3} &= \frac{\omega}{\pi} \int_{t=\alpha/\omega}^{t=\pi/\omega} (E_{1m} \sin \omega t - E_i)\, dt \\ &= \frac{1}{\pi} [E_{1m}(1 + \cos \alpha) - E_i(\pi - \alpha)] \end{aligned} \tag{8-5}$$

Substituting Eq. (8-4) into Eq. (8-5)

$$E_{S3} = \frac{2E_{1m}}{\pi} - kE_S - E_i + \frac{\alpha}{\pi}(E_i - E_T) \tag{8-6}$$

The presence of a term involving α in Eq. (8-6) makes the relationship between the average second-stage winding voltage (which is equivalent to the second-stage flux change) and the signal voltage nonlinear. The nonlinearity is roughly an arccosine term.

In addition to the nonlinearity resulting from the interstage circuit losses, the circuit of Fig. 8-12 is subject to a nonlinearity arising in the load circuit. If R_L can be considered infinite with respect to R_D, the load voltage E_L bears a linear relationship to the input voltage E_S if the nonlinearities of the interstage circuit and of the core properties are neglected. However, it can be shown that for minimum power dissipation in the output circuit for a given useful load power, $R_L = 1.414R_D$. For this condition R_L cannot be considered infinite and E_L may not be linear with respect to E_S.

To illustrate this point, let the gating half-cycle of the second stage be divided into three portions, as shown in Fig. 8-13. The angle α is the firing angle of reactor L_3, β is the firing angle of reactor L_4, and γ is the quiescent firing angle at which $\alpha = \beta$. In Fig. 8-14 the voltages appearing across R_{D1}, R_{D2}, and R_L are shown as functions of time for one gating half-cycle. A mathematical illustration can be developed if it is assumed that:

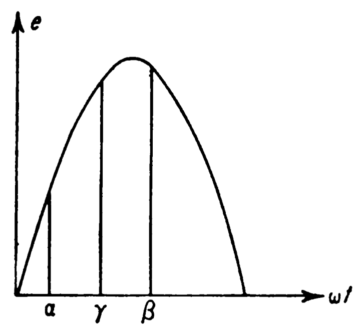

FIG. 8-13. Gating half-cycle of second stage showing firing angles.

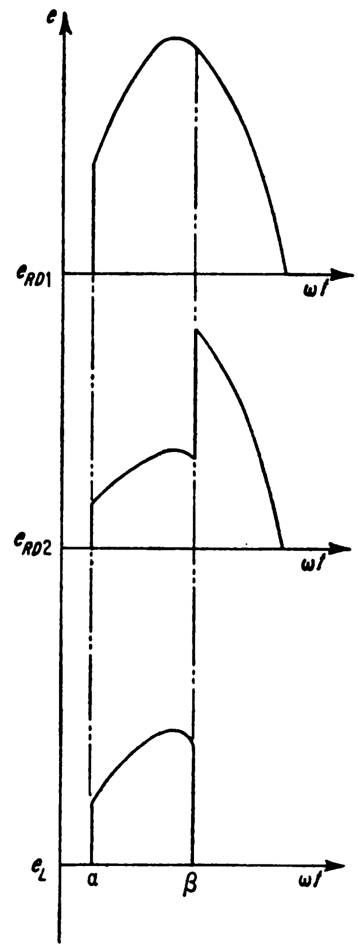

FIG. 8-14. Waveshapes occurring in load circuit during gating.

1. The saturated inductance of the second-stage reactors is negligible.
2. The exciting current of the second-stage reactors is negligible.
3. The second-stage diode forward impedance can be approximated as a linear resistance.
4. The two second-stage reactors have identical characteristics.
5. The source impedance of e_{ac2} is zero.

6. The first-stage and the interstage circuits are linear.

7. The components of the two second-stage gate circuits are identical.

With regard to the circuit of Fig. 8-12 and the above assumptions, the following equations may be written for the three time periods of Fig. 8-13.

$$\begin{aligned} e_{ac2} &= e_{NG3} = e_{NG4} && 0 < \omega t < \alpha \\ e_{ac2} &= i_1 R_{G3} + i_2 R_{D1} = e_{NG4} + i_L R_{D2} && \alpha < \omega t < \beta \\ e_{ac2} &= i_1 R_{G3} + i_2 R_{D1} = i_3 R_{G4} + i_4 R_{D2} && \beta < \omega t < \pi \end{aligned} \tag{8-7}$$

It can be shown that load current i_L can flow only for the condition $\alpha < \omega t < \beta$. For this condition, the following simultaneous equations can be written

$$\begin{aligned} e_{ac2} &= i_1 R_{G3} + i_2 R_{D1} \\ i_2 R_{D1} &= i_L (R_L + R_{D2}) \end{aligned} \tag{8-8}$$

or, since $R_{D1} = R_{D2} = R_D$

$$i_2 = i_L \left(1 + \frac{R_L}{R_D}\right) \tag{8-9}$$

$$i_1 = i_2 + i_L \tag{8-10}$$

Combining Eqs. (8-9) and (8-10)

$$i_1 = i_L \left(2 + \frac{R_L}{R_D}\right) \tag{8-11}$$

Substituting Eqs. (8-9) and (8-11) into Eq. (8-8)

$$e_{ac2} = i_L R_{G3} \left(2 + \frac{R_L}{R_D}\right) + i_L R_D \left(1 + \frac{R_L}{R_D}\right) \tag{8-12}$$

Simplifying this equation, an expression for i_L is obtained for the period $\alpha < \omega t < \beta$

$$i_L = \frac{e_{ac2} R_D}{2R_{G3} R_D + R_L R_{G3} + R_L R_D + R_D^2} \tag{8-13}$$

During the period $\alpha < \omega t < \beta$, the flux change in reactor L_4 is given as

$$\Delta\phi_4 = \frac{1}{\omega N_{G4}} \int_\alpha^\beta e_{NG4}\, d\omega t$$

But Eq. (8-7) yields an expression for e_{NG4} in terms of e_{ac2} and i_L, yielding

$$\Delta\phi_4 = \frac{1}{\omega N_{G4}} \int_\alpha^\beta e_{ac2} \frac{2R_{G4} R_D + R_L R_{G4} + R_L R_D}{2R_{G4} R_D + R_L R_{G4} + R_L R_D + R_D^2}\, d\omega t \tag{8-14}$$

A quantity E_Q will now be defined as the quiescent voltage, representing the average voltage appearing across R_{D1} and R_{D2} under a "no signal" condition. This voltage may be considered as the bias point. Under null conditions, both halves of the amplifier are assumed to be at this bias point and L_3 and L_4 will both fire at the angle γ. Defining e_{ac2} as $E_{2m} \sin \omega t$

$$E_Q = \frac{E_{2m}}{2\pi} \int_\gamma^\pi \sin \omega t \, d\omega t$$
$$= \frac{E_{2m}}{2\pi} (1 + \cos \gamma)$$
$$\gamma = \cos^{-1} \left(\frac{2\pi E_Q}{E_{2m}} - 1 \right) \tag{8-15}$$

Equation (8-15) yields an expression for the quiescent firing angle in terms of the peak value of e_{ac2} and the quiescent voltage resulting from this firing angle.

Assuming the proper polarity of signal (the polarity which results in an advance in the firing angle of reactor L_3), and under the conditions assumed initially, the firing angle of L_4 will retard as the angle of L_3 advances and, with R_L infinite,

$$\int_\alpha^\gamma E_{2m} \sin \omega t \, d\omega t = \int_\gamma^\beta E_{2m} \sin \omega t \, d\omega t \tag{8-16}$$

That is, the volt-second area absorbed by reactor L_3 will differ from the area absorbed under quiescent conditions by the same amount that the area absorbed by reactor L_4 differs from the area absorbed under quiescent conditions. The sign of the change in area is opposite for the two reactors, reactor L_3 absorbing this many less volt-seconds and reactor L_4 this many more.

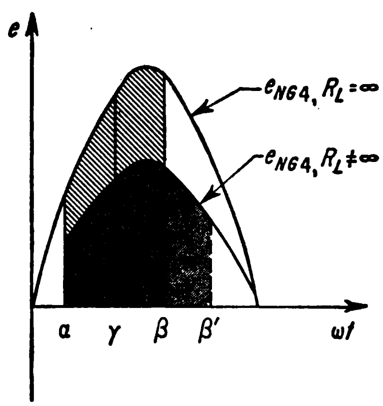

FIG. 8-15. Effect of R_L on gate voltage of reactor L_4.

However, when R_L is not infinite, the situation is not the same. After reactor L_3 fires at α, the voltage across the gate winding of reactor L_4 is no longer e_{ac2} but becomes $e_{ac2} - i_L R_D$, as shown by Eq. (8-7). The volt-second area absorbed by the reactor L_2 during the gating half-cycle, of course, must remain constant whether R_L is present or not, since the flux change during the reset half-cycle is independent of R_L. Thus, if the voltage at the reactor terminals varies with R_L while the volt-second area is independent of R_L, the time, or firing angle, β must also vary with R_L. This effect is shown in Fig. 8-15, where the firing angle in the absence of R_L is designated as β while the angle in the presence of R_L is β'.

The firing angle of reactor L_3, α, is independent of the presence of R_L since R_L has no effect on e_{NG3}. However, if R_L is infinite, reactor L_4 will absorb, in addition to the volt-second area between zero and α (which is also the area absorbed by reactor L_3), the area included between the angles α and β before it fires. But it has already been established in Eq. (8-16) that the area included between the angles α and γ equals the area between γ and β. Therefore, after reactor L_3 fires, reactor L_4 will absorb twice the area between α and γ. It is now possible to derive an expression for the angle α in terms of the quiescent voltage E_Q.

It was seen in Sec. 8-1 that, in a push-pull amplifier, a nonlinearity develops when one-half of the amplifier reaches either full output or cutoff at a different input than is required to bring the other half to cutoff or full output, respectively. In the amplifier under discussion, then, a nonlinearity will result whenever α reaches zero at an input different from that at which β reaches 180°. To ensure linear operation, the parameters involved must be determined in terms of easily controlled variables. An expression for α must first be obtained.

The volt-second area absorbed by reactor L_3 for a given signal is given by

$$\begin{aligned} \mathrm{VSA}_3 &= \frac{E_{2m}}{\omega}\int_\alpha^\gamma \sin \omega t \, d\omega t \\ &= \frac{E_{2m}}{\omega}(\cos \alpha - \cos \gamma) \end{aligned} \tag{8-17}$$

The area absorbed by reactor L_4 from α to π is, from Eq. (8-14)

$$\mathrm{VSA}_4 = \frac{1}{\omega}\int_\alpha^\pi E_{2m} \sin \omega t \, \frac{2R_{G4}R_D + R_LR_{G4} + R_LR_D}{2R_{G4}R_D + R_LR_{G4} + R_LR_D + R_D{}^2}\, d\omega t \tag{8-18}$$

To simplify notation a new variable will be introduced

$$Z = 2R_{G4}R_D + R_LR_{G4} + R_LR_D \tag{8-19}$$

Substituting Eq. (8-19) into Eq. (8-18) and performing the indicated integration

$$\mathrm{VSA}_4 = \frac{E_{2m}}{\omega}\,\frac{Z}{Z + R_D{}^2}(1 + \cos \alpha) \tag{8-20}$$

In a previous paragraph it was established that, after reactor L_3 fires, reactor L_4 will absorb twice the volt-second area between α and γ. Therefore, Eq. (8-20) is equal to twice Eq. (8-17)

$$\frac{E_{2m}}{\omega}\,\frac{Z}{Z + R_D{}^2}(1 + \cos \alpha) = \frac{2E_{2m}}{\omega}(\cos \alpha - \cos \gamma) \tag{8-21}$$

Substituting the expression for γ from Eq. (8-15) into Eq. (8-21) and simplifying

$$\frac{Z}{Z + R_D{}^2}(1 + \cos \alpha) = 2 \cos \alpha - 2\left(\frac{2\pi E_Q}{E_{2m}} - 1\right)$$

from which, by proper manipulation

$$\alpha = \cos^{-1}\left(\frac{4\pi E_Q}{E_{2m}}\frac{Z + R_D^2}{Z + 2R_D^2} - 1\right) \tag{8-22}$$

This, then, is the expression for the values α may have when $\beta = \pi$. Since the quiescent voltage E_Q is an easily controlled variable, it is possible to obtain maximum linearity by varying E_Q to make α zero in Eq. (8-22). Thus,

$$0 = \cos^{-1}\left(\frac{4\pi E_Q}{E_{2m}}\frac{Z + R_D^2}{Z + 2R_D^2} - 1\right)$$

$$1 = \frac{4\pi E_Q}{E_{2m}}\frac{Z + R_D^2}{Z + 2R_D^2} - 1 \tag{8-23}$$

Simplifying Eq. (8-23)

$$E_Q = \frac{E_{2m}}{2\pi}\frac{Z + 2R_D^2}{Z + R_D^2} \tag{8-24}$$

Unless this equation is satisfied, the maximum linear range of the amplifier will not be realized, provided that all the other assumptions have been met. It is common practice, however, to trade off nonlinearities against each other in order to achieve maximum linearity. That is, E_Q might be varied around the value established in Eq. (8-24) in order to compensate for a nonlinearity introduced, for instance, in the interstage circuit.

In addition to the causes of nonlinearities discussed in this section, there is evidence that interwinding capacitance causes nonlinearities. Since this parameter is difficult to measure and has been known to vary from one reactor to another even though the reactors were supposedly wound the same way, not much can be said concerning the effects of this capacitance. If peculiar nonlinearities occur in designs involving thousands of turns, an attempt is usually made to minimize interwinding capacitance.

8-4. DISCONTINUITIES

For the purposes of this text, the subject of discontinuities is distinguished from other types of nonlinearities. The nonlinearities discussed in the preceding section are usually evidenced as somewhat gradual changes in slope when experimental data are examined. Granted that, in many of the illustrations, the change in slope is displayed as occurring abruptly at a point, in actual practice the phenomena tend to result in smoother curves. With the discontinuities to be discussed in this section, however, an abrupt jump in the transfer characteristic is observed. The curve on either side of the jump may or may not have the same slope.

One such discontinuity which has been discussed at some length in the literature is the phenomenon of "core triggering."[4,5] A transfer characteristic showing the nature of this phenomenon is shown in Fig. 8-16. The solid curve was obtained with a load resistance of 500 ohms, the

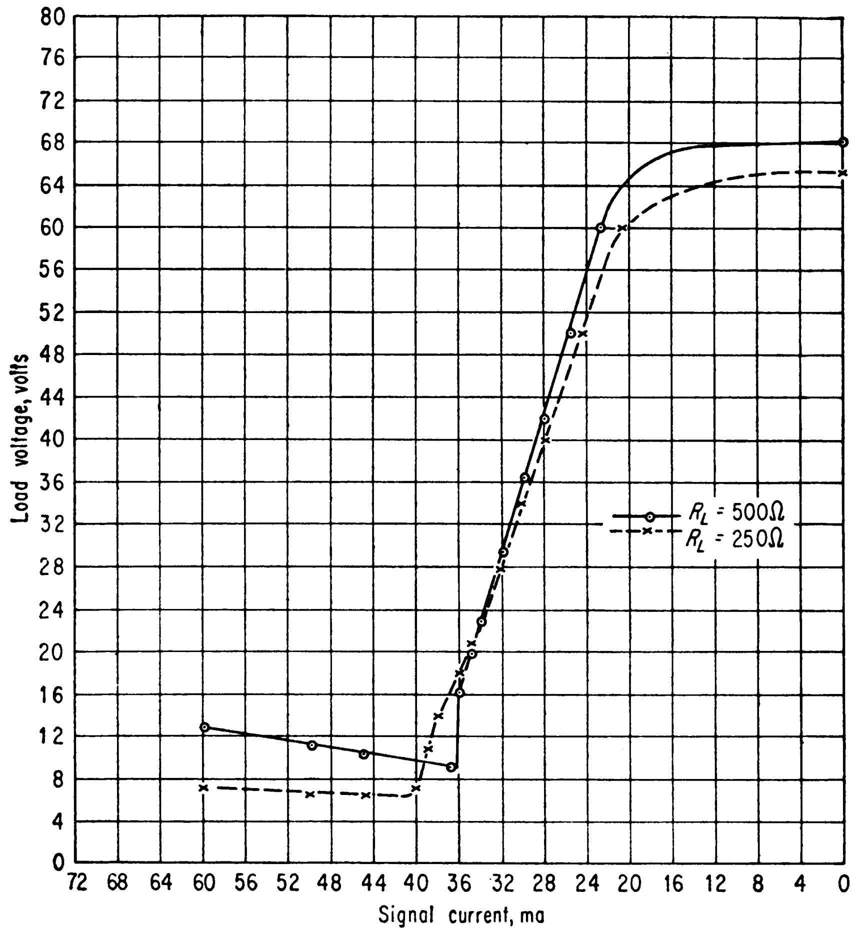

Fig. 8-16. Transfer characteristics showing the influence of load resistance on "triggering."

dashed curve with a load resistance of 250 ohms. The abrupt jump from cutoff to partial output is obvious in the solid curve for the higher load resistance, while the transition is much smoother for the lower value of resistance. Such a "trigger" is the result of insufficient gating volt-seconds applied to the reactor either because of too low a gate voltage or because of too high a total resistance in the gate circuit. In such an underexcited state, the flux never reaches positive saturation when large values of signal are applied. This implies that domain walls exist within the core material at the beginning of each reset half-cycle and the magnetic potential required to achieve a given amount of flux change during a reset period is less than would be required for an equivalent flux change

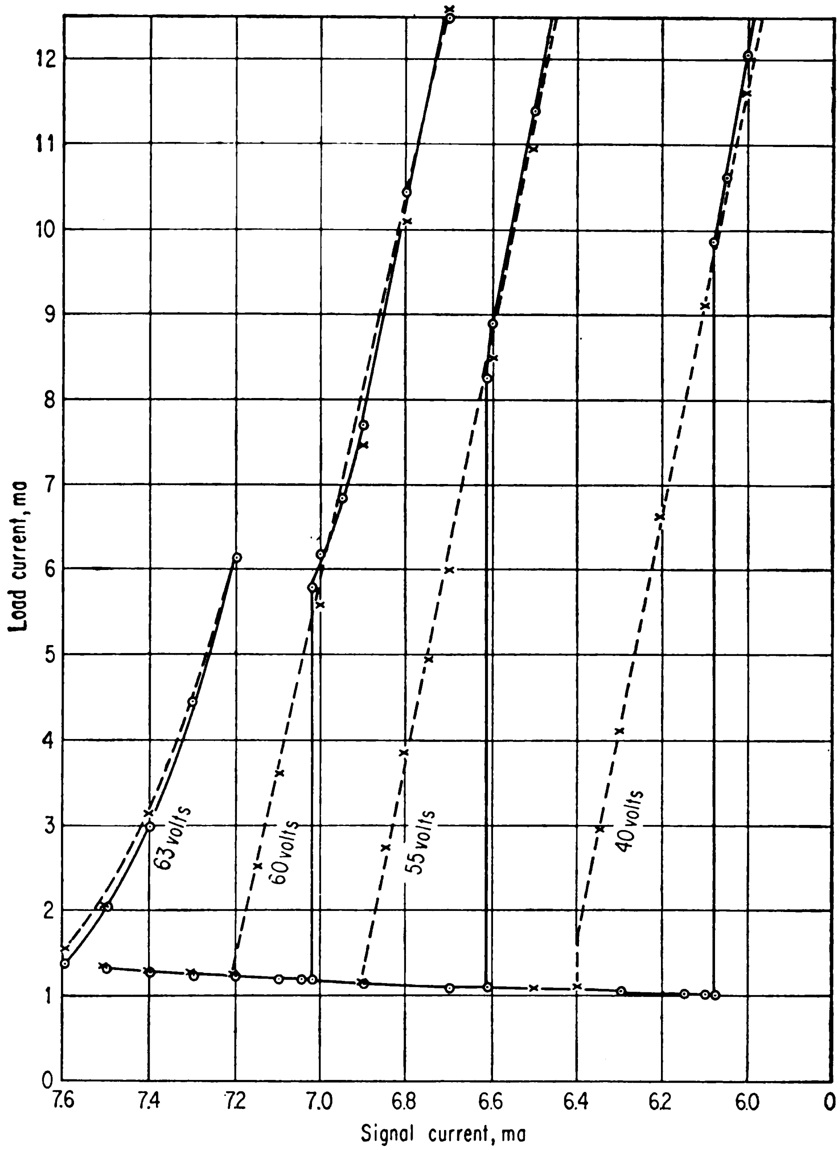

FIG. 8-17. Transfer characteristics showing the influence of gate voltage on "triggering."

if it were necessary to nucleate domain walls first. As the signal parameter is decreased to the point at which the trigger occurs, a condition is reached in which the positive magnetic potential at the end of a gating period leaves the domain walls in a configuration less favorably oriented for easy reset than previously. Accordingly, in the next reset period a somewhat smaller amount of reset is obtained and, in the next gating period, the domains are even less favorably oriented for easy reset. This ratcheting process continues until the flux achieves positive saturation in the gating half-cycle and establishes a steady-state condition in which the flux change during the reset period is considerably less than it was in the steady-state condition which existed before the ratcheting process was initiated. It is important to observe that the second steady-state condition (resulting in appreciable output) is initiated from the first condition with only an infinitesimal change in signal. In fact, it is possible to initiate the ratcheting process with a transient change in supply voltage and thus obtain both steady-state conditions without any change in signal.

To illustrate the extent to which the magnitude of the trigger is dependent on the value of supply voltage, the cutoff regions of several transfer characteristics are shown in Fig. 8-17. These characteristics were obtained with a Logan circuit similar to that described in Chap. 3. It is seen that, for any supply voltage less than 63 volts, the characteristic obtained with decreasing input signal displays a pronounced discontinuity, while the characteristic obtained with increasing input is reasonably smooth. It is possible to obtain a downward trigger but, in general, the magnitude of the downward trigger is much less than that of the upward trigger. A very small downward trigger is observable in Fig. 8-17 in the increasing signal characteristic with a 40-volt supply voltage.

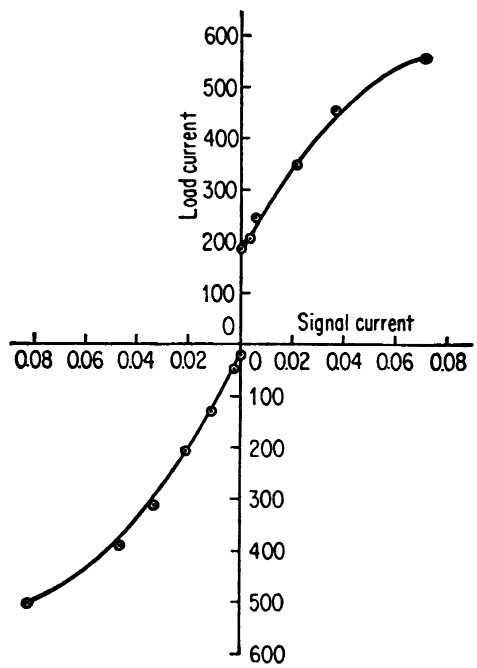

FIG. 8-18. Discontinuity occurring in some multistage push-pull amplifiers.

Another, different type of discontinuity is occasionally found when a multistage push-pull amplifier is used. The nature of this discontinuity is shown in Fig. 8-18. It is obvious that the use of an amplifier with such a characteristic in a feedback control system could lead to serious instabilities. Unfortunately, no logical explanation of this peculiar behavior has been formulated. The discontinuity has been eliminated in designs in which it has appeared by decreasing the gain of the second-stage amplifier through the use of resistances shunting the gate windings of the second-stage reactor.

Since the characteristic of each stage by itself is continuous through the origin, it is apparent that the induced voltages across the second-stage control windings must be influencing the behavior of the first-stage reactors. The mechanism by which this influence is exerted has not been discovered, to the knowledge of the authors, nor has it been demonstrated why the "fix" applied is effective. The comparative rarity of this type of discontinuity has made an analysis of it of less consequence than other more common problems, such as core triggering.

Another type of discontinuity arises from use of an inductive, capacitive, or active load.[6,7] The shape of the discontinuity will vary with the individual case, but in general it resembles the triggering phenomenon. The methods for dealing with such a discontinuity vary with the cause but often involve shunting the load with a low resistance or with a free-wheeling rectifier. Occasionally, tuning the load proves effective, although in most cases the wideband frequency content of the output of a magnetic amplifier reduces the effectiveness of such compensation procedures.

8-5. RECTIFIER LEAKAGE

A discussion of rectifier leakage, once a major problem in magnetic-amplifier design, was reserved until this late chapter because leakage is no longer the plague it once was, except in isolated circumstances. The development of the silicon rectifier with room-temperature leakage current on the order of 10^{-8} amp has relegated the problem of rectifier leakage to the fringe area of magnetic-amplifier design. At times, however, rectifier leakage must be reckoned with. Such cases arise, for instance, when ambient temperatures in excess of 200°C must be considered or when extremely large load currents must be supplied.

The effects of large leakage currents on a transfer characteristic are illustrated in Fig. 8-19. It is apparent that leakage causes a decrease in gain and results in an amplifier which is not at full output with zero signal applied. The amount of signal required to bring the amplifier to cutoff is not affected greatly by large variations in the amount of leakage current, however. The presence of rectifier leakage increases the problems of environmental sensitivity and gain change since the reverse resistance of rectifiers is both nonlinear and temperature-sensitive. These properties result in appreciable change of gain and quiescent operating point as either line voltage or ambient temperature is varied.

Several circuits have been used to minimize the effects of rectifier leakage. A typical approach is illustrated in Fig. 8-20. The circuit shown is a center-tap circuit with a compensation circuit consisting of a winding N_F added to each reactor and connected across the load through rectifiers, REC_3 and REC_4. REC_4 must have leakage characteristics similar to gate circuit rectifiers REC_1 and REC_2. REC_3 need carry only small amounts of current in the forward direction and may be a small area diode with moderate characteristics. In the following qualitative analysis, it will be assumed for simplicity that REC_3 has an infinite

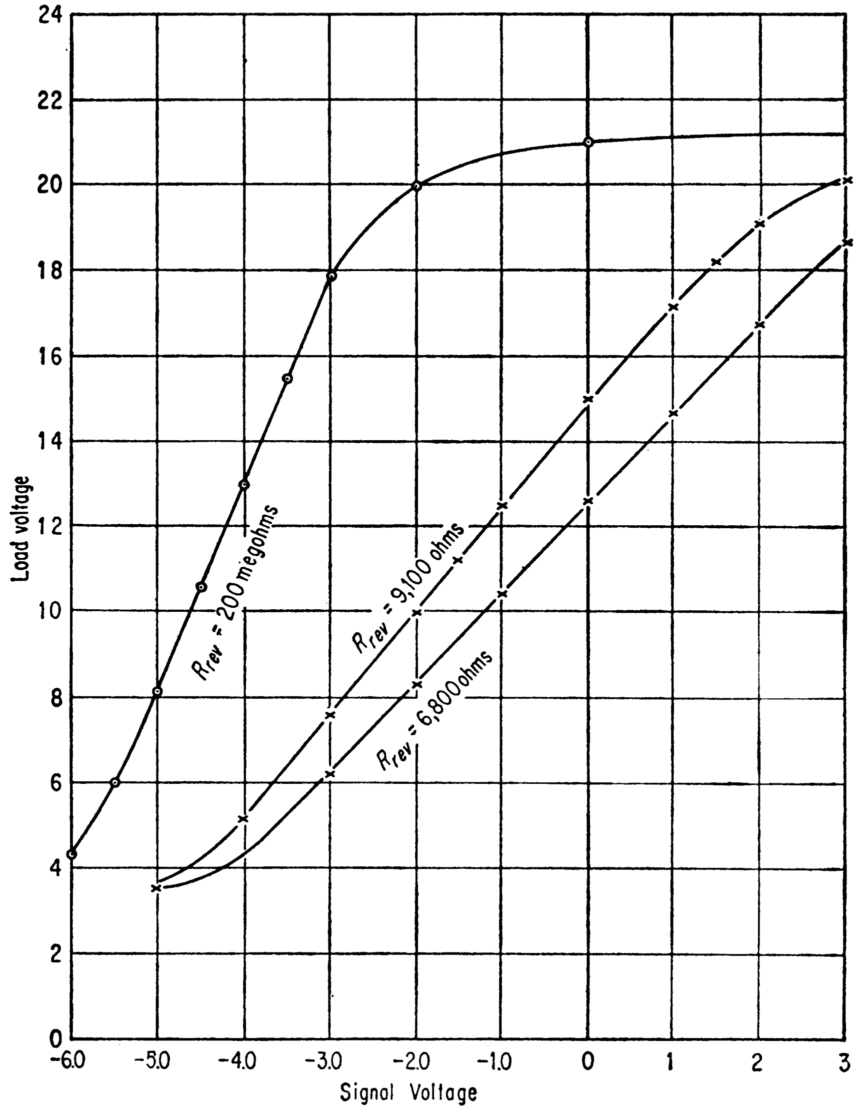

FIG. 8-19. Effect of rectifier leakage on a transfer characteristic.

reverse resistance since leakage in REC_3 will result only in second-order effects.

Let it be assumed that when the control circuit is open and the compensation circuit switch Sw_1 is open, the leakage of rectifiers REC_1 and REC_2 results in the steady-state load voltage waveshape of Fig. 8-21a and the waveshape of Fig. 8-21b across REC_2. If Sw_1 is closed at the

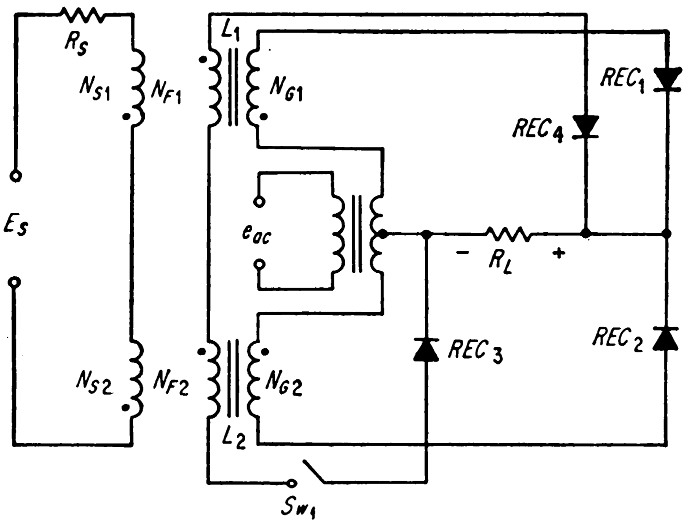

FIG. 8-20. Circuit for minimizing effects of rectifier leakage.

beginning of a reset half-cycle of reactor L_2 and it is assumed that N_F is twice N_G, no current will flow in the compensation circuit until reactor L_1 fires. This is obvious since the voltage developed across N_{F2} must be small while the voltage across N_{F1} is equal to twice e_{ac} and has a polarity which applies reverse voltage to REC_3, which has been assumed to have infinite reverse resistance. After reactor L_1 fires, the voltage across N_{F1} becomes zero and a voltage equal to e_{ac} appears across R_L. This voltage across R_L also appears across REC_4, causing a leakage current to flow through N_{F2}. Since the voltage across REC_2 is twice the voltage appearing across REC_4 and N_{F2} is twice N_{G2}, the ampere-turns are approximately in balance and no further appreciable flux change occurs in reactor L_2 until the end of the reset half-cycle.

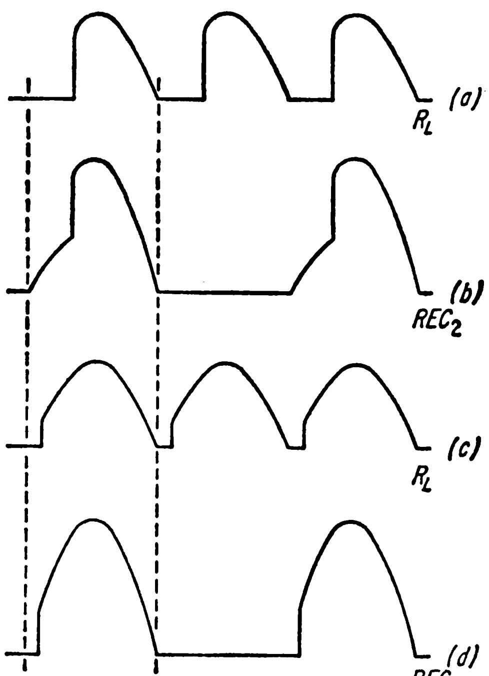

FIG. 8-21. Waveshapes for circuit of Fig. 8-20. (*a*) Load voltage, Sw_1 open; (*b*) rectifier voltage, Sw_1 open; (*c*) load voltage, Sw_1 closed; (*d*) rectifier voltage, Sw_1 closed.

At the start of the reset half-cycle of L_1, leakage occurs in REC_1 until reactor L_2 fires. However, because flux change in reactor L_2 was minimized by the compensation circuit during the reset half-cycle of reactor L_2, this reactor will fire much earlier in its gating half-cycle than reactor L_1 did in the previous half-cycle. Consequently, leakage will cause only a relatively small amount of reset in reactor L_1. This type of ratcheting process will be recognized as the same type of feedback phenomenon discussed in Chap. 3 in connection with the doublet amplifier. The steady-state conditions existing with switch Sw_1 closed are illustrated in Fig. 8-21*c* and *d*. Application of signal increases the complexity of the explanation but the result is the same—the compensation circuit minimizes the deleterious effects of rectifier leakage current.

8-6. EFFECT OF SUPPLY FREQUENCY ON AMPLIFICATION AND SIGNAL-POWER REQUIREMENTS

The previous discussions of amplifier operation and design procedures have, to a large extent, ignored explicit reference to the function of gating frequency. In general, most industrial organizations work in the immediate neighborhood of one fixed frequency and are concerned only with small variations about a nominal. The introduction of high-efficiency d-c to a-c converters, however, makes a discussion of operation at other than common power frequencies of more than academic interest.[8,9]

The most obvious effect of a large change in gating frequency is to change the power which a given core is capable of controlling. The curves presented in Fig. 7-1 were compiled on the basis of a 400-cps gating frequency. From the equation

$$E_{NG} = 4.44 N_G f B_m A$$

it is apparent that the voltage which a given number of turns will control is proportional to frequency. If it is assumed that a reactor has been designed for maximum power output, the maximum current is determined by wire size, and the maximum power a given core is capable of controlling will change, not by the second power, but in direct proportion to a frequency change.

The first-order effect of a frequency change on the gating circuit, therefore, is a proportional change in the power output. Some second-order effects occur, however, which alter this direct relationship. For example, the prefiring gating current is a function of frequency and, as frequency increases, the percentage of maximum load voltage which can be controlled by the signal decreases, assuming again that the reactor will always supply maximum load power. Another second-order effect is an increase in the percentage of supply voltage appearing across the core in the postfiring period as a result of the nonsquareness of the core-material characteristic. Both these second-order effects tend to make the usable change in output power something less than directly proportional to the change in frequency.

It will be recognized that the second-order effects are not linear over a large range of frequencies. In the low-frequency range both the prefiring gate current and the saturated inductive reactance of a reactor are very small and the effect of a twofold increase in each on usable load voltage would be difficult to measure. At high frequencies, however, these parameters are appreciable and a twofold increase would have an immediately recognizable effect.

In addition to first- and second-order effects in the gate circuit which apply to virtually any circuit configuration, a change in gating frequency affects the signal circuit to a greater or lesser degree depending on the circuit configuration considered. In circuits with a very low N^2/R ratio, for example, reset tends to take place very nearly in the same manner as the flux change resulting from a step change in magnetic potential. The manner in which such reset takes place is a function of the magnitude of the step change of magnetic potential as illustrated in Fig. 8-22. In this figure, all flux changes are initiated from the remanent condition. Curve a resulted from a step change of magnetic potential just a little greater than the threshold value. Curve c resulted from a magnetic potential which differed from the threshold value by an amount twice as great as the difference between the threshold value and the magnetic potential required to produce curve a. An intermediate value of magnetic potential resulted in curve b. It will be observed that, for curve b, the flux change is virtually complete in six units of time. For a gating frequency with a half-cycle period longer than six time units, then, the resetting magnetic potential required to obtain complete reset of flux need never exceed, nor even equal, the value used to obtain curve b. However, if the half-cycle period is less than six time units, complete reset cannot be obtained with a magnetic potential equal to that used to obtain curve b, since the reset mechanism will be interrupted by the start of the gating interval. This indicates that, as frequency is increased, larger resetting magnetic potentials are required to obtain complete reset in one resetting interval.

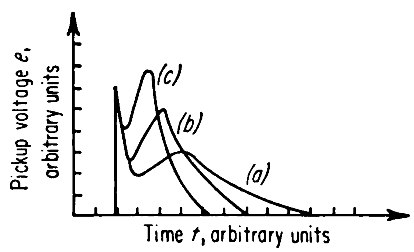

FIG. 8-22. Induced voltage as a function of time for three magnitudes of mmf.

The major effects of supply frequency on amplifier gain, then, can be summarized as a nearly proportional increase due to gate-circuit phenomena and a decrease of unspecified magnitude due to control-circuit phenomena. Curves relating amplifier gain to supply frequency as a function of N^2/R for a bridge amplifier are presented in Fig. 8-23. These curves were obtained on a set of reactors wound specifically to operate over a large frequency range. The load resistance was varied to maintain the maximum average current output constant. The scattering of the points is indicative of the difficulties encountered in trying to measure gain when the characteristic is somewhat curved. A smooth set of points is almost impossible to attain; the best that can usually be achieved is an indication of the trend of the dependent variable.

The foregoing discussion indicates that for a given signal-circuit configuration, the signal power required to control a given set of cores

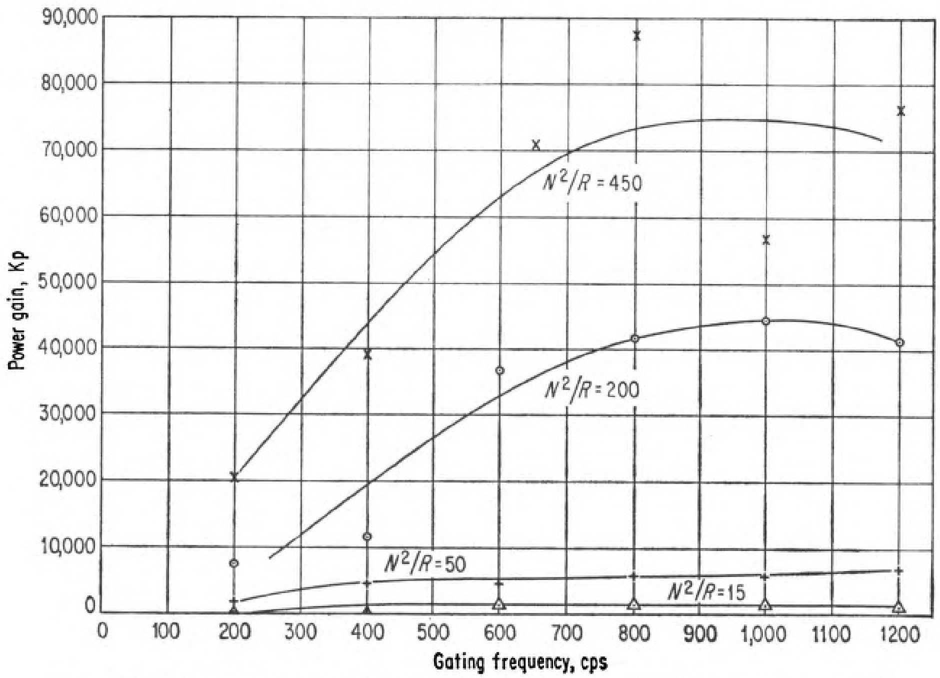

FIG. 8-23. Power gain as a function of frequency (N^2/R as a parameter).

completely increases with increasing frequency. Apart from the problems of providing a source of higher frequency, then, there are indications that it is not always desirable to operate at as high a gating frequency as possible. Where minimum signal-source drain is of concern, it may be that a lower frequency is the preferred alternative.

REFERENCES

1. Collins, H. W.: High-frequency Operation of Self-saturating Magnetic Amplifiers, *Trans. AIEE*, vol. 74, part I, pp. 500–505, 1955.
2. Proposed Standard Terms and Definitions for Magnetic Amplifiers, *Trans. AIEE*, vol. 77, part I, pp. 429–431, 1958.
3. Timmel, F. G., C. C. Glover, and D. H. Mooney: Self-bias in Balanced Magnetic Amplifiers, Conference Paper, AIEE Summer General Meeting, 1954.

4. Batdorf, S. B., and W. N. Johnson: An Instability of Self-saturating Magnetic Amplifiers Using Rectangular Loop Core Materials, *Trans. AIEE*, vol. 72, part I, pp. 223–227, 1953.
5. Finzi, L. A., and D. L. Critchlow: Dynamic Core Behavior and Magnetic Amplifier Performance, *Trans. AIEE*, vol. 76, part I, pp. 229–240, 1957.
6. Leon, H. I., and A. B. Rosenstein: Inductive Load Instability in Magnetic Amplifiers, *Trans. AIEE*, vol. 74, part I, pp. 8–20, 1955.
7. Finzi, L. A., and R. R. Jackson: The Operation of Magnetic Amplifiers with Various Types of Loads, Part I, Load Currents for Given Angle of Firing, *Trans. AIEE*, vol. 73, part I, pp. 270–278, 1954.
8. Bright, R. L.: Junction Transistors Used as Switches, *Trans. AIEE*, vol. 74, part I, p. 120, 1955.
9. Martin, W. A.: Development of the Transistor Inverter at 20 KC Using Power Transistors, *IRE Trans. on Instrumentation*, vol. I-6, pp. 118–122, June, 1957.

9

Applications

The principal object of this book has been to consider self-saturating magnetic amplifiers as a class in considerably greater detail than has been attempted previously in text form. The complete elimination of any discussion of simple reactor circuits has stemmed from the authors' convictions that practically none of the theory concerning the detailed mechanics of operation of simple reactor circuits is conceptually useful as a basis for the consideration of self-saturating circuits.

This concentration of emphasis logically limits the discussion of applications to those involving self-saturating magnetic amplifiers, despite the historical significance of light dimming at Radio City Music Hall. But even beyond this self-imposed restriction, the main preoccupation of this book has been with the presentation of a discussion of the mechanics of operation of self-saturating magnetic amplifiers with sufficient care and detail to provide a firm basis for future design work by the reader as well as for some insight into the origin of certain performance characteristics which are impossible to appreciate from more idealized treatments. For this reason, and because this aspect of the subject is covered fairly adequately in some of the existing treatments,[1–3] the discussion of applications will be quite brief. Illustrative examples will be given, however, together with a tabulation of the more common applications and the circuit types normally used to satisfy the application requirements.

9-1. COMPETITIVE POSITION

The rapid growth and continued application of self-saturating magnetic amplifiers since World War II have come about as a result of extensive military development in this field. Commercial applications have not lagged far behind, however, especially in those areas where magnetic-amplifier costs are competitive with those of less reliable equipment.

It is obvious that the self-saturating magnetic amplifier would not have been applied to the multitude of military and commercial applications now in existence if there were not very definite advantages in its use.

On the other hand, since its use has not excluded both vacuum tubes and transistors, it would also seem obvious that there are certain inherent limitations in this device as there are with all electrical components in use today. The following list of advantages and disadvantages seems, to the authors' point of view, to present the most important items for consideration. They are listed here to stimulate the reader, and in particular the design and application engineer, to compile his own list which would take into account those particular considerations which are pertinent to his own field of application.

A. Advantages

1. The manner in which a magnetic amplifier is constituted leads to ruggedness and a consequent high degree of reliability.
2. Only a low-impedance alternating-voltage power supply is required.
3. Relatively high efficiencies are obtainable with a magnetic amplifier because of the absence of heater power and auxiliary power supplies, and the relatively low wattage dissipation of the low-impedance circuits.
4. The magnetic amplifier is available immediately since no warm-up time is required for heaters or auxiliary power supplies.
5. Isolation is possible between input and output circuits and signals of different voltage levels can be summed in any required proportions by the use of multiple signal windings.
6. The magnetic amplifier is able to handle very heavy load currents. Single units have been developed to control currents up to 160,000 amp.[4]

B. Disadvantages

1. The frequency response of a magnetic amplifier is a function of the frequency of the a-c supply. In some applications this may dictate a higher supply frequency than is readily available.
2. The magnetic amplifier is inherently a low-input impedance device as compared to vacuum tubes. This may be a disadvantage in accepting low-level signals from transducers which are not capable of supplying even the small amounts of current required by a low-input impedance.
3. A pure sinusoidal output waveform is not readily obtainable, since magnetic amplifiers operate by control of firing angle.
4. A source of a-c power is required, which is a disadvantage where only direct current is available.

9-2. CHARACTERISTICS PERTINENT TO A SPECIFIC APPLICATION

As already pointed out in Chap. 7 in the discussion of selection of candidate magnetic-amplifier circuit configurations as a first step in design, it is very important to give careful consideration to the requirements of a particular design specification before any detailed design procedures are initiated. Similarly, it is helpful to review the important characteristics of magnetic amplifiers in general as a background for a more detailed discussion of particular magnetic-amplifier types and their areas of application. Although there will be some duplication between this discussion and that contained in other parts of this book, particularly in Chap. 7, the emphasis here is toward application suitability rather than toward initiating design procedures or explaining the mechanics of operation. Several of these characteristics have already been mentioned as advantages or disadvantages, but with no discussion. A particularly good discussion of these application characteristics has been published by M. G. Say.[5] The discussion here will follow the same format and will incorporate many of the ideas presented there. However, the items will be considered here only as they affect self-saturating magnetic-amplifier applications.

Amplification. As mentioned in Chap. 1, it is more useful to consider the power amplification in self-saturating magnetic amplifiers than the current or voltage amplification because power gain is more directly related to response time and circuit configurations. A power gain of 10^7 is possible for a single-stage magnetic amplifier operating under laboratory conditions, but a more usual value for small single-stage self-saturating magnetic amplifiers with nickel-iron cores is 10^4 to 10^5. For larger units (above approximately 1 kw output) it is desirable from economic considerations to use silicon-iron cores where single-stage power gains of 10^3 to 10^4 are typical. In some cases dynamic response considerations dictate the use of two or three stages to achieve a power gain that could be accomplished in one extremely slow stage.

Input and Output Impedance. Self-saturating magnetic amplifiers are essentially low-impedance devices, especially when compared to vacuum-tube amplifiers. It will be understood that the word impedance in this case is not used in its normal sense, because of the nonlinear relationship between the voltage and current waveforms. At best, the specification of an impedance would involve an average value.

Within these limits, it may be stated that the input impedance is normally determined by external series resistance. In spite of this, it is low when compared to vacuum-tube circuits in order to allow sufficient current to flow through the control windings.

A low-output impedance, nearly always an advantage, is limited by the copper resistance in the gate winding, the impedance of the self-saturating rectifiers, and the saturated inductance of the reactors. In push-pull amplifiers the resistance of the mixing resistors is also a factor. The resistance of the gate winding is limited by the window area of the core and, therefore, by the amount of copper that can be allocated to the gate winding. At higher supply frequencies, the saturated inductance of the cores can appreciably increase the output impedance; at 60 and 400 cps, this is not a significant problem. The impedance of the self-saturating rectifiers is somewhat nonlinear, as pointed out in Chap. 2. Its effect, therefore, tends to decrease as the gate winding voltage is increased.

Static Characteristics. Like other types of d-c amplifiers the self-saturating magnetic amplifier is subject to drift, environmental sensitivity, and gain change. Ambient temperature affects performance and it can be considered a truism that a given level of environmental sensitivity becomes progressively harder to meet as the temperature limits are broadened—at both extremes. This effect is sometimes exaggerated by the inferior electrical, magnetic, or physical properties of the materials which are capable of operating in the wider temperature range. Typical values attainable over the usual military temperature range of -55 to $+85°C$ for a small self-saturating magnetic amplifier would be 2 per cent environmental sensitivity and 5 per cent gain variation with a power gain of several hundred.

Frequency Response. The normal gating frequencies for self-saturating magnetic amplifiers are 50 to 60 cps, 400 cps, and perhaps a few thousand cps. Since the transportation lag of magnetic amplifiers is dictated by the time allowed for reset and since doublet magnetic amplifiers usually require, in addition, at least a few cycles of supply frequency to respond completely, self-saturating magnetic amplifiers have comparatively slow transient response. Therefore, they find their principal sphere of application in control functions where a considerable mass, and a correspondingly appreciable inertia, is involved in the control process. This can occur in the controlled member itself (e.g., the rotor of a motor) or indirectly at some point in the control loop (e.g., the aerodynamic coefficients relating vehicle response to control member deflection or the reaction rate of a chemical process after change of the concentration of the reacting compounds in solution). As a rule of thumb, it is normally considered that the useful bandwidth of a doublet magnetic amplifier should be limited to 10 per cent of the carrier frequency.

Output Waveform. Since control of a self-saturating magnetic amplifier is provided essentially by means of varying the angle of an a-c carrier wave at which the reactor fires, it is difficult to provide an undistorted output waveshape. This feature is no disadvantage for many applications (e.g., the torque in a motor is proportional to the fundamental component of the output—the motor in effect is its own filter). However, for applications in which the output waveform is important, the output filtering required must be charged to the size, weight, and cost of the magnetic amplifying device.

Efficiency. The efficiency of electrical apparatus affects both power consumption and cooling problems. Self-saturating magnetic-amplifier devices are usually more efficient than corresponding electronic units because of the low impedance which can be achieved for the saturated condition and because filament power is not required. Typical efficiencies for single-stage single-ended self-saturating magnetic amplifiers range from 50 per cent for small units (approximately 0.1 watt output) to 80 or 90 per cent for larger units.

Warm-up Time. Self-saturating magnetic amplifiers are available immediately when switched on; there is no need for delay switches and other protective circuitry for starting.

Size and Weight. The size of small self-saturating magnetic amplifiers is generally governed by the requirements of the amplifying characteristics rather than by thermal limitations. If advantage can be taken of a high frequency supply (400–1,600 cps), a magnetic amplifier handling approximately 10 watts can be made to compare favorably with an electronic amplifier and its associated power supply designed to perform the same function.

In the larger units, size is largely determined by temperature rise. In such applications, especially where high load currents are required, the self-saturating magnetic amplifier compares most favorably with competitive devices.

Cost. With few exceptions, the first cost of a self-saturating magnetic amplifier is comparatively high. This is particularly true of small units in which the grain-oriented core materials and complex windings, particularly on toroidal cores, are needed. The market is quite specialized and mass-produced tubes, relays, and rotating machines are extremely competitive.

Reliability. Self-saturating magnetic amplifiers are static solid-state devices and need not contain parts which have an inherently limited life. In construction they resemble the combination of transformers with resistors, capacitors, and rectifiers. The reliability and ability to withstand severe environmental conditions of transformers, resistors, and capacitors are well known. These characteristics for rectifiers are improving and it should be noted that such sophisticated characteristics of semiconducting materials as minority carrier lifetime and alpha cutoff are required for transistor operation, but not for rectifier operation. Hand in hand with the long life of the components, little, if any, routine maintenance or periodic replacement of parts is required. Faults due to coil failure are rare and such breakdowns of apparatus as do occur are usually associated with components such as rectifiers and relays. Low maintenance costs and low incidence of failure, therefore, help to offset the high initial cost. Unless the fault is an easily detected one, servicing is a specialized job and usually necessitates return of the equipment to the manufacturer, or the attention of the manufacturer's field repair specialist.

9-3. LINEAR AMPLIFIERS

In a discussion of applications of self-saturating magnetic amplifiers, it is often the practice to classify the application by the actual use itself. For example, the applications could be divided into the type of loads or devices which are driven by the particular amplifier. This leads to an emphasis on the load, but a rather disjointed treatment of the individual circuit type, since more than one amplifier may be suitable for a given load application. In the following discussion, the several major amplifier types will be treated individually and their most important applications will be noted. The means of classifying the various amplifier types will be the one developed earlier in this book in Chaps. 3 and 5. In other words they will be grouped according to their dynamic characteristics. Those exhibiting time delay, called doublet-type amplifiers, will be treated first. Those without time delay, or fast-response amplifiers, will be treated second. Such special circuit compensation techniques as self-bias and filter output circuits will be treated in a general way with emphasis on the application that demands such compensation techniques.

The three most popular doublet amplifiers are the doubler, the center-tapped, and the bridge, as pointed out in Sec. 3-7. These will be discussed individually in this section in both the single-ended and push-pull variations of the circuits, together with some comment on the use of external feedback.

Doubler Amplifier. A typical doubler circuit, including control and bias windings, is shown in Fig. 9-1*a*. The operation of this circuit has been described in Secs. 3-8 and 5-6. The circuit derives its name from the polarity configuration of the rectifiers. This type of rectifier connection in itself was referred to as the doubler connection in power-supply circuits even before the introduction of self-saturating magnetic amplifiers. With application to self-saturating circuits, the total magnetic-amplifier circuit came to be known as the doubler amplifier. As noted in previous chapters, this circuit has an inherent a-c output. In order to obtain a d-c output with this circuit, some designers have employed the load circuit shown in Fig. 9-1*b*. With the present state of the art, this connection may seem far less desirable for a d-c output current than direct use of the bridge circuit. However, it did have the advantage, before the days of high-quality rectifiers, of requiring only low-quality rectifiers (relatively high back leakage current) for the bridge rectifying circuit. Even the self-saturating doubler rectifiers are not subjected to high back voltages, as discussed in Sec. 5-6. Therefore, early types of plate rectifiers could produce a reasonably high gain amplifier in this type of circuit, whereas a bridge circuit would have been severely hampered.

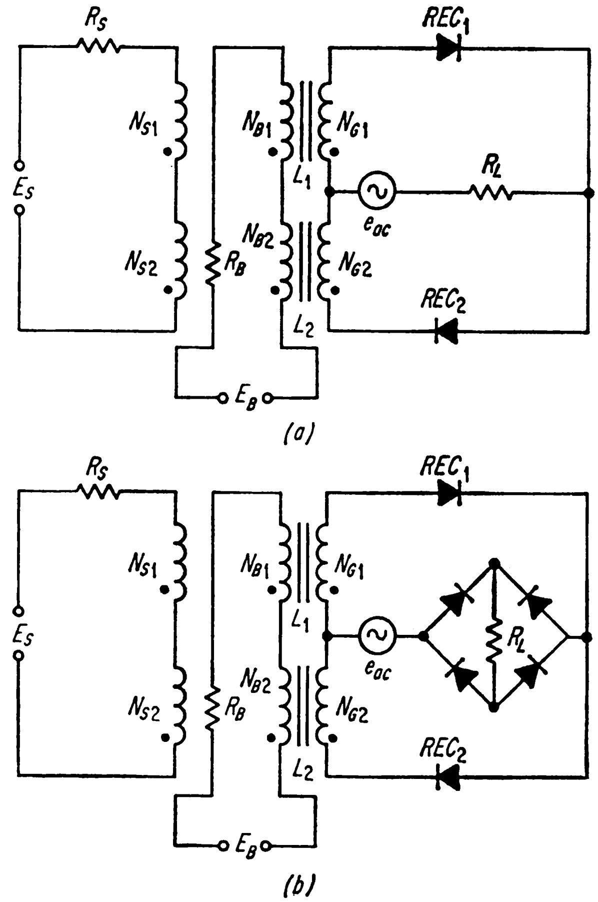

FIG. 9-1. Doubler amplifier. (*a*) A-c output; (*b*) d-c output.

Today, however, the doubler amplifier is treated almost exclusively as an a-c output device and is utilized for such loads as a wide variety of heating elements, a-c relays, alarm or indicating lights, and power-supply regulator circuits. Usually these applications require a fairly large amount of output power of the a-c type without the requirement of an extremely linear amplifier characteristic. The inherent nonlinearity of the circuit has been discussed in detail in the literature[6] and, while it is not a severe handicap for low-gain high-power control applications, it can be a disturbing feature if an extremely high accuracy system is desired. Another, older application of this type of amplifier was in the control of a-c servo motors. However, with the introduction of such circuits as those discussed later in this section, the doubler circuit has frequently been replaced in this application by these more modern amplifiers, particularly in low-power uses. The previously mentioned nonlinearities, as well as the sometimes unpredictable changes in the transfer characteristic of the doubler amplifier, resulting from a highly inductive motor winding, have been the contributing factors in its replacement in these applications.

Bridge Amplifier. A typical magnetic-amplifier bridge circuit, including control and bias windings, is shown in Fig. 9-2. The operation of this circuit has been described in Secs. 3-7 and 3-8. Here again, the name chosen for this amplifier is derived largely from the rectifier configuration; in fact, the basic circuit is simply a bridge rectifier with

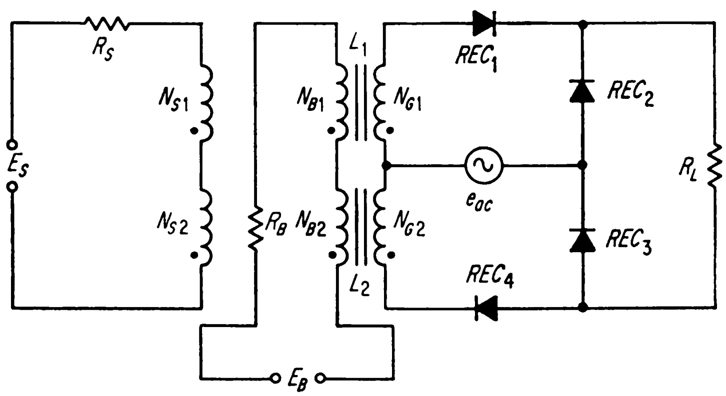

FIG. 9-2. Bridge amplifier.

saturable reactors inserted in two of the four rectifier legs of the bridge. Schematic diagrams of the amplifier often obscure this fact in an effort to make the analysis of the circuit somewhat easier. Obviously this circuit has an inherent d-c output characteristic as compared to the a-c characteristic of the doubler amplifier. Where a d-c output is desired, the bridge would nearly always be preferred to the doubler circuit followed by a bridge rectifier, as shown in Fig. 9-1*b*. The exception to this rule would be the case discussed in the previous paragraphs in an application in which the reduced requirements placed on the back leakage characteristics of the rectifier would be very important. In general, then, a bridge or center-tapped amplifier would be used wherever a d-c load characteristic is desired and, more particularly, the bridge amplifier is employed where the load impedance is somewhat inductive. The reason for this becomes obvious upon examining the circuit in Fig. 9-2 to determine the impedance that the amplifier presents to the load. Looking back into the amplifier from the load-circuit terminals, we find that there is a very-low-impedance unidirectional path for current flow through rectifiers REC_3 and REC_2. This provides a short circuit path for induced currents that would otherwise greatly contribute to backfiring in the magnetic amplifier and upset the linear operation of the circuit. Rather complete treatments of this subject are found in specific literature.[7] In summary, the rectifier configuration for this circuit combines the advantages found in the doubler amplifier of Fig. 9-1*b* with the advantages of "free-wheeling" rectifiers often utilized in reducing the induced current effects of an inductive load. Some of the most common applications of this circuit are d-c power-supply regulator circuits, hydraulic-control valve circuits, and d-c relay coils.

The linearity of this circuit is somewhat better than that of the doubler circuit.[6] This fact, together with the free-wheeling rectifier effect, tends to make the bridge amplifier quite easy for the designer to apply to a wide range of loads and functional applications. In other words, its characteristics are quite easy to predict in an initial design.

Center-tapped Amplifier. Figure 9-3 shows a simple version of a single-ended center-tapped circuit. The operation of this circuit has

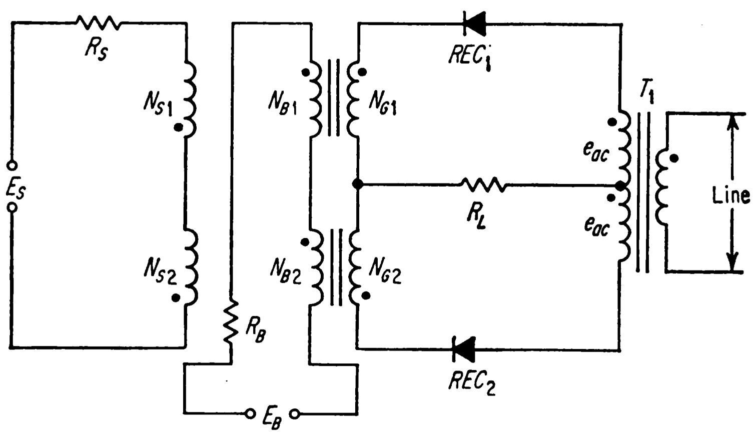

FIG. 9-3. Center-tapped amplifier.

been described in Chap. 5 (see Figs. 5-17 and 5-18). The circuit derives its name from the center-tapped transformer which is required for its gate winding voltage source. This transformer must have twice the nominal load voltage rating with a center tap supplying one terminal of the load circuit. As a single-ended d-c output circuit, the center-tapped circuit has found application comparable to that of the bridge amplifier. It is quite linear but does not have the free-wheeling rectifier characteristic of the bridge amplifier. It will be discussed more fully in a later paragraph in the push-pull version for which the circuit seems more ideally suited.

Push-pull Amplifier Circuits. The problem of designing an efficient push-pull or phase-reversible amplifier is one that has never ceased to intrigue amplifier designers in general. In the field of magnetic amplifiers it has been particularly discouraging to the designer to see the

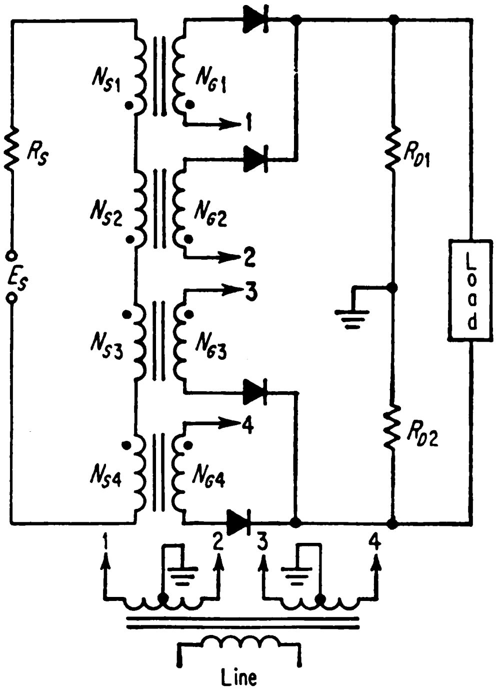

FIG. 9-4. Push-pull center-tapped amplifier.

inherent efficiency of the circuit greatly reduced by the losses introduced in any practical push-pull configuration. Switching techniques have on occasion been tried in order to reverse the polarity of the output voltage at the null point, but since discontinuities thus introduced are quite intolerable to high-performance feedback control systems and since problems of environmental sensitivity are greatly accentuated by such a circuit they will not be considered further. The most popular doublet-type push-pull circuit is the center-tapped circuit shown in Fig. 9-4. This circuit evolves in a straightforward manner from Fig. 9-3 by the addition of two cores and rectifiers and the load-mixing resistors R_{D1} and R_{D2} in an analogous manner to the push-pull configurations considered in Chap. 7. A push-pull bridge circuit is shown in Fig. 9-5 and is formed in a quite similar manner by load resistance mixing. The most interesting point to note between the two circuits in Figs. 9-4 and 9-5 is that the

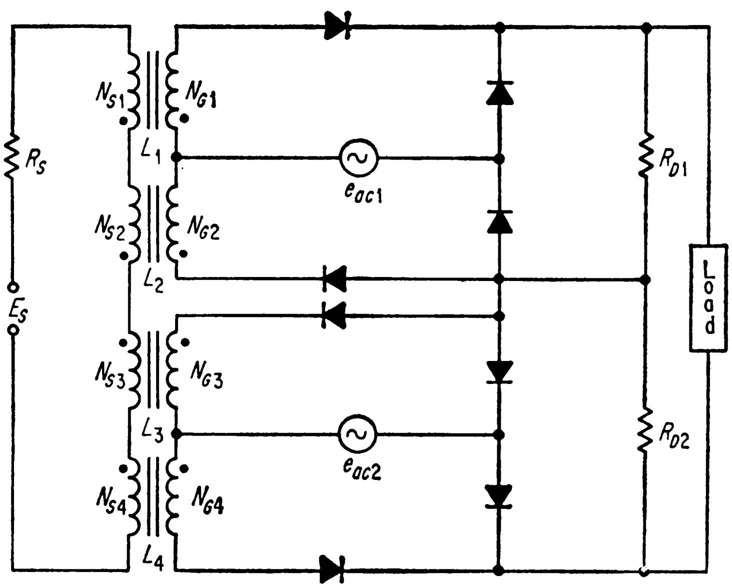

FIG. 9-5. Push-pull bridge amplifier.

center-tapped circuit for the push-pull arrangement requires fewer individual rectifiers; four compared to eight for the bridge circuit. However, as pointed out previously, the bridge circuit does have the free-wheeling rectifier advantage that is extremely useful if the two mixing resistors of Fig. 9-5 can be replaced by the inductive coils in a hydraulic valve or in a differential relay. Such applications are undoubtedly the most efficient use of the push-pull circuit since the efficiency of the amplifier is increased by mixing the effects of the two currents i_1 and i_2 rather than by obtaining a differential voltage across the mixing resistors.

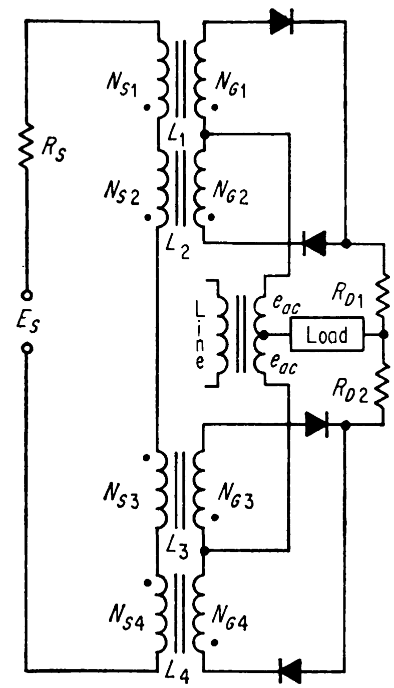

FIG. 9-6. Push-pull doubler amplifier.

A push-pull doubler circuit, shown in Fig. 9-6, can be used to obtain a phase-reversible a-c output voltage or current. However, with enough safeguards built into the circuit for practical operation, its efficiency is impaired and it is seldom used where more modern circuits are practicable. It can be noted from the circuit of Fig. 9-6 that any condition other than perfect class B operation would provide a path for current flow during at least part of a cycle through resistors R_{D1}, R_{D2}, and one core in each of the individual doubler halves of the push-pull circuit. In fact R_{D1} and R_{D2} are inserted to limit such current flow as the bias points of the amplifiers shift because of environmental changes. Naturally these resistors reduce the total efficiency of the circuit.

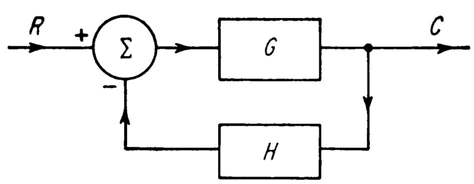

$$\frac{C}{R} = \frac{G}{1 + GH}$$

FIG. 9-7. Block diagram for amplifier with external feedback.

External Feedback. As mentioned in Sec. 5-5, external feedback may be applied to any of the magnetic amplifiers described in this chapter. In a very general way, such a circuit would take the block diagram form of Fig. 9-7. The transfer function at the lower frequencies might be approximated by the methods developed in Chap. 5. If the feedback block H were a simple resistive network, the effects of negative feedback would be a reduction in gain, an increase in the corner frequency, and an increase in linearity. A more generally useful configuration in the servo or feedback-control field is the use of a frequency-sensitive network for H. This allows the designer to synthesize transfer functions required by the total system for the quantity C/R. Naturally, practical limits are soon discovered in such a technique, but the use of frequency-sensitive networks in the feedback block has generally proved to be much more useful and flexible as well as economical in size and weight than the more straightforward technique of attempting to insert filters between amplification blocks in a functional block diagram. For more details on the types of transfer functions that may be synthesized if the transfer function approximations developed in Chap. 5 are properly applied, the techniques pointed out in any text on feedback-control theory are applicable.[8–10]

Another interesting point to note is that external feedback of this type may be applied to the amplifiers discussed in the next section (that is, amplifiers having only a dead time). If $G(s)$ in Fig. 9-7 is equal to $k\epsilon^{-sT_T}$, then the application of a positive feedback network will result in a total amplifier characteristic exhibiting time delay. The total transfer function C/R might then be said to be an artificial doublet amplifier.

Fast-response Amplifiers. Section 3-9 states that single-core building blocks may be combined in such a way that the only frequency-sensitive factor in the transfer function is the inherent dead time of the

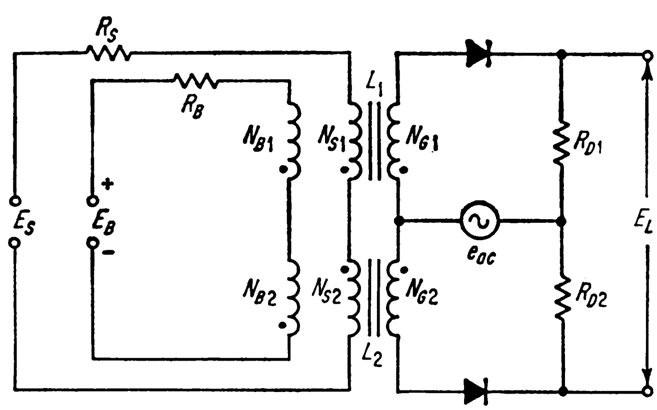

FIG. 9-8. Push-pull Logan amplifier.

single-core amplifier. The following discussion will cover several practical amplifiers of this type.

Figure 9-8 (which is identical with Fig. 7-9) shows the simplest form of a half-wave circuit; that is, the push-pull Logan circuit. This circuit has been rather completely described in the design procedures of Chap. 7 and finds its application mainly as an integral part of the hybrid types of amplifiers. As an individual stage of amplification it has found very little application because of the limited gain per stage and the further restrictions of half-wave output. The magnitude of the fundamental component of ripple inherent in such an output might be a disadvantage unless sufficient gain per stage were available to allow for the inefficiencies of some filtering. This circuit, therefore, is frequently considered as only a building block for the hybrid-type amplifiers discussed in the next paragraph.

It would have to be admitted that the name hybrid amplifier, already existing in the literature for this type of amplifier, is not too descriptive. It was chosen because of the combination of volt-second and ampere-turn control utilized in the same amplifier. However, this title could apply equally well to combinations of semiconductors and saturating devices which might constitute a total amplifier.[11] As pointed out in the

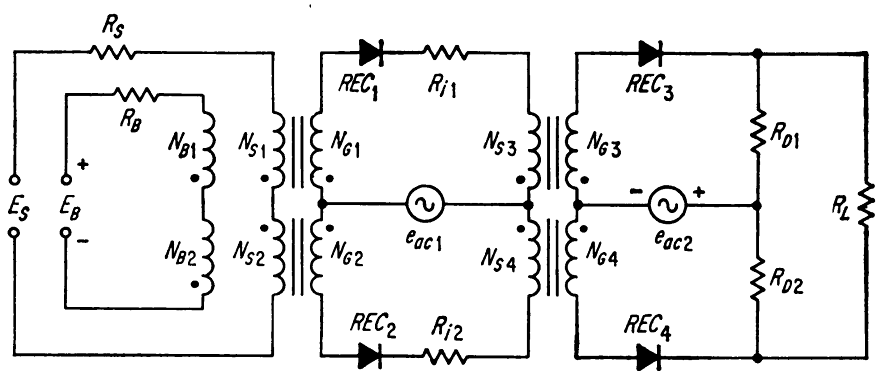

FIG. 9-9. Hybrid III amplifier.

previous paragraph and in Chap. 7, this amplifier is made up of two half-wave circuits coupled together in such a fashion that the firing angle of the power or output cores is slaved to the low-level input cores as shown in Fig. 9-9. If the problems of the interstage coupling are handled in a proper manner by the designer, as outlined in Chap. 7, this amplifier can be a very powerful tool in achieving the gain and response time often required in modern high-performance servo systems. This circuit has so far found its greatest use in servomechanisms employing high-performance hydraulic valves and actuators as well as in some regulator circuits where the transfer function of the feedback-control loop requires a high corner frequency in the magnetic amplifier. With these advantages, the problems of interstage coupling design outlined in Chap. 7 become a small cost to pay in return for the advantages obtained in the feedback-control system.

Other types of hybrid amplifiers may be formed by simply slaving a power stage to the firing angle of a low-level input stage. For instance, the two bridge circuits described in the next paragraph may be converted into hybrid amplifiers by simply supplying their control windings with the output of a half-wave preamplifier as is done with the Hybrid IV in Fig. 7-12.

The half-wave bridge circuit, shown in Fig. 9-10, is a useful modern output amplifier. Perhaps the most annoying drawback of this circuit is the simple fact that no esthetically satisfactory method of drawing the schematic diagram exists. If normal conventions are used, the operation of the circuit is almost completely obscured by the layout of the schematic. The method used in Fig. 9-10, on the other hand, requires verbal explanation to allow the uninitiated reader to appreciate its operation in a reasonable length of time (see also Fig. 3-18). The two windings labeled A and the two windings labeled B are gate windings of equal turns placed on the same core. Therefore, there are only two cores used in the circuit, even though the drawing of the schematic diagram would indicate that there are a total of four cores. In other words this is a

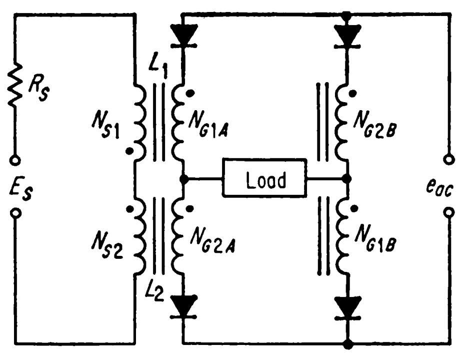

FIG. 9-10. Half-wave bridge amplifier.

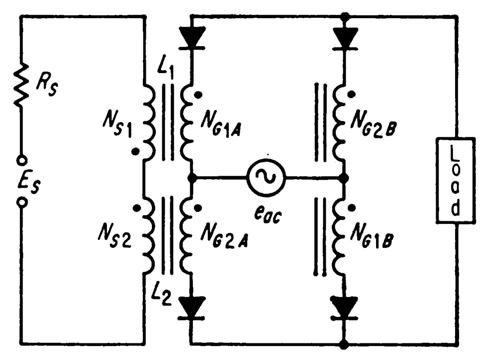

FIG. 9-11. D-c bridge amplifier.

simple bridge circuit of four legs in which gate windings of the self-saturating magnetic amplifier are inserted in each of the four legs. The firing angles of reactors L_1 and L_2 increase and decrease differentially so that at any condition other than the initial bias condition an unbalance would occur in the bridge, causing a current to flow through the amplifier load. This circuit has been rather completely described elsewhere in the literature[12] and has found wide application as a two-phase servo motor control amplifier. In order to limit current flow when both cores are in a saturated condition, it is normally necessary to insert a current limiting resistor in series with the a-c supply. This, of course, reduces the efficiency of the amplifier in a manner similar to that discussed in the paragraph on the push-pull doubler amplifier. Depending, of course, on the absolute magnitude of the power output of the circuit, the series resistor may or may not be a real handicap.

A strikingly similar bridge-circuit configuration, originally proposed by Geyger, is shown in Fig. 9-11. Apologies are made for the fact that this variation is treated here even though it is not a fast-response amplifier. It is treated in this section because of the great schematic similarity between the two circuits. It will be noted from examining Figs. 9-10 and 9-11 that the amplifiers differ mainly in the reversal of position of the load and the gate winding voltage sources. In effect, this simply means that current can only flow in one direction through the load circuit in the amplifier of Fig. 9-11. This bridge was, in fact, first applied by its inventor to the problem of supplying current to a two-phase induction servo motor. In this application, the cores are biased to a 90° firing point at null, supplying half-cycle pulses of d-c current to the servo motor. This causes a damping field to be induced in the motor and is quite advantageous in certain control applications. As the firing angles of the reactors vary from the null point as a result of an input signal, a fundamental frequency component of current is forced to flow through the motor. This fundamental component is a maximum when one core is saturated throughout a gating half-cycle and the other core unsaturated so that in the maximum output condition the output waveform is one unidirectional half-wave pulse of current every other half-cycle. A more complete discussion of this amplifier can be found in the literature.[1]

The question of single-ended versus push-pull circuits in this section is not as appropriate as it was in the discussion of doublet amplifiers since in this section the circuits are essentially push-pull by their very nature. The single-ended version of any of the above circuits would be a trivial one-core laboratory model.

Special Compensation Techniques. When applied to an actual system in industrial or military practice, most of the circuits shown in the figures in this chapter contain additional refinements which might seem superfluous to a beginner in the field. These refinements to a basic circuit are not unique to the magnetic-amplifier field and, in fact, are probably more common in the field of electron-tube amplifiers. One such embellishment found in magnetic amplifiers is the self-bias circuit already discussed in some detail in Chap. 8. It is of interest at this point in our general discussion of types of amplifiers to point out that this circuit can only be applied to push-pull amplifiers in which the output voltage or the current is obtained by the summation of two single-ended voltages or currents. For example, in the push-pull bridge or center-tapped circuits, a current which is equal to the sum of the two single-ended halves of the circuit is readily obtainable. In this case the output current is equal to the difference between these two currents. However, in the doubler push-pull circuit there is no handy way to obtain such a current for self-bias without unduly complicating the total circuit. Again, in the case of the fast-response amplifiers, wherever the push-pull circuit is of such a nature as to allow a current to flow which is the sum of the two halves of the amplifier, an adequate self-bias current may be obtained. This may be done in the case of the half-wave circuits and the hybrid types.

Another type of compensation that often occurs is a method for ensuring linearity of the amplifier in spite of the existence of an inductive load. This subject has been rather thoroughly covered in the transactions of the AIEE, and it was pointed out in the previous discussion of the bridge circuit in this section that the free-wheeling rectifier path of the bridge amplifier provides inherent correction of the effects of an inductive load. Other forms of compensation discussed in the literature include correction of the power factor by use of a parallel capacitance and the reduction of the effect of the inductance by addition of series resistance.[7]

Filtering of the output of a magnetic amplifier is often resorted to when the waveform will have a detrimental effect. Considerable care must be exercised by the designer in the application of such filters, not only because of the time delay that may be introduced, but also because of another factor. This factor is of importance when the time constants of the output filter allow only "peak charging" of the capacitors in the filter. When this occurs, the duty cycle resulting from high-amplitude narrow-width pulses may have a detrimental effect upon the rectifiers under certain conditions. An advantage which may be gained from the use of output filters is the increase in voltage gain which may result from use of a proper time constant filter. This may be accomplished in several of the half-wave circuits where the charge on the capacitor may increase the average output voltage obtained from the half-wave circuit over a complete cycle.

9-4. SWITCHING AMPLIFIERS

In order to improve system reliability in many applications, bistable, or relay, types of magnetic amplifiers may replace the conventional moving armature and contact types of relays. To achieve such an on-off circuit with a self-saturating magnetic amplifier, application of sufficient positive feedback to achieve an infinite or even a negative slope gain curve will result in the amplifier switching from a minimum to a maximum output condition with the application of a minute increment of input signal. Such on-off amplifiers have been discussed quite completely in the literature[13,14] and the individual magnetic-amplifier circuits, before the application of positive feedback, are really no different from those already discussed in this chapter.

Another field of growing application is that of the logic circuits (often referred to as "and," "or," and "not"). However, a reference to existing literature[14,15] in the field would be deemed sufficient inasmuch as these circuits need not have an amplification function, but perform

TABLE 9-1

Application / Circuit	Power supply regulators: A-c	Power supply regulators: D-c	D-c motor speed control	Generator output regulator	Analogue computer circuits	Low-level d-c signal amplifiers	Two-phase servo motor control	Logic circuits	Switching devices	Hydraulic valve control	Preamplifiers and intermediate amplifiers	Heater control	Pulse-width modulation	Circuit diagram (see Fig. Nos.)
Doubler amplifier	X						O	X	X			X		SE:9-1 PP:9-6
Center-tapped amplifier		X		X	X	X		X	X	X	X			SE:9-3 PP:9-4
Bridge amplifier		X	X	X	X	O		X	X	X	O	X		SE:9-2 PP:9-5
Hybrid III					X	O				X	X			9-9
Hybrid IV							X							7-12
Half-wave bridge							X							9-10
D-c bridge							X							9-11
Logan amplifier								X			PP		SE	SE:3-1 PP:9-8
Ramey amplifier								X	X					3-9

SE = single-ended amplifiers.
PP = push-pull amplifiers.
X = often used.
O = used infrequently.

certain types of logic upon certain combinations of input signals in order to accomplish a specific function in digital computing circuits. In most cases, however, the circuits do exhibit the characteristics of a self-saturating Logan- or Ramey-type amplifier. By building up combinations of some of these circuits, the so-called pulse line or shift register may be evolved, again from building blocks similar to the Logan or Ramey circuits.

9-5. CLASSIFICATION OF APPLICATIONS

While a classification of amplifiers by types of loads does not lend itself to a logical discussion of amplifier circuits, as pointed out in Sec. 9-3, it would seem a useful extension of Table 7-1 and the preceding discussions in this chapter to outline general applications as in Table 9-1. This table is intended as a general quick-reference guide, particularly for users rather than designers of amplifiers, and could be made more detailed by any practitioner in a specialized field of application. All circuits discussed in Chap. 9 are included and the types of applications, while not exhaustive, are felt to be at least representative.

In Table 9-1, types of applications are listed across the top and amplifier-circuit types are listed on the left-hand side. For reference, the figure numbers of the circuit diagrams of each circuit type are given in the extreme right-hand column. Where common usage seems to favor a push-pull configuration as against a single-ended type, the symbols *PP* or *SE* are used to denote the favored configuration. Again, where usage favors a particular circuit type for a given application but another amplifier may be used occasionally, the distinction is made through use of an *x* for the most-used type and an *o* for the less-used type. It is interesting to note that the bridge and center-tapped amplifiers seem to be the most generally useful configurations.

REFERENCES

1. Geyger, W. A.: "Magnetic Amplifier Circuits," 2d ed., McGraw-Hill Book Company, Inc., New York, 1957.
2. Storm, H. F.: "Magnetic Amplifiers," John Wiley & Sons, Inc., New York, 1955.
3. Milnes, A. G.: "Transductors and Magnetic Amplifiers," MacMillan and Company, Ltd., London, 1957.
4. Rosenstein, A. B.: 160,000 Ampere High Speed Magnetic Amplifier Design, *Trans. AIEE*, vol. 74, part I, pp. 90–97, 1955.
5. Say, M. G.: "Magnetic Amplifiers and Saturable Reactors," George Newnes, Ltd., London, 1954.
6. Pittman, G. F., Jr.: Notes on the Control Mechanism of Self-Saturating Magnetic Amplifiers, Conference Paper, AIEE Summer General Meeting, 1953.
7. Storm, H. F.: Magnetic Amplifiers with Inductive D-c Load, *Trans. AIEE*, vol. 73, part I, pp. 466–475, 1954.

8. Truxal, J. G.: "Automatic Feedback Control System Synthesis," McGraw-Hill Book Company, Inc., New York, 1955.
9. Ahrendt, W. R., and J. F. Taplin: "Automatic Feedback Control," McGraw-Hill Book Company, Inc., New York, 1951.
10. Chestnut, Harold, and R. W. Mayer: "Servomechanisms and Regulating System Design," John Wiley & Sons, Inc., New York, 1951.
11. Attura, G. M.: "Magnetic Amplifier Engineering," McGraw-Hill Book Company, Inc., New York, 1959.
12. Lufcy, C. W., P. W. Barnhart, and A. E. Schmid: An Improved Magnetic-servo Amplifier, *Trans. AIEE*, vol. 71, part I, pp. 281–289, 1952.
13. Radus, R. J., R. W. Roberts, O. R. Reiley, and C. V. Fields: Magnetic Amplifiers for Replacement of Relays, *Proc. Natl. Electronics Conf.*, vol. 12, p. 454, 1956.
14. Morgan, R. E.: A New Static Magnetic Switching Circuit Using Combined "And" and "Or" Functions, CP 57-101, AIEE Winter General Meeting, 1957.
15. Evans, W. G., W. G. Hall, and R. I. VanNice: Magnetic Logic Circuits for Industrial Control Systems, *Trans. AIEE*, vol. 75, part II, pp. 166–171, 1956.

Index